APPENDIX D

CATEGORY D
SEPARATE EFFECT TESTING

PHENOMENA DESCRIPTIONS AND RATIONALES FOR IMPORTANCE RANKING, APPLICABILITY, AND UNCERTAINTY

This appendix provides a description for each phenomenon appearing in Table 3-4, Separate Effect Testing PIRT. Entries in the Table D-1, columns 1 and 2, follow the same order as in Table 3-5. Table D-1, column 3, also documents the PIRT-panel developed rationales for three types of Panel findings.

First, rationales are provided for the importance (High, Medium, or Low) assigned by the panel to each phenomenon. Because importance ranking was established by a vote of the panel members, a rationale is provided whenever one or more panel members voted a particular rank, i.e., High, Medium or Low. If there were no votes for a given importance rank, "No votes" is entered.

Second, the PIRT panel considered the applicability of the baseline PIRT to a broader set of circumstances, e.g., different fuel arrays, cladding types, reactor types, and burnups to 75 GWd/t. The specific question addressed by the PIRT panel was as follows: "Could the importance ranking assigned for the given phenomenon in the baseline PIRT be for different for other fuel arrays, cladding types, reactor types, or burnups?" If this question is answered with a "no", the following entry appears in Table C-1: "Baseline PIRT importance rank is applicable." If this question is answered with a "yes", the rationale is entered. Additional details are presented in the footnotes to Table 3-5.

Third, the PIRT panel considered the current state of knowledge or uncertainty regarding each phenomenon. The phenomenon is characterized as "known (K)" if approximately 75-100% of full knowledge and understanding of the phenomenon exists. The phenomenon is characterized as "partially known (PK)" if between 25-75% of full knowledge and understanding of the phenomenon exists. The phenomenon is characterized as "unknown (UK)"if less than 25% of full knowledge and understanding of the phenomenon exists. Because the uncertainty ranking was established by a vote of the panel members, a rationale is provided whenever one or more panel members voted a particular uncertainty, i.e., known, partially known, or unknown. If there were no votes for a given uncertainty level, "No votes" is entered

There were several phenomena for which no importance rank was recorded. In such cases "No rationale recorded" is entered.

Table D-1. PWR and BWR LOCA. Category D– Separate Effect Testing

Subcategory (Test type)	Phenomena (Parameter)	Definition and Rationale (Importance, Applicability, and Uncertainty)
Oxidation rate, oxygen distribution, effect of chemistry on solubility (vote=15)†	Specimen selection: Alloy type	Composition or designation of the metal utilized in fuel-rod fabrication
Separate effect test to measure the steam oxidation kinetics at high temperature in Zirconium alloys used for cladding.		H(3) Data (B&W-10227) show that the 2nd layer develops differently on different alloys. Initial oxide layer may be different between alloys and thus behave differently. M(2) Similar to rationale for high but the oxide kinetics do not change and the other differences may not affect brittleness. L(0) No votes. Fuel: N Clad: NA Reactor: N Burnup: N K(2): Data, judgement PK(2): Judgement, no data UK(1): Data, judgement

† The Separate Effect Testing category was developed by considering the types of separate effect experiments that might be conducted to develop needed data. The panel defined six test types and the phenomena associated with each. Prior to voting on the phenomena themselves, the panel voted on the importance of each test type.

Table D-1. PWR and BWR LOCA. Category D– Separate Effect Testing (continued)

Subcategory (Test type)	Phenomena (Parameter)	Definition and Rationale (Importance, Applicability, and Uncertainty)
Oxidation rate, oxygen distribution, effect of chemistry on solubility (vote=15) Separate effect test to measure the steam oxidation kinetics at high temperature in Zirconium alloys used for cladding.	Specimen selection: Thickness and morphology of pre-existing oxide	The total amount of oxide formed on the cladding and whether the oxidation is uniform or nodular, and whether there is extensive cracking and spalling. H(1) Thickness and morphology controls passage to the metal, even though the oxidation rates are the same. M(2) Hydrogen pickup during corrosion may affect oxide rates. Some early irregularities in oxide rate data exist and may be due to corrosion layer. L(2) Data (French and Japan) show that only the thin dense oxide layer controls the oxidation rate at high temperature and this layer is independent of the initial oxide. Fuel: N Clad: NA Reactor: N Burnup: N K(2): Data PK(3): Data (incomplete) UK(0): No votes

Table D-1. PWR and BWR LOCA. Category D– Separate Effect Testing (continued)

Subcategory (Test type)	Phenomena (Parameter)	Definition and Rationale (Importance, Applicability, and Uncertainty)
Oxidation rate, oxygen distribution, effect of chemistry on solubility (vote=15) Separate effect test to measure the steam oxidation kinetics at high temperature in Zirconium alloys used for cladding.	Specimen selection: Burnup, including fluence	The amount of burnup to which the fuel rod used for the specimen was exposed. H(3) Burnup per se may not be so important but there could be effects such as precipitate dissolution for which testing is needed. M(1) Burnup per se may not be so important but there could be effects such as precipitate dissolution for which testing is needed, but the effect is not expected to be so pronounced. Discovery of unknown effects may occur if testing takes place. L(1) Irradiation damage is expected to be annealed out. Fuel: N Clad: N Reactor: N Burnup: NA K(1): Data PK(4): Data, judgement UK(0): No votes

Table D-1. PWR and BWR LOCA. Category D– Separate Effect Testing (continued)

Subcategory (Test type)	Phenomena (Parameter)	Definition and Rationale (Importance, Applicability, and Uncertainty)
Oxidation rate, oxygen distribution, effect of chemistry on solubility (vote=15) Separate effect test to measure the steam oxidation kinetics at high temperature in Zirconium alloys used for cladding.	Specimen selection: Pre-existing hydrogen content and distribution	Amount and distribution of hydrogen associated with fuel rod clad segment. This hydrogen may be in solution in the metal or may exist combined with the metal as a discrete hydride phase. H(1) Affects oxygen repartition during oxidation and oxygen solubility in the beta phase. M(3) Initial amount of hydrogen has a slight impact on the cladding strain during the ballooning phase and a very low impact on oxidation at high temperature and behavior upon quench; the initial H distribution has no impact. High concentration of hydrogen stabilizes beta phase and is conducive to thicker layer of load-bearing prior beta phase. L(1) The available testing by the Japanese and French indicate a relatively minor effect of hydrogen content on nonirradiated or irradiated cladding high temperature oxidation. Fuel: N Clad: NA Reactor: N Burnup: NA K(2): Data PK(2): Data, judgement UK(0): No votes

Table D-1. PWR and BWR LOCA. Category D– Separate Effect Testing (continued)

Subcategory (Test type)	Phenomena (Parameter)	Definition and Rationale (Importance, Applicability, and Uncertainty)
Oxidation rate, oxygen distribution, effect of chemistry on solubility (vote=15) Separate effect test to measure the steam oxidation kinetics at high temperature in Zirconium alloys used for cladding.	Conduct of Test-During Oxygen potential	Related to partial pressure of oxygen in system. H(3) The oxygen availability directly controls the alpha and oxide layer developments and the hydrogen pickup. Condition of steam starvation must be avoided to have a valid test. The oxygen potential is the boundary condition that determines oxidation rate. M(1) The development of an appropriate environment is essential to obtaining meaningful results. However, the measurement of oxygen potential may not be necessary to ensure a prototypical environment. L(0) No votes. Fuel: N Clad: N Reactor: N Burnup: N K(1): Data. Judgement PK(2): Data, Judgement UK(0): No votes.

Table D-1. PWR and BWR LOCA. Category D– Separate Effect Testing (continued)

Subcategory (Test type)	Phenomena (Parameter)	Definition and Rationale (Importance, Applicability, and Uncertainty)
Oxidation rate, oxygen distribution, effect of chemistry on solubility (vote=15) Separate effect test to measure the steam oxidation kinetics at high temperature in Zirconium alloys used for cladding.	Conduct of Test-During Temperature and time	Measurement of the time-varying temperature. H(5) May affect oxygen distribution and hydrogen pickup. Key parameter needed to analyze the tests. Since the corrosion process is such a strong function of temperature, accurate measurement of the temperature during the test is essential to providing meaningful results. M(0) No votes. L(0) No votes. Fuel: N Clad: N Reactor: N Burnup: N K(2): Data, Judgement PK(2): Data, Judgement UK(0):

Table D-1. PWR and BWR LOCA. Category D– Separate Effect Testing (continued)

Subcategory (Test type)	Phenomena (Parameter)	Definition and Rationale (Importance, Applicability, and Uncertainty)
Oxidation rate, oxygen distribution, effect of chemistry on solubility (vote=15) Separate effect test to measure the steam oxidation kinetics at high temperature in Zirconium alloys used for cladding.	Conduct of Test-During Total steam pressure	Total steam pressure H(1) Recent Korean testing on oxide at temperatures below 1800 F shows that the impact of pressure on oxidation rate could be important in small break LOCA M(3) Available experimental results do not show large effects for low burnup Zircaloy; to be confirmed at high burnup and for alternative cladding alloys. Not a key parameter but should be measured to check the experimental conditions are the same. Available testing information indicates measurable differences in high temperature cladding corrosion rate for different steam pressures. L(1) As long as steam starvation is prevented, total steam pressure is less important. Fuel: N Clad: N Reactor: N Burnup: N K(3): Data, Judgement PK(1): Data, Judgement UK(0): No votes.

Table D-1. PWR and BWR LOCA. Category D– Separate Effect Testing (continued)

Subcategory (Test type)	Phenomena (Parameter)	Definition and Rationale (Importance, Applicability, and Uncertainty)
Oxidation rate, oxygen distribution, effect of chemistry on solubility (vote=15) Separate effect test to measure the steam oxidation kinetics at high temperature in Zirconium alloys used for cladding.	Conduct of Test-During Weight gain	On-line measurement of the gain in mass of the test specimen. Used to measure the total amount of oxygen absorbed during the high temperature oxidation phase. H(4) Very important parameter to measure because it is directly linked with the equivalent cladding reacted (ECR) used for a LOCA criterion. Less accurate than direct O measurement (integrate Temperature distribution effects and end effects) but very useful in relative. M(1) Weight gain is a primary measure of corrosion, however, the more important measure in this case would be performed by metallography (differentiation between oxide, oxygen-stabilized alpha-phase, and remaining beta phase). L(0) No votes. Fuel: N Clad: N Reactor: N Burnup: N K(5): Data, Experience, Judgement PK(0): No votes. UK(0): No votes.

Table D-1. PWR and BWR LOCA. Category D– Separate Effect Testing (continued)

Subcategory (Test type)	Phenomena (Parameter)	Definition and Rationale (Importance, Applicability, and Uncertainty)
Oxidation rate, oxygen distribution, effect of chemistry on solubility (vote=15) Separate effect test to measure the steam oxidation kinetics at high temperature in Zirconium alloys used for cladding.	Conduct of Test-During Steam consumption	On-line measurement of the level of steam consumption during the LOCA transient H(1) This is a primary indicator of oxidation. M(2) Crosscheck measurement for the weight gain. Useful data but less precise than the post test measurement when the high temperature oxidation is non-uniform along the rod. L(2) The use of steam consumption was suggested as an alternate, independent assessment of oxygen absorbed, however, the more direct measurement is performed with metallography and weight gain. Steam consumption is not easily measured and is not necessarily an accurate indication of the degree of total oxidation (because of steam condensation). Fuel: N Clad: N Reactor: N Burnup: N K(3): Data, Experience, Judgement PK(2): Judgement UK(0): No votes.

Table D-1. PWR and BWR LOCA. Category D– Separate Effect Testing (continued)

Subcategory (Test type)	Phenomena (Parameter)	Definition and Rationale (Importance, Applicability, and Uncertainty)
Oxidation rate, oxygen distribution, effect of chemistry on solubility (vote=15) Separate effect test to measure the steam oxidation kinetics at high temperature in Zirconium alloys used for cladding.	Conduct of Test-During One-sided vs. two-sided	Whether oxidation is allowed on both the interior and exterior surfaces of the tube to model both oxidation processes as will occur during an accident. H(2) Two-sided oxidation is important in order to reproduce the specific oxidation conditions inside the balloon (stagnant steam conditions inducing a higher hydrogen pickup). A true simulation of the actual condition is essential to avoid overlooking unanticipated effects; such as the role of inner surface fission products, presence of a zirconium liner, or other possible differences. M(3) Both kind of tests are doable. The analysis should take into account the test conditions. Two-sided oxidation may have slightly different kinetics; at least it is worth investigating. L(1) High-temperature oxidation is controlled primarily by the process of oxygen transport across the oxide layer. Fuel: N Clad: N Reactor: N Burnup: N K(2): Data PK(3): Data, Judgement: Prior work has shown, for example, that the presence of a zirconium liner does not significantly affect the cladding high temperature corrosion behavior. However, all possible effects have not necessarily been quantified. UK(0): No votes.

Table D-1. PWR and BWR LOCA. Category D– Separate Effect Testing (continued)

Subcategory (Test type)	Phenomena (Parameter)	Definition and Rationale (Importance, Applicability, and Uncertainty)
Oxidation rate, oxygen distribution, effect of chemistry on solubility (vote=15) Separate effect test to measure the steam oxidation kinetics at high temperature in Zirconium alloys used for cladding.	Conduct of Test-PTE Oxide thickness	Post test measurement of the oxide thickness that developed during the high temperature phase of the LOCA transient. H(5) One of the most pertinent measurements. Oxide thickness is the most important parameter of oxidation. Key parameter for the interpretation and analysis of the test. Posttest metallography is the primary and most reliable quantification, however the measurement is not necessarily just oxide thickness, also region of oxygen-stabilized alpha layer and remaining beta layer. Useful parameter to measure primary item studied. M(0) No votes. L(0) No votes. Fuel: N Clad: N Reactor: N Burnup: N K(3): Data, Experience PK(1): Data, Judgement UK(0): No votes.

Table D-1. PWR and BWR LOCA. Category D– Separate Effect Testing (continued)

Subcategory (Test type)	Phenomena (Parameter)	Definition and Rationale (Importance, Applicability, and Uncertainty)
Oxidation rate, oxygen distribution, effect of chemistry on solubility (vote=15) Separate effect test to measure the steam oxidation kinetics at high temperature in Zirconium alloys used for cladding.	Conduct of Test-PTE Characteristic α–β morphology	Measurement of the thickness and morphology of the different metallurgical layers that formed during the LOCA transient. H(5) Key parameter to analyze the test. Alpha and beta layer thicknesses and the degree of alpha "incursion" are important oxidation parameters that influence the mechanical properties of the cladding. Relative amounts of alpha and beta determine the behavior of oxidized clad. Note: Posttest metallography is the primary and most reliable quantification, however the measurement is not necessarily just oxide thickness, also region of oxygen-stabilized alpha layer and remaining beta layer. M(0) No votes. L(0) No votes. Fuel: N Clad: N Reactor: N Burnup: N K(3): Data, Experience, Judgement PK(2): Data, Judgement UK(0): No votes.

Table D-1. PWR and BWR LOCA. Category D– Separate Effect Testing (continued)

Subcategory (Test type)	Phenomena (Parameter)	Definition and Rationale (Importance, Applicability, and Uncertainty)
Oxidation rate, oxygen distribution, effect of chemistry on solubility (vote=15) Separate effect test to measure the steam oxidation kinetics at high temperature in Zirconium alloys used for cladding.	Conduct of Test-PTE Oxygen distribution	Distribution of oxygen either dissolved or existing as an oxide phase in the cladding. H(5) Oxygen content in the beta phase is important for embrittlement. Key parameter that governs the behavior upon quench of the cladding. Posttest metallography is the primary and most reliable quantification, however the measurement is not necessarily just oxide thickness, also region of oxygen-stabilized alpha layer and remaining beta layer. Distribution of oxygen in prior beta layers is an important oxidation parameter that strongly influences the mechanical properties. M(0) No votes. L(0) No votes. Fuel: N Clad: N Reactor: N Burnup: N K(2): Data, Experience, Judgement PK(2): Data, Judgement UK(0): No votes.

Table D-1. PWR and BWR LOCA. Category D– Separate Effect Testing (continued)

Subcategory (Test type)	Phenomena (Parameter)	Definition and Rationale (Importance, Applicability, and Uncertainty)
Oxidation rate, oxygen distribution, effect of chemistry on solubility (vote=15) Separate effect test to measure the steam oxidation kinetics at high temperature in Zirconium alloys used for cladding.	Conduct of Test-PTE Hydrogen pickup and distribution	Amount and distribution of H absorbed by the cladding during the LOCA transient. H(4) Hydrogen pickup in the beta phase is important for brittleness. The amount of H usually picked-up is small. It can be locally very high in case of early failure of the cladding during the ballooning phase followed with steam ingress. Hydrogen content and distribution in the prior beta layer are important parameters that influence the mechanical properties of the cladding. M(2) Prior work by the Japanese and French have shown the pre- and post-test hydrogen content and distribution to be not so influential for practically achievable hydrogen levels, however, the amount of hydrogen absorbed during the test is an item of active interest and deserves characterization. L(0) No votes. Fuel: N Clad: N Reactor: N Burnup: Y(1): More important for high-burnup fuel K(3): Data, Judgement PK(2): Data, Judgement UK(0): No votes.

Table D-1. PWR and BWR LOCA. Category D– Separate Effect Testing (continued)

Subcategory (Test type)	Phenomena (Parameter)	Definition and Rationale (Importance, Applicability, and Uncertainty)
Quench tests, quench rate, Tquench, etc. (vote=14) Separate effect test to determine the thermal shock resistance of cladding when quenched after high temperature oxidation.	Specimen selection: Hydrogen content and distribution	Amount and distribution of hydrogen associated with fuel rod clad segment. This hydrogen may be in solution in the metal or may exist combined with the metal as a discrete hydride phase. H(3) Affects oxygen solubility in the beta phase and post-quench ductility. Hydride dissolves during oxidation at high temperatures and most hydrogen atoms are concentrated in the beta phase. Hydrogen content and distribution in the transformed beta phase are important parameters that influence clad resistance to thermal-shock failure. M(2) Data show low impact of H on clad behavior upon quench. Prior testing has demonstrated that quench behavior is not significantly affected by the amount of prior hydrogen (oxygen embrittlement is more important), distribution of prior hydrogen (homogenization occurs during the high temperature period), or hydrogen absorbed during the high temperature oxidation reaction (hydrogen absorption is minimal). However, this is an item of active interest and deserves a characterization. L(0) No votes. Fuel: N Clad: N Reactor: N Burnup: N K(2): Data PK(2): Data, Judgement UK(0): No votes.

Table D-1. PWR and BWR LOCA. Category D– Separate Effect Testing (continued)

Subcategory (Test type)	Phenomena (Parameter)	Definition and Rationale (Importance, Applicability, and Uncertainty)
Quench tests, quench rate, Tquench, etc. (vote=14) Separate effect test to determine the thermal shock resistance of cladding when quenched after high temperature oxidation.	Specimen selection: Alloy type	Composition or designation of the metal utilized in fuel-rod fabrication H(2) May affect oxygen distribution and hydrogen pickup. Stability of beta phase and mechanical properties of the load-bearing prior beta layer are significantly influenced by the addition of Nb, therefore, thermal-shock resistance of M5 and Zirlo is expected to differ from that of Zircaloy. M(2) In general, differences among the characterized zirconium based materials have shown differences in high-temperature oxidation and quench behavior to be relatively minor. However, specific details on the newer materials are not available to the reviewer and so bets are hedged. L(1) Data show no significant impact of the Alloy type on the behavior upon quench Fuel: Y(1): M5- or Zirlo-clad fuels Clad: N Reactor: Y(1): PWR Burnup: N K(1): Data PK(2): Data UK(1): Judgement

Table D-1. PWR and BWR LOCA. Category D– Separate Effect Testing (continued)

Subcategory (Test type)	Phenomena (Parameter)	Definition and Rationale (Importance, Applicability, and Uncertainty)
Quench tests, quench rate, Tquench, etc. (vote=14) Separate effect test to determine the thermal shock resistance of cladding when quenched after high temperature oxidation.	Specimen selection: Thickness and morphology of pre-existing oxide	The total amount of oxide formed on the cladding during in-reactor operation and whether the oxidation is uniform or nodular, and whether there is extensive cracking and spalling. H(3) These parameters influence the degree of transient oxidation and hydrogen uptake, the two properties that strongly influence clad resistance to thermal shock. It is important to use representative cladding even though data shows little effect. M(3) Oxidation characteristics are less important than associated hydrogen pickup. However, non-prototypical fabrication conditions may artificially enhance its impact. For example, oxide layers produced under a gaseous mixture of noble gas and steam is dense and protective while oxide layer produced under irradiation is defective and non-protective. Data show that pre-existing oxide has no significant impact on the clad resistance upon quench. Nevertheless the clad thinning associated to a thick pre-existing oxide layer affects slightly the stress field in the cladding and the overall clad behavior during the LOCA transient. In general, differences among the characterized zirconium based materials have shown differences in high-temperature oxidation and quench behavior to be relatively minor. However, specific details on the newer materials are not available to the reviewer and so bets are hedged. L(0) No votes. Fuel: N Clad: N Reactor: N Burnup: N K(3): Data PK(1): Data UK(1): No rationale provided

Table D-1. PWR and BWR LOCA. Category D– Separate Effect Testing (continued)

Subcategory (Test type)	Phenomena (Parameter)	Definition and Rationale (Importance, Applicability, and Uncertainty)
Quench tests, quench rate, Tquench, etc. (vote=14) Separate effect test to determine the thermal shock resistance of cladding when quenched after high temperature oxidation.	Specimen selection: Burnup	The amount of burnup and cladding fluence to which the fuel rod used for the specimen was exposed. H(2) High burnup alters several important properties of cladding and the nature of pellet-cladding interface which influence the resistance to thermal-shock failure. If the fuel rod is full of fuel, the fuel morphology will influence the quenching. Full rod fuel morphology (fragmentation, rim characteristics, bonding, etc.) is important). M(2) The clad temperature during a LOCA transient is large enough to anneal all irradiation defects. At the time of quench there is no irradiation damages left in the cladding. Prior testing by the French and Japanese have shown a relatively minor if any effect of pre-existing oxide thickness. However, high burnup specimens should be selected to address the question of unknown or previously otherwise uncharacterized effects. Independently of the other degradation variables (O, H, etc) burnup may not be important but it's good to preserve prototypicality. L(0) Fuel: Y(1): MOX (agglomerates) in case of full rod Clad: N Reactor: N Burnup: N K(2): Data PK(2): Data, Judgement: Much is known (Data), but this testing is intended to also address the unknown. UK(1): No rationale recorded.

Table D-1. PWR and BWR LOCA. Category D– Separate Effect Testing (continued)

Subcategory (Test type)	Phenomena (Parameter)	Definition and Rationale (Importance, Applicability, and Uncertainty)
Quench tests, quench rate, Tquench, etc. (vote=14) Separate effect test to determine the thermal shock resistance of cladding when quenched after high temperature oxidation.	Conduct of Test-During Axial constraints	Manner in which test specimen is constrained by fittings to simulate potential in-reactor axial constrains during the core reflood phase. H(6) Phebus 219 rod 18 shows that constraints can affect test outcome. Japanese test shows the restraint can affect brittleness results. M(0) No votes L(0) No votes Fuel: N Clad: N Reactor: N Burnup: N K(0): No votes PK(5): Data UK(1): Data (incomplete), judgement

Table D-1. PWR and BWR LOCA. Category D– Separate Effect Testing (continued)

Subcategory (Test type)	Phenomena (Parameter)	Definition and Rationale (Importance, Applicability, and Uncertainty)
Quench tests, quench rate, Tquench, etc. (vote=14) Separate effect test to determine the thermal shock resistance of cladding when quenched after high temperature oxidation.	Conduct of Test-During Azimuthal quenching	Simulation of azimuthal heat flux gradient during testing. H(1) This is the type of effect that should be tested using a limiting case so that it can be disposed of as a problem or investigated further. M(3) In rupture processes, any asymmetry in stress field enhances the rupture. Impact is expected to be of the second order. L(1) Azimuthally localized nonuniform partial quenching is less prototypic and should be avoided in the test. Fuel: N Clad: N Reactor: N Burnup: N K(0): No votes. PK(4): Data, Judgement UK(1): No rationale provided

Table D-1. PWR and BWR LOCA. Category D– Separate Effect Testing (continued)

Subcategory (Test type)	Phenomena (Parameter)	Definition and Rationale (Importance, Applicability, and Uncertainty)
Quench tests, quench rate, Tquench, etc. (vote=14) Separate effect test to determine the thermal shock resistance of cladding when quenched after high temperature oxidation.	Conduct of Test-During Empty/full	Conduct of test using specimens that have either had the fuel removed (empty) or retained the fuel (full). H(4) In the case of fuel relocated into the balloon, the clad is less susceptible to rewetting due to enhanced heat transfer to the cladding associated with the stored energy and the residual power of the fuel. The desire is to perform a separate effect test to understand the behavior of the cladding, as opposed to confusing interactions introduced by the presence of fuel pellets. The effect of the fuel pellets will be assessed during the integral testing. Intact fuel and the state of fuel-cladding gap or bonding influence important parameters such as clad ID oxidation, hydrogen uptake, and clad mechanical constraints. M(2) Data showing the importance of the presence of the fuel within the rod during the quenching are not available. Needs testing. L(0) No votes. Fuel: N Clad: N Reactor: N Burnup: Y(1): More important at high burnup. K(1): ANL and JAERI data, judgment PK(4): Data, Judgement: Some pellet effects have been hypothesized, but the point here is that this is to be a separate effects test – and so it should be a separate effects test (no pellets). UK(0): No votes.

Table D-1. PWR and BWR LOCA. Category D– Separate Effect Testing (continued)

Subcategory (Test type)	Phenomena (Parameter)	Definition and Rationale (Importance, Applicability, and Uncertainty)
Quench tests, quench rate, Tquench, etc. (vote=14) Separate effect test to determine the thermal shock resistance of cladding when quenched after high temperature oxidation.	Conduct of Test-During One-sided vs. two-sided	The quench is applied either on the external side of the cladding or on both sides. The latter simulates the case of a rod that burst during the blow down phase. H(2) The magnitudes of total oxidation, hydrogen pickup, temperature gradient during quench, and thermal stress are influenced significantly by this choice. Internal oxidation in the vicinity of the rupture provides significant hydride production, which affects the results. M(4) In a real quench process, at the balloon height, the cladding suffers both mechanisms, i.e., two-sided near the burst opening and one-sided at the opposite azimuth. Data show low impact on the result. The thought is that the primary parameter affecting quench behavior is the remaining beta phase, and not so much where that is (ID in one-sided test or mid-thickness on two-sided tests). However, there should be at least a few tests of the actual condition (two-sided) to confirm that a significant difference in performance does not occur. L(0) No votes. Fuel: N Clad: N Reactor: N Burnup: N K(1): Data PK(4): Data, Judgment UK(0): No votes.

Table D-1. PWR and BWR LOCA. Category D– Separate Effect Testing (continued)

Subcategory (Test type)	Phenomena (Parameter)	Definition and Rationale (Importance, Applicability, and Uncertainty)
Quench tests, quench rate, Tquench, etc. (vote=14) Separate effect test to determine the thermal shock resistance of cladding when quenched after high temperature oxidation.	Conduct of Test-During Cooldown before quench	The cladding needs to cool down naturally from the oxidation temperature to the quenching temperature. H(6) The important parameters are the relative values of the beta and alpha transition temperatures, which controls some mechanical properties, and the quench initiation temperature. The test should be as prototypical as possible to avoid undesirable artifacts. French testing has demonstrated a significant difference between a fast quench and a fast quench preceded by a slow cooldown phase that is more prototypical of the actual condition. Cooldown rate strongly influences O and H distributions and the microstructure and the mechanical properties of the prior beta layer. M(0) No votes. L(0) No votes. Fuel: N Clad: N Reactor: N Burnup: N K(4): Data PK(2): Data, Judgement UK(0): No votes.

Table D-1. PWR and BWR LOCA. Category D– Separate Effect Testing (continued)

Subcategory (Test type)	Phenomena (Parameter)	Definition and Rationale (Importance, Applicability, and Uncertainty)
Quench tests, quench rate, Tquench, etc. (vote=14) Separate effect test to determine the thermal shock resistance of cladding when quenched after high temperature oxidation.	Conduct of Test-During Clad temperature at time of the quench	Clad temperature at the time the quench occurs. It depends on the rod environment. It has an impact on the metallurgical morphology of the clad. H(5) Whether quench occurs before or after the completion of beta-to-alpha phase transformation is a major parameter that influences the magnitude of thermal stress and the properties of the prior-beta phase. M(1) Hobson's ring tests showed that even for the same level of oxidation, the mechanical properties were different for different high temperature levels. This difference may or may not affect the quench behavior, and may or may not be significant when all temperatures are below 2200 F, however, it suggests that a range of pre-quench temperatures be explored to confirm no unexpected differences in behavior exist. L(0) No votes. Fuel: N Clad: N Reactor: N Burnup: N K(3): Data, Judgement PK(4): Data, Judgement UK(0): No votes.

Table D-1. PWR and BWR LOCA. Category D– Separate Effect Testing (continued)

Subcategory (Test type)	Phenomena (Parameter)	Definition and Rationale (Importance, Applicability, and Uncertainty)
Quench tests, quench rate, Tquench, etc. (vote=14) Separate effect test to determine the thermal shock resistance of cladding when quenched after high temperature oxidation.	Conduct of Test-During Cycling of quenching	Repeated loading of the test segment via dryout followed by quenching. H(1) Several thermal shocks may result in a higher probability of failure. M(2) Before permanent reflood, a cladding may encounter several partial and temporary rewetting and dryout periods. This phenomenon may enhance the clad failure. low impact of the cycles are expected on the overall behavior of the cladding. Should be checked through a separate effect tests series (phase equilibria and transformation kinetics tests). L(3) The most severe thermal shock is produced at the first quenching. Not sure why this is being considered. It's not the expected case. Fuel: N Clad: N Reactor: N Burnup: N K(0): No votes. PK(2): Data, Judgement UK(3): No information on cyclic quenching, but also not convinced it will happen.

Table D-1. PWR and BWR LOCA. Category D– Separate Effect Testing (continued)

Subcategory (Test type)	Phenomena (Parameter)	Definition and Rationale (Importance, Applicability, and Uncertainty)
Quench tests, quench rate, Tquench, etc. (vote=14) Separate effect test to determine the thermal shock resistance of cladding when quenched after high temperature oxidation.	Conduct of Test-During Temperature history	Measurement of the time-varying temperature throughout oxidation and quenching. H(4) Temperature history is the primary factor that determines oxidation, hydrogen uptake, and the mechanical properties of the load-bearing prior beta layer. M(2) The key parameter is the clad temperature before quench. To measure the local clad temperature during the quench might be useful for the analysis but the measurement has not to be intrusive (risk of experimental artifacts). Knowledge of the actual temperature prior to the slow cool down phase, and during the slow cool down phase are important to know that we attained the desired pre-quench conditions. However, measurement during the quench is less critical (you get what you get and will likely not be able to measure it precisely). L(0) No votes. Fuel: N Clad: N Reactor: N Burnup: N K(3): Data, judgement PK(3): Data, Judgement UK(0): No votes.

Table D-1. PWR and BWR LOCA. Category D– Separate Effect Testing (continued)

Subcategory (Test type)	Phenomena (Parameter)	Definition and Rationale (Importance, Applicability, and Uncertainty)
Quench tests, quench rate, Tquench, etc. (vote=14) Separate effect test to determine the thermal shock resistance of cladding when quenched after high temperature oxidation.	Conduct of Test-During Pre-thinning of cladding	The specimen has experienced the ballooning phase of the LOCA transient before being quenched. H(4) The idea here was that the cladding tested should represent the as-thinned condition resulting from pre-transient oxidation, since the remaining metal thickness pre-test determines the remaining ductile ligament after high temperature oxidation (as opposed to using the a section of the fuel rod for the test that exhibits unusually low corrosion (like the bottom of the rod for PWRs). Since this pre-transient metal loss can be significant (perhaps 10%), this effect can significantly influence the quench test results by correspondingly reducing the remaining ductile region. Pre-thinning influences directly the thickness of the load-bearing prior-beat layer available for a given transient as well as the magnitude of thermal stress. M(2) The clad thinning of the ballooned area of the cladding can be taken into account through calculation (geometrical effect only). The residual stresses related to the clad straining are annealed during the high temperature oxidation phase. L(0) No votes. Fuel: N Clad: N Reactor: N Burnup: N K(1): Data PK(5): Data, Judgement UK(0): No votes.

Table D-1. PWR and BWR LOCA. Category D– Separate Effect Testing (continued)

Subcategory (Test type)	Phenomena (Parameter)	Definition and Rationale (Importance, Applicability, and Uncertainty)
Quench tests, quench rate, Tquench, etc. (vote=14) Separate effect test to determine the thermal shock resistance of cladding when quenched after high temperature oxidation.	Conduct of Test-During Quench mass flow rate	Delivery rate of water used to quench the rod. H(0) No vote. M(1) Important for the thermal-hydraulic conditions. L(3) Low impact is expected. It is expected that a significant variation in mass flow rate can be permitted and will result in effectively equivalent quench characteristics. Fuel: N Clad: N Reactor: N Burnup: N K(0): PK(4): Data, Calculation, Judgement UK(0):
Quench tests, quench rate, Tquench, etc. (vote=14) Separate effect test to determine the thermal shock resistance of cladding when quenched after high temperature oxidation.	Conduct of Test-PTE Equivalent cladding reacted (ECR) at location of failure	The percentage of Zr atoms that would have reacted with oxygen to form ZrO2 if all oxygen absorbed into the cladding were used to form ZrO2. H(7) Primary parameter used to understand, extend and evaluate results. M(0) L(0) Fuel: N Clad: N Reactor: N Burnup: N K(4): Data PK(2): Judgement based on data and calculations UK(0):

Table D-1. PWR and BWR LOCA. Category D– Separate Effect Testing (continued)

Subcategory (Test type)	Phenomena (Parameter)	Definition and Rationale (Importance, Applicability, and Uncertainty)
Quench tests, quench rate, Tquench, etc. (vote=14) Separate effect test to determine the thermal shock resistance of cladding when quenched after high temperature oxidation.	Conduct of Test-PTE Metallography	Metallographic examination to determine the morphology of the material, and which can be related to phase formation during quench. H(6) Metallography is the primary means to determine the degree of oxidation, phase structure, and the microstructure of the prior beta layer. M(0) No votes. L(0) No votes. Fuel: N Clad: N Reactor: N Burnup: N K(3): Data, Judgement PK(2): Data, Judgement UK(0): No votes.
Quench tests, quench rate, Tquench, etc. (vote=14) Separate effect test to determine the thermal shock resistance of cladding when quenched after high temperature oxidation.	Conduct of Test-PTE Fragment/non-fragment	Determine if the cladding embrittlement has led to cladding fragmentation H(6) Fragmentation of the cladding means risk of fuel dispersal and subsequent coolability concern. M(0) No votes. L(0) No votes. Fuel: N Clad: N Reactor: N Burnup: N K(2): Data, judgement PK(3): Data, Judgement UK(0): No votes.

Table D-1. PWR and BWR LOCA. Category D– Separate Effect Testing (continued)

Subcategory (Test type)	Phenomena (Parameter)	Definition and Rationale (Importance, Applicability, and Uncertainty)
Quench tests, quench rate, Tquench, etc. (vote=14) Separate effect test to determine the thermal shock resistance of cladding when quenched after high temperature oxidation.	Conduct of Test-PTE Characterization of tubing integrity	Perform leak test on the cladding to detect a potential crack. H(3) The determination of cladding failure is the primary objective of test. Agree with the medium definition but give it more weight. M(5) To establish the limit of failure upon quench the cladding integrity has to be defined and checked. L(0) No votes. Fuel: N Clad: N Reactor: N Burnup: N K(2): Data, Judgement PK3): Data, Judgement UK(0): No votes.

Table D-1. PWR and BWR LOCA. Category D– Separate Effect Testing (continued)

Subcategory (Test type)	Phenomena (Parameter)	Definition and Rationale (Importance, Applicability, and Uncertainty)
Phase equilibria and transformation kinetics-chemistry effects (vote=11) Measurement of phase equilibria and phase transformation kinetics that can provide fundamental data relevant to the cladding behavior during LOCA events.	Specimen selection: Hydrogen content and distribution	Amount of hydrogen in the sample and where it is located. H(4) Hydrogen affects the alpha, alpha plus beta, and beta boundaries. Data show that hydrogen content has an impact on phase transformation temperature and kinetics. Hydrogen is a strong beta stabilizer which influences phase equilibria, transformation kinetics, and the structure of prior beta layer. M(1) This type of information is useful in explaining, and possibly extrapolating the observations, but does not represent direct confirmation that criteria are met or not met. As such this whole category is rated at a lower level than some of the other more performance related characterizations. L(0) No votes. Fuel: N Clad: Y(1): More important for M5 and Zirlo. Reactor: N Burnup: Y(1): More important for high-burnup fuel. K(3): Data PK(2): Data, Judgement UK(0): No votes.

Table D-1. PWR and BWR LOCA. Category D– Separate Effect Testing (continued)

Subcategory (Test type)	Phenomena (Parameter)	Definition and Rationale (Importance, Applicability, and Uncertainty)
Phase equilibria and transformation kinetics-chemistry effects (vote=11) Measurement of phase equilibria and phase transformation kinetics that can provide fundamental data relevant to the cladding behavior during LOCA events.	Specimen selection: Alloy type	Composition or designation of the metal utilized in fuel-rod fabrication H(4) Alloying elements such as Sn and Nb affect the alpha, alpha plus beta, and beta boundaries. Nb-bearing M5 and Zirlo behave significantly different from zircaloy. Affects the phase equilibria and the transformation kinetics. M(1) This type of information is useful in explaining, and possibly extrapolating the observations, but does not represent direct confirmation that criteria are met or not met. As such this whole category is rated at a lower level than some of the other more performance related characterizations. L(0) No votes. Fuel: N Clad: N Reactor: Y(1): PWR Burnup: N K(2): Data PK(3): Data, Judgement UK(0): No votes.

Table D-1. PWR and BWR LOCA. Category D– Separate Effect Testing (continued)

Subcategory (Test type)	Phenomena (Parameter)	Definition and Rationale (Importance, Applicability, and Uncertainty)
Phase equilibria and transformation kinetics-chemistry effects (vote=11) Measurement of phase equilibria and phase transformation kinetics that can provide fundamental data relevant to the cladding behavior during LOCA events.	Specimen selection: Oxygen content	Amount of oxygen either dissolved or existing as an oxide phase in the cladding. H(3) Oxygen is a strong alpha stabilizer. Total amount of oxygen will affect phase equilibria. M(3) Data show low impact of initial oxide per se. Only Hydrogen related to the pre-transient oxide plays a role. L(0) No votes. Fuel: N Clad: N Reactor: N Burnup: N K(4): Data, Judgement PK(1): Data, Judgement UK(0): No votes.

Table D-1. PWR and BWR LOCA. Category D– Separate Effect Testing (continued)

Subcategory (Test type)	Phenomena (Parameter)	Definition and Rationale (Importance, Applicability, and Uncertainty)
Phase equilibria and transformation kinetics-chemistry effects (vote=11) Measurement of phase equilibria and phase transformation kinetics that can provide fundamental data relevant to the cladding behavior during LOCA events.	Specimen selection: Fluence	Fast neutron fluence experienced by the specimen H(0) No votes. M(2) At 62 GWd/t, the major factor is hydrogen pickup; however, the effect of fluence is less certain at higher burnups. L(3) Irradiation damages are quickly annealed during the transient. Second-phase precipitates are amorphized by irradiation, irradiation damages are annealed out rapidly at >550°C. Do not see how this will influence the result of the test. Fuel: N Clad: Y(1): Not well known for M5 and Zirlo. Reactor: N Burnup: N K(2): Data, judgement PK(3): Data, Judgement UK(0): No votes.

Table D-1. PWR and BWR LOCA. Category D– Separate Effect Testing (continued)

Subcategory (Test type)	Phenomena (Parameter)	Definition and Rationale (Importance, Applicability, and Uncertainty)
Phase equilibria and transformation kinetics-chemistry effects (vote=11) Measurement of phase equilibria and phase transformation kinetics that can provide fundamental data relevant to the cladding behavior during LOCA events.	Determination of hydrogen and oxygen solubilities in α and β phases as a function of hydrogen, oxygen, and temperature for relevant alloys	Establishes the relationship between oxygen and hydrogen potential and phase compositions. H(4) These parameters are necessary to allow relevant modeling and analysis. M(1) Seems to be redundant with establishing the phase diagram. Data directly influence assessment of the validity of the current LOCA embrittlement criteria for high-burnup operation and for new types of alloy. L(0) No votes. Fuel: N Clad: Y(1): More important for M5 and Zirlo Reactor: N Burnup: Y(1): More important at high burnup K(1): Data, judgement PK(4): Calculations, Data, Judgement UK(0): No votes.

Table D-1. PWR and BWR LOCA. Category D– Separate Effect Testing (continued)

Subcategory (Test type)	Phenomena (Parameter)	Definition and Rationale (Importance, Applicability, and Uncertainty)
Phase equilibria and transformation kinetics-chemistry effects (vote=11) Measurement of phase equilibria and phase transformation kinetics that can provide fundamental data relevant to the cladding behavior during LOCA events.	Determination of time constants for limiting mechanisms for phase transformation during heating as a function of hydrogen, heating rate and cooling rate	Phase transformations often require time to transform from one phase to the other, and kinetic transport mechanisms often control the reaction rates. H(3) Should be known for relevant calculation and analysis. Knowing these transport mechanisms may allow the determination of reaction kinetics. M(1) Seems to be redundant with establishing the phase diagram. L(1) Alpha-to-beta transformation kinetics during the heatup phase are very fast. Beta-to-alpha transformation during the cooldown phase is not limited by cooling rate; that is, depending on cooling rate, either diffusionless martensitic transformation or transformation via nucleation and growth are possible. However, transformation microstructure and the degree of O and H redistribution during the transformation are strongly influenced by the cooling rate. Fuel: N Clad: N Reactor: N Burnup: N K(2): Data, Judgement PK(3): Data, Judgement UK(0): No votes.

Table D-1. PWR and BWR LOCA. Category D– Separate Effect Testing (continued)

Subcategory (Test type)	Phenomena (Parameter)	Definition and Rationale (Importance, Applicability, and Uncertainty)
Phase equilibria and transformation kinetics-chemistry effects (vote=11) Measurement of phase equilibria and phase transformation kinetics that can provide fundamental data relevant to the cladding behavior during LOCA events.	Determination of diffusion coefficient of oxygen in individual phases	Need definition H(1) Drives the level of clad embrittlement. M(1) Seems to be redundant with establishing the phase diagram. L(1) A significant database is available for Zr and Zircaloy. Fuel: N Clad: N Reactor: N Burnup: N K(2): Data PK(1): Data, Judgement UK(0): No votes.
Phase equilibria and transformation kinetics-chemistry effects (vote=11) Measurement of phase equilibria and phase transformation kinetics that can provide fundamental data relevant to the cladding behavior during LOCA events.	Determination of the retained β and transformed β-phase morphology and oxygen plus hydrogen redistribution during β - α transformations (cooling), including Niobium-rich alloys	Defined by title. H(2) Rated higher simply because this is the bottom line; other items are needed to develop an analytical representation. These factors play direct and very important roles, which determine the clad resistance to thermal shock and the post-quench mechanical properties. M(0) No votes. L(0) No votes. Fuel: N Clad: N Reactor: N Burnup: N K(0): No votes. PK(2): Data, Judgement UK(0): No votes.

Table D-1. PWR and BWR LOCA. Category D– Separate Effect Testing (continued)

Subcategory (Test type)	Phenomena (Parameter)	Definition and Rationale (Importance, Applicability, and Uncertainty)
Mechanical Properties at high temperature, e.g., ≥ 300 C (vote=10) Creep and burst tests Designed to investigate creep and burst behavior of cladding at high temperature	Specimen selection: Pre-existing oxide	The total amount of oxide formed on the cladding during in-reactor operation and whether the oxidation is uniform or nodular, and whether there is extensive cracking and spalling. H(1) Directly influences burst and creep strengths. M(2) Data show that impact is limited to related Hydrogen content and clad thinning. L(1) The pre-existing oxide thickness determines the remaining metal thickness, which directly determines the creep and burst behavior. However, over the ranges of practical interest, the variations are not expected to be all that significant. Fuel: N Clad: N Reactor: N Burnup: N K(4): Data, Judgement PK(0): No votes. UK(0): No votes.

Table D-1. PWR and BWR LOCA. Category D– Separate Effect Testing (continued)

Subcategory (Test type)	Phenomena (Parameter)	Definition and Rationale (Importance, Applicability, and Uncertainty)
Mechanical Properties at high temperature, e.g., ≥ 300 C (vote=10) Creep and burst tests Designed to investigate creep and burst behavior of cladding at high temperature	Specimen selection: Alloy and initial thermomechanical treatment	Composition or designation of the metal utilized in fuel-rod fabrication and the thermomechanical treatment. H(5) Alloy type may affect the burst behavior. Beta favoring or alpha favoring may impact the mechanical behavior . Data are needed to do relevant analysis. Creep behavior is known to vary significantly with thermomechanical treatment and alloy type. M(1) Do not expect a big influence of cladding type at high temperature. L(0) No votes. Fuel: N Clad: Y(1): More important for M5 and Zirlo. Reactor: N Burnup: N K(2): Data PK(2): Data, Judgement UK(1): No rationale provided.

Table D-1. PWR and BWR LOCA. Category D– Separate Effect Testing (continued)

Subcategory (Test type)	Phenomena (Parameter)	Definition and Rationale (Importance, Applicability, and Uncertainty)
Mechanical Properties at high temperature, e.g., ≥ 300 C (vote=10) Creep and burst tests Designed to investigate creep and burst behavior of cladding at high temperature	Specimen selection: Hydrogen content	Total amount of pre-existing hydrogen in the material. H(2) Affects burst behavior (alpha to beta transformation). M(4) Data show some hydrogen impact on the mechanical properties at high temperatures. The French have reported an effect of cladding creep strength with hydrogen content. Hydrogen content influences phase stability and burst behavior. Creep failure at <550C during a LOCA is of less concern. Do not expect a large effect. L(0) No votes. Fuel: N Clad: Y(1): Important for M5 and Zirlo Reactor: N Burnup: N K(1): Data PK(4): Data, Judgement UK(0): No votes.

Table D-1. PWR and BWR LOCA. Category D– Separate Effect Testing (continued)

Subcategory (Test type)	Phenomena (Parameter)	Definition and Rationale (Importance, Applicability, and Uncertainty)
Mechanical Properties at high temperature, e.g., ≥ 300 C (vote=10) Creep and burst tests Designed to investigate creep and burst behavior of cladding at high temperature	Specimen selection: Fluence (radiation damage)	Level of radiation damage in cladding after in-reactor irradiation. H(1) Irradiation hardening is known to affect the cladding creep behavior. Alternate effects, such as precipitate dissolution, are not as well characterized. M(1) At 62 GWd/t, the major factor is hydrogen pickup; the importance of fluence at higher burnups is less certain. L(3) Irradiation damages are annealed at the test temperature. Irradiation damages are virtually annealed out rapidly at >600°C. Fuel: N Clad: N Reactor: N Burnup: N K(3): Data PK(2): Data, Judgement UK(0): No votes.

Table D-1. PWR and BWR LOCA. Category D– Separate Effect Testing (continued)

Subcategory (Test type)	Phenomena (Parameter)	Definition and Rationale (Importance, Applicability, and Uncertainty)
Mechanical Properties at high temperature, e.g., ≥ 300 C (vote=10) Creep and burst tests Designed to investigate creep and burst behavior of cladding at high temperature	Conduct of Test-During Strain profile as a f(r, θ, z, t)	Measurement of local strain variation with strain gages and similar equipment, such that the full strain distribution is known. H(4) These data are used to validate the thermomechanical models. In the interest of creep deformation, an accurate history of the deformation behavior during the test is essential to characterize differences in behavior. Relative to burst behavior, characterization of the resulting burst strain may be sufficient without detailing temporal characterization. Difficult to obtain this data, but useful and with high importance if we can get it. M(1) Data are needed to develop models. L(0) No votes. Fuel: N Clad: N Reactor: N Burnup: N K(3): Data, Judgement PK(1): Data, Judgement UK(0): No votes.

Table D-1. PWR and BWR LOCA. Category D– Separate Effect Testing (continued)

Subcategory (Test type)	Phenomena (Parameter)	Definition and Rationale (Importance, Applicability, and Uncertainty)
Mechanical Properties at high temperature, e.g., ≥ 300 C (vote=10) Creep and burst tests Designed to investigate creep and burst behavior of cladding at high temperature	Conduct of Test-During Pressure as f(t)	Internal pressure in the rod as a function of time. H(5) To allow proper interpretation of the test, the internal pressure versus time should be measured. The creep deformation history cannot be interpreted without a corresponding temporal characterization of the driving force (pressure). M(0) No votes. L(1) A pressure history is needed to develop models. Fuel: N Clad: N Reactor: N Burnup: N K(3): Data, Calculation PK(2): Data, Calculation, Judgement UK(0): No votes.

Table D-1. PWR and BWR LOCA. Category D– Separate Effect Testing (continued)

Subcategory (Test type)	Phenomena (Parameter)	Definition and Rationale (Importance, Applicability, and Uncertainty)
Mechanical Properties at high temperature, e.g., ≥ 300 C (vote=10) Creep and burst tests Designed to investigate creep and burst behavior of cladding at high temperature	Conduct of Test-During Temperature as f(t)	Measurement of the time-varying temperature. H(5) Impacts mechanical resistances of the specimen. Phase transformation and distribution and subsequent cladding mechanical properties depend on the clad temperature. To use the test results as a validation database for the calculation codes, the time-varying clad temperature should be measured. Creep is a very sensitive function of the cladding temperature and therefore the temperature must be known. Burst and creep behaviors are sensitive to clad maximum temperature. Obviously need to know temperature. M(0) No votes. L(0) No votes. Fuel: N Clad: N Reactor: N Burnup: N K(4): Data, Calculation PK(1): Data, Judgement UK(0): No votes.

Table D-1. PWR and BWR LOCA. Category D– Separate Effect Testing (continued)

Subcategory (Test type)	Phenomena (Parameter)	Definition and Rationale (Importance, Applicability, and Uncertainty)
Mechanical Properties at high temperature, e.g., ≥ 300 C (vote=10) Creep and burst tests Designed to investigate creep and burst behavior of cladding at high temperature	Conduct of Test-During Temperature profile as f(θ) and f(z)	Measurement of azimuthal and axial variations of temperature. H(4) Phase transformation and distribution, and subsequent cladding mechanical properties, depend on the clad temperature. To use the test results as a validation database for the calculation codes, the time-varying clad temperature should be measured. M(1) Burst strain is known to be sensitive to circumferential temperature differences. Measurement of the circumferential temperature distribution would be needed to best interpret the testing results. L(0) No votes. Fuel: N Clad: N Reactor: N Burnup: N K(3): Data, Calculation PK(2): Data, Judgement UK(0): No votes.

Table D-1. PWR and BWR LOCA. Category D– Separate Effect Testing (continued)

Subcategory (Test type)	Phenomena (Parameter)	Definition and Rationale (Importance, Applicability, and Uncertainty)
Mechanical Properties at high temperature, e.g., ≥ 300 C (vote=10) Creep and burst tests Designed to investigate creep and burst behavior of cladding at high temperature	Conduct of Test-During Open (actively pressurized) or closed	The test is conducted either with closed ends tube (constant number of moles) or with open ends (controlled pressure). H(5) It is crucial to represent the actual pressure evolution of a full-length rod. Knowledge and control of the internal pressure is essential to obtaining useful characterizations of creep and burst behavior which probably leads to open (actively pressurized) tubes. The pressure in a closed tube would vary with heatup and with cladding deformation. Affects test. M(0) No votes. L(1) Closed burst is a better simulation. Fuel: N Clad: N Reactor: N Burnup: N K(4): Data, Judgement PK(1): Data, Judgement UK(0): No votes.

Table D-1. PWR and BWR LOCA. Category D– Separate Effect Testing (continued)

Subcategory (Test type)	Phenomena (Parameter)	Definition and Rationale (Importance, Applicability, and Uncertainty)
Mechanical Properties at high temperature, e.g., ≥ 300 C (vote=10) Creep and burst tests Designed to investigate creep and burst behavior of cladding at high temperature	Conduct of Test-During Biaxiality ratio	The state of stress experienced by the cladding during testing. H(5) There is preliminary information on the impact of axial stress on the cladding rupture; additional experimental results are needed. Burst at <830°C (deformation controlled by prism slip in the highly anisotropic alpha phase) is sensitive to biaxial ratio. Influences failure limit. M(2) The most directly useful testing would simulate the actual cladding stress state. L(0) No votes. Fuel: N Clad: N Reactor: N Burnup: N K(2): Data PK(2): Data, Judgement UK(0): No votes.

Table D-1. PWR and BWR LOCA. Category D– Separate Effect Testing (continued)

Subcategory (Test type)	Phenomena (Parameter)	Definition and Rationale (Importance, Applicability, and Uncertainty)
Mechanical Properties at high temperature, e.g., ≥ 300 C (vote=10) Creep and burst tests Designed to investigate creep and burst behavior of cladding at high temperature	Conduct of Test-During Load and displacements, i.e., σ and ε behavior	Determination of the stress-strain response of the material using uniaxial testing. H(5) Objective of the test. The ability of the cladding material to withstand mechanical loadings is directly related to the basic mechanical properties; primarily ductility but also strength. Development of the material stress-strain curve provides information necessary to understand possible performance differences in the cladding capability with increasing exposure. Therefore, accurate measurement of these quantities is essential. Important for code development. M(0) No data. L(0) No data. Fuel: N Clad: N Reactor: N Burnup: N K(3): Data, Calculation, Judgement PK(2): Data, Judgement UK(0): No data.

Table D-1. PWR and BWR LOCA. Category D– Separate Effect Testing (continued)

Subcategory (Test type)	Phenomena (Parameter)	Definition and Rationale (Importance, Applicability, and Uncertainty)
Mechanical Properties at high temperature, e.g., ≥ 300 C (vote=10) Creep and burst tests Designed to investigate creep and burst behavior of cladding at high temperature	Conduct of Test-During Strain rate	The rate at which the strain is applied. H(2) Relevant parameter. Primary test parameter to be fixed and measured. M(1) Available testing has demonstrated that strain-rate effects exist. However, for the purpose of tensile property testing, the strain rate should be relatively quick (to best reflect true elastic-plastic behavior and avoid creep-induced inaccuracies), and within the practical range of achievable test strain rates relative to the target, spurious strain rate effects are not expected. L(0) No votes. Fuel: N Clad: N Reactor: N Burnup: N K(2): Data PK(1): Data, Judgement UK(0): No votes.

Table D-1. PWR and BWR LOCA. Category D– Separate Effect Testing (continued)

Subcategory (Test type)	Phenomena (Parameter)	Definition and Rationale (Importance, Applicability, and Uncertainty)
Mechanical Properties at high temperature, e.g., ≥ 300 C (vote=10) Creep and burst tests Designed to investigate creep and burst behavior of cladding at high temperature	Conduct of Test-During Circumferential (hoop)/axial (not ring)	Whether the uniaxial test should be done by a ring test or by an axial test. H(5) Relevant for non-isotropic materials. Primary test parameters to be measured. M(1) Appropriate test should be used L(0) No votes. Fuel: N Clad: N Reactor: N Burnup: N K(2): Data PK(1): Data, Judgement UK(0): No votes.
Mechanical Properties at high temperature, e.g., ≥ 300 C (vote=10) Creep and burst tests Designed to investigate creep and burst behavior of cladding at high temperature	Conduct of Test-PTE Post-test strain	Perform strain measurements at the failure locations. H(8) Relevant parameter. A key output of the burst characterization is the rupture strain, as input to flow blockage assessment. The most important test objective; needed to develop models. M(0) No votes L(1) Relevance of the data is low especially if the internal pressure evolution is not prototypical. Fuel: N Clad: N Reactor: N Burnup: N K(3): Data, Judgement PK(2): Data, Judgement UK(0): No votes.

Table D-1. PWR and BWR LOCA. Category D– Separate Effect Testing (continued)

Subcategory (Test type)	Phenomena (Parameter)	Definition and Rationale (Importance, Applicability, and Uncertainty)
Mechanical Properties at low temperature, e.g., ≤ 300 C (vote=10) Post oxidation and quench ductility test	Post oxidation and quench ductility tests, e.g., 1. Axial tensile 2. Ring tensile 3. Ring compression 4. Impact 5. Bending	To simulate a post LOCA seismic event two types of mechanical tests are suggested: four-point bending test (Note 1) and impact test to simulate the impact between the grid dimples and the rods (Note 2). H(4) The best testing to perform is four-point bend testing, supplemented by ring testing. Four-point bend testing addresses the post-LOCA performance limit of greatest interest, while ring testing provides supplementary insight into the fundamental mechanical properties as and aid in interpretation of the four-point bend testing results. The order of higher importance is--impact test followed by ring-compression test. M(1) Axial tensile test is a convenient test that can identify the most vulnerable spot along the cladding length, however, post-quench axial tensile loading is not expected to occur or to be insignificant in magnitude (Note 4). L(1) Ring-tensile stress in a burst cladding is either negligible or insignificant in post-quench phase. Fuel: N Clad: N Reactor: N Burnup: N K(1): Data, Judgement PK(3): Data, Judgement UK(0): No votes.

Table D-1. PWR and BWR LOCA. Category D– Separate Effect Testing (continued)

Subcategory (Test type)	Phenomena (Parameter)	Definition and Rationale (Importance, Applicability, and Uncertainty)

Notes:

1. The specimen should be a least 50-cm long (one span) and should contain its gap closed fuel pellet stack. The loading to be applied to the specimen should be limited to a given deflection (during a seismic event the maximum deflection for a 4-m fuel assembly is currently less than 25-mm).
2. The specimen should be 5 to 10 cm long and should include its fuel pellet stack. The loading is a pulse whose magnitude and width are respectively 165 N and 2-3 ms
3. In order to get immediately comparable data to those from which the criteria were deduced in 1973, perform the new test with a ring compression process. Ring tensile tests may be very severe (recent Halden results on dried-out rods). The relevance of the mechanical test is the key. The loading applied to the specimen should be prototypical. It is imperative that the right type of testing be performed to determine the most relevant characterization. These types of test are most applicable to post-quench modes of loading (due to various hydraulic, handling, and other mechanical forces) and deformation of the ballooned, burst, and oxidized cladding. Bending test is addressed in separate below (i.e., ability to withstand post-LOCA seismic events and aftershocks).
4. Test results should be interpreted very carefully, because according to previous studies in ANL and JAERI, the most vulnerable spot produced in burst cladding is strongly influenced by the selected heating method, the degree of temperature nonuniformity near the burst region, and oxidation and hydrogen uptake from the clad inner surface.

Table D-1. PWR and BWR LOCA. Category D– Separate Effect Testing (continued)

Subcategory (Test type)	Phenomena (Parameter)	Definition and Rationale (Importance, Applicability, and Uncertainty)
Seismic tests Test type: 4--point bending Separate effect test that addresses the ability of the fuel rod to withstand a post-LOCA seismic event without shattering	Specimen selection: Alloy type	Composition or designation of the metal utilized in fuel-rod fabrication H(4) May affect oxygen distribution and hydrogen pickup. Hydrogen pick-up fraction of the alloy during operation will be a primary parameter since very little hydrogen is absorbed during the LOCA transient. Very little, if any, of this type of testing has been performed to date and therefore a judgement of the relative importance of various parameters is difficult and necessarily speculative at this time. It is proposed for this category that all identified parameters be assigned High Importance but Unknown. The effects of O, H, hydrides, and the microstructure of prior beta layer are strongly influenced by alloy type. M(0) No votes. L(0) No votes. Fuel: N Clad: Y(1): More important for M5 and Zirlo Reactor: N Burnup: N K(1): Data PK(1): Data, Judgement UK(2): Lack of data

Table D-1. PWR and BWR LOCA. Category D– Separate Effect Testing (continued)

Subcategory (Test type)	Phenomena (Parameter)	Definition and Rationale (Importance, Applicability, and Uncertainty)
Seismic tests Test type: 4--point bending Separate effect test that addresses the ability of the fuel rod to withstand a post-LOCA seismic event without shattering	Specimen selection: Thickness and morphology of pre-existing and transient oxides	The total amount of oxide formed on the cladding and whether the oxidation is uniform or nodular, and whether there is extensive cracking and spalling. H(3) Oxide related clad thinning will slightly affect the mechanical behavior of the cladding. Very little, if any, of this type of testing has been performed to date and therefore a judgement of the relative importance of various parameters is difficult and necessarily speculative at this time. It is proposed for this category that all identified parameters be assigned High Importance but Unknown. These parameters strongly influence the thickness, O and H contents, and hydriding behavior of the load-bearing prior beta layer. M(1) Oxidation characteristics less important than hydrogen characteristics. L(0) No votes. Fuel: N Clad: N Reactor: N Burnup: N K(3): Data, Calculation PK(0): No votes. UK(1): Lack of data

Table D-1. PWR and BWR LOCA. Category D– Separate Effect Testing (continued)

Subcategory (Test type)	Phenomena (Parameter)	Definition and Rationale (Importance, Applicability, and Uncertainty)
Seismic tests Test type: 4--point bending Separate effect test that addresses the ability of the fuel rod to withstand a post-LOCA seismic event without shattering	Specimen selection: Burnup	The amount of burnup and cladding fluence to which the fuel rod used for the specimen was exposed. H(2) Very little, if any, of this type of testing has been performed to date and therefore a judgement of the relative importance of various parameters is difficult and necessarily speculative at this time. It is proposed for this category that all identified parameters be assigned High Importance but Unknown. Major factor that influences the material structure and properties. M(1) At 62 GWd/t, the major factor is hydrogen pickup; however, the importance of fluence at higher burnups is unclear. L(1) The irradiation damages have been annealed during the LOCA transient and will not affect the post-LOCA mechanical behavior of the cladding. Fuel: N Clad: N Reactor: N Burnup: N K(2): Data, Judgement PK(1): Data, Judgement UK(1): Lack of data

Table D-1. PWR and BWR LOCA. Category D– Separate Effect Testing (continued)

Subcategory (Test type)	Phenomena (Parameter)	Definition and Rationale (Importance, Applicability, and Uncertainty)
Seismic tests Test type: 4--point bending Separate effect test that addresses the ability of the fuel rod to withstand a post-LOCA seismic event without shattering	Specimen selection: Pre-existing and transient hydrogen content and distribution	Amount and distribution of pre-existing hydrogen associated with fuel rod clad segment. This hydrogen may be in solution in the metal or may exist combined with the metal as a discrete hydride phase. H(4) Affects oxygen solubility in the beta phase and post-quench ductility in the absence of burst. Since the cladding during the LOCA absorbs little Hydrogen, the initial Hydrogen content will play a key role during the post-LOCA mechanical tests. The initial Hydrogen distribution has no importance. Very little, if any, of this type of testing has been performed to date and therefore a judgement of the relative importance of various parameters is difficult and necessarily speculative at this time. It is proposed for this category that all identified parameters be assigned High Importance but Unknown. Post-quench hydride distribution is the major factor that influences the mechanical properties, especially at <200°C. M(0) No votes. L(0) No votes. Fuel: N Clad: N Reactor: N Burnup: N K(2): Data, Judgement PK(1): Data, Judgement UK(1): Lack of data

Table D-1. PWR and BWR LOCA. Category D– Separate Effect Testing (continued)

Subcategory (Test type)	Phenomena (Parameter)	Definition and Rationale (Importance, Applicability, and Uncertainty)
Seismic tests Test type: 4--point bending Separate effect test that addresses the ability of the fuel rod to withstand a post-LOCA seismic event without shattering	Specimen selection: With or without ballooning	Determining whether the four-point bending test should be performed on a fuel rod section that includes a ballooned region. H(4) The clad geometry change (clad thinning and diameter increase) will affect the mechanical behavior of the rod. The unanswered question is whether the seismic loads will cause unacceptable failure elsewhere. Ballooning and burst influence strongly clad ID-side oxidation, hydrogen uptake, and hydriding, producing weak spots near the burst opening. M(0) No votes. L(0) No votes. Fuel: N Clad: N Reactor: N Burnup: N K(1): Data, Judgement PK(2): Data, Judgement UK(0): No votes.

Table D-1. PWR and BWR LOCA. Category D– Separate Effect Testing (continued)

Subcategory (Test type)	Phenomena (Parameter)	Definition and Rationale (Importance, Applicability, and Uncertainty)
Seismic tests Test type: 4--point bending Separate effect test that addresses the ability of the fuel rod to withstand a post-LOCA seismic event without shattering	Conduct of Test-During Temperature	The temperature at which the test is conducted. H(3) Ductility may vary a lot with temperature. Variations in performance with test temperature have been demonstrated by Hobson's ring tests. The more critical issue is to define the relevant temperature range, and then maintenance of that temperature during the test should be achievable and enforced. With the extent of embrittlement anticipated in the test sample, the maintenance of the intended temperature range is critical for obtaining meaningful test results. Bending temperature (<200°C) is a major factor that influences test results. M(0) No votes. L(1) The post LOCA tests are isothermal. Fuel: N Clad: N Reactor: N Burnup: N K(0): No votes. PK(4): Data, Experience, Judgement UK(0): No votes.

Table D-1. PWR and BWR LOCA. Category D– Separate Effect Testing (continued)

Subcategory (Test type)	Phenomena (Parameter)	Definition and Rationale (Importance, Applicability, and Uncertainty)
Seismic tests Test type: 4--point bending Separate effect test that addresses the ability of the fuel rod to withstand a post-LOCA seismic event without shattering	Conduct of Test-During Strain rate (displacement ratio)	Measurement of the strain versus time H(3) Relevant parameter. The objective of the test is to measure the response of the rod to an imposed deflection. Strain rate effects can be expected; prototypical strain rates are needed to ensure meaningful test results M(1) No rationale provided (ANL) L(0) No votes. Fuel: N Clad: N Reactor: N Burnup: N K(0): Data PK(3): Data, Judgement UK(0): No votes.

Table D-1. PWR and BWR LOCA. Category D– Separate Effect Testing (continued)

Subcategory (Test type)	Phenomena (Parameter)	Definition and Rationale (Importance, Applicability, and Uncertainty)
Seismic tests Test type: 4--point bending Separate effect test that addresses the ability of the fuel rod to withstand a post-LOCA seismic event without shattering	Conduct of Test-During ASTM specification	The shape of the contact points and the way to apply the loading should follow the ASTM specification to avoid undesirable experimental artifact (local stress concentration) H(2) Relevant specification to avoid non-prototypical loading of the rod. M(1) It may be difficult to apply it for ballooned, burst, and nonuniformly oxidized and hydrided cladding. L(0) No votes. Fuel: N Clad: N Reactor: N Burnup: N K(1): Data PK(3): Data, Calculation, Judgement UK(0): No votes.

Table D-1. PWR and BWR LOCA. Category D– Separate Effect Testing (continued)

Subcategory (Test type)	Phenomena (Parameter)	Definition and Rationale (Importance, Applicability, and Uncertainty)
Seismic tests Test type: 4--point bending Separate effect test that addresses the ability of the fuel rod to withstand a post-LOCA seismic event without shattering	Conduct of Test-During Appropriate bending moment	During a seismic event the fuel assembly is submitted to a prototypical bending moment . H(4) The tests have to be prototypical. The loading to be applied to the specimen should be limited to a given deflection (during a seismic event the maximum deflection for a 4-m fuel assembly is currently less than 25-mm). The application of an appropriate bending moment is essential to obtaining meaningful results. However, it is also anticipated that once the prototypical bending moment is demonstrated to be successful, the bending moment will be increased to determine margin to the critical bending moment for failure and whether the consequences of failure are truly unacceptable from the consideration for maintenance of coolable geometry. M(0) No votes. L(0) No votes. Fuel: N Clad: N Reactor: N Burnup: N K(1): Data, Judgement PK(3): Data, Calculation, Judgement UK(0): No votes.

Table D-1. PWR and BWR LOCA. Category D– Separate Effect Testing (continued)

Subcategory (Test type)	Phenomena (Parameter)	Definition and Rationale (Importance, Applicability, and Uncertainty)
Seismic tests Test type: 4--point bending Separate effect test that addresses the ability of the fuel rod to withstand a post-LOCA seismic event without shattering	Conduct of Test-During Cycling	Apply a cyclic loading on the rod to simulate the seismic event. H(3) Cycling induces metal fatigue. By the very nature of the post-LOCA seismic event, cycling can be anticipated, although at a relatively low frequency. It is well-known from fatigue studies that the allowable strain amplitude decreases with increasing number of cycles; the quantification of this reduction would be needed if it appears that the expected loading approaches the level for unacceptable consequences with a single cycle. However, if considerable margin to fracture/unacceptable consequences exists then multiple cycle testing may not be necessary. M(0) No votes. L(1) The magnitude of the seismic load is low enough to avoid plastic deformation of the clad and the number of cycles is not large enough to create fatigue damage. No cumulative damage is expected. Fuel: N Clad: N Reactor: N Burnup: N K(1): Data, Judgement PK(3): Data, Judgement UK(0): No votes.

Table D-1. PWR and BWR LOCA. Category D– Separate Effect Testing (continued)

Subcategory (Test type)	Phenomena (Parameter)	Definition and Rationale (Importance, Applicability, and Uncertainty)
Seismic tests Test type: 4--point bending Separate effect test that addresses the ability of the fuel rod to withstand a post-LOCA seismic event without shattering	Conduct of Test-PTE Characterize integrity	Define the level of fragmentation of the cladding after the post-LOCA mechanical test. H(4) The objective of the test is to define the LOCA limits (%ECR and max clad temperature) that provoke clad fragmentation and potential subsequent core coolability concern by allowing extended fuel dispersal. These limits are beyond those leading to a simple loss of clad integrity. Characterization of post-test geometry is critical to the determination of whether an acceptable geometry has been maintained (when demonstrating the prototypical bending load case), or whether a truly unacceptable condition is developed with fracture (when the test is extended to intentionally develop fracture). M(0) L(0) Fuel: N Clad: N Reactor: N Burnup: N K(1): Data, Judgement PK(1): Data, Judgement UK(2): Lack of data

Table D-1. PWR and BWR LOCA. Category D– Separate Effect Testing (continued)

Subcategory (Test type)	Phenomena (Parameter)	Definition and Rationale (Importance, Applicability, and Uncertainty)
Seismic tests Test type: 4--point bending Separate effect test that addresses the ability of the fuel rod to withstand a post-LOCA seismic event without shattering	Conduct of Test-PTE Characterize local hydrogen	Amount and distribution of hydrogen associated with fuel rod clad segment. This hydrogen may be in solution in the metal or may exist combined with the metal as a discrete hydride phase. H(4) Primary parameter that could impair the clad resistance. Only the initial amount is important. The Hydrogen distribution has no impact since it becomes uniform during the LOCA transient. A characterization of the hydrogen and oxygen distribution would aid in the interpretation of the test results. The fracture characteristics and susceptibility are expected to be directly related to these embrittling agents. Hydride morphology, orientation, number density, and distribution influence test result significantly. M(0) No votes. L(0) No votes. Fuel: N Clad: N Reactor: N Burnup: Y(1): More important at high burnup K(1): Data PK(2): Data, Judgement UK(0): No votes.

Table D-1. PWR and BWR LOCA. Category D– Separate Effect Testing (continued)

Subcategory (Test type)	Phenomena (Parameter)	Definition and Rationale (Importance, Applicability, and Uncertainty)
Simulation of fuel relocation	Specimen selection: Burnup	The amount of burnup to which the fuel rod used for the specimen was exposed. H(4) Fuel morphology (fragmentation, rim characteristics, bonding, etc.) is important. The nature of the bonding between the pellet and the cladding changes with the burnup increase. It will affect the potential for fuel relocation. The segment burnup level can determine the extent of pellet-cladding bonding and corresponding susceptibility to fuel relocation during ballooning and rupture. Fuel and rim-zone microstructure and the state of bonding with cladding are strongly influenced by fuel burnup. M(0) No votes. L(0) No votes. Fuel: Y(1): MOX agglomerates Clad: N Reactor: N Burnup: N K(1): Data PK(3): Data, Judgement UK(0): No votes.

Table D-1. PWR and BWR LOCA. Category D– Separate Effect Testing (continued)

Subcategory (Test type)	Phenomena (Parameter)	Definition and Rationale (Importance, Applicability, and Uncertainty)
Simulation of fuel relocation	Specimen selection: Fuel type (MOX)	Composition of the fuel, i.e., a specified MOX composition. H(2) May affect the amount of fine grain material after relocation. Fuel structure and mechanical properties are influenced by fuel type. M(1) The consequence of fuel fragments relocation (higher local decay heat and higher cladding temperature) could be more effective with MOX fuel than with UO2 fuel. Nevertheless the viscoplastic properties of the MOX should impair the fuel fragments relocation at high burnup. L(1) No significant differences in pellet-cladding bonding behavior or pellet cracking behavior are anticipated or have been observed with MOX fuel, and therefore no significant differences in relocation behavior are anticipated. Fuel: N Clad: N Reactor: N Burnup: N K(1): Data PK(2): Data, Judgement UK(1): Judgement

Table D-1. PWR and BWR LOCA. Category D– Separate Effect Testing (continued)

Subcategory (Test type)	Phenomena (Parameter)	Definition and Rationale (Importance, Applicability, and Uncertainty)
Simulation of fuel relocation	Specimen selection: Alloy type	Composition or designation of the metal utilized in fuel-rod fabrication H(2) May affect burst (beta favoring or alpha favoring additions). Ductile burst and brittle failure by thermal shock and post-quench forces are influenced strongly by cladding alloy type. M(1) In general, compositional differences have not been observed to significantly affect cladding burst behavior. However, if significant differences in burst behavior occurred, the relocation characteristics could be similarly significantly altered. L(1) Data show no significant impact of alloy type on the balloon size that could influence the fuel fragments relocation. Fuel: N Clad: N Reactor: N Burnup: N K(2): Data PK(1): Data, Judgement UK(1): Judgement

Table D-1. PWR and BWR LOCA. Category D– Separate Effect Testing (continued)

Subcategory (Test type)	Phenomena (Parameter)	Definition and Rationale (Importance, Applicability, and Uncertainty)
Simulation of fuel relocation	Specimen selection: Chemical and mechanical bonding	Chemical and mechanical bonding between the fuel pellet and the cladding prior to the test. H(4) Fuel morphology (bonding) is important. It will affect the potential for fuel fragmentation relocation. It is speculated that bonding could significantly affect the relocation characteristics by impeding pellet fragment movement. However, this effect has not been demonstrated. Major factor that influences fuel slumping and potential release of fuel particles upon burst and subsequent fragmentation. M(0) No votes. L(0) No votes. Fuel: N Clad: N Reactor: N Burnup: N K(0): No votes. PK(3): Data, Judgement UK(1): Lack of data

Table D-1. PWR and BWR LOCA. Category D– Separate Effect Testing (continued)

Subcategory (Test type)	Phenomena (Parameter)	Definition and Rationale (Importance, Applicability, and Uncertainty)
Simulation of fuel relocation	Specimen selection: Cracking	Crack pattern and crack density of the fuel pellets prior to the test. H(2) Controls the rubble bed characteristics after relocation. Degree of fuel cracking directly influences the potential for fuel relocation and release. M(0) No votes. L(2) Beyond a given burnup the number of cracks is stable. In general the macroscopic fuel pellet cracking pattern develops early in life and does not change significantly with elevated exposures. Therefore, this contribution to fuel relocation susceptibility is not expected to be a dominant parameter during this test series. Fuel: N Clad: N Reactor: N Burnup: N K(1): Data PK(3): Data, Judgement UK(0): No votes.

Table D-1. PWR and BWR LOCA. Category D– Separate Effect Testing (continued)

Subcategory (Test type)	Phenomena (Parameter)	Definition and Rationale (Importance, Applicability, and Uncertainty)
Simulation of fuel relocation	Conduct of Test-During With or without blowdown	Determination of whether blowdown processes must be simulated in the test. H(0) No votes. M(1) During the blowdown phase of the LOCA transient, fuel stored energy is redistributed in the pellet and the clad. This redistribution produces a decrease of the pellet centerline temperature and increases the pellet rim and clad temperatures. Due to these temperature transients, the central part of the pellet will suffer a contraction while the rim and the clad will experience an expansion. These adverse effects could induce fuel mechanical stresses and fragmentation. The expansion and contraction inside the fuel pellet may affect bonding and fuel debris sizes. L(2) Vibration loads occurring during the blowdown phase may cause additional pellet fragment movement. In general, pellet fragments are relatively constrained within the fuel rod by the column geometry, as evidenced by characterization of fuel column geometry in hot cells. Therefore, this effect is not considered to significantly contribute to relocation susceptibility later during the cladding heatup and rupture phases. Fuel thermal contraction and cladding heatup during the blowdown phase increases the pellet-cladding gap and possibly facilitates pellet fragment relocation. Cladding heatup rate and temperature, either with or without a blowdown, are the primary factors that influence burst shape and dimensional changes. Fuel: N Clad: N Reactor: N Burnup: N K(0): No votes. PK(1): Data, Experience, Judgement UK(2): Judgement

Table D-1. PWR and BWR LOCA. Category D– Separate Effect Testing (continued)

Subcategory (Test type)	Phenomena (Parameter)	Definition and Rationale (Importance, Applicability, and Uncertainty)
Simulation of fuel relocation	Conduct of Test-During Blowdown temperature transients for fuel and cladding	Simulation of the temperature response of the fuel and cladding during the blowdown phase of a large-break LOCA. H(2) Important parameters that influence cladding burst and dimensional changes. M(0) No votes. L(1) Pellet fragment movement. In general, pellet fragments are relatively constrained within the fuel rod by the column geometry, as evidenced by characterization of fuel column geometry in hot cells. Therefore, this effect is not considered to significantly contribute to relocation susceptibility later during the cladding heatup and rupture phases. Fuel thermal contraction and cladding heatup during the blowdown phase increases the pellet-cladding gap and possibly facilitates pellet fragment relocation. Cladding heatup rate and temperature, either with or without a blowdown, are the primary factors that influence burst shape and dimensional changes. Fuel: N Clad: N Reactor: N Burnup: N K(1): Data, Judgement PK(2): Data, Experience, Judgement UK(0): No votes.

Table D-1. PWR and BWR LOCA. Category D– Separate Effect Testing (continued)

Subcategory (Test type)	Phenomena (Parameter)	Definition and Rationale (Importance, Applicability, and Uncertainty)
Simulation of fuel relocation	Conduct of Test-During Pre- and post-burst test phases (2)	Look at the impact of fuel fragment relocation on the cladding temperature during the high temperature oxidation phase and the quenching phase. H(1) Data of fuel relocation determines the impacted phases. M(3) Needs in pile test to be prototypical (heating source should come from the fuel). If the objective is as speculated above, this test would help to characterize at which point in time the bulk of the relocation occurs. However, most rods that balloon also burst and it is not clear that a separation in time would significantly affect the LOCA performance (i.e., whether relocation occurs instantaneously to fill the ballooned region as opposed to instantaneous relocation on burst). Burst shape and dimensional changes are influenced by clad phase at the time of ballooning and burst. L(0) No votes. Fuel: N Clad: N Reactor: N Burnup: N K(1): Data, Judgement PK(3): Data, Calculation, Judgement UK(0): No votes.

Table D-1. PWR and BWR LOCA. Category D– Separate Effect Testing (continued)

Subcategory (Test type)	Phenomena (Parameter)	Definition and Rationale (Importance, Applicability, and Uncertainty)
Simulation of fuel relocation	Conduct of Test-During Internal pressure and moles of gas	The amount of gas in the rod upper plenum, for a given initial pressure in the test rod. H(3) Driving force for relocation, together with gravity. It is crucial to have a pressure evolution representative of a full-length rod. Internal gas pressure is the driving force for fuel fragments relocation. To be prototypical the amount of gas within the rod prior to the test has to be maintained constant. The internal pressure is a measured parameter, not an input data. Initial pressure is the primary factor that determines the burst temperature and shape and potential release of fuel particles from rim zone at burst. Plenum gas inventory is a secondary factor. M(1) If gas flow is the primary relocation mechanism, then an accurate simulation of that gas flow would be needed to obtain the most meaningful results. However, it is anticipated that similar relocation behavior would be obtained over a relatively wide range of gas flows. L(0) No votes. Fuel: N Clad: N Reactor: N Burnup: N K(0): No votes. PK(4): Data, Calculations, Judgement UK(0): No votes.

Table D-1. PWR and BWR LOCA. Category D– Separate Effect Testing (continued)

Subcategory (Test type)	Phenomena (Parameter)	Definition and Rationale (Importance, Applicability, and Uncertainty)
Simulation of fuel relocation	Conduct of Test-During Flow induced vibration	During ballooning and after burst, the fuel rod vibration induced by the flow can favour crumbling of the fuel pellet stack. H(0) No votes. M(2) Fuel column axial gaps have been observed to form and continue during normal reactor operation. This results suggests that fuel column shakeout is not likely with normal flow-induced vibration even over very extended periods. It is further noted that with cladding perforation, steam ingress will promote fuel pellet oxidation that has been observed, with failed fuel during normal reactor operation, to cause effective blockage within the fuel rod to preclude fuel downward fuel pellet fragment motion, again overriding the effects of flow induced vibration. Secondary driving force. L(2) Potential impact of rod vibration is expected to be small. Ballooning and burst occur after blowdown, and steam-flow-induced vibration during and after blowdown would be insignificant. Fuel: N Clad: N Reactor: N Burnup: N K(0): No votes. PK(2): Data, Judgement UK(1): Judgement

Table D-1. PWR and BWR LOCA. Category D– Separate Effect Testing (continued)

Subcategory (Test type)	Phenomena (Parameter)	Definition and Rationale (Importance, Applicability, and Uncertainty)
Simulation of fuel relocation	Conduct of Test-During Exterior rod constraints	Manner in which test specimen is constrained by surrounding rods to simulate potential in-reactor behavior. H(1) Prior ballooning experiments have shown that coplanar ballooning is not likely, and therefore balloons may not be constrained by adjacent ballooned sections. However, the constraints provided by adjacent non-ballooned rods can still provide a significant restriction on the amount of cladding ballooning and corresponding fuel relocation. M(1) Rod constraints during ballooning may affect the fuel distribution at the relocation site. L(2) The purpose of these tests is to analyze the separate effect of fuel fragment relocation. Exterior constraints influence ballooning shape to some extent. Fuel: Y(1): Most modern BWR fuel designs use part-length fuel rods resulting in zones where there is a significant gap between adjacent rods (because rods in certain lattice locations terminate at a lower elevation). This design feature may permit greater ballooning and relocation at those elevations. However, the fuel rods at those peculiar locations would correspondingly experience a circumferential temperature gradient, which is known to reduce the resulting burst strain. Clad: N Reactor: N Burnup: N K(0): No votes. PK(4): Data, Judgement UK(0): No votes.

Table D-1. PWR and BWR LOCA. Category D– Separate Effect Testing (continued)

Subcategory (Test type)	Phenomena (Parameter)	Definition and Rationale (Importance, Applicability, and Uncertainty)
Simulation of fuel relocation	Conduct of Test-During Balloon size and burst size	Determination of the dimensions of the ballooned area and the cladding breach during the test. H(4) Affects the amount of relocated fuel in the balloon. The balloon and burst size represents the maximum potential volume for relocation. Directly influence the potential for fuel relocation, slumping, and release at and after burst. M(0) No votes. L(1) Balloon size and burst size are measured after the test. No need to measure it on-line Fuel: N Clad: N Reactor: N Burnup: N K(1): Judgement PK(2): Data, Judgement UK(0): No votes.

Table D-1. PWR and BWR LOCA. Category D– Separate Effect Testing (continued)

Subcategory (Test type)	Phenomena (Parameter)	Definition and Rationale (Importance, Applicability, and Uncertainty)
Simulation of fuel relocation	Conduct of Test-During Length	Longitudinal dimension of the fuel rod segment to be tested. H(2) The driving force for fuel fragments relocation is the internal gas pressure in the plenum. For high burnup fuel rods the axial gas transport is significantly impaired. A short rod would favor the plenum gas participation The rod length has to be prototypical to avoid experimental bias. At the least, the length between two grids must be tested. M(1) The amount of fuel above the ballooned/burst section defines the potential fuel volume to be relocated. However, the size of the ballooned/burst region defines the maximum possible relocated fuel volume. Therefore, if the ballooned/burst location can be defined with reasonable certainty, sufficient length can be provided above that region to enable prototypic relocation. L(1) Length more than about 15 times of the pellet length (6 inches) is sufficient. Fuel: N Clad: N Reactor: N Burnup: N K(1): Calculation PK(3): Data, Judgement UK(0): No votes.

Table D-1. PWR and BWR LOCA. Category D– Separate Effect Testing (continued)

Subcategory (Test type)	Phenomena (Parameter)	Definition and Rationale (Importance, Applicability, and Uncertainty)
Simulation of fuel relocation	Conduct of Test-PTE Granularity of dispersed material	Granularity of dispersed fuel fragments is measured to get relevant information on the fuel density in the relocated fuel fragments zone. H(3) The equivalent fuel density of the relocated fragments allows codes to simulate the local overheating of the cladding. Major factor that influences the potential for fuel relocation and release. M(1) Smaller pellet fragments would be expected to result in easier fuel movement and possibly a higher density of relocated fuel. However, pellet cracking patterns are established early in life and do not vary greatly with increased exposure, so a widely varied granularity of material, prior to dispersal, is not expected. L(0) No votes. Fuel: N Clad: N Reactor: N Burnup: N K(0): No votes. PK(4): Data, Judgement UK(0): No votes.

Table D-1. PWR and BWR LOCA. Category D– Separate Effect Testing (continued)

Subcategory (Test type)	Phenomena (Parameter)	Definition and Rationale (Importance, Applicability, and Uncertainty)
Simulation of fuel relocation	Conduct of Test-PTE Thermography	Non-intrusive measurement of the temperature differences of the tested fuel rod. H(1) Provides the fuel distribution in 3D. M(0) No votes. L(2) Low added value Fuel: N Clad: N Reactor: N Burnup: N K(0): Data PK(2): Data, Judgement UK(1): Judgement

Table D-1. PWR and BWR LOCA. Category D– Separate Effect Testing (continued)

Subcategory (Test type)	Phenomena (Parameter)	Definition and Rationale (Importance, Applicability, and Uncertainty)
Simulation of fuel relocation	Conduct of Test-PTE Thermal diffusivity of rubble bed	Self defined. H(1) Output parameter. M(1) Probably difficult to do, but would be useful in quantifying the effective thermal properties of the rubble mass (This assumes that in the ballooned/burst region if the material is still there – it may be worthwhile to capture this just prior to burst although there may not be significant relocation at that time if gas flow is the primary relocation mechanism), otherwise this is best done analytically. L(1) No rationale provided. Fuel: N Clad: N Reactor: N Burnup: N K(0): No votes. PK(2): Data, Judgement UK(1): Judgement

Table D-1. PWR and BWR LOCA. Category D– Separate Effect Testing (continued)

Subcategory (Test type)	Phenomena (Parameter)	Definition and Rationale (Importance, Applicability, and Uncertainty)
Simulation of fuel relocation	Conduct of Test-PTE Strain profile of cladding as f(θ,z)	Measure the shape and the size of the ballooned area of the tested fuel rod. H(3) The purpose of this test is to assess the amount and characteristics of relocation. A determining aspect of that process is the amount of ballooning (free volume to which the fuel may relocate), and therefore this volume should be known in any assessment of relocation characteristics. Note that the circumferential variation of cladding strain should also be determined. Axial variation of clad circumferential strain is a parameter that directly influences the potential for fuel relocation and slumping. M(1) Will give some indications on potential impact of the balloon the shape (magnitude and extension) on the amount of relocated fuel. L(0) No votes. Fuel: N Clad: N Reactor: N Burnup: N K(1): Judgement, Calculation PK(3): Data, Judgement UK(0): No votes.

Table D-1. PWR and BWR LOCA. Category D– Separate Effect Testing (continued)

Subcategory (Test type)	Phenomena (Parameter)	Definition and Rationale (Importance, Applicability, and Uncertainty)
Simulation of fuel relocation	Conduct of Test-PTE Burst size	Size of the opening in the cladding after the burst. H(3) This is taken to be the effective surface area of the bulged region that was removed as a result of the burst. Similar to the preceding item, the hole size will be a determining factor in the amount of relocated fuel retained within the ballooned region. Burst opening size and burst circumferential strain are parameters that directly influence the potential for fuel relocation and release at and after burst. M(0) No votes. L(1) If the internal pressure is not maintained (prototypal case) the opening is small. Fuel: N Clad: N Reactor: N Burnup: N K(2): Data PK(2): Data, Judgement UK(0): No votes.

Table D-1. PWR and BWR LOCA. Category D– Separate Effect Testing (continued)

Subcategory (Test type)	Phenomena (Parameter)	Definition and Rationale (Importance, Applicability, and Uncertainty)
Simulation of fuel relocation	Conduct of Test-PTE Material balance (in-rod and dispersed)	Determination of the mass of fuel remaining within the tested fuel rod and the mass that left the fuel rod through the rupture. H(2) This is the primary result to be quantified in this test series, to be correlated with the ballooned region and burst size. It is the amount of lost material that is of interest as it could possibly contribute to such effects as flow blockage, etc. M(0) L(2) This information is covered by the local measurement of the fuel density. Fuel: N Clad: N Reactor: N Burnup: N K(1): Judgement PK(2): Data, Judgement UK(1): Judgement

APPENDIX E

EXPERIMENTAL DATABASES

The experimental databases identified in Section 4 of this report are further discussed in this appendix. The author of each contribution is identified. The contributed documentation exhibits some style differences. References providing additional details for each test program are provided at the end of each contributed entry.

E-1. Separate Effect Tests

E-1.1. Cladding Tests (United States)

The information regarding this test series was provided by panel member A. Motta of the Pennsylvania State University and M. Billone of Argonne National Laboratory.

Argonne National Laboratory (ANL) and The Pennsylvania State University (PSU) are working together on a program to investigate cladding properties and to test loss-of-coolant accident (LOCA) acceptance criteria at high burnups.[1, 2, 3] Although the main focus of the program is to investigate fuel behavior under LOCA conditions, related mechanical properties testing is being done under both LOCA conditions and rod ejection accident (REA) conditions.

Ring Tensile Tests. The tests at relatively low temperatures and high strain rates appropriate for rod ejection accident conditions are being performed. The objectives are two-fold: to understand the degradation in cladding failure behavior at high burnup and to obtain stress-strain relationships that will serve as inputs to codes. High-burnup fuel rods (about 70 GWd/t) from the H. B. Robinson PWR are expected to be available for these tests along with related archival fresh tubing. Although the fuel has not arrived at the time of this writing, high-burnup specimens (about 50 GWd/t) from TMI-1 are available and have been used for preliminary testing along with non-irradiated Zircaloy-4 tubing. Oxidation kinetics and phase transformation characteristics are also being measured on high-burnup specimens.

Axial Tensile Tests. Similar testing will be done on axial tensile specimens electromachined from de-fueled portions of irradiated fuel rods and from non-irradiated tubing specimens. These tests will be performed over the same temperature range and strain-rate range as the ring-stretch tests mentioned above. The combination of the axial and the hoop stress-strain properties will allow validation and improvement of the models used in fuel rod codes for predicting the mechanical behavior of an anisotropic alloy such as Zircaloy.

Biaxial Tube Burst Tests. Biaxial tube burst tests are the most informative and the most difficult to perform, and they consume the largest amount of specimen material, which is a significant consideration when testing irradiated fuel material. These tests will be done in a more limited temperature range of 300 °C–400 °C, but they will explore the effects on deformation and failure of stress biaxiality ratios

from 1:1 to 2:1 at high strain rate. In principle, the tests can be run with the fuel intact or with the fuel removed. Some tests will be run with the fuel removed to generate baseline data for code validation along with data that can be compared to other such studies on non-irradiated and medium-burnup cladding.

Post Quench Ductility Tests. Four-point bending tests will be performed after quenching to determine remaining ductility in oxidized cladding. Other post-quench ductility tests are being considered at the time of this writing.

Oxidation Kinetics. Oxidation kinetics are being measured on high-burnup specimens to determine the effect of pre-LOCA oxidation (corrosion) on the allowable oxidation for regulatory considerations. Phase transformation characteristics and their effect on high-temperature oxidation are also being studied.

References for Cladding Tests (United States)

1. A. B. Cohen, et al., "Modified Ring Stretch Tensile Testing of Zr-1Nb Cladding," Proc. USNRC Water Reactor Safety Information Meeting, NUREG/CP-0162 **2**, 133–149 (October 20–22, 1977).
2. T. M. Link, D. A. Koss and A.T. Motta, "Failure of Zircaloy Cladding under Transverse Plane-strain Deformation," N*uclear Engineering and Design* **186** 379-394 (1998).
3. D. W. Bates, et al., "Influence of Specimen Design on the Deformation and Failure of Zircaloy Cladding," *Proc. ANS International Meeting on Light Water Reactor Fuel Performance,* Park City, Utah, 1201–1210 (April 10–13, 2000).

E-1.2. Cladding Mechanical Property Tests (Japan)

The information regarding this test series was provided by panel member T. Fuketa of the Japan Atomic Energy Research Institute (JAERI).

Mechanical property tests for fuel cladding have been carried out at JAERI, applying different testing method and specimen configuration according to the purpose.[1] They are ring tensile tests, axial tensile tests, and tube burst tests. The most general and reliable method to quantitatively examine the mechanical property of materials is the uniaxial tensile test. Therefore, the test is applied to examine the mechanical property changes after temperature transients expected in LOCAs. The specimens are electro machined from artificially hydrided Zircaloy-4 cladding, annealed at temperatures ranging from 873 °K–1373 °K for 300 s in argon flow, and tensile tested at room temperature and 573 °K. Strength and ductility changes are obtained as a function of hydrogen concentration and annealed temperature. Recent test results showed that ß-quenched Zircaloy cladding with a high hydrogen concentration over 500 wtppm exhibits very low ductility at room temperature. The data obtained will be used to evaluate results from thermal shock tests and be provided as input to codes. Similar tests are planned with oxidized and hydrided specimens and high burnup specimens. The modified ring tensile test with machined specimen currently being developed might be applied in those tests, because of an advantage on the necessary specimen volume.

References for Cladding Mechanical Property Tests (Japan)

1. T. Fuketa, F. Nagase, T. Nakamura, H. Sasajima and H. Uetsuka, "JAERI Research on Fuel Rod Behavior during Accident Conditions," *Proceedings of the 27th Water Reactor Safety Information Meeting*, Bethesda, Maryland, U.S.A., October 25-27, 1999, NUREG/CP-0169, 341-354 (2000).

E-1.3. LOCA Separate Effects Tests (France)

EDGAR program. The separate phenomena which are covered by the EDGAR programs are: (1) the phase transformation kinetics during heat-up and cooling down, and (2) the mechanical properties of the cladding (creep strain rate, time to rupture, diametral strain at rupture). Based on the hypothesis that most of the irradiation defects are annealed during the heat-up, some tests are made on prehydrided specimens to simulate the impact of irradiation on both mechanical and oxidation behaviors. Tests on pre-hydrided samples are performed at different hydrogen content levels.

The EDGAR program is complementary to the LOCA integral tests (such as the LOCA criteria test performed at ANL). The integral tests programs are devoted to the study of the whole behavior of cladding materials during a LOCA. The knowledge of the elementary behaviors of the claddings will allow the interpretation of these integral LOCA tests and, more specifically, the extrapolation of these tests results to other in-reactor LOCA transients.

TAGCIS-TAGCIR-HYDRAZIR-CINOG Program Test Series. The French LOCA test program consisted of four different test series, with their specific purposes. All the tests involved well-defined double-sided oxidation and thermal shock tests on empty 17X17 Zr-4 cladding samples in a steam environment:

- The TAGCIS test series (1991-1993) included more than 110 thermal shock tests on as-fabricated or pre-oxidized Zr-4 cladding samples. This series investigated the thermal shock behavior of non-irradiated cladding having an initial corrosion similar to the end-of-life corrosion of a high burn up fuel rod.
- The TAGCIR test series (1993-1996) included 25 oxidation and thermal shock tests on irradiated Zr-4 cladding samples from high burnup fuel rods irradiated for 5 cycles up to 60-63 GWd/t in a commercial EDF nuclear power plant (corrosion from 60 to 100-120 μm).
- The HYDRAZIR test series (1996-1999) included oxidation and thermal shock tests (at different cooling rates) on non-irradiated as fabricated and pre-hydrided Zr-4 cladding samples (0 to 5000 ppm H). One of the objectives of this series was to investigate the impact of pre-accident hydriding on transient oxidation and quenching behavior. The interest in hydrogen impact came from the TAGCIR test series that showed that the behavior of irradiated zircaloy under LOCA conditions could possibly be related to the hydrogen.

- The CINOG test series (1997- 2001) included oxidation and thermal shock tests on as-fabricated Zr-4 samples. This series was devoted mainly to the licensing of new or advanced alloy under LOCA conditions.

The experimental process for assessing the ECR values for the TAGCIR test series was based on the metallographic measurements of the different metallurgical phases layers thickness and the subsequent calculation of the total amount of oxygen present in the cladding. In the more recent HYDRAZIR and CINOG test series, the same test facility provided, in terms of the measured local cladding temperature, both the high temperature oxidation kinetic through weight gain measurements and the final quenching behavior.

In all cases, the cladding was assumed to have failed as soon as it could not withstand an internal over-pressure of 1 bar of argon and small bubbles were detected on the sample surface. This methodology was extremely conservative since such a threshold was well below the fragmentation limit.

E-2. Integral Tests

E-2.1. LOCA Tests (United States)

The primary purpose of these tests is to evaluate the performance of high burnup fuel relative to the NRC cladding embrittlement criteria defined in 10CFR50.46. The criteria relevant to this research effort are:

1. The calculated maximum fuel element cladding temperature shall not exceed 2200 °F
2. The calculated total oxidation of the cladding shall nowhere exceed 0.17 times the total cladding thickness before steam oxidation.

Within the ANL test plan, the LOCA integral tests will be conducted on fuel rod segments (300-mm long) with the as-irradiated cladding outside diameter (OD) and inside diameter (ID) oxide layers and the fuel intact. In this way, the high burnup effects of the oxide layers, the associated hydrogen pickup due to waterside corrosion, and the fuel cladding contact and/or bonding will be present in the tests. The central 150-200 mm of the test sample will be uniformly (within 25 °C) heated. The specimen will be pressurized, stabilized at 300 °C, heated at 5 °C/s to 1204 °C, held at 1204°C at a time corresponding to a calculated equivalent cladding reacted (ECR) of °17%, slow cooled to 750 °C–800 °C, and water-quenched. The calculation of the ECR vs. time at 1204°C will be made using the ANL "A Model", with model parameters adjusted based on the results of the oxidation test results at 1204 °C. A minimum of three tests will be run. The time for the first test will be set to yield ECR ≅ 17% including the in-reactor-formed oxide layers. The second test will be run at a longer time corresponding to ECR>30% in an effort to produce thermal-shock failure of the cladding. Based on these two results, an intermediate time-ECR test will be run (e.g., 17% ECR excluding the in-reactor oxide layer) to help determine margin to failure. Additional tests (up to 3) may be run based on what is learned from the first three tests.

As the planned tests with high burnup fueled cladding are first-of-a-kind relative to previous tests that have been conducted, there are other important responses that will be studied to resolve the effects of high burnup operation on LOCA-relevant phenomena. During the 5 °C/s rise to 1204 °C, the cladding will balloon and burst. Of interest from the ANL tests are the circumferential magnitude and axial extent of the ballooning, the geometry of the burst, possible fuel particle relocation to the ballooned and burst region, and the effects of these phenomena on the circumferential and axial temperature profile. To the extent practical, these phenomena will be observed, described and quantified. In terms of post-test analyses, the ECR, the phase distribution, and the hydrogen content will be measured in the ballooned-and-burst region and either in the thermal-quench-failed region (if different from the ballooned-and-burst region) or in a non-ballooned, non-burst, non-failed axial location for the tests in which thermal-shock failure does not occur. The ECR values based on data will be compared to the calculated ECR values to determine the degree of conservatism associated with the models.

The rods, grid spans, locations within the grid spans and the times (in terms of ECR values for Limerick BWR LOCA integral tests are identified in Table E-1. The results of the tests using the irradiated fueled cladding samples will be compared to results obtained with non-irradiated cladding samples. Another option that is available for isolating the effects of tight fuel-cladding bonding is to defuel samples, fill the cladding with alumina or zirconia pellets and run these samples through the same the same temperature history. However, because of the anticipated low cladding oxide thickness and hydrogen content, it is difficult to justify such tests. The tests on the BWR Zircaloy-2 archive (or near archive) cladding can be run outside the hot cell in the LOCA Criteria Mockup.

Table 3-1. LOCA Integral Test Matrix for Limerick BWR Fuel Rods

Material Condition	Fuel Rod ID	Grid Span (Location from bottom in mm)	Test Time in Terms of Calculated ECR	Post-Test Examinations
Irradiated	F9	5 (70-370)	≅17%	M, O, P
		6 (70-370)	>30%	M, O, P, F
	J4	6 (70-370)	17%<ECR<30%	M, O, P
		5(70-370)	TBD	TBD
	J6	6(70-370)	TBD	TBD
		5(70-370	TBD	TBD
Archive	---	---	17%	M, O, P
			17-30%	M, O, P
			>30%	M, O, P, F

(All tests are to be run at a peak cladding temperature (PCT) of 1204 °C; TBD = to be determined, M = metallography, O = oxygen analysis, H = hydrogen analysis, P = profilometry, F = fractography)

E-2.2. LOCA Tests (Japan)

The information regarding this test series was provided by panel member T. Fuketa of the Japan Atomic Energy Research Institute (JAERI).

This test series[1] examines the rod-burst, oxidation and reflooding stages, similar to the tests performed at ANL. To systematically investigate the influence of burnup extension on failure-bearing capability of the cladding during quench, pre-hydrided, pre-oxidized, and/or irradiated claddings as well as high burnup claddings are tested. A 600-mm-long cladding with end plugs is pressurized to 5 MPa with Argon gas and heated in a steam flow at a rate of 10 K/s to a target temperature ranging 800 °C to 1250 °C. Annular alumina pellets are contained in the cladding to simulate the heat capacity of UO_2 pellets. After the isothermal oxidation period at the target temperature, the cladding is slowly cooled to 700 °C and finally water-quenched by reflooding from the bottom end. Cladding axially expands during heat up and oxidation, and shrinks during cooling and quench. The shrinkage of the cladding may be restricted between spacer grids in the bundle geometry. Then, the cladding is quenched fixing both ends, for a conservative condition, to examine the influence of restricting the cladding shrinkage and consequent tensile loading during the quench in some part of the present tests.

Oxide layer thickness, hydrogen content and increase of circumference by ballooning are measured in the post-test examination to characterize the cladding failure. Failure-bearing capability will be evaluated based on ECR calculated both from oxidation temperature-time and measured oxide layer thickness.

Tests have now been performed with artificially hydrided cladding (non-irradiated) to examine the separate effect of hydrogen absorption during operation. The test results obtained thus far indicate that the restriction of the cladding shrinkage during quench has a large influence on the failure boundary for the oxidized condition and it is even larger in pre-hydrided claddings. Therefore, the tests with pre-hydrided claddings under controlled axial loading condition will be added. Preparation of high burnup cladding specimens is now in progress, and the tests with high burnup PWR fuel claddings (about 42 MWd/t) are to be started beginning in 2002.

References for LOCA Tests (Japan)

1. F. Nagase, M. Otomo, M. Tanimoto, and H. Uetsuka, "Experiments on High Burnup Fuel Behavior under LOCA Conditions at JAERI," *Proc. ANS International Meeting on Light Water Reactor Fuel Performance,* Park City, Utah (April 10-13, 2000).

E-2.3. BWR Transient Dryout and Rewet Tests

The anticipated transient without scram (ATWS) instability and the LOCA have been identified as key events for the evaluation of fuel performance for a BWR. In ATWS instability the BWR will be at low flow for natural circulation and experience power oscillations. During these oscillations, the high power fuel bundles may undergo periodic boiling transition and rewet following each power

pulse. As long as the PCT remains below the minimum film boiling temperature, rewet will occur and excessive fuel heat up is avoided. However, if the cladding temperature exceeds the minimum film boiling temperature (approximately 600 °C [1100 °F]) following a power pulse the fuel may not rewet and substantial fuel heat up can occur. The following material is based on information found in Refs. 1 through 31.

Data for transient dryout, post dryout heat transfer and transient rewet have been obtained since the mid 1960s. The data include simple geometry tests as well as full scale simulated fuel bundles.

Simple geometry data[1,2,3] have typically been obtained in tubular and annular geometries and include steady state as well as transient tests. These tests typically give well defined thermal hydraulic data and are excellent for model qualification. They do not, however, provide information on the cross sectional variation of thermal hydraulic conditions in a rod bundle. The maximum PCT for these tests goes well beyond the minimum film boiling temperature, where rewet is not obtained. These tests therefore provide valuable information on boiling transition, film boiling heat transfer and rewetting.

Similar tests have been obtained in simple rod bundles,[4,5,14] typically 4x4 rod bundles. In these tests both steady state and transient tests have been performed. The steady state tests were used to obtain information on film boiling heat transfer, while the transient tests were used to obtain additional information on transient dryout and rewet. The transients were either simple power and flow transients where either the power was temporarily raised or the flow temporarily reduced to obtain a boiling transition, or they were simulation of a reactor turbine trip or recirculation pump trip. These tests also give PCTs beyond the minimum film boiling temperature and provide valuable information on boiling transition, film boiling heat transfer and rewetting.

BWR fuel vendors perform extensive critical power tests for each new fuel product that is developed. Steady state critical power data over a range of parameters covering normal steady state operation as well as the expected range of parameters for operational transients is obtained. These data are used to develop a fuel-type-specific critical power correlation. In addition a few transient tests are usually performed in order to demonstrate the applicability of the correlation under transient conditions.[6,7,8,11,19,27,28.29,30,31] The transient tests are simulated turbine trip and recirculation pump trip events, and in one instance a reactor instability was simulated. Since the transient tests are intended to demonstrate the applicability of the critical power correlation under transient conditions, the PCT typically does not exceed the saturation temperature by more than 100 °C–200 °C and thus does not provide data beyond the minimum film boiling temperature.

Numerous LOCA experiments have provided information on transient dryout, film boiling heat transfer and transient rewet. These tests include data from the BDHT,[15] TLTA,[16] FIST,[17,18] FIX,[9,10,21,22,23] TBL,[24] and ROSA-III[25,26] test facilities, which are all scaled simulations of BWRs. The upper range of PCTs for these tests is approximately 870 °C (1600 °F). High temperature data up to 1150 °C (2100 °F) have

been obtained in GE's core spray heat transfer test facility and from the GOTA test facility and similar facilities at Hitachi and Toshiba.[20]

Finally in-pile tests have been performed, where nuclear fuel rods have been subject to boiling transition during power and flow transients. Even though the primary purpose of these tests was to evaluate the thermal and mechanical response of the fuel, these tests also provide valuable data on transient dryout and rewet. The early data in the van Houten report[13] were collected for exposures up to 20 GWd/t and PCTs up to 1700 °C. The later data from the Halden test reactor[13] had exposures up to 40 GWd/t and PCTs up to 950 °C.

The transient dryout and rewet tests are summarized in the Table E-2.

Table E-2. Transient Dryout and Rewet Tests.

Geometry	Test Type	PCT	References
Simple Geometry Tests			
Tubular and Annular	Steady State and Transient	850 °C	1, 2, 3
Simple Rod Bundles			
4X4 Rod Bundles	Steady State Film Boiling Flow and Power Transients Simulated Turbine and Pump	715 °C	4, 5, 14
Full Scale Rod Bundles			
	Simulated Turbine and Pump Trips for 8X8, 9X9 and 10X10 Rod Bundles		6, 7, 8, 11, 19, 27, 28, 29, 30, 31
LOCA			
Scaled Simulation of a BWR.	BDHT, TLTA, FIST, FIX, TBL, ROSA	870 °C	9, 10, 15, 16, 17, 18, 21, 22, 23, 24, 25, 26
Core Spray Heat Transfer	CSHT, GOTA. Toshiba, Hitachi	1150 °C	20
In-Pile Data			
	Flow and Power Transients	1700 °C	12, 13

Note: Minimum Film Boiling Temperature 600 °C.

References for BWR Transient Dryout and Rewet Tests

1. A. W. Bennet, et. al., "Studies of Burnout in Boiling Heat Transfer to Water in Round Tubes with Non-Uniform Heating," Atomic Energy Research Establishment document AERE-R55076, Harwell (1966).
2. A. Era, et. al., "Heat Transfer in the Liquid Deficient Region for Steam Water Mixtures at 70 kg/cm2 Flowing in Tubular and Annular Conduits," Centro Infomazioni Studi Esperienze, SpA document CISE-R-184 (1966).

3. D. C. Groeneveld, "An Investigation of Heat Transfer in the Liquid Deficient Region," Atomic Energy Canada, Ltd. Document AECL3281, Ottawa (1966).

4. G. L. Yoder, et. al., Dispersed Flow Boiling Heat Transfer Data Near Spacer Grids in a Rod Bundle, *Nuclear Technology* **60**, 304-313 (1983).

5. G. L. Yoder, D. G. Morris, and C. B. Mullins, "Rod Bundle Burnout Data and Correlation Comparisons," *Nuclear Technology* **68**, 355-369 (1985).

6. O. Nylund, et. al., "Post Dryout in Connection with BWR Main Circulation Pump Trip," European Two-Phase Flow Group Meeting, Munich (June 1986).

7. R. Persson, L. Nilsson, and H. Gustafson, "FIX-II — Transient Dryout Tests Summary Report," Studsvik Report NP-86/35, Nykoping (1986).

8. "General Electric BWR Thermal Analysis Basis (GETAB): Data, Correlation and Design Application," General Electric document NEDO-10959A (January 1977).

9. L. Nilsson, R. Persson, and H. Wijkstrom, "FIX-II — LOCA Blowdown and Pump Trip Heat Transfer Experiments," Summary Report for the First Experimental Period," Studsvik Report NP-83/325 (1984).

10. L. Nilsson and R. Persson, "FIX-II — LOCA Blowdown and Pump Trip Heat Transfer Experiments," Summary Report for the Second Experimental Period, Studsvik Report NP-85/42, 1985.

11. J. S. Nunez and B. Matzner, "Critical Power, pressure Drop and Transient Tests, 81 Rod Bundle with KWU Spacers AHl6 and AHl7," General Electric document NEDC-21984 (1978).

12. M. A. McGrath, B. C. Oberlander Mykiebust et. al., "Dryout Fuel Behaviour Tests in lFA613, Summary of Inpile Results and PIE Data," EHPG Meeting, Loen (May 1999).

13. R. van Houten, "Fuel Rod Failure as a Consequence of Departure from Nucleate Boiling or Dryout," United States Nuclear Regulatory Commission document NUREG-0562 (June 1979).

14. B. S. Shiralkar, et. al., "Transient Critical Heat Flux — Experimental results, GEAP-13295, AEC Research and Development Report (1972)

15. K. V. Moore, et. al., "Analysis of the GE BWR Blowdown Heat Transfer Program, Test 4906 (AEC Standard Problem 4)," Electric Power Research Institute document EPRI-280 (January 1975).

16. L. S. Lee, G. L. Sozzi, and S. A. Allison S. A., "BWR Large Break Simulation Tests — BWR BlowdownlEmergency Core Cooling Program, "General Electric document GEAP-24962-1, NUREG/CR-2229, EPRI NP-1783, Volumes 1 & 2 (March 1981).

17. W. S. Hwang, Md. Alamgir, and W. A. Sutherland, "BWR FIST Phase I Test Results," United States Nuclear Regulatory Commission document NUREG/CR-371 1 (November 1983).

18. W. A. Sutherland, Md. Alamgir J. A. Findlay, and W. S. Hwang, "BWR Full Integral Simulation Test (FIST) Phase II Test Results and TRAC-BWR Model Qualification," United States Nuclear Regulatory Commission document NUREG/CR-4128, GEAP-30876, EPRI NP-3988 (June 1985).

19. X. M. Chen, J. G. M. Andersen, L. Klebanov, and T. Anegawa, "A Transient Subchannel Analysis Method for BWR Fuel Bundles," NUTHOS-5 (1997)

20. F. D. Shum, et. al., "SAFER Model for Evaluation of Loss-of-Coolant Accidents for Jet Pump and Non-Jet Pump Plants, Volume 1, SAFER — Long Term Inventory Models for BWR Loss-of-Coolant Analysis," General Electric document NEDO-30996A (October 1987).

21. L. Nilsson and P. A. Gustafsson, "FIX-II – LOCA Blowdown and Pump Trip Heat Transfer Experiments, Summary Report for Phase 2: Description of Experimental Equipment Part 1. Main Text," Studsvik Report NR-83/238 Part 1 of 3, (February 1983).

22. L. Nilsson L., et al., "FIX-II LOCA Blowdown and Pump Trip Heat Transfer Experiments, Experimental Results from LOCA Test No. 5052," Studsvik Report NR-83/323, (March 1984).

23. O. Sandervag, and D. Wennerberg, "FIX-II _ Experimental Results of Test 3025 (ISP-15)," Studsvik Report NR-83/283 (July 1983).

24. M. Naitoh, M. Murase, and R. Tsutsumi, "Large Break Integral Test with TBL- 1 (Hitachi BWR Integral Facility)," 9'th Water Reactor Safety Information Meeting, National Bureau of Standards, Gaithersburg, Maryland (October 1981).

25. Y. Anoda,et. al., "ROSA-III System Description Report Fuel Assembly No. 4," JAERI-M 9363 (February 1981).

26. Y. Anoda et. al., "Experimental data of the ROSA-III Integral test Run 912 (5% Slit Break Test without HPCS Actuation," Japan Atomic Energy Research Institute document JAERI-M [illegible] (July 1982).

27. G. Preusche and Z, Stosic, "Post-Dryout Methodology for BWRs," Siemens AG/KWU, Fachtagung der KTG-Fachgruppe "Brennelemente und Kernbauteile", Karlsruhe, Mats (2000).

28. M. Kitamura, T. Mitsutake, K. Kamimura, N. Abe, S. Morooka, and J. Kimura, "BWR 9X9 Rod Assembly Thermal Hydraulic Test (4), Cladding Temperature Behavior During Power Increase," 1998 Fall Meeting, Atomic Energy Society of Japan (1998).

29. M. Kitamura, T. Mitsutake, K. Kamimura, N. Abe, S. Morooka, and J. Kimura, "BWR 9X9 Rod Assembly Thermal Hydraulic Test (5), Cladding Temperature Behavior During Flow Coast Down Event," 1998 Fall Meeting, Atomic Energy Society of Japan (1998).

30. N. Abe, S. Mimura, S. Ebata, S. Morooka and T. Anegawa, "Post-BT Test Analysis by Best Estimate Thermal-Hydraulic Code TRACG," ICONE (1999).

31. J. G. M. Andersen, et. al., "TRACG Qualification," General Electric document NEDE-32177P Revision 2. (January 2000).

E-2.4. Dryout Effects on High Burnup Fuel (Halden Reactor Project-Norway)

The information regarding this test series was provided by panel-member W. Wiesenack.

Background. The objective of the dry-out test series was to provide information on the consequences for fuel of short-term dry-out incidents in a BWR. The experimental method employed was, on an individual basis, to expose fuel rod with different burnups to single or multiple dry-out events; to follow this by either unloading or continued operation in the reactor; and to finish with post irradiation examination and testing with emphasis on fuel clad properties. The test series was co-sponsored by the Halden Project's joint program and TEPCO (Japan).

Testing program. The test series comprised three loadings of IFA-613. Each rod was contained in a stainless steel channel within the rig so that the coolant conditions for each rod could be controlled individually. In this way separate dry-out scenarios were effected for each rod. Thermocouples attached to the surface of the test rods were used to monitor clad surface temperature and clad elongation was monitored by way of an extensometer. The first and second loading operated for a month after dry-out while the rods in the last loading were unloaded directly after the dry-out procedure. In neither case did any fuel failures develop.

The in-pile dry-out experiments with the third (and last) set of fuel rods in IFA-613 were completed in January '98 (HWR-552, HP-1036) and the post irradiation examination (PIE) on all eight rods in the three test series were finished in September '98 (Kjeller hot cell).

Summary of results. In total, 2 rods with fresh Zr-2 and Zr-4 and 6 rods with clad pre-irradiated to 22-40 MWd/kg (Zr-2, Zr-2 with liner and Zr-4) were individually exposed to reduced or no-flow conditions in a heated light water loop within the Halden reactor. Dry-out occurred over the upper region of each rod, with 6 rods developing PCTs in the range 950 °C–1200 °C.

An overview of the condition of the rods in terms of clad surface condition, rod dimensions and hydriding was achieved using non-destructive PIE techniques such as profilometry and neutron radiography. Clad and fuel microstructure and clad mechanical properties were investigated with destructive PIE techniques including ceramography, metallography, microhardness and ring tensile testing. It was observed that while dry-out had not affected the fuel microstructure, significant changes had been induced in the clad. These included high temperature corrosion resulting in moderate growth of the outer surface oxide layer and H_2 pick-up (hydriding formation). Some of the rods also exhibited uniform and localised clad creep-down into pellet-pellet interfaces and in the most severely tested rods that clad

had undergone the α to β phase transformation. This material exhibited reduced ultimate tensile strength and brittle fracture. However, significant improvements of ductility were observed in clad that had been exposed to less severe in-pile transients where a small α-phase grain structure was retained and hydrogen pick-up was minimal. None of the rods failed, during either the dry-out phase or the subsequent steady-state normal operation.

Applications. The data obtained will be used to assess and modify existing rules/regulations in member countries on the continued operation with fuel elements subjected to short-term dry-out transients in boiling water reactors.

APPENDIX F

DESCRIPTION OF PWR FUEL AND CLADDING STATE AT HIGH BURNUP[†]

The extended operational exposure that accompanies high burnup causes changes to the fuel and cladding that may affect the fuel rod's ability to withstand the accident without losing its integrity (Fig. F-1). These changes, which occur gradually over the life of the fuel rod, can be considered as initial conditions for the accident.

There are many changes that occur to the fuel and cladding as a result of prolonged exposure to the irradiation field present in a reactor core, and to the corroding environment and high temperature. The combination of high temperature, radiation damage, transmutation, mechanical stresses and chemical reactions causes the microstructure of cladding and fuel to evolve considerably during reactor exposure. These changes in microstructure, microchemistry, and macroscopic characteristics of pellet and cladding are responsible for the changes in material behavior observed at high burnup. These changes are very complex and difficult to predict in a mechanistic fashion. Of the many changes to the fuel and cladding, it is important to discern which are of greatest importance to determining fuel rod behavior during an accident. We list some of the more important material degradation phenomena below, recognizing that the list may not be inclusive. The changes to the fuel and cladding are important to both pressurized water reactor (PWR) and boiling water reactor (BWR) fuel types. A discussion specific to the changes to BWR fuel and cladding is presented in Appendix G.

F.1. Cladding Changes

The main degradation mechanisms to Zircaloy-4 cladding include uniform waterside corrosion, hydriding, and radiation damage.

Uniform waterside corrosion occurs throughout the reactor exposure. The corrosion rates depend on many factors including alloy chemistry and thermomechanical treatment, coolant chemistry, radiation-induced changes to cladding microchemistry, and irradiation temperature. For cladding with burnups in excess of 50 GWd/t , the oxide thickness can exceed 100 μm depending on fuel duty, i.e., power and temperature versus time and burnup. The burnup level at which any given oxide thickness is reached for a given alloy is dependent on the fuel duty. The more modern alloys such as ZIRLO and M5, can have lower corrosion rates than standard Zr-4 and low-Sn Zr-4 at similar burnup. All of the zirconium alloys examined to date show a change in corrosion rate when the oxide exceeds a certain thickness (20–30 μm in thickness), which indicates a change in corrosion regime, termed **breakaway corrosion.** Therefore, it is likely that even the new modern alloys such as ZIRLO will eventually experience breakaway corrosion. The question with

[†] See Acknowledgments for authorship information.

the new modern alloys is the burnup level at which breakaway corrosion will be observed.

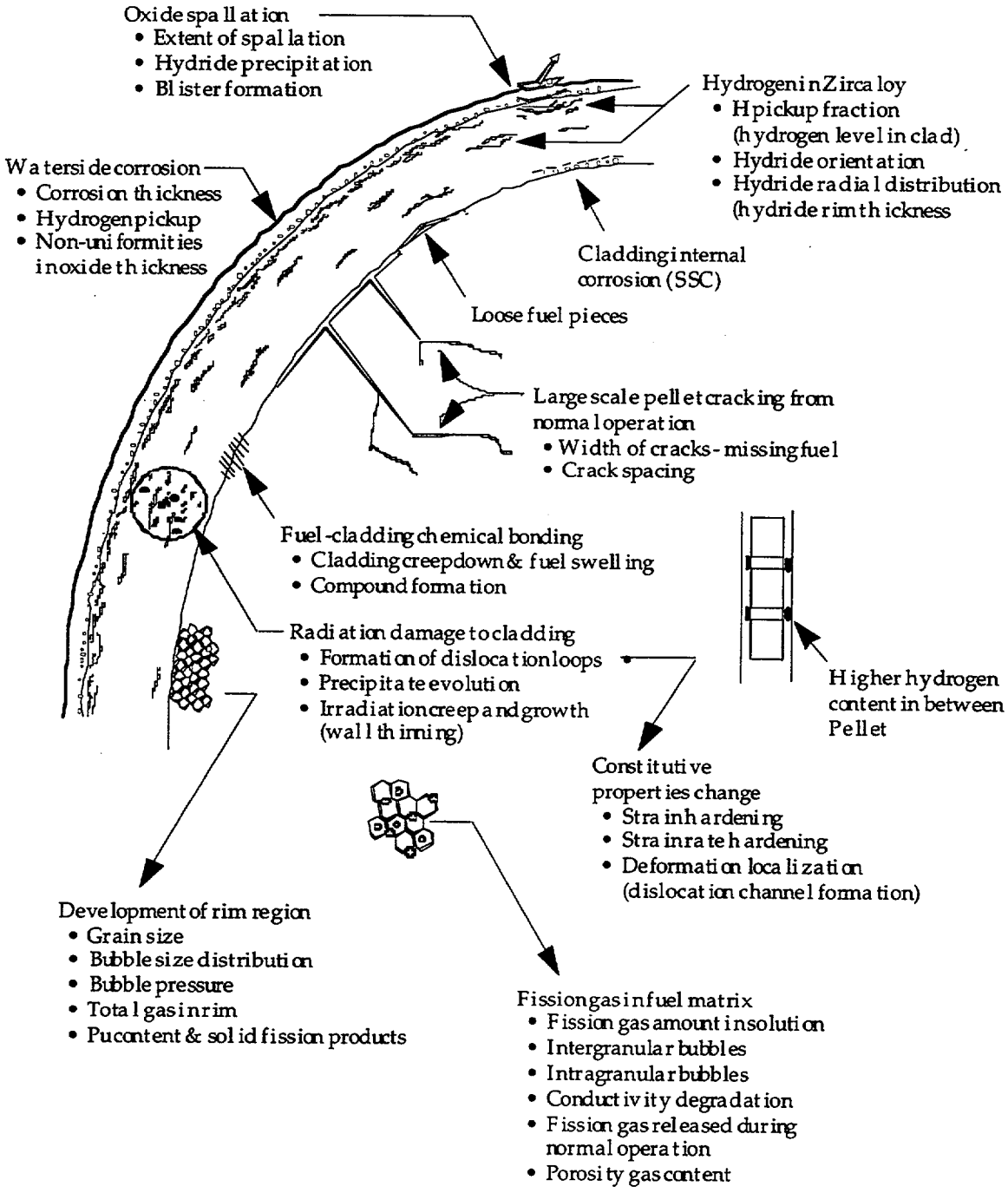

Fig. F-1. Fuel state at high burnup

For example, fuel that experiences a high fuel duty will experience breakaway corrosion at a lower burnup level than fuel with a lower fuel duty. One of the concerns with large oxide thicknesses is the higher probability of **oxide delamination**, whereby portions of the oxide layer are detached from the adherent oxide creating an oxide region with worse heat conduction characteristics. Ultimately the detached oxide can break off (**oxide spalling**), creating a thinner oxide. The associated temperature gradients created by spalling have been shown to influence hydride blister formation in the spalled region.[F-1] The hydride blister is brittle, and its presence has been shown to affect overall cladding ductility.

The main concerns associated with the uniform corrosion process are the potential for oxide spalling resulting in hydride blisters, which affect the overall cladding ductility; loss of thermal conductivity; non-uniform wall thinning (non-uniform oxide); and overall wall thinning.

Hydriding occurs as hydrogen is absorbed into the cladding as a result of uniform corrosion of the cladding (roughly 15%–20% of the hydrogen generated by the corrosion reaction is absorbed into the alloy). This hydrogen precipitates as hydrides throughout the cladding thickness at corrosion thicknesses greater than 50 microns (μm). When the overall hydrogen level is high enough (>1000 parts per million [ppm]), the cladding is brittle when tested at reactor temperature. It is possible that lower levels of hydrogen (600-800 ppm) can affect cladding ductility, especially at lower temperature.

However, lower levels of hydrogen, can also degrade the overall cladding ductility depending on the hydride distribution. Hydrogen has high mobility but low solubility in Zircaloy is very low, so hydrogen will tend to precipitate out in any cold spot formed in the material. For example, there is a much greater hydride concentration near the surface of the cladding creating a **hydride rim** with local hydrogen levels higher than 1000 ppm. In addition to being radially localized, the axial distribution of hydrogen is also non-homogeneous, with greater concentration in the region in-between the fuel pellets due to the slightly lower heat fluxes and lower temperatures at pellet interfaces.

The main concerns associated with hydriding are: (a) lower ductility and/or embrittlement resulting from an overall change in constitutive properties, and (b) creation of weak spots in cladding resulting from the formation of a hydride rim, and/or hydride blisters.

Radiation damage. When irradiated to 30 GWd/t (corresponding to a fast fluence of ~10^{22} n/cm^2, E>1 MeV) the cladding suffers an amount of damage calculated at about 20 dpa (displacements per atom)[F-2]. The dpa level is roughly proportional to the fluence or burnup, so that 60GWd/t corresponds to about 40 dpa and 75 GWd/t to 50 dpa. This very high level of displacements is translated mostly into radiation-induced dislocation loops, both <a> and <c> type that form from the agglomeration of point defects. Although the overall <a> dislocation density saturates after about one month of reactor irradiation at a level comparable to that found in cold-worked,

stress-relieved (CWSR) cladding, the <c> type dislocations evolve over a more extended period of time. In addition there are microchemical changes in the alloy related to irradiation induced intermetallic precipitate amorphization and dissolution, which can **change corrosion resistance** and hydrogen pickup.

The **constitutive response** of the cladding is also affected by the radiation damage, in particular the dislocation loop microstructure formed under irradiation. The yield stress increases, and the uniform strain decreases, i.e. the material undergoes **hardening** and ductility decrease. The increase in dislocation loop density decreases the strain hardening coefficient of the material. At the microscopic level, these loops can also influence deformation localization at the microscopic level (dislocation channeling); the effects of these microscopic processes on macroscopic deformation and failure are not clear at the moment. There is also **cladding creepdown**, which can cause the gap to be closed, creating the conditions for fuel-clad chemical bonding to develop.

The main concerns relating to radiation damage are (a) radiation hardening and possible embrittlement, (b) change of corrosion resistance through microchemical changes, (c) mechanical property changes and (d) deformation localization (e.g., dislocation channeling, possibly leading to easier axial crack propagation).

F.2. Fuel Changes

During normal operation fission gas is formed inside the UO_2 fuel, and distributes itself largely into five inventories: *(i)* gas dissolved in the UO_2 matrix, *(ii)* gas in intragranular (matrix) bubbles, *(iii)* gas in intergranular (on grain boundaries) bubbles *(iv)* gas released to the rod void volume and (*v*) gas in fuel porosity. The amount of gas dissolved in the UO_2 matrix is small, as the solubility of fission gases in UO_2 is low. Contributions *(ii)* and *(iii)* result in fuel swelling with consequent pellet-cladding mechanical interaction (PCMI) and contribution *(iv)* is the result of fission gas release (FGR), which increases the internal rod pressure and results in hoop stress on the cladding. The exact partitioning of these gases among the three inventories are dependent on the power history, temperature, fuel microstructure, etc.

Rim Formation. Because of Uranium-238 resonance neutron capture at the UO_2 pellet surface, the amount of plutonium formed in the fuel is greater at the edge of the pellet than in the center. This causes the fission rate at the pellet surface to slowly increase with burnup while the fission rate in the bulk of the pellet decreases. The ratio of fission at the edge of the pellet to the center may be as high as 3 at high burnups. Such a region is called the **rim region** and its thickness is approximately 100–300 μm. The rim region is formed when the local burnup at the rim exceeds approximately 60 GWd/t (40-45 GWd/t radial averaged). The **rim region** has a characteristic microstructure that consists of sub-micron size grains with bubbles under high gas pressures and has high porosity (20-30%). Some of these bubbles may be in non-equilibrium with the matrix because there are large strain fields

around the smaller bubbles and there is further evidence that they exist within the interior of the pellet as well as on the rim if the irradiation temperatures are low.

The main concerns with the formation of the rim region concern its effects on (a) the amount of fission gas loading and (b) the lubrication (by shearing during deformation, the rim could reduce the friction coefficient between cladding and fuel).

Fuel restructuring and large cracking. These phenomena occur at low burnups when a significant fuel-cladding gap exists. The fuel-cladding gap is either very small or non-existent (as evidenced by chemical bonding) in high burnup fuel even when the fuel is at hot zero power (reactor coolant is still hot). Therefore, these phenomena are not likely to occur in high burnup fuel.

Microcracking. The mechanical stresses and thermal stresses present in the fuel during the RIA transient can cause **microcracking** to occur at the grain boundaries weakened by gas bubbles. The microcracking and its extent can affect both fission gas swelling and deformation.

Pellet-cladding Interface. As burnup increases, a metallurgical or chemical bond starts to form between the cladding and the fuel, so that **fuel-cladding bonding** occurs. Clearly the development of this bond depends on the establishment of clad-fuel contact resulting from creepdown and fuel swelling. At intermediate stages, the friction coefficient will increase but without perfect bonding. It is important to determine the friction coefficient so that we can determine the stress state and failure mode of the cladding during pellet-cladding PCMI.

F.3. References

F-1. M. Garde, G. P. Smith, and R. C. Pirek, "Effects of Hydride Precipitate Localization and Neutron Fluence on the Ductility of Irradiated Zircaloy-4," in *11th International Symposium on Zr in the Nuclear Industry*, vol. STP 1295. Garmisch-Partenkirchen: ASTM, 1996, pp. 407.

F-2. "Standard Practice for Neutron Radiation Damage Simulation by Charged-Particle Irradiation," American Society for Testing and Materials Standard Practice E521-96 (1996).

APPENDIX G

DESCRIPTION OF BWR FUEL AND CLADDING STATE AT HIGH BURNUP[†]

During irradiation, the fuel and cladding experience changes in geometry, material macrostructure and microstructure, mechanical properties, and other physical and performance characteristics. It is considered that some of these changes could possibly affect the fuel rod's ability to maintain its integrity when subjected to an accident. Figure G-1 presents a qualitative characterization of some of these fuel and cladding changes. These changes, which occur generally gradually over the life of the fuel rod, can represent initial conditions for the accident.

Of the many changes experienced by the fuel and cladding, it is important to discern which of these are of greatest importance in determining fuel rod behavior during the power oscillations. Some of the more important phenomena are presented and discussed below, recognizing that the list may not be inclusive. The changes to the fuel and cladding indicated in Figure G-1 are possible, and have been observed, in both pressurized water reactor (PWR) and boiling water reactor (BWR) fuel types, although to varying extents. Recognizing that the power oscillations are a BWR event, the following discussion will attempt to clarify the applicability of the various phenomena as currently recognized in modern commercial BWR fuel.

G.1. Cladding Changes

The cladding material applied in BWRs is Zircaloy-2, most predominately in the annealed, fully recrystallized condition with a zirconium-based inner liner, although cold-worked stress relieved material and non-liner applications also exist. The zirconium liner can contain varying amounts of alloy additions, intended for post-defect corrosion resistance. The primary change mechanisms identified for the cladding are waterside corrosion, hydriding, and radiation damage.

Cladding corrosion occurs through direct exposure of the cladding outer surface to a high temperature, highly oxidizing environment enhanced by the radiation field. The effects of cladding corrosion are wall thinning, increased heat transfer resistance, and cladding hydrogen absorption. In general, the BWR suppliers have progressively refined the cladding material processing to minimize the occurrence of nodular corrosion, thereby resulting in a generally uniform corrosion morphology. Where cladding corrosion distributions are typically peaked at the higher elevations in PWRs, the corrosion distributions are generally flatter along the fuel rod length in a BWR, with possible peaking at the lower elevations. Circumferential variations in cladding oxide layer thickness are observed in BWRs, but are generally minor in magnitude. Where cladding corrosion thicknesses of up to or greater than 100 μm has been observed in PWRs, BWR cladding corrosion is significantly less, typically less than 50 μm at exposures up to ~62 GWd/MTU peak rod average exposure, as observed to date.

[†] See Acknowledgments for authorship information.

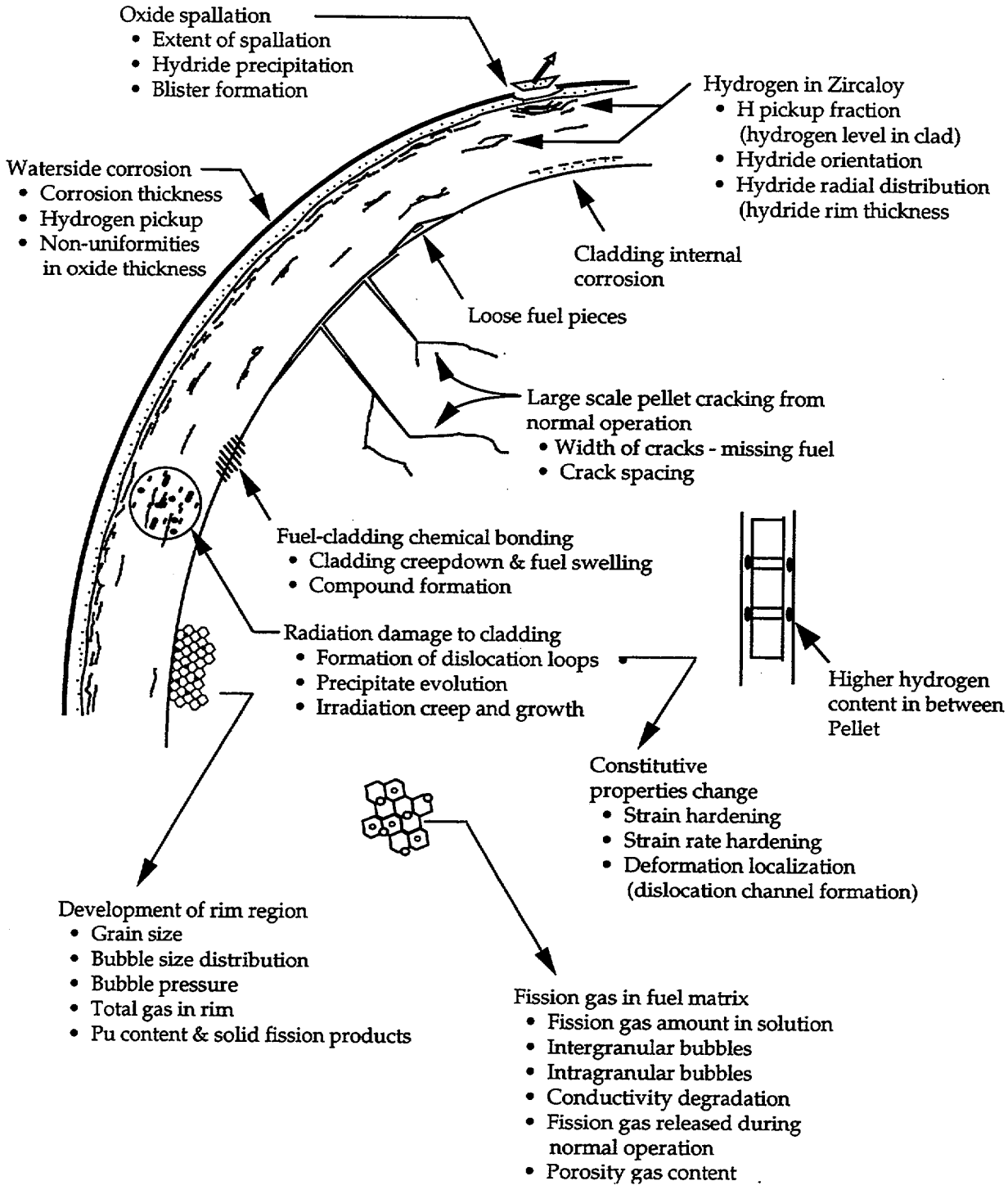

Fig. G-1. Fuel and Cladding State

An important consideration is oxide layer cracking, delamination, and spalling. Oxide layer cracking and delamination can lead to an acceleration in the oxide layer growth rate. Spalled oxide regions result in a cooler cladding metal temperature during operation than exists under the adjacent unspalled oxide regions. The

presence of such "cold spots" can promote redistribution of any hydrogen absorbed from the cladding outer surface corrosion process, thereby leading to hydride localizations and even bulk hydride formation (observable as bulges or blisters) in the outer region of the cladding. Such bulk hydride formation regions are highly embrittled and are often accompanied with partial cladding cracks even in the absence of applied loading by the fuel pellets (caused simply by the volume expansion associated with the conversion of zirconium to zirconium hydride). Where significant accelerated corrosion and oxide layer spalling has been observed in PWRs, similar conditions are typically not observed in BWRs with modern cladding materials.

Corrosion localizations have been observed at fuel assembly spacer locations, adjacent to Inconel components (typically referred to as "shadow corrosion"). Although accelerated localized corrosion, leading to fuel rod failure, has occurred at one BWR with an earlier cladding material type, in general, the available characterizations indicate that this localization develops relatively quickly, but then remains relatively stable, at least to exposure levels characterized to date (~62 GWd/MTU peak rod average exposure).

BWRs operate with several water chemistry options: Hydrogen Water Chemistry, Zinc Injection, and Nobel Metal Chemical Addition. To date, no unacceptable changes in the cladding corrosion performance have been observed under these water chemistry options.

In summary, in BWRs with modern cladding, the primary effects of interest from the corrosion process are (1) wall thinning, (2) increased heat transfer resistance, and (3) the effects of corresponding hydrogen pickup.

Hydriding occurs as hydrogen, liberated by the cladding outer surface corrosion process, is absorbed into the cladding. Typically, less than 20% of the hydrogen generated by the corrosion reaction is absorbed by the cladding. This absorbed hydrogen generally precipitates as circumferentially oriented zirconium hydride stringers when the amount of absorbed hydrogen exceeds the solubility level. Available testing has demonstrated no adverse influence of hydrogen on elevated temperature irradiated Zircaloy ductility (total elongation) for hydrogen contents up to at least 850 ppm[G-1]. At higher hydrogen levels, something in excess of 1000 ppm, the cladding ductility can be reduced at operating temperatures. Most typically, BWR cladding hydrogen content is <200 ppm, as characterized at ~50 GWd/MTU rod average exposure for modern BWR cladding materials. Although higher levels (less than 600 ppm) have been observed in older cladding types at elevated exposures (up to ~65 GWd/MTU rod average exposure), even this level is below that required to significantly affect the cladding mechanical properties.

At high hydrogen levels (in excess of 1000 ppm) a dense hydride rim can form near the cladding outer surface, primarily as observed in PWR fuel applications. Hydride localizations have also been observed at "cold spots" occurring at pellet-pellet interfaces (adjacent to pellet chamfers), and more significantly, at spalled oxide

locations as discussed previously. With the generally lower hydrogen concentration observed in BWR fuel, dense hydride rims or extreme localizations at pellet-pellet interfaces have not typically been observed, although the general tendency of hydride accumulations toward the cladding outer surface or near pellet-pellet interfaces has been observed.

Another consideration, although not typically observed in either PWR or BWR applications is the development of radially oriented hydrides, which, in significant concentration, could affect the cladding ductility.

In summary, in BWRs with modern cladding, the primary considerations with cladding hydrogen content are (1) the impact, if any, on the cladding mechanical properties, and (2) the effect of hydride localizations to form weak, damage-susceptible regions. In general, these considerations have not been found to be significant for the hydrogen contents observed in modern BWR cladding to date.

Radiation Damage to the cladding material occurs as a direct consequence of exposure to fast neutrons. This radiation damage is manifested as radiation-induced dislocation loops, both <a> and <c> type that form from the agglomeration of point defects. Although the overall <a> dislocation density saturates very early in life, the <c> type dislocations evolve over a more extended period of time. The effect of this damage is a strengthening of the material, with a corresponding reduction in ductility, and increased irradiation-induced stress-free growth (occurs in the absence of an applied stress). Additionally, microchemical changes occur as the irradiation induces intermetallic precipitate amorphization and dissolution, which can alter the mechanical properties, corrosion resistance and possibly also the hydrogen pickup of the cladding material.

In addition to irradiation-induced growth of the cladding material, irradiation also induces cladding creep in response to the applied fuel rod internal-external pressure difference and pellet expansion loadings.

In summary, the primary considerations relative to cladding radiation damage are (1) radiation hardening and the corresponding mechanical properties impact, and (2) deformation caused by irradiation-induced growth and creep.

G.2. Fuel Changes

Fission Products. During normal operation, solid and gaseous fission products are generated within the UO_2 fuel pellet. Whereas the solid fission products generally remain at the birthsite, the gaseous fission products are more mobile and distribute largely into five separate inventories: *(i)* gas dissolved in the UO_2 matrix, *(ii)* gas in intragranular (matrix) bubbles, *(iii)* gas in intergranular (on grain boundaries) bubbles *(iv)* gas released to the fuel rod void volume and (*v*) gas in fuel porosity. The amount of gas dissolved in the UO_2 matrix is limited by the solubility in UO_2. Solid fission products result in a progressive swelling of the fuel material with irradiation exposure. Gaseous fission product inventories *(iii)*, and to a lesser extent

(ii) and (v), under high temperature low restraint conditions, can also result in fuel swelling with consequent pellet-cladding contact. Inventory *(iv)* is referred to as fission gas release (FGR) and produces an increase in the fuel rod internal pressure and corresponding cladding loading. The exact partitioning of the fission gases among the identified inventories is dependent primarily on the fuel pellet microstructure and thermal operating history.

Rim Formation. As a result of Uranium-238 resonance neutron capture at the UO_2 pellet periphery, the amount of plutonium formed in the fuel pellet is greater at the pellet periphery than in the center. This plutonium buildup causes a significant increase in the fission rate at the pellet periphery, relative to the fission rate in the bulk of the pellet. At elevated exposures, the result of this elevated fission rate is to produce a highly porous, fine grained structure. This altered structure region is called the **rim region.** The size of the rim region increases relatively progressively with increased exposure above ~40-45 GWd/MTU pellet average exposure. The primary considerations with the formation of the rim region are (1) possible increased fission gas release, (2) possible increased resistance to heat transfer, and (3) possible increased gaseous swelling under high rim temperature conditions. It is noted that the pellet rim may provide a cushion, or lubricating, effect that may reduce the consequences of pellet-cladding mechanical interaction.

Fuel restructuring and macrocracking. During the initial rise to power, the thermal stresses caused by the pellet radial temperature gradient cause the pellet to crack (primarily radially). With the release of strain energy, the cracked pellet segments relocate outwards toward the cladding (called fuel relocation or restructuring). With continued irradiation, additional outward movement of the pellet segments can occur. At ~mid-life exposures, the combined effects of pellet relocation, fuel irradiation swelling, and cladding creepdown result in a closed pellet-cladding gap. From this point, (1) a reduction in the fuel pellet expansion (such as caused by a power decrease) can result in partial gap opening, and (2) additional fuel expansion (by progressive fuel swelling or as a result of a power increase) can cause pellet radial cracks to (partially) close, thereby increasing the effective pellet stiffness, and imposing loading and deformation of the cladding. No particular change in this behavior is expected at elevated exposures.

Microcracking. During a rapid reactivity pulse where the pellet rim can experience significant heatup, and in the absence of significant constraint provided by the cladding, gas bubble expansion at the grain boundaries (most notably at the pellet rim) could lead to grain boundary cracking (decohesion). The result would be a release of fission gases to the fuel rod void volume with an increase in the fuel rod internal pressure and applied cladding pressure loading, with a subsequent reduction in the local pellet expansion. In the presence of significant cladding constraint, gas bubble expansion would be suppressed with a corresponding reactive increased loading of the cladding, likely with no significant fission gas release until release of the applied hydrostatic stress such as would occur on cooling. Additional pellet cracking can also occur on cooling, resulting in additional fission gas release,

but correspondingly also reducing the gaseous swelling potential for the next heatup cycle.

Pellet-Cladding Interface. With the onset of pellet-cladding contact, a bond layer develops between the fuel pellet and the cladding. At elevated exposure, the magnitude (bond layer thickness) and extent (circumferential and axial surface coverage) increases. The development of this bond layer affects the ability of the pellet and cladding to move independently (effective friction), and thereby affects load transfer from the pellet to the cladding and the subsequent cladding stress state. The bond layer can fracture during cooldown or power reductions, leading to an intermediate state.

G.3. References

G-1. S. B. Wisner, R. B. Adamson, "Combined Effects of Radiation Damage and Hydrides on the Ductility of Zircaloy-2", Nuclear Engineering and Design, 185 (1998), pages 33-49.

APPENDIX H

MEMBERS OF THE HIGH BURNUP FUEL PIRT PANEL

Carl A. Alexander

Carl Alexander is Chief Scientist of Battelle's government sectors operation. He has a B.S. in Mathematics from Ohio University, a M.S. in Physics from the same institution, and a Ph.D. in Ceramic Engineering received in 1961 from The Ohio State University. From 1962 to 1985 he was a member of the engineering and graduate faculty of The Ohio State University, with joint appointments as Adjunct Professor of Nuclear Engineering as well as Ceramics and Materials Engineering. He has also served as Adjunct Professor at the University of Maryland and Southampton University in the U.K. His specialty is nuclear fuels and thermodynamics. He performed some of the first loss-of-coolant simulations in the late 1950s early 1960s. He contributed to Wash-1400 in which he showed the importance of cesium iodide as a transport medium in a LOCA. He performed several studies of fission product release with real fuels at very high temperatures and has evaluated a number of complexes involving urania and Zircalloy at very high temperatures.

Jens G. M. Andersen

Jens G. Munthe Andersen is a principal engineer at Global Nuclear Fuel. He has a M.S. in Nuclear Engineering for the Technical University in Denmark and obtained a Ph.D. in Nuclear Engineering from the same institution in 1974. From 1971 to 1978 he was employed by Risø National Laboratory in Denmark. From 1978 Dr. Andersen has been employed by General Electric Nuclear Energy and since January 2000 by Global Nuclear Fuel (a joint venture of GE, Toshiba and Hitachi). He is currently leader of the Methods and Process Development team at Global Nuclear Fuel. Dr. Andersen has 29 years experience in the nuclear field. He has been primarily engaged in developing computer programs for boiling water reactor transient and safety analysis. He has participated in numerous PIRT panels and the application of the CSAU methodology to BWR.

John A. Blaisdell

John Blaisdell is a Senior Consulting Engineer at Westinghouse Electric Company (CE Nuclear Power, LLC). He received his BS degree in Mechanical Engineering from Clarkson University in 1961 and a Ph.D. in Mechanical and Aerospace Engineering from North Carolina State University in 1969. Dr. Blaisdell has worked in the nuclear industry for that past 29 years. His experience includes work on the PWR FLECHT-SEASET experimental program, including test specification development and review and correlation of results; development of best-estimate small break LOCA analytical methods; and supervising the development of mathematical models of fuel behavior during a LOCA. He was the Manager of Safety Analysis at Northeast Utilities where he managed the development of plant-

specific probabilistic safety analyses (PSAs) for four nuclear units and the in-house development of transient and LOCA analysis capability. He was also a project manager at Yankee Atomic Electric Company where he managed the development of a best-estimate containment analysis for the Maine Yankee power plant. This work included facilitating a PIRT panel and managing the development of the methodology to statistically combine the results of the mass and energy calculations with the containment response calculations. Dr. Blaisdell is currently involved in the LOCA and non-LOCA safety analyses for both PWRs and BWRs.

Brent E. Boyack

Brent E. Boyack is the facilitator for the High Burnup Fuel PIRT Panel. He is a registered professional engineer. He obtained his B. S. and M. S. in Mechanical Engineering from Brigham Young University. He obtained his Ph.D. in Mechanical Engineering from Arizona State University in 1969. Dr. Boyack has been on the staff of the Los Alamos National Laboratory for 19 years; he is currently the leader of the software development team, continuing the development, validation, and application of the Transient Reactor Analysis Code (TRAC). Dr. Boyack has over 30 years experience in the nuclear field. He has been extensively engaged in accident analysis efforts, including design basis and severe accident analyses of light water, gas-cooled, and heavy-water reactors; reactor safety code assessments and applications; safety assessments; preparation of safety analysis reports; and independent safety reviews. He chaired the MELCOR and CONTAIN independent peer reviews and was a member of the Code Scaling, Applicability and Uncertainty or CSAU technical program group. He has participated in numerous PIRT panels. He has over 70 journal and conference publications and is an active member of the American Nuclear Society.

Bert M. Dunn

Bert M. Dunn obtained his B. S. in Physics from Washington State University in 1968 and his M. S. in Physics from Lynchburg College in 1973. Mr. Dunn has worked in LOCA and Safety Analysis for the Babcock and Wilcox Company (B&W) and Framatome Technologies (FTI) for 28 years. Mr. Dunn has served as the lead technically for the development of the B&W and FTI LOCA evaluation models for once through and recirculating steam generator plants. He has worked with both deterministic and best estimate LOCA evaluation techniques. He has also been technical lead for method development and application of boron dilution accident methods and pressurized thermal shock evaluation methods. He is currently employed as an Advisory Engineer with responsibility for the development of LOCA and Safety Analysis techniques for evaluation of advanced cladding materials. This includes test specification development, review and correlation of results, and the incorporation of results into requisite analytical methods. Mr. Dunn has been primary author on several company topical reports covering both methods development and accident analysis.

Derek B. Ebeling-Koning

Derek B. Ebeling-Koning is Manager of BWR Fuel and Engineering Analysis at Westinghouse Electric Company. He received his B.S. degree in Nuclear Engineering from Rensselaer Polytechnic Institute in 1977. He received his M.S. and Ph.D.degrees in Nuclear Engineering in 1979 and 1983, from Massachusetts Institute of Technology. He has worked for the last 17 years in BWR and PWR safety analysis, initially for Westinghouse Electric, then ABB Combustion Engineering starting in 1991 (now a subsidy of Westinghouse Electric.) His expertise includes methods and modeling of two-phase flow; BWR LOCA analysis, PWR operational transients and containment analysis; and a lead role in developing and licensing of ABB BWR reload analysis methodology in the U.S. Dr. Ebeling-Koning is a member of the ANS and ASME, and technical reviewer for several industry journals.

Toyoshi Fuketa

Toyoshi Fuketa is a Principal Engineer in the Fuel Safety Research Laboratory at the Japan Atomic Energy Research Institute (JAERI). He obtained his B. S., M. S. and Ph.D. in Mechanical Engineering Science from Tokyo Institute of Technology, Japan, in 1982, 1984 and 1987, respectively. Dr. Fuketa has been involved in the Nuclear Safety Research Reactor (NSRR) project to study behavior of LWR and research reactor fuels under reactivity accident and severe accident conditions and to evaluate the thresholds, modes, and consequences of fuel failure in terms of the fuel enthalpy, fuel burnup, coolant conditions, and fuel design. His research interests include fuel-coolant interactions, fuel failure mechanisms and transient fission gas behavior. He was engaged in small-scale steam explosion experiments at Sandia National Laboratories, Albuquerque, from 1988 to 1990, as a visiting scientist.

Georges Hache

Georges HACHE is a PIRT expert on LOCA fuel behavior from the French Nuclear Safety and Protection Institute (IPSN). He graduated from the French Ecole Polytechnique in 1973 and Ecole des Mines de Paris in 1976 (colleges of university level, admission to which is by strict examination). After ten years in the French nuclear inspectorate, he joined the IPSN Safety Research Division at Cadarache in 1986. He was involved in the development and assessment of safety computer codes, describing fuel and fission products behavior during severe and design basis accidents of light water and fast breeder reactors (SCANAIR, ICARE2, ESCADRE...), including definition and interpretation of safety tests in the CABRI and PHEBUS reactors. After having led the safety software development and assessment team for a period of seven years, he is now senior scientific adviser to the head of the Division. He has been engaged in international cooperative efforts including the OECD / CSNI Rasplav program and a task force on fuel safety criteria.

Lawrence E. Hochreiter

L.E. (Larry) Hochreiter is a professor of Nuclear and Mechanical Engineering at the Pennsylvania State University and does research and teaching in the areas of two-phase flow and heat transfer, reactor thermal-hydraulics, fuel rod design, and nuclear reactor safety. He recieved a BS degree in Mechanical Engineering from the Universtiy of Buffalo and a MS and Ph.D degrees in Nuclear Engineering from Purdue University. While at Pennsylivania State University, Dr. Hochreiter has developed a detailed reflood heat transfer PIRT to guide the design and instrumentation of the NRC Rod Bundle Heat Transfer program, located at Penn State. Before joining the Penn State University in 1997, Dr. Hochreiter was a Consulting Engineer at the Westinghouse Electric Corporation for nearly 26 years and was responsible for the development, testing validation, and licensing of Westinghouse safety analysis methods. He developed the large-break Loss Of Coolant Accident (LOCA) PIRT for the Westinghouse Best-Estimate Methodology. He also participated in and helped develop the Westinghouse small-break LOCA PIRT. Dr. Hochreiter also developed several PIRTs for the Westinghouse advanced AP600 design for the accident analysis methods and presented these PIRTs to the NRC and the ACRS.

S. E. "Gene" Jensen

S. E. "Gene" Jensen is an experienced engineer with 38 years of involvement in nuclear safety applications and development. Mr. Jensen obtained his BS degree in 1961 from Montana State and his MS degree from the University of Idaho both in Chemical Engineering. He is a registered professional engineer. He spent the first 14 years of his career at the Idaho National Engineering Laboratory working in various phases of the nuclear safety test engineering program. He became involved with the early regulatory support activities including the development of the Water Reactor Evaluation Model (WREM) to perform LOCA analyses according to the NRC ECCS Rule which came out in 1975. In 1975, Mr. Jensen joined Exxon Nuclear Company (since purchased by Siemens), where he was instrumental in developing LOCA ECCS Evaluation Models for both PWRs and BWRs and obtaining NRC approval of these models. Mr. Jensen has spent 24 years with what is now Siemens Power Corporation all of which were involved with safety analysis applications and development including both transient and LOCA analysis. His most recent involvement has been as the technical lead in developing a PWR Realistic LOCA methodology for Large Break LOCA. Mr. Jensen is a member of both ANS and AIChE.

Siegfried Langenbuch

Siegfried Langenbuch is head of the reactor dynamics division of GRS. He obtained his Diploma in Physics from the University of Munich in 1969. The objective of his Dr. degree work was the development of an efficient spatial- and time-dependent 3D-neutronics model for studying reactivity initiated accidents. His research interests were code development for neutron dynamics and thermo-fluid dynamics

of the reactor core, including the coupling of 3D-neutronics models with plant system codes. In addition, he has experience in safety review of nuclear design, thermal design, and accident analysis of BWRs and PWRs as well as of VVERs and RBMKs of Russian design. He is a member of national and international working groups for the requirements of nuclear design. He has numerous publications in the field of reactor core dynamics.

Frederick J. Moody

Frederick J. Moody is a Consulting Engineer in Thermal-Hydraulics, who has participated in numerous NRC - sponsored peer review groups and Technical Program Groups, involving the analysis of postulated nuclear reactor accidents. He received his Ph.D. in Mechanical Engineering from Stanford University in 1971. He completed 41 years of reactor and containment safety analyses at the General Electric Nuclear Energy Division, where he developed various industry-standard analytical models for studies involving pipe and component rupture blowdown of high pressure steam and water mixtures, containment pressure and jet impingement loads, waterhammer forces associated with pipe flow accelerations, dynamic and thermal response of nuclear reactor core components during accident conditions, and fluid-structure interaction of submerged structures. He has taught numerous engineering courses as an adjunct professor for 28 years at San Jose State University, as an in-plant instructor at General Electric, and more recently as an instructor for professional development courses sponsored by the American Society of Mechanical Engineers. He has authored numerous journal papers, written an engineering textbook, *Introduction to Unsteady Thermo-Fluid Mechanics* (Wiley Interscience, 1990), and co-authored *The Thermal-Hydraulics of a Boiling Water Nuclear Reactor*, 2nd Ed., ANS Press, 1993.

Arthur T. Motta

Arthur T. Motta has worked in the area of radiation damage to materials with specific emphasis in Zr alloys for the last fifteen years. He received a B.Sc. in Mechanical Engineering and an M.Sc. in Nuclear Engineering from the Federal University of Rio de Janeiro, Brazil, and a Ph.D. in Nuclear Engineering from the University of California, Berkeley. He worked as a research associate for the CEA at the Centre for Nuclear Studies in Grenoble, France for two years and as a post-doctoral fellow for AECL at Chalk River Laboratories, Canada, before joining Penn State in 1992. The research programs he developed at Penn State include mechanical behavior of Zr alloys, advanced techniques for characterization of Zr alloys, and its oxides, defects in intermetallic compounds and phase transformation under irradiation. He has expertise in transmission electron microscopy, charged particle irradiation, mechanical testing, positron annihilation spectroscopy and theoretical expertise on phase transformations under irradiation and microstructural evolution under irradiation. He has recently authored review articles on amorphization under irradiation and on zirconium alloys in the nuclear industry. He was recently guest editor for a special issue of the Journal of Nuclear Materials, and was a member of a

DOE panel to evaluate research needs on radiation effects on ceramics for radioactive waste disposal.

Mitchell E. Nissley

Mitchell E. Nissley obtained his B. S. and M. Eng. degrees in Nuclear Engineering from Rensselaer Polytechnic Institute. Mr. Nissley has been on the staff of the Westinghouse Electric Company for 18 years; he is currently the leader of the team responsible for the development, licensing and application of the various realistic large break LOCA analysis codes and methodologies employed by Westinghouse. His contributions to the nuclear industry include the development and licensing of critical heat flux correlations for advanced PWR and VVER fuel designs, and the development and licensing of realistic large break LOCA evaluation models for Westinghouse PWR designs (cold leg injection, upper plenum injection and AP600). He has numerous journal and conference publications.

Katsuhiro Ohkawa

Katsuhiro Ohkawa is an advanced technical engineer at Westinghouse Electric Company. He received his BS in Physics from Sophia University in Tokyo, MS (1978) and PhD (1983) in Nuclear Science and Engineering from Rensselaer Polytechnic Institute. His experience at Westinghouse includes the development of Liquid Metal Advanced Nuclear Plants, BWR and PWR safety methods. Since 1990, he has been involved in the development of CSAU based Best Estimate Large Break. Currently he is involved in the development of Best Estimate Small Break LOCA Methodology.

Kenneth L. Peddicord

Kenneth L. Peddicord is Associate Vice Chancellor and Professor of Nuclear Engineering at Texas A&M University. He received his B.S. degree in Mechanical Engineering from the University of Notre Dame in 1965. He obtained his M.S. degree in 1967 and his Ph.D. degree in 1972, both in Nuclear Engineering from the University of Illinois at Urbana-Champaign. From 1972 to 1975, Dr. Peddicord was a Research Nuclear Engineer at the Swiss Federal Institute for Reactor Research (now the Paul Scherrer Institute) where he worked in the plutonium fuels program. From 1975 to 1981, Dr. Peddicord was Assistant and Associate Professor in the Department of Nuclear Engineering at Oregon State University. From 1981 to 1982, he was a Visiting Scientist at the EURATOM Joint Research Centre in Ispra, Italy where he was involved in the Super Sara Severe Fuel Failure Programme. In 1983, Dr. Peddicord joined Texas A&M University as Professor of Nuclear Engineering. He has served as Head of the Department of Nuclear Engineering (1985-88), Associate Dean for Research (1988-91), Interim Dean of Engineering (1991-93), and Director of the Texas Engineering Experiment Station (1991-93). Since 1994, he has been Associate Vice Chancellor of the Texas A&M University System. Dr. Peddicord serves as the representative of the A&M System to the Governing Board of the Amarillo National Resource Center for Plutonium. Dr. Peddicord's research

interests are in the performance and modeling of advanced nuclear fuels. Since 1995, he has been a participant in joint DOE-Minatom activities on excess plutonium disposition and nuclear materials safety. Dr. Peddicord has 120 publications in technical journals and conferences. He is a registered professional engineer in the state of Texas and has been a member of the American Nuclear Society since 1975.

Gerald Potts

Mr. Potts of Global Nuclear Fuel received a Bachelor of Science degree in Mechanical Engineering from the University of California, and a Master of Science degree in Mechanical Engineering from Santa Clara University. Mr. Potts has accumulated 28 years experience in the commercial nuclear power industry within the General Electric Nuclear Energy division. Mr. Potts' responsibilities and experience include fuel rod thermal-mechanical design, fuel rod thermal-mechanical performance and licensing basis analytical model development, and fuel integrity assessment under normal steady-state operation, anticipated operational transient, and accident conditions.

Joe Rashid

Joe Rashid is a Fellow of the ASME and a registered Nuclear Engineer. His general field of expertise is computational thermo-mechanics, structural mechanics and material constitutive modeling. He acquired his graduate and undergraduate education in mechanics at the University of California Berkeley, receiving the PhD degree in 1965. Having received his education at the birth place of the Finite Element Method in the early sixties, Dr. Rashid was among the pioneering contributors to its development, in particular three-dimensional computations. Dr. Rashid's three and a half decades career in the nuclear industry began with the gas-cooled reactor technology at General Atomics in San Diego, followed by an eight-year career in BWR technology at General Electric in San Jose, and finally at ANATECH Corp. which he founded in 1978. At General Atomics, his work in the mechanics of concrete reactor vessels and nuclear fuel particles led to the development of the smeared-crack model, which was adopted in finite element codes as the basic model for the cracking analysis of brittle materials. At GE, he was responsible for the development of the industry's first two-dimensional fuel rod behavior code for the analysis of the then-emerging pellet-clad interaction (PCI) problem. At ANATECH, Dr. Rashid undertook the development of the transient fuel analysis code FREY for the Electric Power Research Institute (EPRI). In the aftermath of the Three Mile Island accident, EPRI's collaboration with Sandia in reactor containment research, with Dr. Rashid as the principal investigator for EPRI, led to the institutionalization of the leak-before-break concept for reactor containment structures, thereby profoundly affecting risk assessment of loss of coolant accidents. He participated in severe accident work with Sandia and EPRI, which included the development of constitutive models and analysis methods for the creep rupture of pressure vessel lower head under loss of coolant accident. He participated in the expert review process for NUREG-1150, and was nominated by

NRC to chair an international expert panel for OECD'sVessel Investigation Project. Dr. Rashid's publications in the various fields of activity in which he had primary contributions exceed 100, which include journal articles, reports and white papers.

Richard J. Rohrer

Richard J. Rohrer serves as a member of the High Burn-up Fuel Phenomena Identification and Ranking Table (PIRT) Panel. He is a registered professional engineer in the state of Minnesota. He obtained a B.S. in Nuclear Engineering from the University of Illinois, and an M.S. in Nuclear Engineering from the University of Wisconsin in 1983. He also holds an M.S. in Management from Cardinal Stritch College, and a Senior Reactor Operator Certification for the Monticello Nuclear Generating Plant. Mr. Rohrer has over 16 years experience supporting operations of nuclear power reactors, including licensing, reactor engineering, probabilistic safety assessment, core design, accident analysis, and transient analysis. He currently manages projects for the Monticello Nuclear Generating Plant in the Nuclear Analysis and Design group with Nuclear Management Company. Mr. Rohrer is a member of the American Nuclear Society and has published five technical papers on probabilistic safety assessment and Boiling Water Reactor stability. In addition, he is an active participant in the Electric Power Research Institute's Robust Fuel Program.

James S. Tulenko

James S. Tulenko is Chairman of the Nuclear and Radiological Engineering Department and a Professor of Nuclear Engineering at the University of Florida. He received his B.A. with honors in Engineering Physics from Harvard College and his M.A. in Engineering Physics from Harvard University in 1960. After military service in the Corps of Engineering, he obtained a M.S. in Nuclear Engineering from the Massachusetts Institute of Technology in 1963. In 1980 he obtained a M.E.A. from George Washington University. Professor Tulenko's professional activities have included all aspects of the nuclear fuel cycle. He has over 35 years of experience in fuel design, fuel operation and fuel performance. Professor Tulenko was Manager of Nuclear Development at United Nuclear Corporation where he patented the water hole thermalization concept now utilized in all boiling water reactors. He also was project engineer for one of the first Plutonium reloads in a commercial reactor. He served as Manager of Physics for Nuclear Materials and Equipment (NUMEC) Corporation where he headed up nuclear physics activities. He later served as Manager of Physics and Manager of Nuclear Fuel Engineering for the Nuclear Power Division of Babcock and Wilcox. In 1979 he was made a Fellow of the American Nuclear Society (ANS) for his contributions to the fuel cycle. In 1980 he received the Silver Anniversary Exceptional Service Award of the ANS for his outstanding contributions to the Nuclear Fuel Cycle in the first 25 year of the ANS. In 1997 he received the Mishima Award of the ANS given for outstanding contributions to Nuclear Material Research. He also was awarded the Glenn Murphy Award of the American Society of Engineering Education given to the Outstanding Nuclear Engineering Educator. He is a Board Member of the National

Nuclear Accrediting Board of the Institute of Nuclear Power Operations and a Board Member of the American Nuclear Society. He is also a Commissioner of the Engineering Accreditation Commission. He has over 100 journal and conference publications and has consulted for a variety of government agencies and commercial companies.

Keijo Valtonen

Keijo Valtonen is a Chief Inspector with the Radiation and Nuclear Safety Authority of Finland. He obtained his degree from the University of Helsinki where he majored in reactor physics and thermal hydraulics. His primary duties since 1975 have been fuel, nuclear and thermal-hydraulic design of reactor cores; transient and accident analysis for Loviisa (VVER-440 type PWR) and Olkiluoto (ABB-Atom type BWR); and operator qualification, including oral licensing examinations and review of operator instructions. He has reviewed plant feasibility studies, including those for the VVER-1000, ABB-Atom BWR 90, Siemens PWR, and SECURE and PIUS. He has reviewed numerous feasibility studies for new fuel designs, including VVER Zr 1% Nb, BNFL-VVEF fuel, ABB 8x8, SVEA 64, SVEA 100, Siemens 9x9, GE12 and Siemens ATRIUM 10. He has participated in safety reviews for the RBMK. He has engaged in research work on the transient behavior of BWR and PWR reactor cores, BWR stability analysis, validation of TRACB and RAMONA computer codes, PWR boron dilution, and several fuel transient behavior studies for VVER and BWR reactors. He has been engaged in international cooperative efforts including IAEA and OECD development of safety criteria for future nuclear reactors, regulatory approaches to severe accident issues for the OECD/CNRA, a state-of-the-art report on BWR stability, the European Union's safety RBMK safety review, the OECD/CSNI task force of fuel safety criteria.

Nicolas Waeckel

Nicolas Waeckel is a visiting senior engineer from EDF to EPRI. During his stay at EPRI he managed the Working Group 2 (response in transient) within the Robust Fuel Program. Nicolas Waeckel was the Technical Leader and Manager of the Nuclear Fuel design and Survey Group at Electricité de France (EDF) Septen. At EDF he developed and managed fuel R&D programs including fuel R&D programs addressing RIA and LOCA issues. He developed and managed activities in areas of nuclear fuel rod and nuclear fuel assembly design, design methodologies and fuel rod performance code development (normal operation conditions and accidental conditions). He represented EDF in interacting with the French Safety Authorities on many key issues (RIA, LOCA, fuel assembly distortion, burn-up extension, etc...). From 1984 to 1990, he was in charge of the FBR and the LWR Structural Mechanics Design Group thereafter. He has developed several design methodologies (buckling of thin shells, creep-fatigue and progressive deformations) and participated to the writing of the RCCMR (design rules for the FBRs). He managed 15 PhD students and 20 contracts with Universities, CEA and Novatome. He has authored papers and reports in areas of mechanical design of thin structures (buckling, creep-fatigue, ratchetting and fracture mechanics) and nuclear fuel design and performance (PCMI,

High burn-up properties, RIA and LOCA). He obtained an MS in Civil Engineering from the National Institute of Applied Sciences in Lyon (France) in 1978, a PhD in 1981 and a Sciences Doctorate in 1983 from the same Institute. The topic of his Sciences Doctorate Thesis was the impact of initial geometrical defect on buckling of FBR related thin structures.

Wolfgang Wiesenack

Wolfgang Wiesenack is the acting general manager of the OECD Halden Reactor Project. He obtained an MS in nuclear engineering from the University of Hanover, Germany, in 1976 and a PhD in nuclear engineering and LWR fuel behavior modeling from the same university in 1983. Dr. Wiesenack had a research assistant position at the University of Hanover, working on LOCA analysis (RELAP 4) and modeling of LWR fuel behavior in normal operating conditions. He joined the OECD Halden Reactor Project in 1984. As senior reactor physicist he was responsible for the core physics calculations of the Halden reactor, including nuclear design studies of experimental rigs, core loadings and updating of the reactor's safety report. He was also responsible for the data acquisition of the reactor and implemented a completely renewed system. As the head of the Data Acquisition & Evaluation division, he was in direct contact with many aspects of fuels and materials behaviour under steady state and ramping and transient conditions. He was actively engaged in the execution of the IAEA code comparison exercise FUMEX to which the Halden Project provided the data. He was also a member of the FRAPCON peer review team. He is a member of the German nuclear society.

APPENDIX I

TUTORIAL PRESENTATIONS TO THE PIRT PANEL

This appendix contains information presented to the PIRT panel with the objective of assisting the panel members to develop a common understanding of LOCA phenomena and fuel behavior in PWRs and BWRs.

I-1 PWR Large-Break LOCA: Impact of High Burnup Fuel

Panel members Lawrence E. Hochreiter, Mitchell E. Nissley, and Bert Dunn prepared this review for the PIRT panel.

I-1.1. Introduction

The Large-Break Loss of Coolant Accident (LBLOCA) will be examined for two different types of Pressurized Water Reactors (PWRs). First, the typical response of a Westinghouse plant, using the approved Appendix K Evaluation Model (EM) will be examined, then the plant response using the approved Westinghouse best estimate calculation will be examined. The response of a Babcock and Wilcox lowered loop PWR will also be examined. In addition to the system response for these plant designs, the fuel temperature and cladding behavior will be examined.

A LOCA is defined as a failure of the main reactor coolant piping which is sufficiently large enough to cause a safety injection signal in which the Emergency Core Cooling system (ECCS) is initiated. This is usually a break which is larger than 3/8 of an inch. Breaks smaller than this size are classified as leaks since the normal plant charging systems have sufficient make-up flow to prevent draining of the reactor coolant system. There are two classifications of breaks; Small Breaks are breaks that are less than one square foot in flow area, and large breaks are breaks that are larger than one square foot in area up to and including a full size double-ended guillotine rupture of the main reactor piping. A Double-Ended cold Leg Guillotine break (DECLG) can have a flow area of approximately nine square feet.

The LBLOCA has been used as the design basis accident for the light water reactors, and it's really a "battleship in the desert" type of approach in which the vendor is asked to analyze this accident without regard to the probability of the accident occurring. The real purpose of analyzing the accident is to verify that the design and function of the emergency core cooling systems, which are provided for the safety of the plant, which recover the plant and limit the fuel damage to acceptable levels. The LBLOCA is used as a calculation exercise, basically to verify the performance of the emergency core cooling system.

In 1965 and earlier, the LOCA was defined as the failure of the largest connecting pipe to the reactor coolant main piping, which is the pressurizer surge line. This is a hot leg

break. This break is a "good break", because all the flow has go to go through the core to go out through the break, so very good core cooling is obtained. About 1966, the break was moved to the failure of the main reactor coolant piping, which was a much more severe break because the break was larger and not all the flow would go through the core. This change resulted in very high-calculated fuel rod cladding temperatures. As a result, additional safety equipment was added to plants. On the Westinghouse plants, cold leg accumulators were added and the low-head pumped systems were up graded and so forth.

There were a whole series of safety concerns that were occurring in the late 1960s and early 1970s, when a large number of these plants were being ordered, and the power for the plants was increasing very rapidly. There were a series of hearings that were held in the early 1970s called the Core Cooling Hearings, and these hearings provided the basis for the regulations that came out in 10 CFR 50.46 and Appendix K of the General Design Criteria. The regulations that were a result of those hearings were acceptance criteria on the performance of the safety systems and the resulting temperatures and oxidation levels and cool ability of the core that were allowable for light water reactors. The requirements included: the peak allowable fuel rod cladding temperature cannot exceed 2200 degrees Fahrenheit; the local cladding oxidation cannot exceed 17 percent; the core-wide oxidation cannot exceed one percent; the core must maintain a coolable core geometry; (This was never really well defined, in a sense, because fuel rod ballooning and bursting is allowed to occur, but the intent here is that a rod-like geometry exists in the core, because the heat transfer database is based on a rod-like geometry to generate the heat transfer models and correlations that are used to calculate the performance of the fuel); and ensure that the safety systems provide long-term cooling of the core to remove the decay energy. These are the criteria that have been used to evaluate the performance of the plant safety systems, by analysis, using a calculation model of the plant. In addition to the criteria, the results of the Core Cooling Hearings were to develop a detailed list of modeling requirements, which were specified in Appendix K of the General Design Criteria, which reflected the safety analysis knowledge at that time. This froze safety analysis technology in a 1972 timeframe and it was very difficult to improve the models at that time. One had to license new models that still conformed to the Appendix K requirements, which were very prescriptive. The results of applying the Appendix K Evaluation Models for the plant safety analysis resulted in lower linear heat rates for the plants. The LBLOCA became the limiting transient for Westinghouse plants and the LBLOCA is usually the most limiting transient for the other vendor's designs as well.

In 1988, after a substantial NRC confirmatory research program that lasted almost 20 years, in cooperation also with EPRI and with industry, there was a significant amount of effort spent to try to determine the conservatisms in the requirements in Appendix K, and to provide a database which could be used then to perform more realistic calculations of the LBLOCA accident. One approach was to realistically model the plant response to the accident. That is, given the accident, how to more realistically calculate

the performance of the safety systems and the performance of the reactor system itself? This was actually something that the NRC was encouraged to do immediately after the Appendix K rule came out, by the American Physical Society. It was felt that the NRC would be better served if it had best-estimate analysis capability, because the NRC could then make better judgments regarding how the reactor system responded to the accident.

In 1988, after the confirmatory research program was complete and the margins associated with the Appendix K evaluation models could be quantified, the rule was changed to allow the use of best-estimate methodology. The modified rule permitted the additional experimental information that had been generated to improve the analysis capability. The ECC performance requirements remained the same, however, the main difference now was that a best-estimate approach could be used which resulted in a more accurate model which could better predict the performance of reactor safety systems such that a higher linear heat generation rate could be calculated for the plant. So in a sense, the best-estimate calculations have regained margin in terms of kilowatts per foot for the plants using improved safety analysis methods and the results of the confirmatory research program.

I-1.2. The Large-Break LOCA Transient Behavior

Figure 1 shows a schematic of a Westinghouse four-loop plant. In Westinghouse designs, the power per loop is roughly the same, approximately 300 megawatts each for each loop. In this fashion, the pumps, steam generators and piping sizes are the same for a 2,3, and 4-loop plant design. As seen in the figure, there are a steam generator, hot leg, loop seal, reactor coolant pump, and cold leg for each loop. When doing a LOCA analysis, the worst break location must be determined. Typically, for a large break LOCA, the worst break location is in the cold leg. The cold leg, at the pump discharge, has been found to be the most limiting-break location for all the designs, not only Westinghouse but other designs as well.

For a large break in the main reactor cooling piping system, the break flow area is very large (typically 9 square feet) so that the transient is very rapid. There are three periods for the large-break LOCA: blowdown, refill, and reflood as shown in Fig. 2. The blowdown period which is approximately 30 seconds long is when the initial inventory that is in the reactor system, is lost out the break. The passive cold leg accumulators will start to inject as the plant depressurizes and there can be some high pressure pumped safety injection also occurring as the plant is depressurizing. The timing of these systems is design specific and depends on the set point pressure of the accumulators and the start-up time of the emergency diesels for the plant.

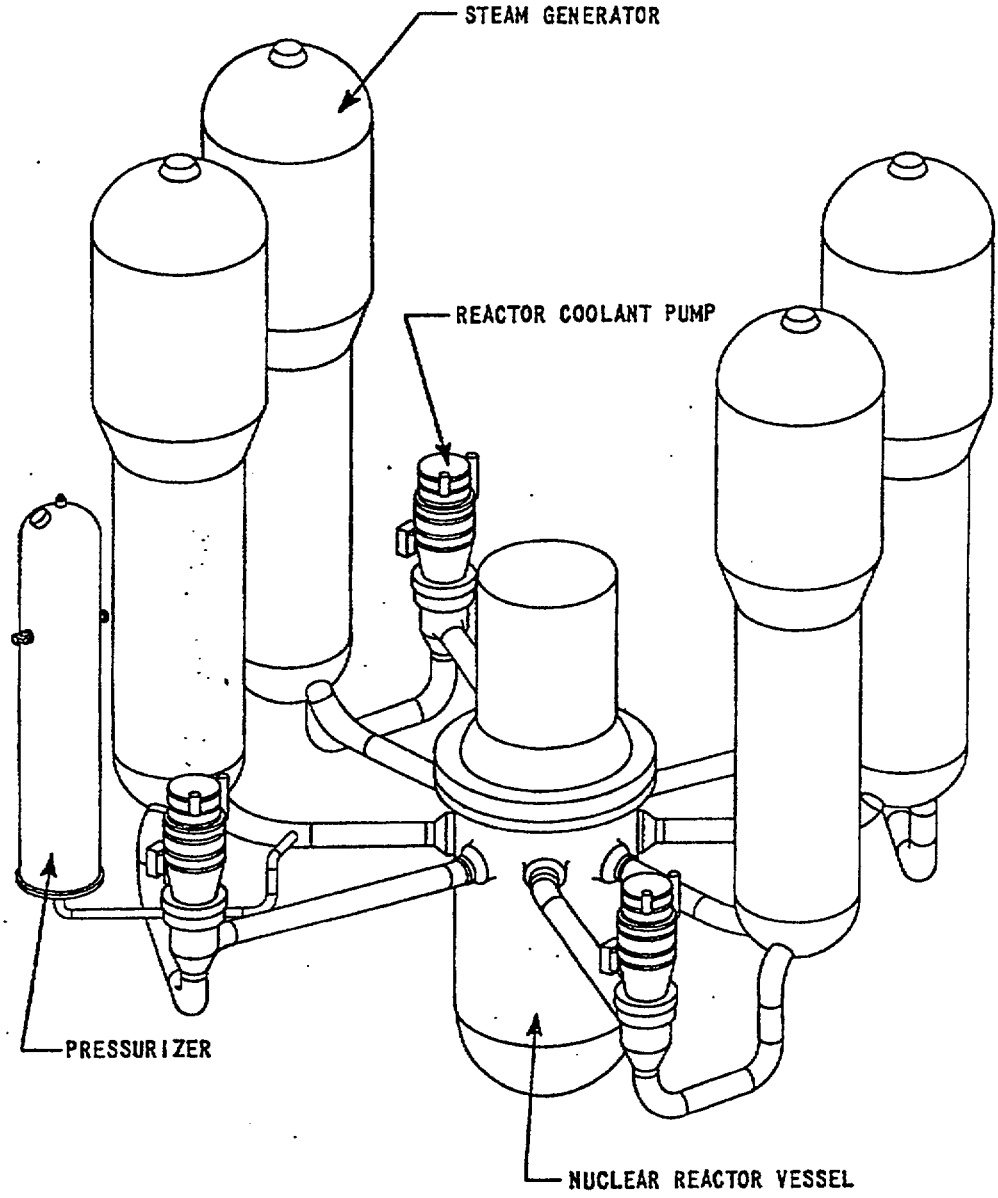

Westinghouse NUCLEAR STEAM SUPPLY SYSTEM

MB 3595

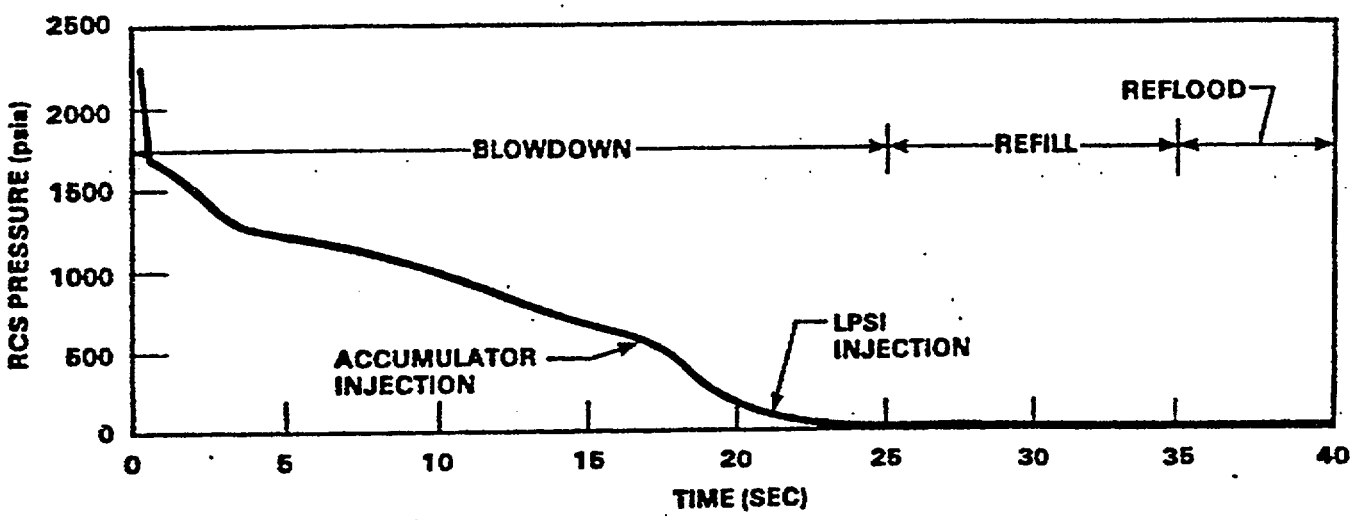

The blowdown is a very rapid transient and there will be flow reversals that occur in the core. The core will quickly go through critical heat flux, and the reactor will shut down due to voiding in the core. No credit is taken for control rods to shutdown the fission reaction in the core, at least for PWRs. The core flow reversals that occur depend on the pump and break interaction, and depend upon how many loops there are in the plant, which means how many pumps there are in the plant. One can calculate more upflow or more downflow depending on the number of pumps (loops) and the break size. This will result in different degrees of cooling depending on whether the flow is up or down in he core and the amount of liquid carried in the flow. The high-pressure safety injection will automatically initiate for most plants during blowdown, but this is a very low flow, high head system. Most of the water that is injected from this system basically goes straight out the break.

Cold leg accumulators will initiate in the Westinghouse plants and in the Babcock & Wilcox plants at a set point pressure of approximately 600 psi. These are passive injection systems. The accumulators are large tanks full of cold borated water, which are isolated from the primary system by check valves, and when the system pressure drops below the set pressure in the check valves these tanks start to inject. In the Combustion Engineering plants most of the cold leg accumulators are set at a set point pressure, 200 psi, so there is a longer delay before those accumulators start to inject.

ECCS bypass occurs during blowdown as shown in Fig. 3. ECCS bypass means that the accumulator flow that is injected into an intact cold leg can be entrained by the steam flow coming up the downcomer and swept around the downcomer annulus and out the break. If there is a high upflow in the downcomer annulus, the flow that is injected can go around the annulus and out the break instead of penetrating down the annulus to fill the vessel as seen in Fig. 3. In the original Appendix K rules, there were stipulations on the amount of credit that can be taken for the injection flow from the accumulators. It

was determined that the accumulator flow would be bypassed until it could be shown that the steam flow up the vessel was low enough that the liquid flow from the accumulators could flow down the downcomer into the lower plenum.

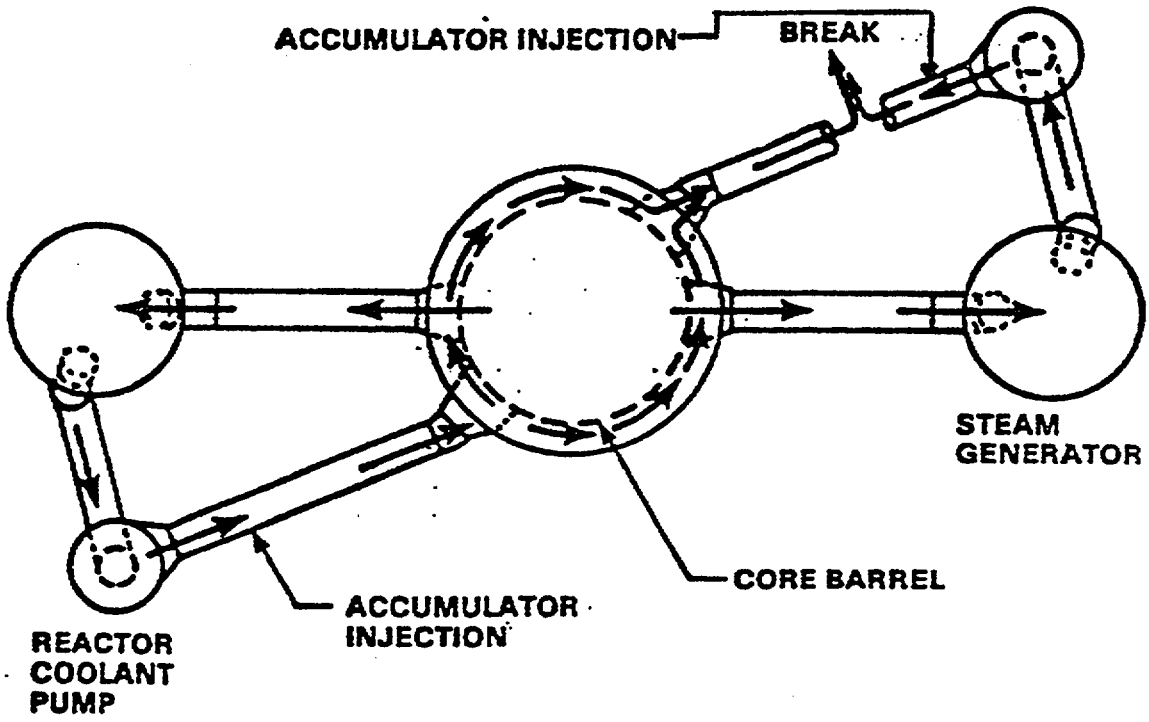

Cold Leg Break Steam Flow Path

Since the 1972 core cooling hearings, there have been full-scale tests run on ECC bypass in Germany as part of the NRC program of confirmatory research. What was observed in those experiments was that for situations in which there was accumulator injection in the loops on the opposite side of the break, the flow from these accumulators would penetrate into the downcomer and begin to refuel the lower plenum, so ECC bypass earlier would actually end earlier. The experiments also showed that the accumulator in the broken loop was completely lost and the accumulator in the cold leg next to the broken cold leg would also bypass a large fraction of its flow during blowdown. Best estimate computer codes have been used to predict the accumulator flows and bypass flow rates in a more accurate manner. However, the code predictions tend to underestimate the amounts of water, which penetrate the downcomer and hence, over-predict the amount of accumulator water, which is bypassed. This is a conservative bias in the best-estimate computer codes.

Toward the end of blowdown, the minimum vessel inventory is reached because most of the initial reactor coolant system inventory is blown out the break.

Now as indicated earlier, there are three phases for the large break LOCA. The blowdown lasts approximately 30 seconds. This is when the primary inventory is vented out the break; the core goes through DNB, voids, and shuts down. The cladding heats up and this is primarily due to the stored energy temperatures of 1600 degrees Fahrenheit can be exceeded. The next period is refill, which is approximately ten seconds in duration, during which refill of the reactor vessel begins, primarily filling the lower plenum to the bottom of the heated length of the fuel rods, and to beginning to reflood the core.

During the "refill period," the lower plenum is being refilled. ECC bypass is ended, and the core is in a stagnant steam environment and is heating up almost adiabatically. There can be some radiation heat transfer to the guide tube thimbles and rod-to-rod radiation heat transfer.

The low-pressure safety injection system starts to activate since the reactor system has depressurized and the reflood process has begun. Figure 4 shows the reflood process as the core begins to reflood. Fuel rod burst can occur in this time period because the cladding temperatures are very high. They are generally in excess of 1600 degrees Fahrenheit, and now the system pressure is very low, so the differential pressure across the cladding from the inside of the cladding to the system itself is very large, and clad ballooning and failure can occur in this timeframe.

Again the safety systems that the plant has to cope with the LBLOCA transient are shown in Fig. 5. There are the cold leg accumulators where there is typically one per loop, one per cold leg. There is a high pressure (high head) safety injection system with injection into each loop. Some plants also have intermediate pressure injection systems.

All plants have low pressure safety injection systems, which inject into the cold legs.

The different safety injection systems will initiate at different pressure levels depending on the plant design. The systems are loaded on emergency diesels, so in the analysis the start time of the diesel and the delay times of the signals to start the systems must be considered. These pump systems pull suction from the refueling water storage tank, which is outside the containment. The refueling water storage tank typically contains about 350,000 gallons of borated water. The pump systems will inject water from the tank up to 20 minutes and then will automatically switch over and pull suction from the reactor sump. It is the pump systems that provide the long-term decay heat removal, post accident, long term cooling for the core. The highest flows into the reactor vessel come from the accumulator and then the next highest flow comes from the low pressure injection systems.

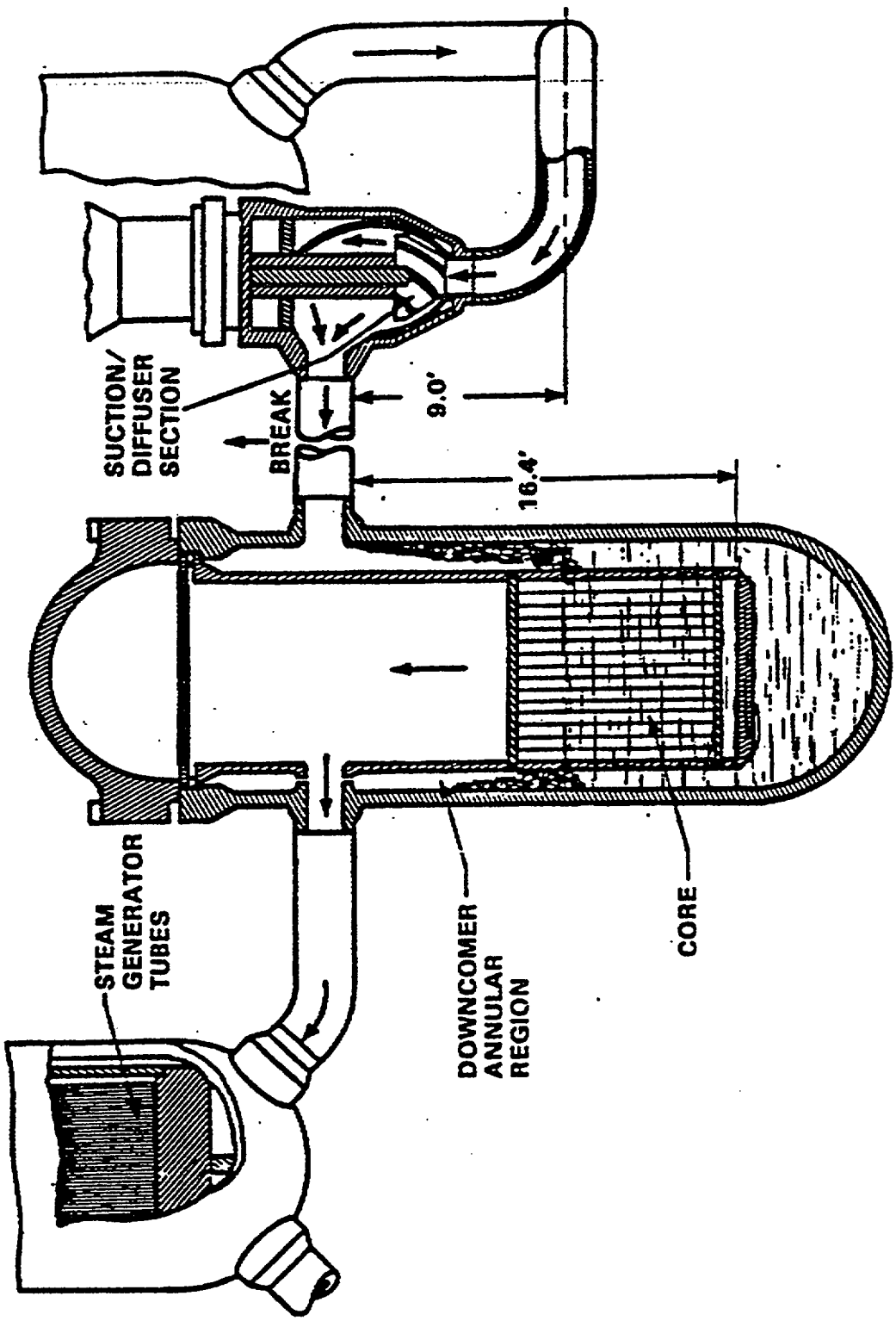

Cold Leg Break Steam Flow Path Schematic Drawing

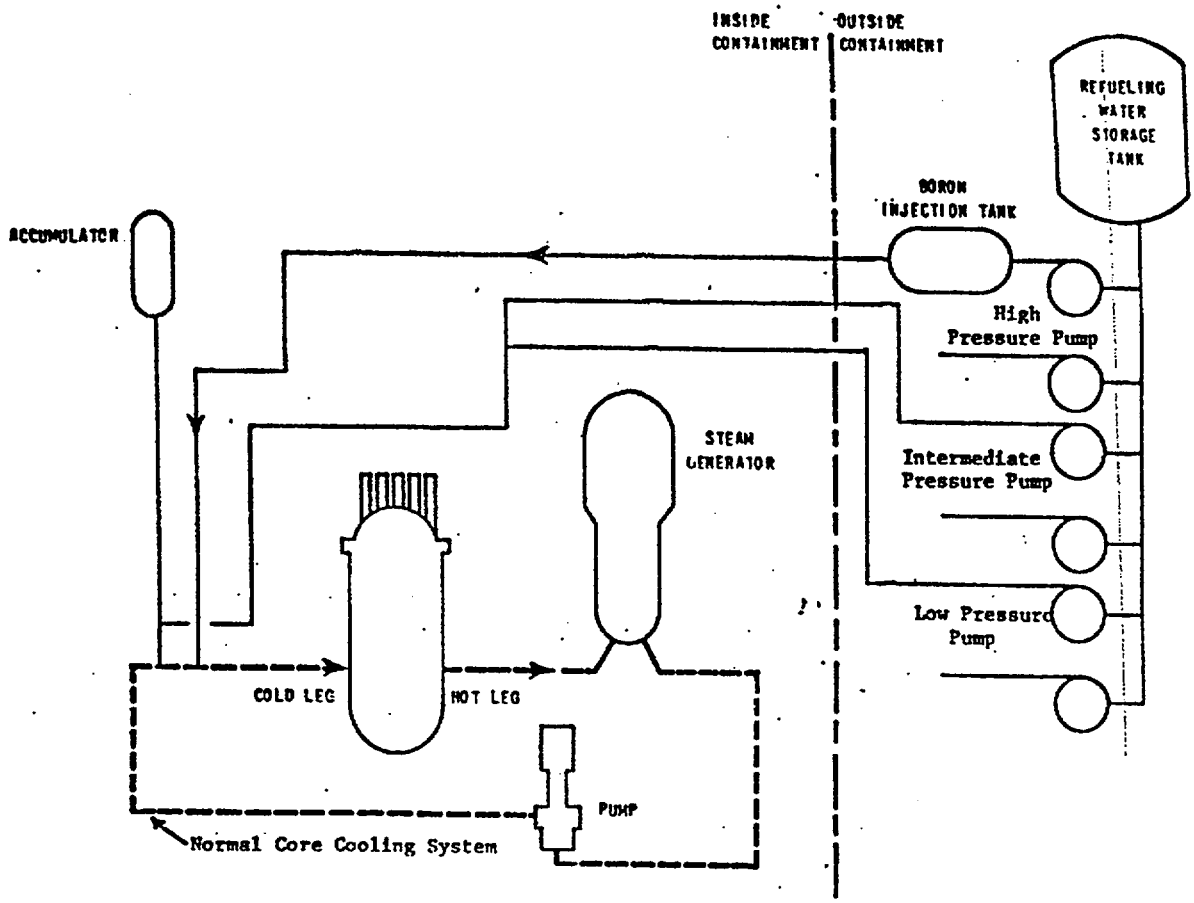

Once the lower plenum is refilled, the core then begins to reflood as seen in Fig. 4. Reflood typically starts at about 40 seconds after the accident and can last until up to 600 seconds before the core is completely quenched and the fuel rods are approximately at the saturation temperature in the entire core. The accumulators are designed and sized such that there is sufficient water in the accumulators to fill the downcomer with water. This provides a driving head for reflood. The reflooding situation is a passive gravity-driven situation. Basically, the accumulators fill the downcomer, which provides 16 feet of driving head to force the flow into the core. The flow goes into a hot core, generates a two-phase mixture, provides cooling and exists the core, goes through the hot leg, into the hot steam generators through the cross over leg, through the reactor coolant pump (which acts as a large resistance), to the cold leg, into the downcomer annulus, around the annulus and out the break. The reflood flow path is shown in Fig. 4 and the details of the reflood process in the core are shown in Fig. 6. Since the system is depressurized so that the primary pressure now is well below the secondary side pressure, the steam generators secondary side is much hotter as compared to the primary side saturation temperature. The stagnant water on the secondary side (note, the secondary side is isolated for the transient) is typically 500 to 525 degrees Fahrenheit, so as a two phase mixture is swept into the steam generator tubes on the primary side, it will all evaporate or a large fraction of it will evaporate.

This will result in an increased steam flow rate of superheated steam leaving the steam generator, which will result in a large pressure drop across the reactor coolant pump since the pump is a large hydraulic resistance. Since, there is only 16 feet of water in the downcomer to force flow to the core and to overcome the pressure drops in the steam generator and the reactor coolant pump. Therefore, the flooding rate into the core is very low; typically it is one-inch per second or less for the majority of the reflood transient. This is called the "steam binding effects" for PWR reflooding.

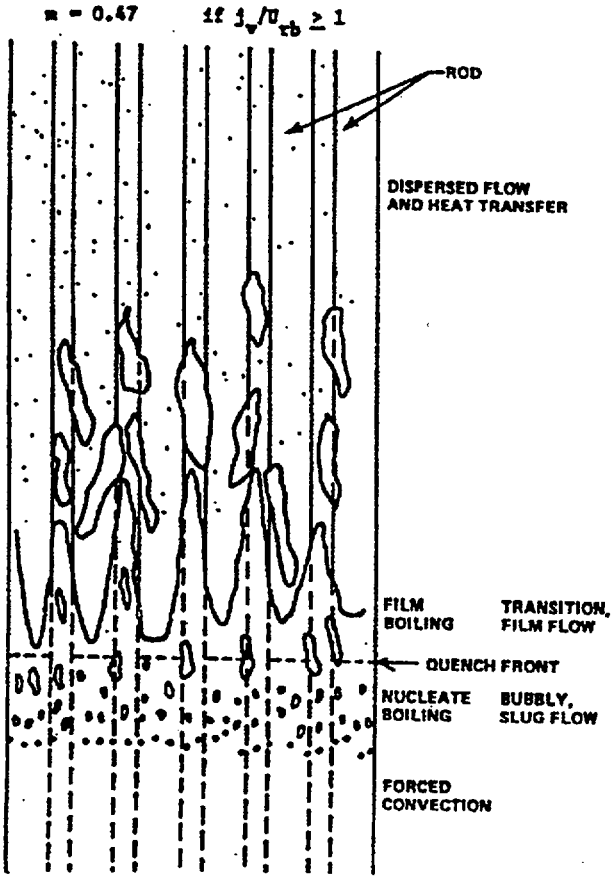

Typical Conditions in Rod Bundle During Reflood

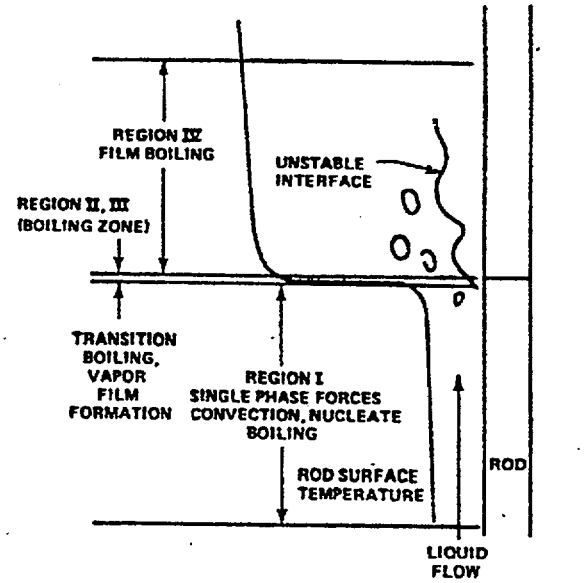

Hydrodynamic and Heat Transfer Regions Near Quench Front

If the plant design has a very low containment back pressure, like a Westinghouse ice condenser plant, the steam specific volume is very large at low pressure, such that for the same mass that gets evaporated there is a much larger volume of steam that has to vented resulting in larger pressure drops in the steam generator and pump such that the flooding rate for these designs are even lower.

The important thing to note is that reflood is a gravity driven process. Pumps are injecting flow into the cold legs. The best they can do is keep this downcomer filled. Once the downcomer is filled, all subsequent water that is injected spills out of the break. After this point, no amount of pumping capacity contributes to putting cooling water in the core.

The peak cladding temperature, while it's different for different designs, for the Westinghouse plants, it will generally occur at reflood, either at the beginning or later during the reflood transient. For the B&W plant that is shown, the peak cladding temperature is calculated to occur at the very beginning of reflood.

Reflood is most critical portion of the transient. The heat transfer is generally the lowest here. The fuel rods will continue to heat up as the quench front advances and the peak cladding temperature is being pushed up the fuel as the quench front moves up.

The fuel rods are being cooled by dispersed flow boiling, heat transfer regime as seen in Fig. 6. If the rods have not burst during refill, they generally will burst during reflood, which results in flow blockage within the core. The flow blockage results in flow diversion and an additional peak cladding temperature penalty. As indicated earlier, the core flooding rates are low. In a Westinghouse plant they quickly drop below one inch a second flooding rate, so it take a long time to fill the reactor vessel and to provide the cooling. The dispersed, two-phase nonequilibrium mixture of superheated steam and drops cools the fuel rods. The calculated peak cladding temperatures exceed 1800 ^{0}F such that zirconium/water reaction can occur at these high cladding temperatures. The PCT generally occurs during reflood. The fuel rods will eventually cool down and quench. It takes approximately 5 minutes to quench the core.

I-1.3. Westinghouse Appendix K Evaluation Model LBLOCA Calculations for a Four Loop PWR

Calculations have been performed for a four-loop Westinghouse PWR using an approved Appendix K type of an evaluation model. One of the requirements of Appendix K is that different break sizes be simulated by changing the discharge coefficient on the break. The event timing for different break sizes are given in Fig. 7 and the calculated results for the different break sizes are given in Fig. 8. As Fig. 8 indicates, the 0.6 Double-Ended Cold Leg Guillotine (DECLG) is the most limiting break for this particular plant. The most limiting break size is plant size and type dependent and must be determined by performing a series of calculations for different break sizes or discharge coefficients to obtain a break spectrum. Figure 7 gives the timing for the

different DECLG transients for this plant. As the figure indicates, for the 0.6 DECLG the accumulator injection occurs at approximately 15 seconds, pump injection occurs at about 30 seconds, and blowdown ends at approximately 30 seconds. The bottom core recovery, which means the end of refill, occurs 13 seconds later (approximately 43 seconds). With blowdown ending at 30 seconds, the accumulators are empty at 53 seconds. This is the time period to fill the lower plenum and to fill the downcomer with the remaining flow in the accumulator, so a large fraction of the accumulator flow has been lost in this Appendix K analysis. A large fraction of the accumulator flow is lost because they have started injecting at 15 seconds but credit is taken only for the flow, filling the vessel toward the end of blowdown at 30 seconds. The hot rod has burst during the refill period in this case and the peak cladding temperature is occurring approximately three minutes into the transient as indicated in Figs. 7 and 8. Figure 8 gives the calculated value and location of the peak cladding temperatures for this range of breaks. For the most limiting break size, and the peak cladding temperature was calculated to be 2000 ^{0}F and it occurred at the eight foot elevation. . The calculated PCT is below the Appendix K limits and the local zirconium/water reaction is only 8 %, which is also under the limit of 17 % such that this represents an acceptable licensing calculation for this plant. The fuel rod burst occurred at six feet, the peak power location, but peak temperature occurred at eight feet as indicated in Fig. 8. What is usually found is that the peak, even with a symmetrical power shape, is usually above the peak power location. Therefore, power shapes, which are more limiting, are those shapes in which the power is skewed to the top of the core. The peak location is displaced toward the top of the core because reflooding is from the bottom of the core, and this tends to push the peak temperature location up the rod.

Time	C_D = 0.4 DECLG (Sec)	C_D = 0.6 DECLG (Sec)	C_D = 0.8 DECLG (Sec)
Break	0	0	0
Reactor trip signal	0.777	0.751	0.735
SI-signal	1.65	1.33	1.15
Intact loop accumulator injection	20.00	15.10	12.50
Pump injection	30.65	30.33	30.15
End of bypass	38.029	29.348	25.334
End of blowdown	38.035	29.348	25.334
BOC time	53.637	43.601	39.175
Intact loop accumulators empty	60.247	53.441	50.225
Hot rod burst time	57.08	40.00	44.26
Peak clad temperature (PCT) time	67.44	165.32	89.92

LARGE BREAK LOCA RESULTS FUEL CLADDING DATA

MINIMUM SAFEGUARDS

	C_D = 0.4 DECLG	C_D = 0.6 DECLG	C_D = 0.8 DECLG
RESULTS			
Peak clad temperature, F	1804.1	2014.0	1776.0
Peak clad temperature location, ft	7.00	8.00	8.00
Local Zr/H_2O reaction, maximum %	2.64	5.39	2.27
Local Zr/H_2O reaction, location for maximum reaction, ft	6.25	8.00	6.25
Total Zr/H_2O reaction, %	<0.30	<0.30	<0.30
Hot rod burst location, ft	6.25	6.00	6.25

Figure 9 shows the calculated core flows during the blowdown period. There is stagnation initially in the core and the flow exits out of the top and the bottom of the core. As blowdown continues, there is a positive core flow period and then core flow period during blowdown. This is caused by the interaction of the main reactor coolant pumps, the break, and the flow resistances between the core and the break. The pump flow in this case is for a four-loop plant, which is greater than the break flow early in time before the pumps cavitate. The difference between the break flow and the pump flow results in positive flow through the core, so the core heat transfer improves. But at some time, the pumps cavitate and loose their pumping capability. The break is still demanding the same flow, so the flow then reverses through the core and there is a negative flow through the core, which also provides some core cooling. For a Westinghouse three-loop plant, this zero flow point on Fig. 9 would shift upward because now instead of having three pumps to provide the flow to the break, there are only two, remembering that the cold leg pipe size (break size) is the same for all Westinghouse plants. If a two-loop plant is examined, all the flow is negative, or down through the core, during blowdown because the break demands more flow than the one pump can provide.

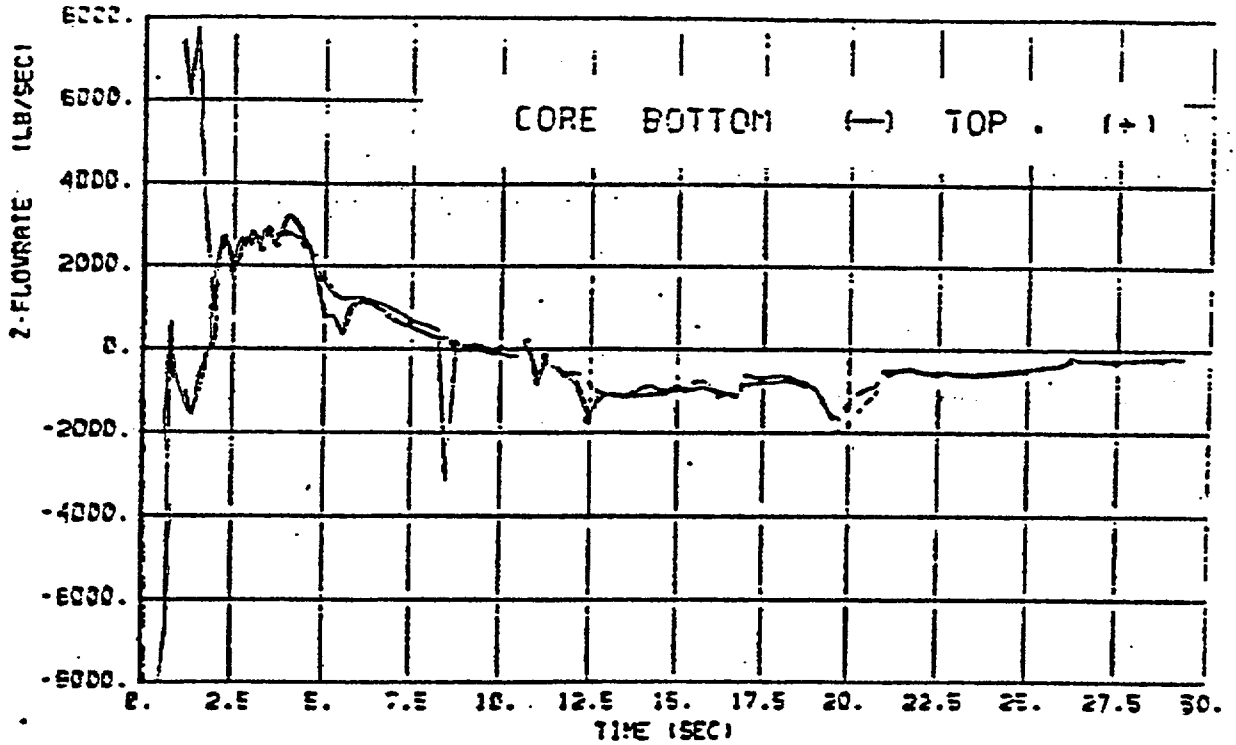

The pressure transient is shown in Fig. 10 and indicates that the containment pressure is reached in approximately 30 seconds. The accumulators begin injecting when the pressure typically reaches 600 psi. Again the accumulators are a passive injection system which provide high flow but for a relatively short period of time. The accumulator injection flow is shown in Fig. 11. In a four loop plant there are three accumulators that are injecting into the intact cold legs.

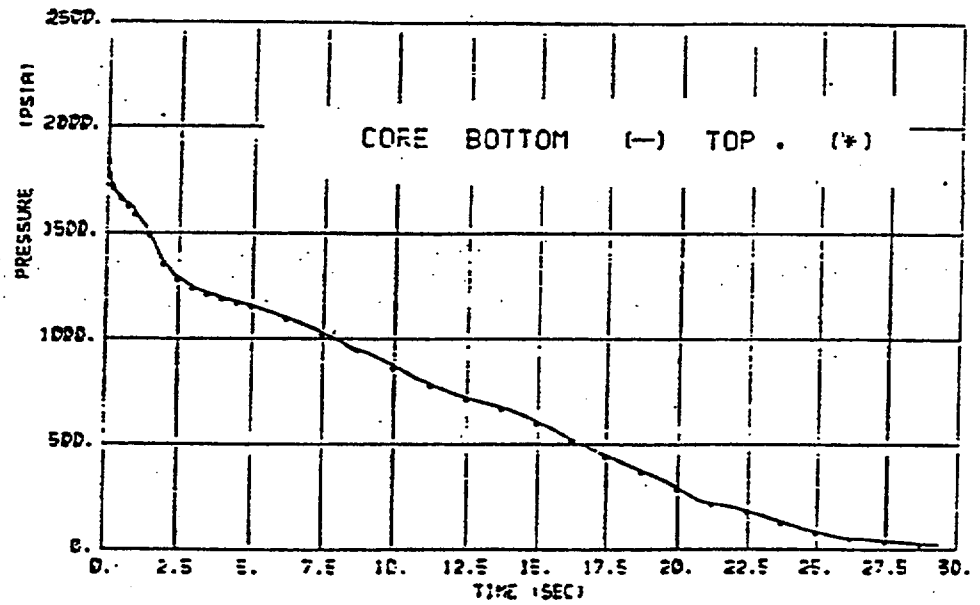

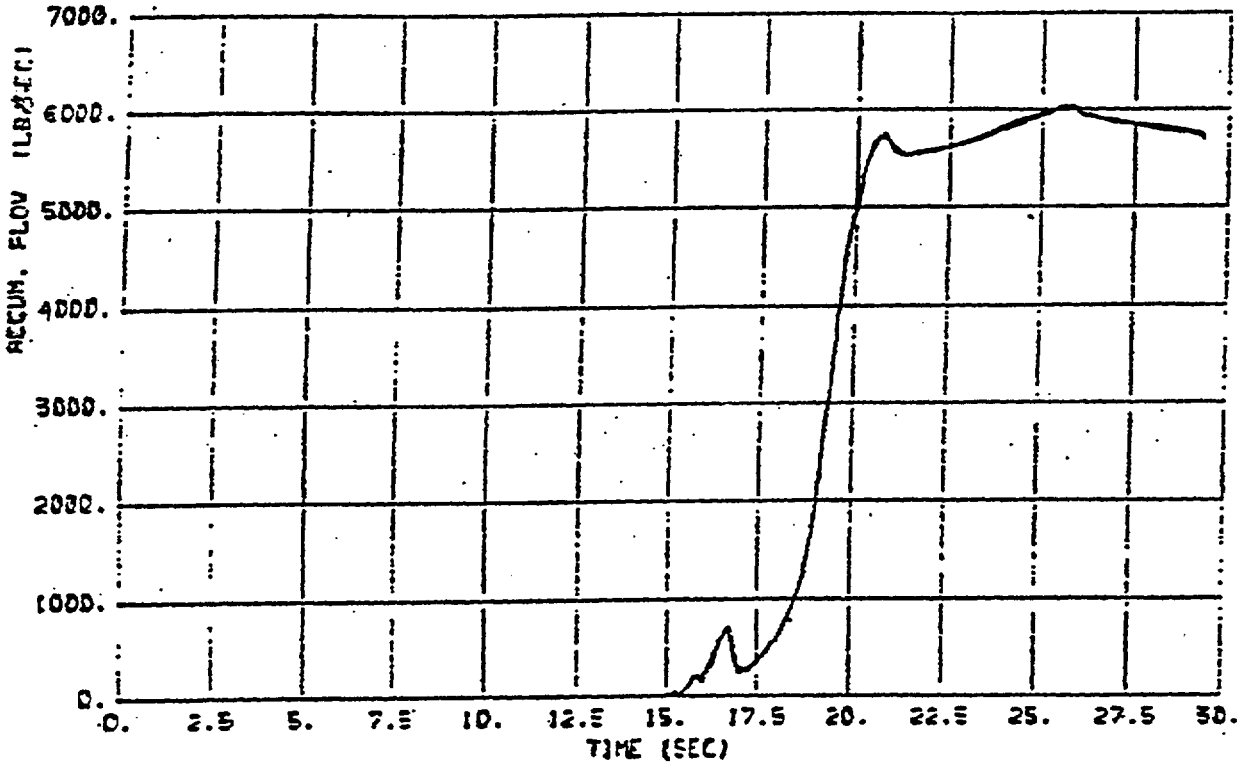

In the reflood period, the downcomer level increases and provides the driving head to force the water into the core. To overcome the pressure drop in the loops. a liquid level in the core is built up as seen in Fig. 12. The downcomer level is the effective driving head to provide cooling into the core. The fuel rod quench front moves up the fuel rods as the core level increases resulting in cooling of the upper elevations of the core such that the temperature turn over and the rods will eventually quench.

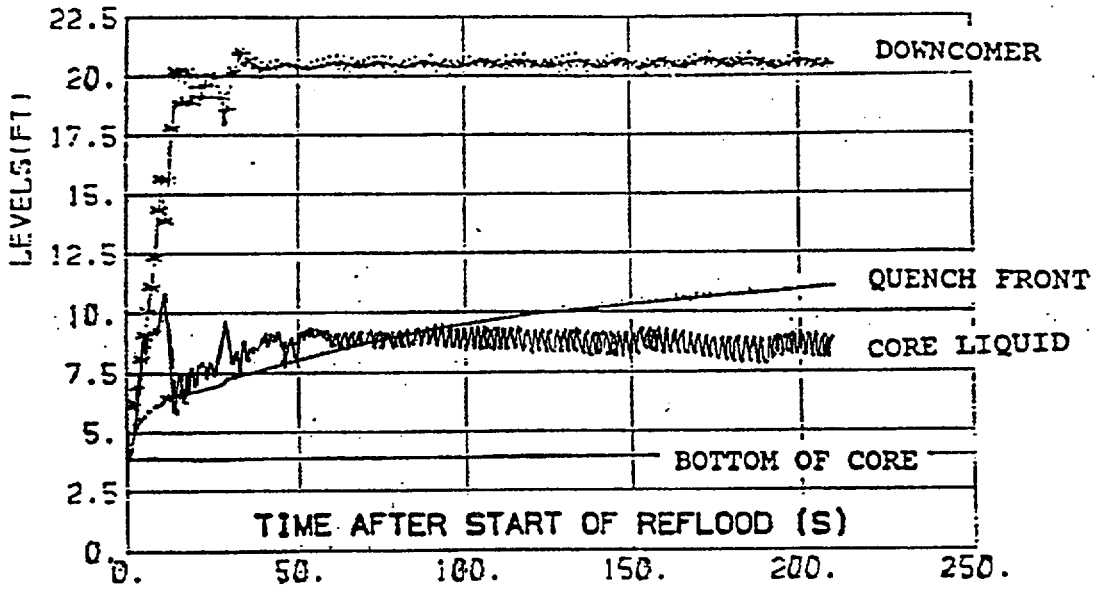

The calculated hot rod temperatures at the burst location and the peak location are shown in Fig. 13. In this calculation, the hot rod peak cladding temperature is located approximately two-feet above the burst location. When ballooning and burst occurs, the gap conductance in the fuel rod at the location of burst is significantly reduced because the cladding has moved away from the pellet. Therefore, the pellet is thermally isolated from the cladding such that the cladding acts like a large fin. Since there's less stored energy, in the cladding, it is much easier to cool, so the cladding easily cool at the burst location. The fuel rod burst location is usually not the limiting peak cladding temperature location. However, there are cases when it can be. This becomes very plant specific.

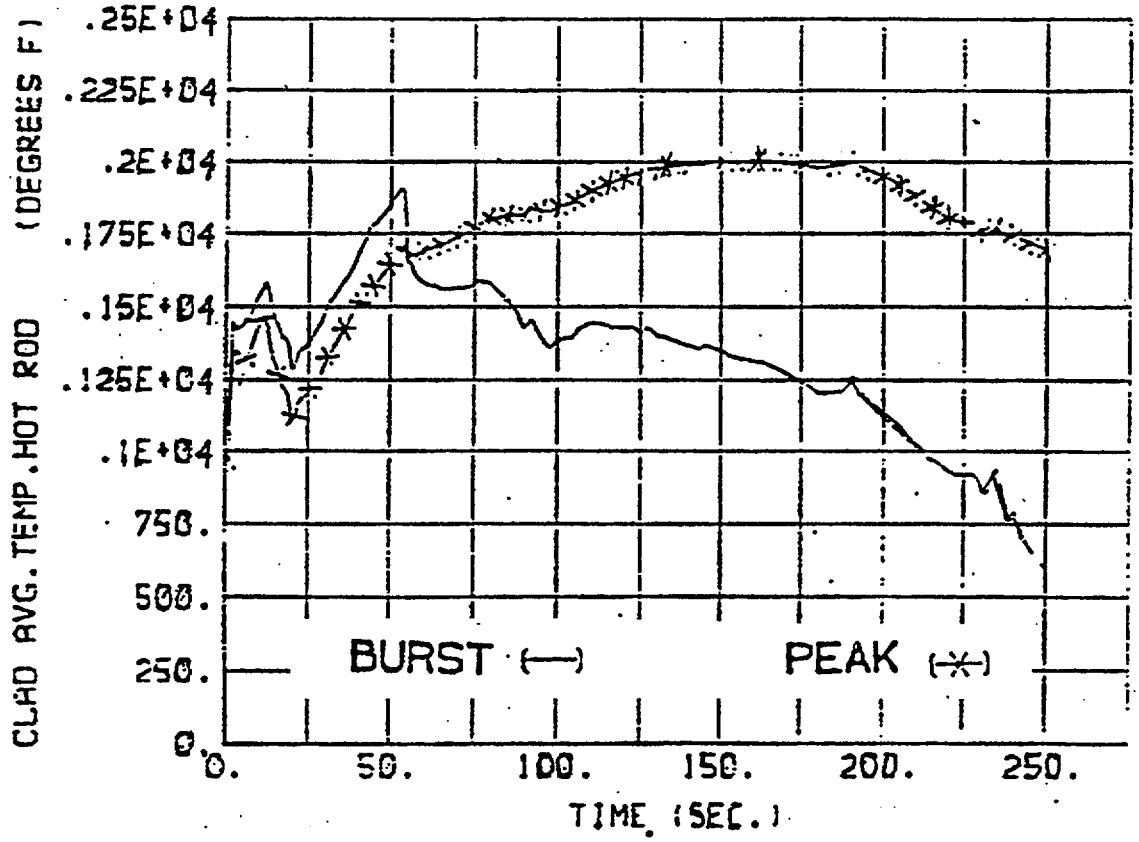

The peak cladding temperature location, in this calculation, is at the eight-foot elevation on the rod, whereas this burst location is at the six-foot elevation on the rod. Double-sided zirconium/water reaction is considered at the burst location. However, as the temperature plot indicates, the cladding temperature decreases upon burst such that the effects of double-sided reaction are not significant. In the Appendix K calculations, there is no direct fuel-coolant heat transfer. All heat transfer assumes the presence of the cladding and the thermal resistance of the fuel pellet-clad gap. The fuel is assumed to stay within the rod and fuel is assumed to stay in a rod like geometry, even in the burst zone.

I-1.4. Babcock and Wilcox Lowered Loop Appendix K Evaluation Model LBLOCA Calculations

Next, a Babcock and Wilcox (B&W) lower loop Appendix K Evaluation Model calculation will be examined. This plant design has lowered primary loops and uses once through steam generators. The break of interest is an 8.5 square foot DECLG break on the pump discharge. The rated plant power is 2772 MWt. The calculation uses a bottom peaked power shape, which is limiting for this plant design, since the PCT occurs at the very beginning of reflood which will be explained shortly.

Figure 14 shows the B&W plant. There are two unique features. One is the once-through steam generator, so this is like a Three Mile Island type unit, and there are barrel check valves in the upper downcomer. The purpose of these check valves is to provide a vent path for flow, reflood flow that would be coming out of the core. Instead of having to go up the long and high hot leg configuration (the candy-cane) and down through the hot steam generator, the flow can vent out through the check valves in the upper plenum to the downcomer, around the downcomer annulus and can go out through the break. The vent valves provide a short circuit flow path to the break. There are approximately 10 large vent valves around the vessel. These are basically flapper valves and are shown in Fig. 15. During normal operation they are held closed because of the positive pressure difference in the downcomer, relative to the upper plenum, because of the pump flow entering the downcomer. During reflood there is a higher pressure in the core and upper plenum so that the flapper valves can open and vent out the two-phase mixture from the core directly to the downcomer annulus, which then flows to the break. This process short-circuits the reflooding portion of the transient because there is no need to force the flow through the huge, hot, once-through steam generators because the reflood flow can vent out through the vent valves. Therefore, reflood is not the limiting portions of the transient for this type of plant design. The time period that is more limiting in this design is the end of refill just before the beginning of reflood.

The pressure transient is shown in Fig. 16 for the B&W plant during the blowdown period. Since this for a double-ended break, the blowdown proceeds very quickly and the vessel is basically depressurized in 30 seconds. For this design there will again be a short positive core flow but a very, very strong negative flow down to the core, as seen in Fig. 17. At the end of blowdown, the reverse flow through the core diminishes because by the end of blowdown, there is little water remaining in the reactor system.

Because a vent path through the barrel check valves to the downcomer and break exists, the loop resistance is negligible and the calculated flooding rate into the core is much higher than a typical Westinghouse plant as shown in Fig. 18. The flooding rate into the core for a Westinghouse plant would be typically be around one inch a second. The flooding rate for the B&W plant is typically two inches a second.

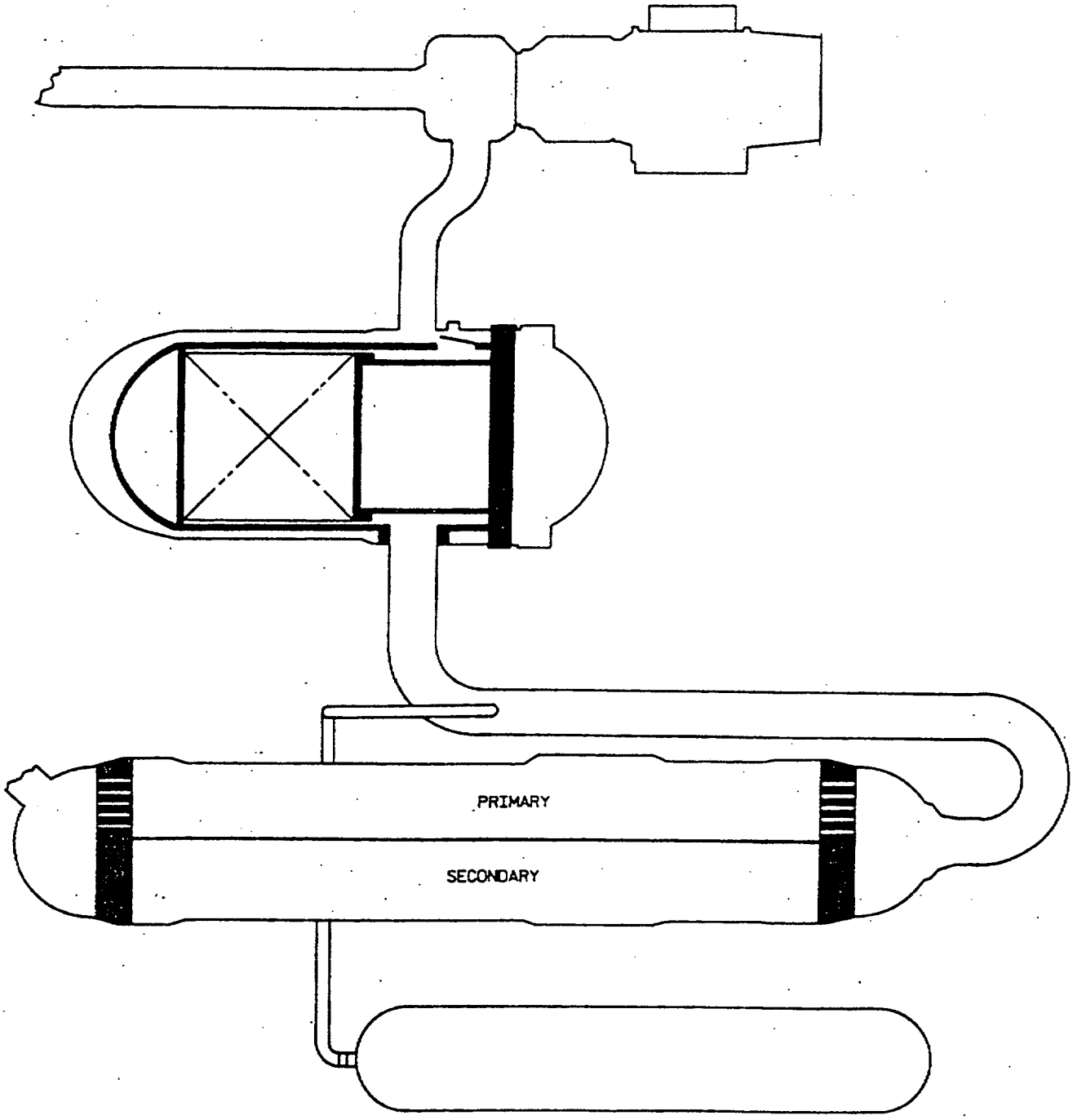
PRIMARY
SECONDARY

Figure 1. Vent Valve Arrangement (B&W 136214E)

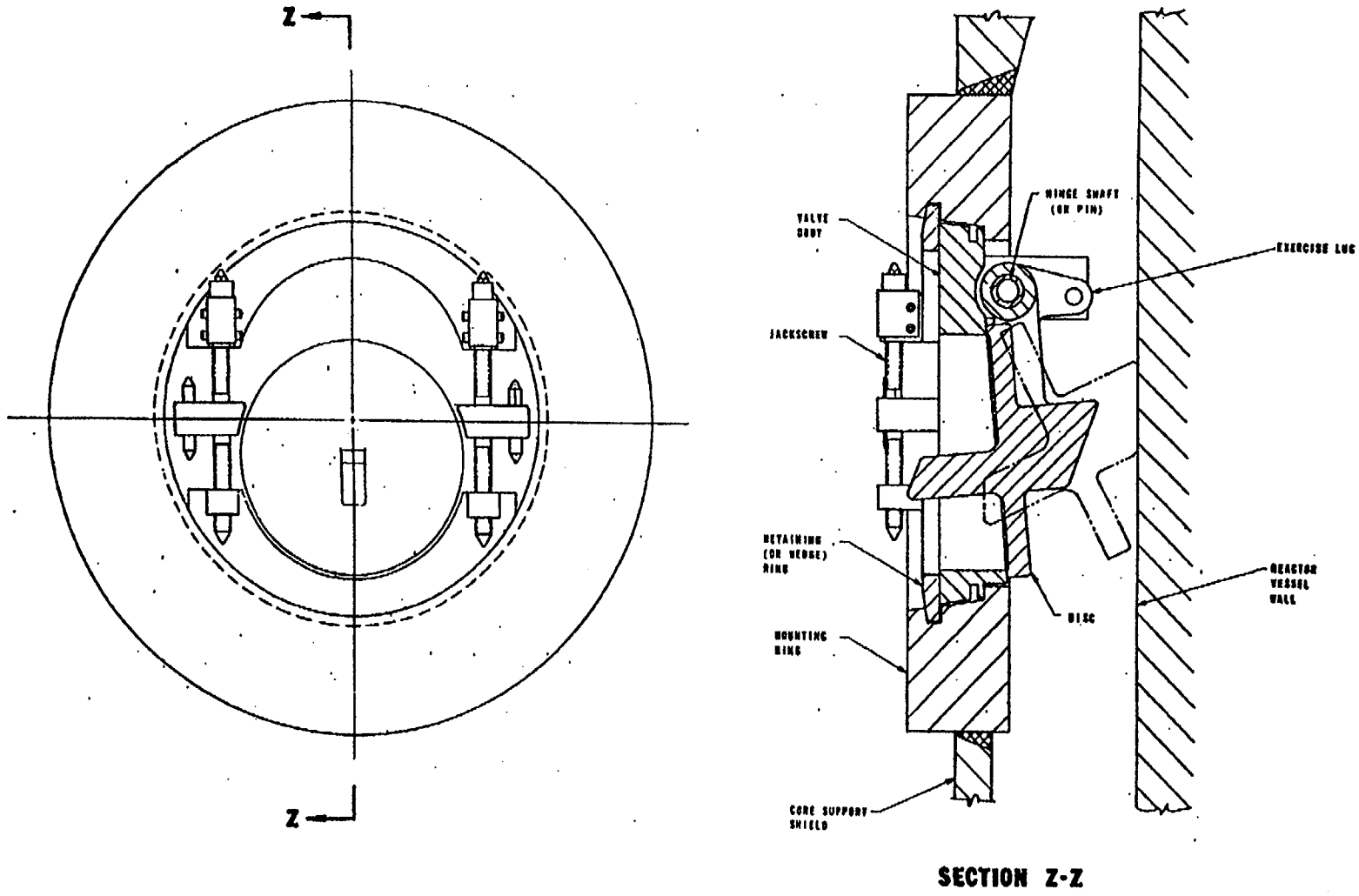

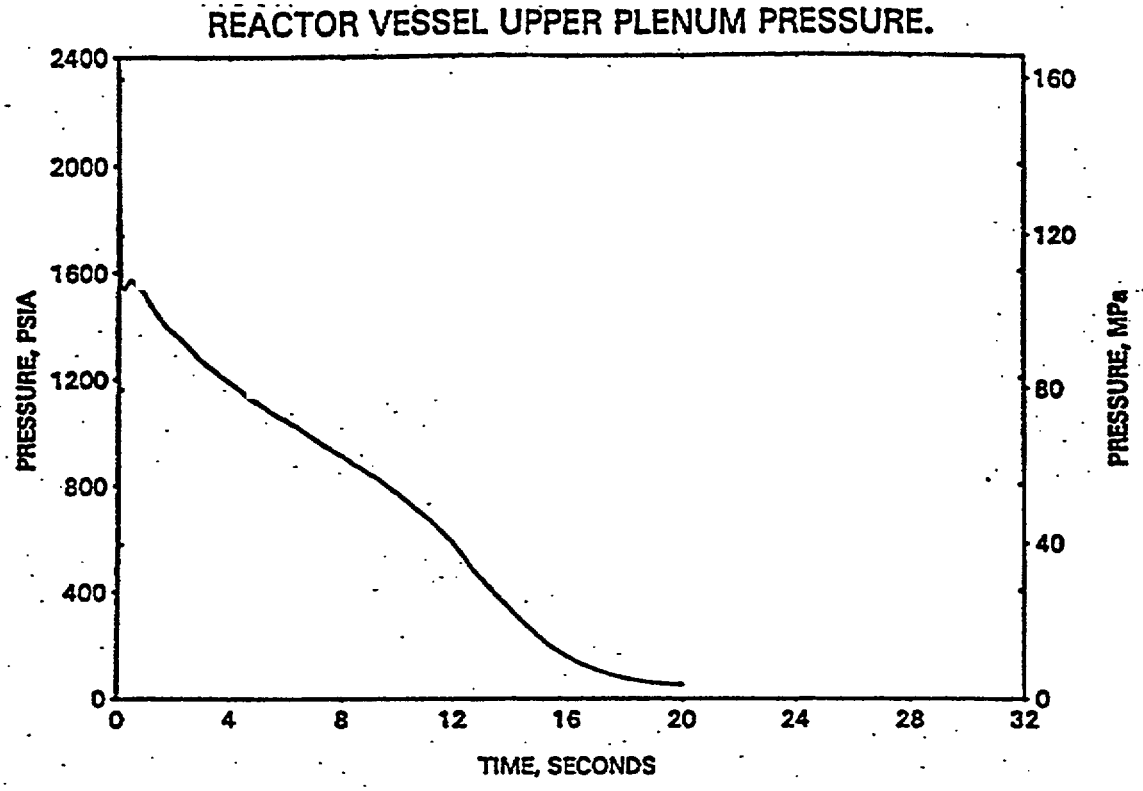
REACTOR VESSEL UPPER PLENUM PRESSURE.
PRESSURE, PSIA
2400
2000
1600
1200
800
400
0
PRESSURE, MPa
160
120
80
40
0
0
4
8
12
16
20
24
28
32
TIME, SECONDS

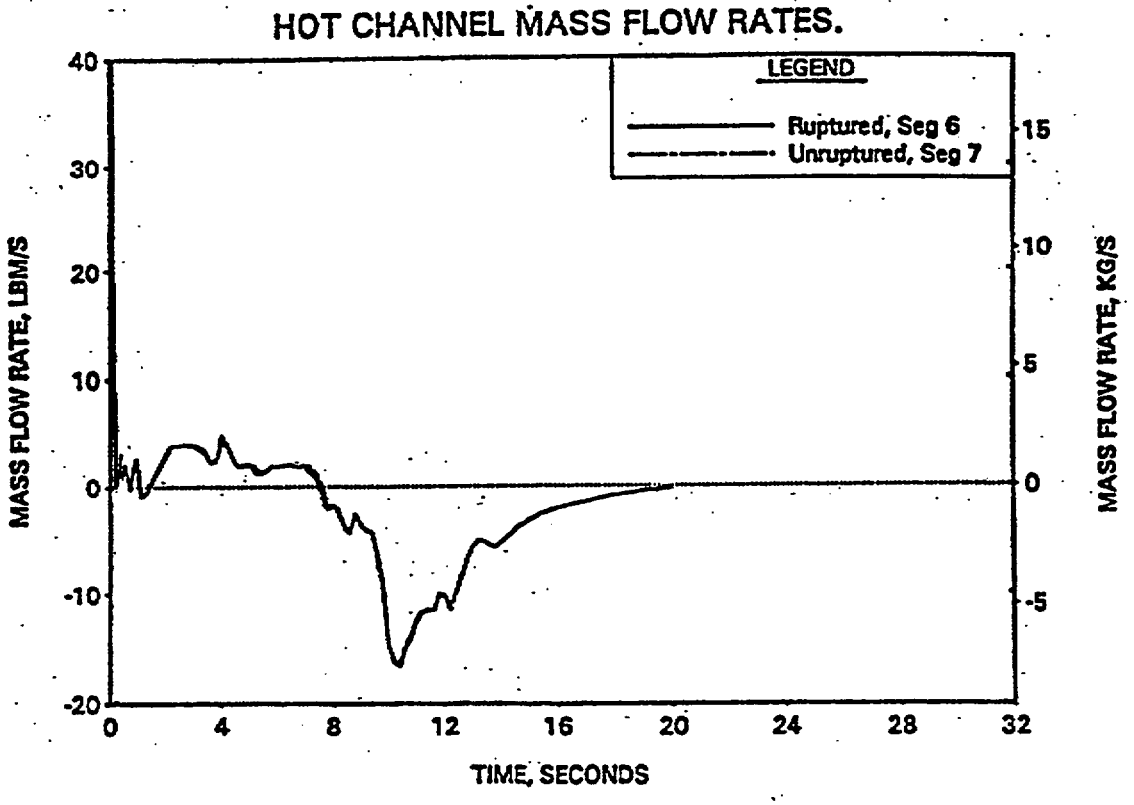
HOT CHANNEL MASS FLOW RATES.
LEGEND
Ruptured, Seg 6
Unruptured, Seg 7
MASS FLOW RATE, LBM/S
40
30
20
10
0
-10
-20
MASS FLOW RATE, KG/S
15
10
5
0
-5
0
4
8
12
16
20
24
28
32
TIME, SECONDS

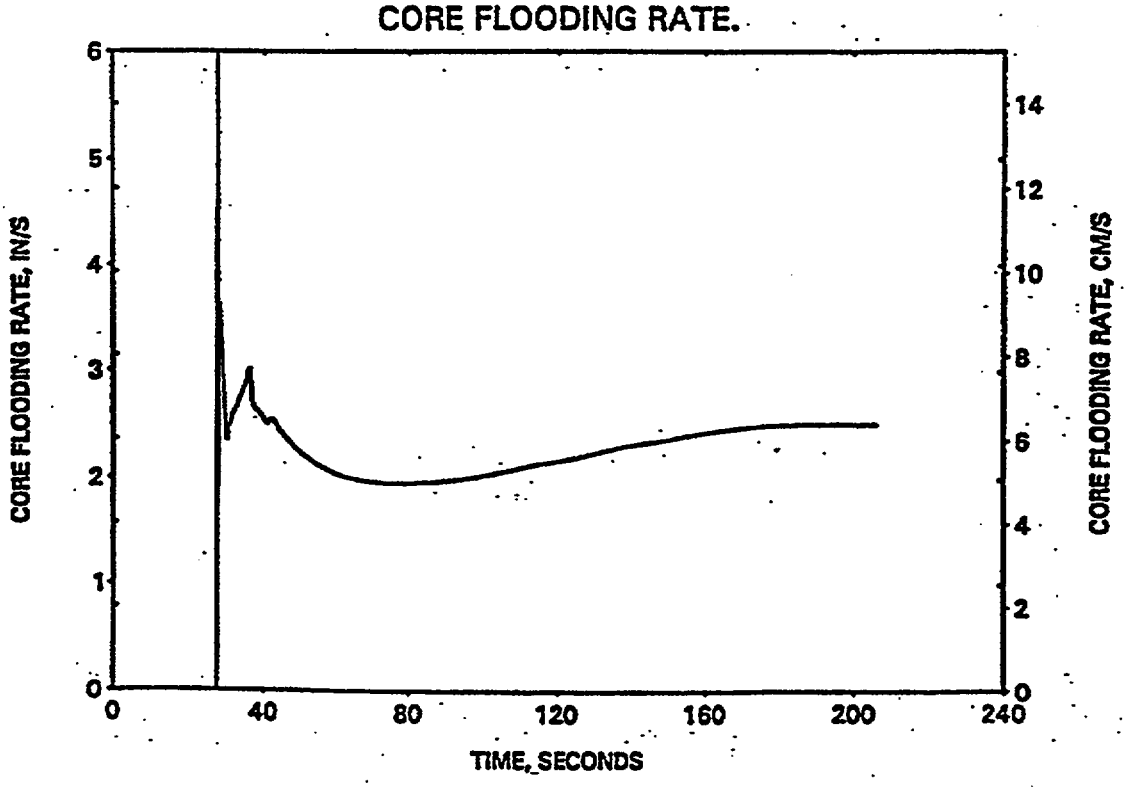

The peak cladding temperatures that are calculated for this design typically occur at the end of the refill period or beginning of the reflood time period. Given the good reflooding heat transfer behavior, with the higher reflood rates due to the vent valves, the peak cladding temperatures quickly turn over and the rods and quench.

As a result, B&W plants tend to have higher allowable linear heat rates because the vent valve plants are not reflood limited. The calculated peak clad temperatures are occurring during the end of blowdown and the refill period, where the PCT then is more controlled by the stored energy in the fuel and not by the duration of the reflood transient, as it was in the Westinghouse plant.

The limiting axial power profile is located 2.5 feet from the core inlet at the bottom of the core. The reason for this location is because of the downflow period at the end of blowdown and the beginning of refill in which the flow is coming down through the vessel. For this flow situation, it is more conservative to have power peaking at the bottom of the core further from the source of cooling, which in the B&W plant case is the upper plenum during blowdown.

The calculated LBLOCA transients for the B&W plant are also shorter as compared to the Westinghouse transients, since reflood is not limiting. Examining Figs. 19 and 20 for these calculations, the PCTs occur earlier as indicated in the figures and the whole transient is much shorter compared to the Westinghouse plant, so there is a real benefit in having barrel check valves. Figures 19 and 20 show both the cladding and fuel

temperatures at the burst location as well as at the peak non-burst location. At the burst location, the cladding has deformed and has moved away from the fuel pellet so it takes longer for the fuel temperature to decrease (Fig. 19) as compared to the fuel temperature at the non-burst location in which the fuel/cladding gap heat transfer coefficient is larger (Fig. 20).

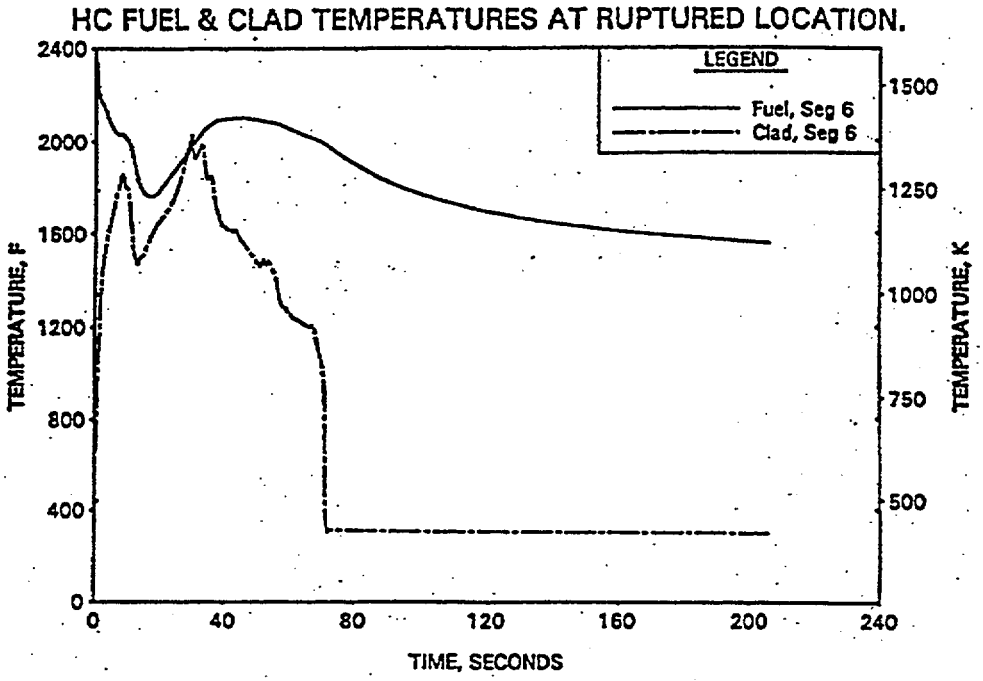

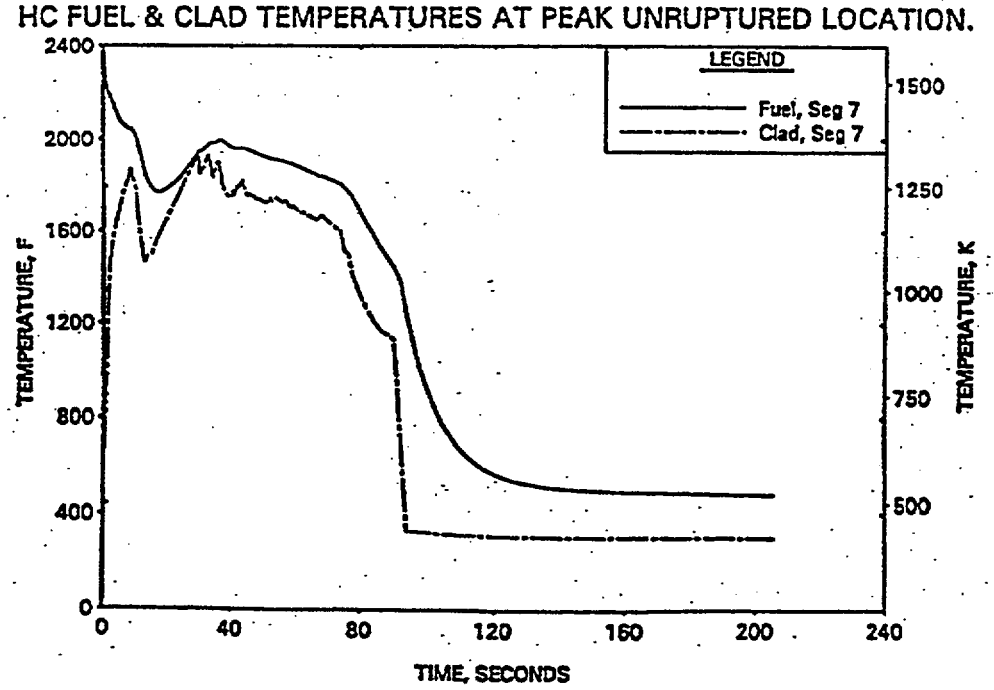

I-1.5. Westinghouse Best-Estimate Model LBLOCA Calculations for a Four-Loop Plant

The previous calculations, which were shown, were Appendix K type calculations using the types of models that were approved in the 1972 timeframe. There have been improvements and modifications made to these models, but generally these models used the prescriptive approach given by Appendix K. Next, a sample best estimate calculations, again for a Westinghouse plant, will be examined. Now these calculations use a best estimate code, in this case WCOBRA/TRAC. The analysis conforms to the rule change in 1988 that allows using a best estimate computer program.

The timeframes for the best-estimate transient are pretty much the same as the Appendix K calculation for the Westinghouse plant as seen in Fig. 21. There is still have roughly a 30 second blowdown period followed by a 10 second refill period, and then a reflood period that can last up to 5 minutes until the core is completely quenched. The change that is different in these calculations is that they are performed using a best estimate method, which gives a more accurate representation of the plant response to the imposed LBLOCA transient. The calculated allowable peak linear heat rates are higher for the best-estimate calculations, as compared to the Appendix K calculation. The Appendix K models and requirements were more limiting as compared to the best-estimate models. As a result, the allowable peak linear heat rates for the best-estimate calculations are higher, so the peak kilowatts per foot in the analysis that is being analyzed is higher.

The benefit of the best-estimate calculations, relative to Appendix K calculations, is that best-estimate LBLOCA calculations would allow the plant to operate at higher kilowatts per foot since the safety analysis of the plant would be performed at higher kilowatts per foot limit.

The temperatures that are calculated using the best-estimate analysis are shown in Fig. 22 for this particular plant. In a best estimate methodology, the nominal value PCT is calculated and then the uncertainties are convoluted in a statistical fashion to calculate a 95th percentile PCT value, replaces the Appendix K value as the licensing basis for the plant. The PCT values shown in Fig. 22 are not that dissimilar from what was shown earlier for older Appendix K calculations. The difference is that the best-estimate calculations are done at higher kilowatts per foot, so that there are temperatures that are typically 16-17-1800 ^{0} F at blowdown and approximately 2000 ^{0} F during reflood. The best-estimate calculations still must conform to the same original 10CFR50.46 requirements that the Appendix K calculations had to achieve. The difference is that the same criteria can be achieved with best-estimate calculations, but at a higher linear heat rate.

BLOWDOWN	0 sec.	Break occurs
		Reactor trip (pressurizer pressure or high containment pressure)
		Pumped SI signal (pressurizer pressure or high containment pressure)
		Accumulator injection begins
		Pumped ECCS injection begins (offsite power available)
		Containment heat removal system starts (offsite power available)
	20-25 sec.	End of bypass
		End of blowdown
REFILL		Pumped ECCS injection begins (loss of offsite power)
		Containment heat removal system starts (loss of offsite power)
	35-40 sec.	Bottom of core recovery
REFLOOD		Accumulators empty
	5 min.	Core quenched
LONG TERM COOLING		Switch to cold leg recirculation on RWST low level alarm
		Switch to hot leg/cold leg recirculation

BEST ESTIMATE LARGE BREAK LOCA TIME SEQUENCE OF EVENTS

BEST ESTIMATE LARGE BREAK LOCA ANALYSIS RESULTS

Component	Blowdown Peak	First Reflood Peak	Second Reflood Peak
$PCT^{average}$	<1508°F	<1681°F	<1384°F
$PCT^{95\%}$	<1760°F	<1976°F	<1964°F
Maximum Oxidation		<11%	
Total Oxidation		<0.89%	

Having higher linear heat rates allows the utility to operate the plant in a more cost effective manner. The best-estimate analysis methods identify LOCA margin that is kilowatts per foot margin that can be used to more efficiently operate the plant. LOCA margin can be used to make changes in the design, usually in the fuel, which requires the use of higher kilowatts per foot. For example, removing the fixed poison rods in the guide tube thimbles in a PWR fuel assembly, which requires higher allowable peak linear heat rates. Another example is using lo-lo leakage loading patterns so the fuel on the edge of the core is almost dead, such that the power is pushed into the center of the core, resulting in higher kilowatts per foot. As fast as LOCA margin is developed, it is used by the utility to improve the cost effectiveness of the plant. Therefore, similar peak cladding temperatures are calculated using the best-estimate methods, however, the plant now operates more efficiently or is using more efficient fuel designs such that the fuel cycle costs are lower.

Figure 23 shows the locus of peak cladding temperatures anywhere in the core. The peak is occurring at the value is that is nearly 2000 ^{0}F, and it is occurring at about 9.7 feet. The PCT is occurring at roughly the same time frame as in the previous Appendix K analysis. Again, while the PCT is about the same, kilowatts per foot, and the integrated power in a hot assembly in the best-estimate analysis is higher than in the Appendix K analysis.

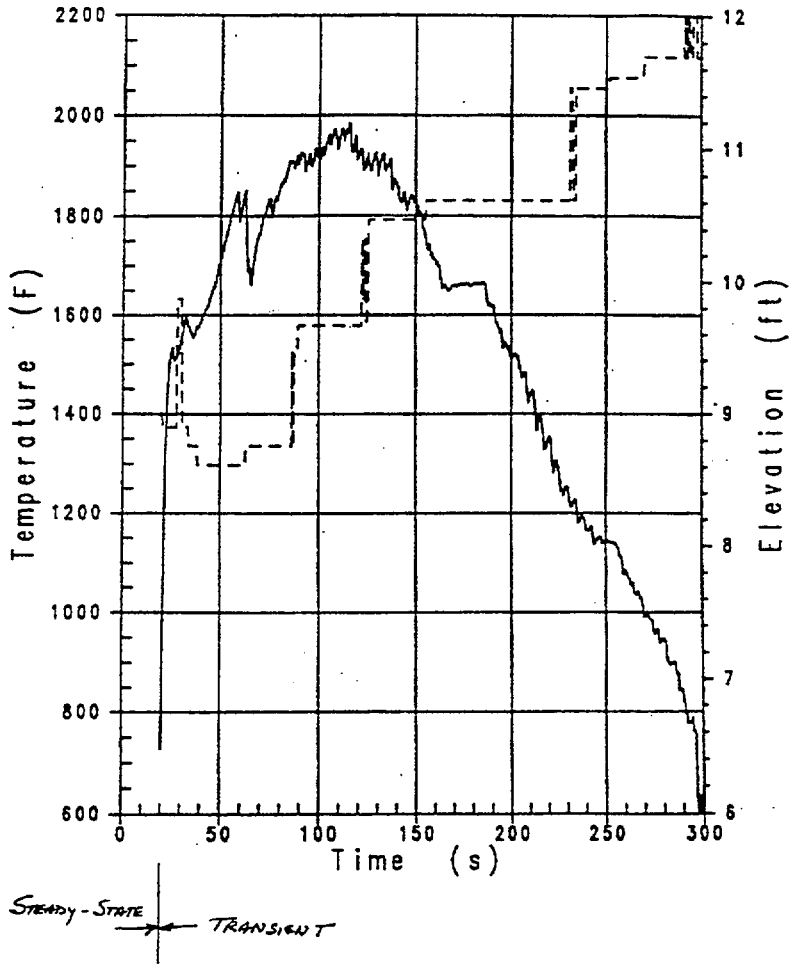

Figure 24 shows the flow rate at the top of the core. In this figure and in the following figures, there is an initial steady state period before the transient, which is modeled in WCOBRA/TRAC as indicated on the figures. At 20 seconds, the break opens and the transient begins. Figure 24 shows the flow reversals during blowdown as well as the flow out of the core during the reflood period.

Figure 25 shows the calculated pressurizer pressure and indicates that the system pressure is quickly down to containment pressure in 30 seconds after the break is initiated.

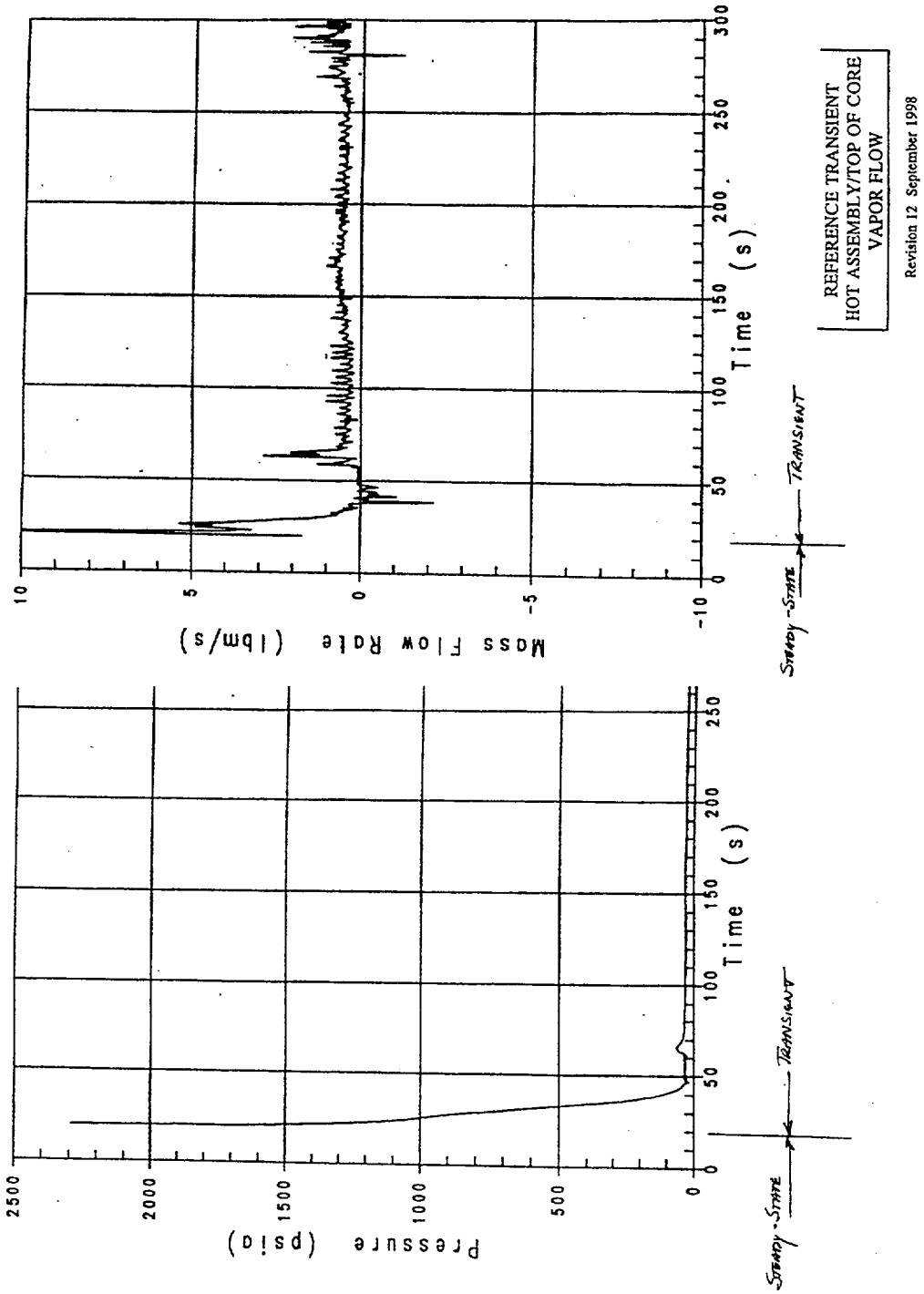

Figure 26 shows the liquid inventory in the lower plenum, and indicates that most of the water is initially blown out of the lower plenum, even in a best-estimate calculation. But the cold leg accumulators begin to inject and the lower plenum is quickly refilled and stays water filled for the remainder of the transient. The time period during which the water has been blown out of the lower plenum is the minimum mass inventory in the vessel. The real point of interest is how quickly the emergency core cooling systems refill the vessel.

Figure 27 is a plot of the reactor vessel water mass and shows how quickly the ECC refills the vessel. Most of the water inventory is due to the accumulator injection, which is then followed by the pumped injection, which maintains the mass inventory in the system.

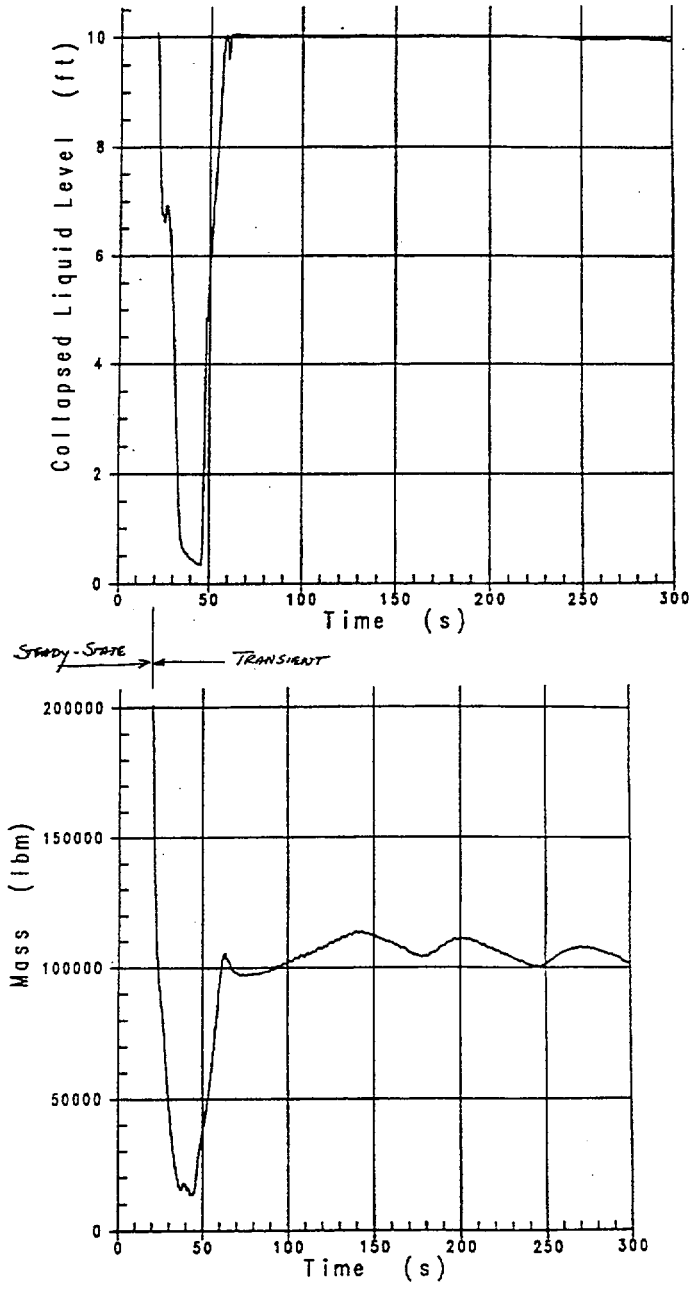

Figure 28 shows the accumulator flow from one cold leg accumulator, which injects very rapidly the vessel. The accumulator injection recovers the mass in the vessel and the pump system continues to inject and maintains flow into the vessel for an extended period of time as seen in Fig. 29.

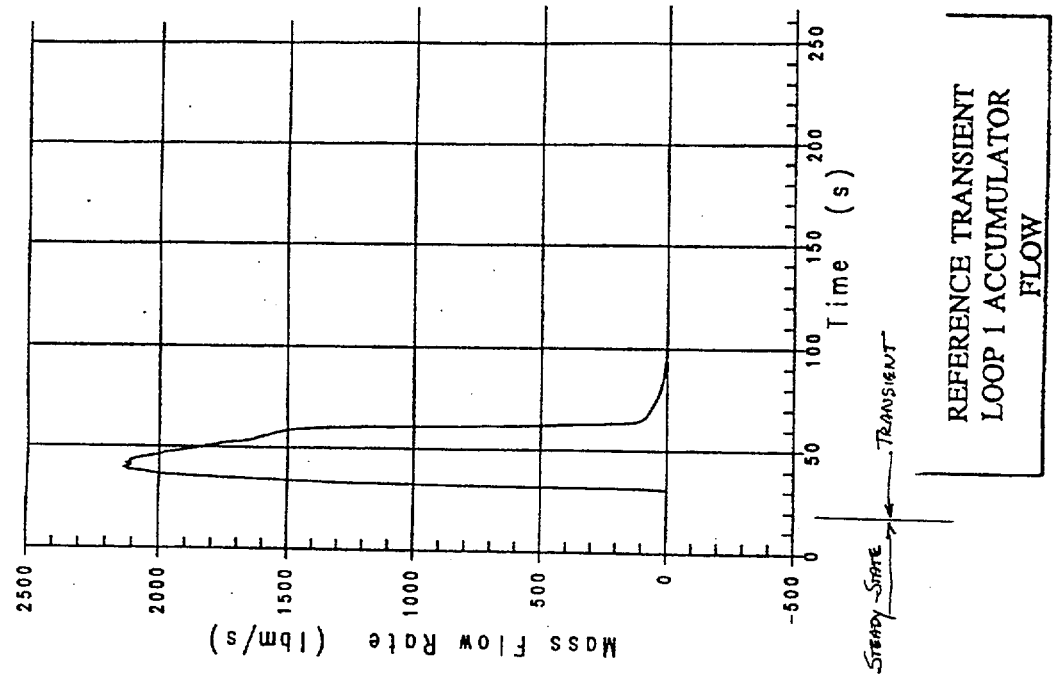

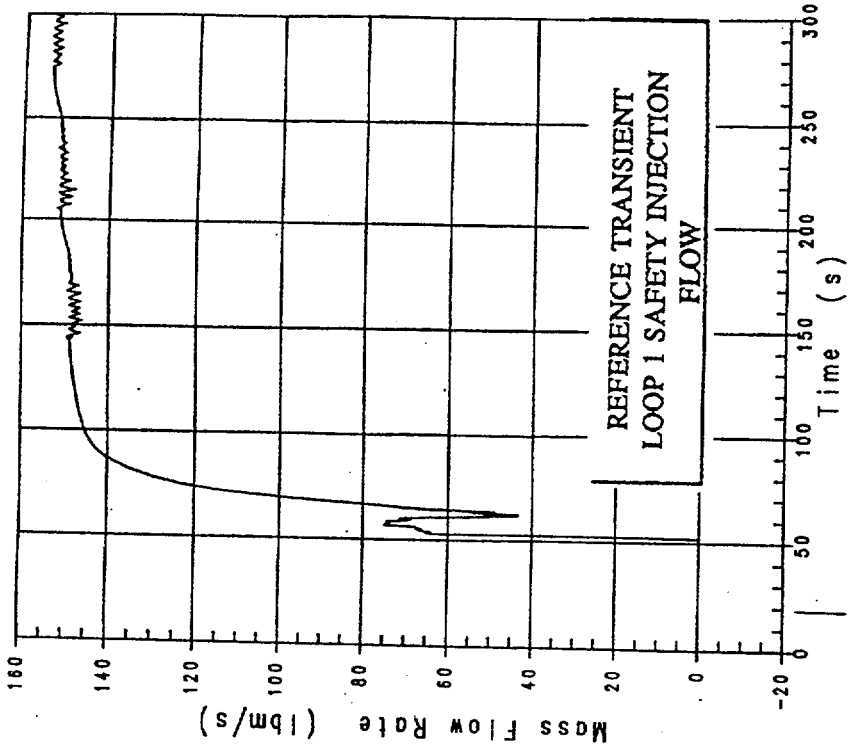

The accumulator injection also fills the downcomer such that the liquid level increases as seen in Fig. 30. It is the level in the downcomer that provides the driving head for flow to enter the core and to begin reflood as seen in Fig. 31. In this calculation, level in the downcomer is recovered with the accumulator injection, and then it is maintained due to the pump injection. At the same time, the flow from the downcomer increases the liquid level in the core, since the head in the downcomer is forcing water into the core. This is what provides the reflood cooling which results in turning the fuel rod temperature around (PCTs) in the reflood portions of the transient. As Fig. 31 indicates, the core level is initially recovered early in reflood and then remains approximately as constant.

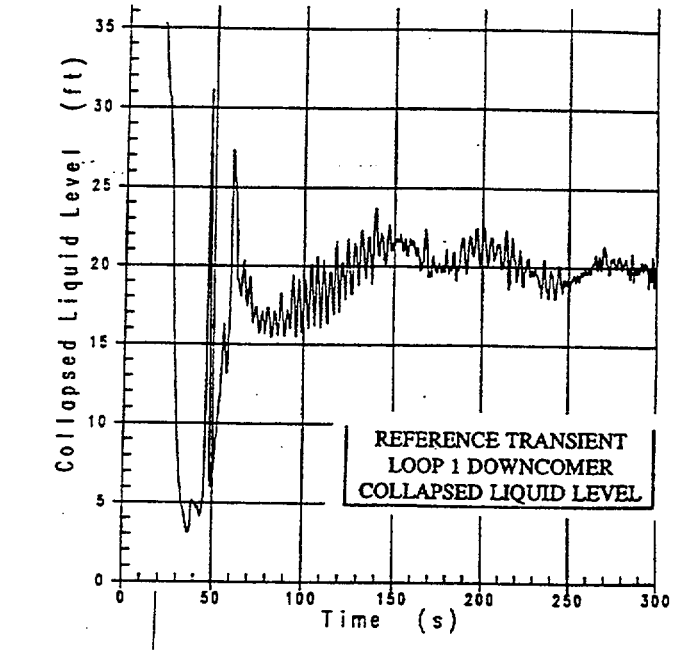

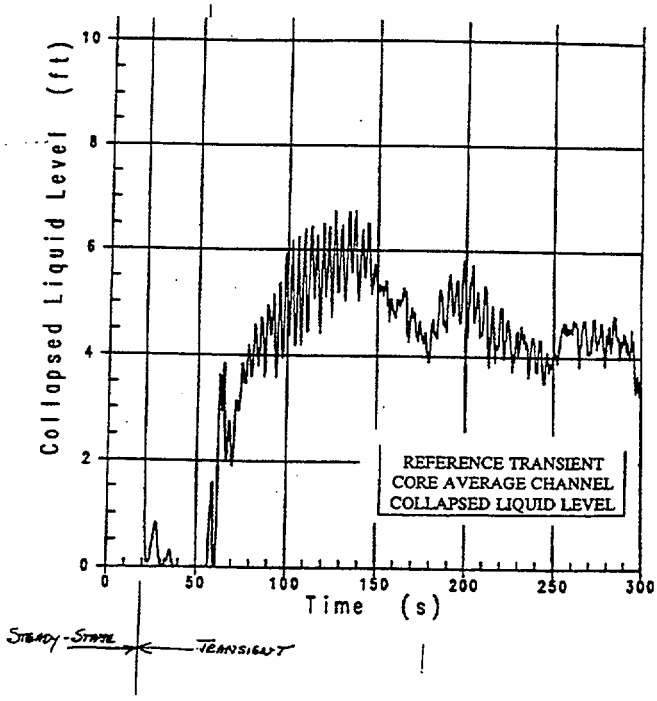

I-1.6. Effects of High Burnup on the LBLOCA Calculations

In this part of the presentation, the effects of high burnup on the LBLOCA were examined and some conclusions on burnup effects were developed from the LBLOCA analysis. Figure 32 shows calculated fuel rod internal pressures for two different fuel rod codes. This solid line is the FUELROD code, which is a PC code that is used at Penn State in a Reactor Engineering class. The dashed line in Fig. 32 is FRAPCON code calculation. These are calculations have been done for the same fuel rod design, plenum design, and power history. The result is for rod internal pressures, which reflect the differences between the codes, primarily the fission gas release model in each of the codes. Comparison calculations have been made between FRAPCON and FUELROD at Penn State and everything else agrees pretty well except for the amount of fission gas that is released in the calculations. So there can be a range of calculated internal pressures for the rod design. The purpose of showing these two calculations is to indicate that there can be a range of internal pressures. For high burn-up fuel, the fuel rod internal pressure can exceed the system pressure. The FUELROD code calculated an internal pressure of about 2700 psi inside the rod during operation at approximately 80,000-MWd/metric ton burn-up, where as FRAPCON calculated a little over 2000 psi.

Looking at a loading pattern for core, most of the designs today are going to lower power on the outside of the core to basically provide some degree of shielding to the reactor vessel. Utilities are using these low leakage loading patterns so the powers of the outer row of assemblies are very low relative to a normalized power of unity. An example of such a loading pattern is shown in Fig. 33. The fuel assemblies on the outside edge of the core represent once and sometimes twice burned fuel assemblies, so burned fuel assemblies are moved out to the outside edge, and the fresh assemblies are loaded into the center regions of the core. The once and twice burned assemblies are the assemblies which are going to have the higher initial internal pressure in the fuel rods because they have been in the core for a longer time, but at the same time, they are the low powered assemblies. Most of the burned assemblies are loaded on the outside edge of the core. However, there are loading patterns that load a twice-burned assembly in the very center of the core to act as a power suppresser or poison. This twice-burned assembly can be driven to higher powers, then the edge assemblies, by the high power fresh assemblies, which surround it.

Considering the core nodding scheme used in the WCOBRA/TRAC Model that was used for the best-estimate calculations as seen in Fig. 34, WCOBRA/TRAC models this type of a loading pattern with different types of assemblies and different fuel rods. There is a unique representation for the low power fuel assemblies. All the low powered edge assemblies are lumped together as a single channel in the calculation. The interior of the core region, in the center, is broken up into fuel assemblies, which are under open holes, support columns or freestanding mixers, or fuel assemblies, which are under guide tubes. There is a separate channel, which represents the hot assembly.

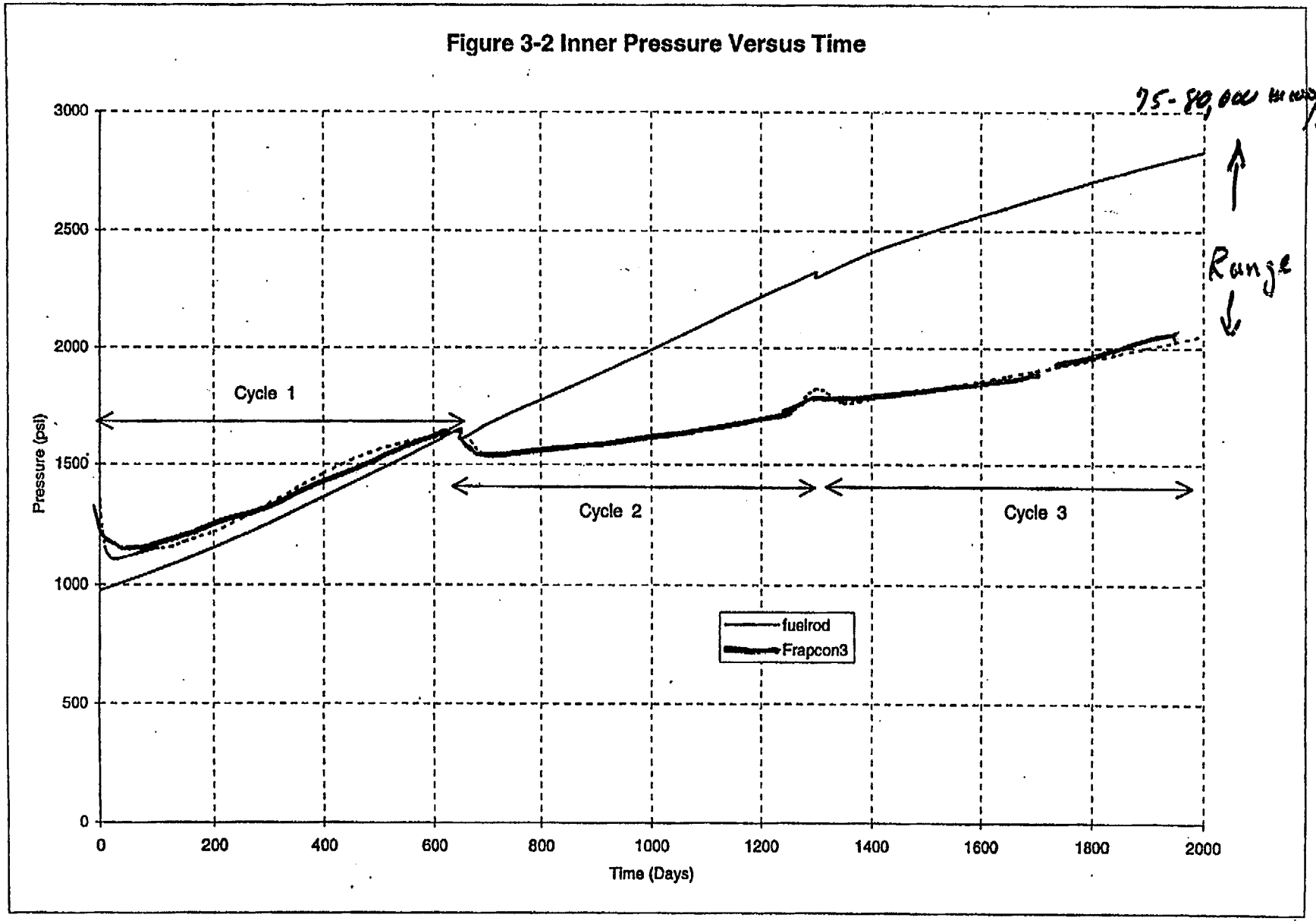
Figure 3-2 Inner Pressure Versus Time
75-80,000 MWD/T
Range
Pressure (psi)
3000
2500
2000
1500
1000
500
0
Cycle 1
Cycle 2
Cycle 3
fuelrod
Frapcon3
0
200
400
600
800
1000
1200
1400
1600
1800
2000
Time (Days)

21180 MWD/MTU
10 PPM
1.383 CORE F-DELTA-H
1.629 CORE FQ

10B .884 .911 1.048 62410	12 1.333 1.374 1.625 26256	10A .908 .951 1.094 52628	11 1.028 1.062 1.211 48482	11 1.000 1.023 1.165 48393	11 1.070 1.137 1.318 47051	12 1.186 1.337 1.590 22856	9A .403 .606 .696 46228
12 1.333 1.374 1.625 26256	11 1.079 1.117 1.285 49664	12 1.328 1.383 1.627 28247	12 1.295 1.371 1.609 28172	11 1.061 1.160 1.339 45940	12 1.309 1.381 1.629 27871	12 1.105 1.306 1.546 22638	10B .344 .622 .719 46783
10A .908 .951 1.094 52628	12 1.328 1.383 1.626 28233	11 1.050 1.104 1.266 49430	11 1.053 1.109 1.260 45876	11 1.044 1.096 1.251 49101	12 1.254 1.357 1.596 26814	11 .702 .969 1.115 40675	
11 1.028 1.062 1.211 48482	12 1.294 1.371 1.608 28156	11 1.053 1.109 1.261 45866	11 1.069 1.174 1.355 46474	12 1.299 1.373 1.611 28363	12 1.109 1.311 1.542 23311	10A .381 .673 .773 43262	
11 1.000 1.023 1.165 48393	11 1.061 1.160 1.339 45960	11 1.044 1.097 1.251 49090	12 1.299 1.373 1.611 28363	12 1.164 1.343 1.580 24853	11 .587 .920 1.050 38364		
11 1.070 1.137 1.318 47051	12 1.309 1.381 1.628 27871	12 1.254 1.357 1.596 26816	12 1.109 1.311 1.542 23313	11 .587 .920 1.049 38369			
12 1.186 1.337 1.590 22856	12 1.105 1.306 1.547 22646	11 .703 .969 1.115 40631	10A .382 .674 .773 43257				
9A .403 .606 .696 46228	10B .344 .622 .718 46790						

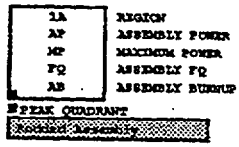

REGION IDENT.	NUMBER OF ASSEMBLIES	POWER SHARING	BURNUPS TOTAL	CYCLE
9A	4	.403	46228	6908
10B	9	.404	48523	7241
10A	12	.557	46382	11047
11	64	.949	45585	20622
12	68	1.240	26163	26163

CYCLE 10 ASSEMBLYWISE POWER AND BURNUP AT
21180 MWD/MTU, HFP, ARO, EQUILIBRIUM XENON

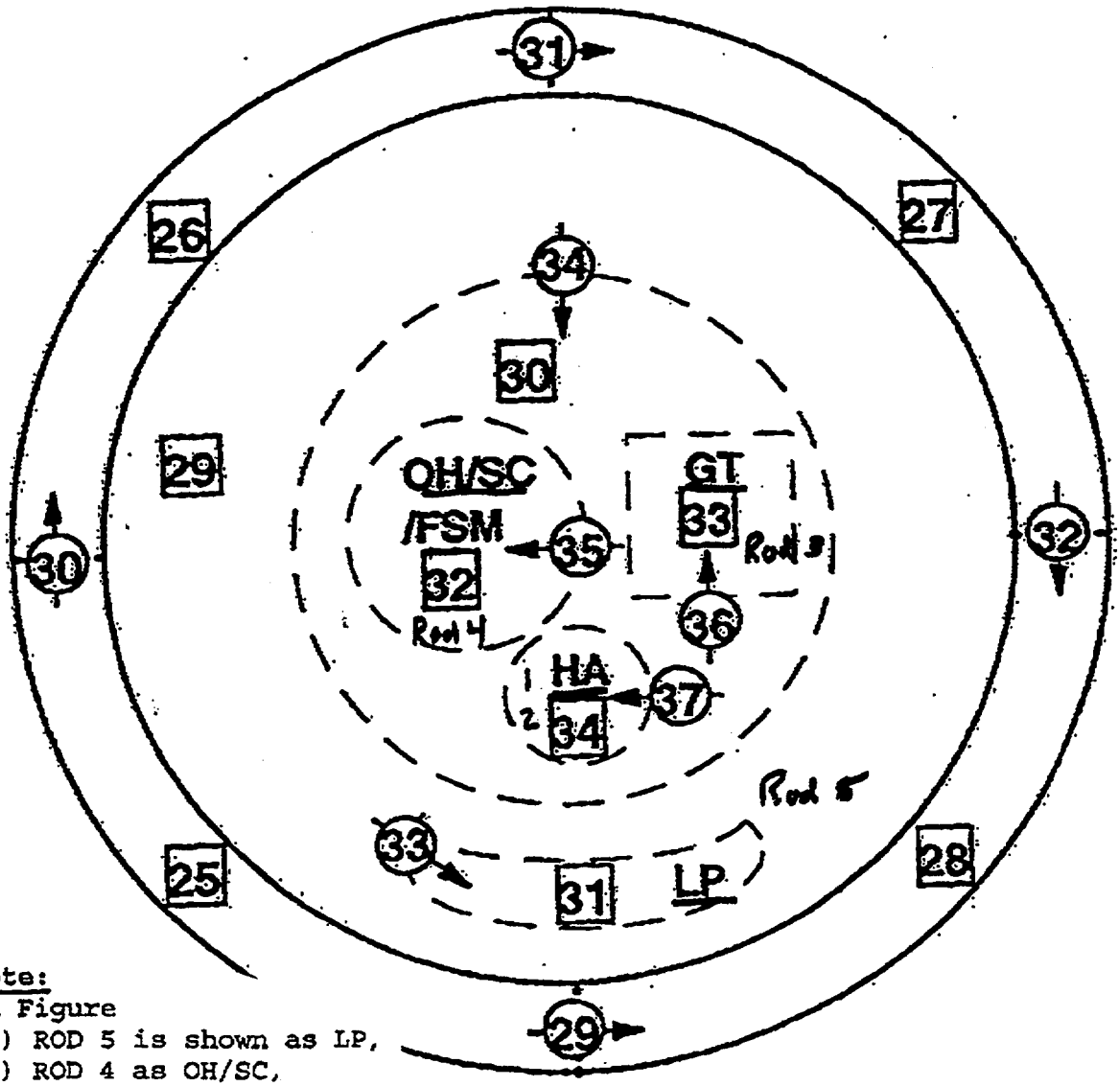

Note:
In Figure
(1) ROD 5 is shown as LP,
(2) ROD 4 as OH/SC,
(3) ROD 3 as GT,
(4) ROD 2 as HA, and
(5) ROD 1 is HOT rod.

In the LOCA calculation that is done, there are typically have five fuel rods which model the different assemblies in the core. There is a fuel rod representing the low power region; a fuel rod representing those fuel assemblies under guide tubes and fuel rod representing fuel assemblies under open hole support columns and free-standing mixers, (these are generally at the same power). There are also two fuel rods, which are modeled, in the hot assembly. There is the hot assembly average rod, which determines the hot assembly fluid conditions, and the hot rod, which is the highest powered rod in the core. The hot rod has included all the engineering uncertainties which makes it the hottest rod. Therefore, there are a total five rods, which are represented in the COBRA TRAC core model.

The calculated temperature response for these rods is shown in Fig. 35. In this figure, Rod 1 is the hot rod, and has a relative power of 1.73 and a delta H value of 1.73; Rod 2 is the hot assembly average rod, and it has a relative power of 1.66. These are the rods, which represent the inner region of the core, Rods 3 and 4; and the Rod 5 represents the fuel assemblies on the outside edge of the core. So Rod 5 would represent the majority of the rods, which have been once, or usually twice, burned. This figure shows the temperature response of the different fuel rods to the LOCA transient as calculated and indicates that the hot assembly, of course, has the highest fuel rod temperatures. Rods 3 and 4 which represent the majority of the fuel rods in the core itself, have lower temperatures, approximately 1400 °F, and then Rod 5 which represents the rods on the outside edge of the core have even much lower temperatures like 400 °F.

Figure 36 shows the corresponding fuel rod internal pressures, in psi, for each of the rods. In this particular calculation the hot rod burst was locked out, that is, the calculation prevented the hot rod from bursting even though it would have been calculated to burst. This was done to obtain a more conservative estimate of the hot rod PCT. The time at which the hot rod would have burst (Rod 1 in Fig. 35), can be obtained form examination of the hot assembly average rod, Rod 2 in Fig. 35. Rod 2, which is the hot assembly average rod is calculated to burst. Rod 1 would have been calculated to burst almost at the same time, perhaps a little earlier than Rod 2. Both Rods 1 and 2 would have burst in this calculation.

Rods 3 and 4, which represent the majority of the rods in the core are calculated to not burst. Rods 3 and 4 are mostly once-burned rods. Some of them could be a little more than once-burned rods. Rod 5, which represents the low power assemblies on the edge of the core, which have the highest internal gas pressure are also not calculated to burst.

Now, compare the calculated temperatures and internal pressures from Figs. 35 and 36 to the burst criteria in NUREG-0630 shown in Fig. 37. Rods 3 and 4 lie outside the amount of burst data that is given so these rods would not be calculated to burst. Rod 5 is at such a low temperature that even though it has a high internal pressure it is not calculated to burst. Rods 1 and 2 would be calculated to burst, not because they have a high pressure but because they are at such a high temperature.

To make Rods 3 and 4 burst, they would have to have the internal pressure increase from 600 psi to approximately 1000 psi, such that their points would lie on the NUREG-0630 burst curve. So those rods would have to have much higher pressure to be calculated to burst. However, these rods are not at such a high pressure and hence they are not calculated to burst in the calculation. In addition to the higher internal pressure, the fuel rod must also achieve high temperatures to burst. For a very high burnup rod, calculated temperatures in excess of 1200 degrees Fahrenheit are required for burst. Both the internal pressure and cladding temperature must be met for the fuel rod to be calculated to burst. As a rule of thumb, a high burnup rod, which would tend to be at relatively low power, would have to heat up to 1300 F (700 C) in order to burst.

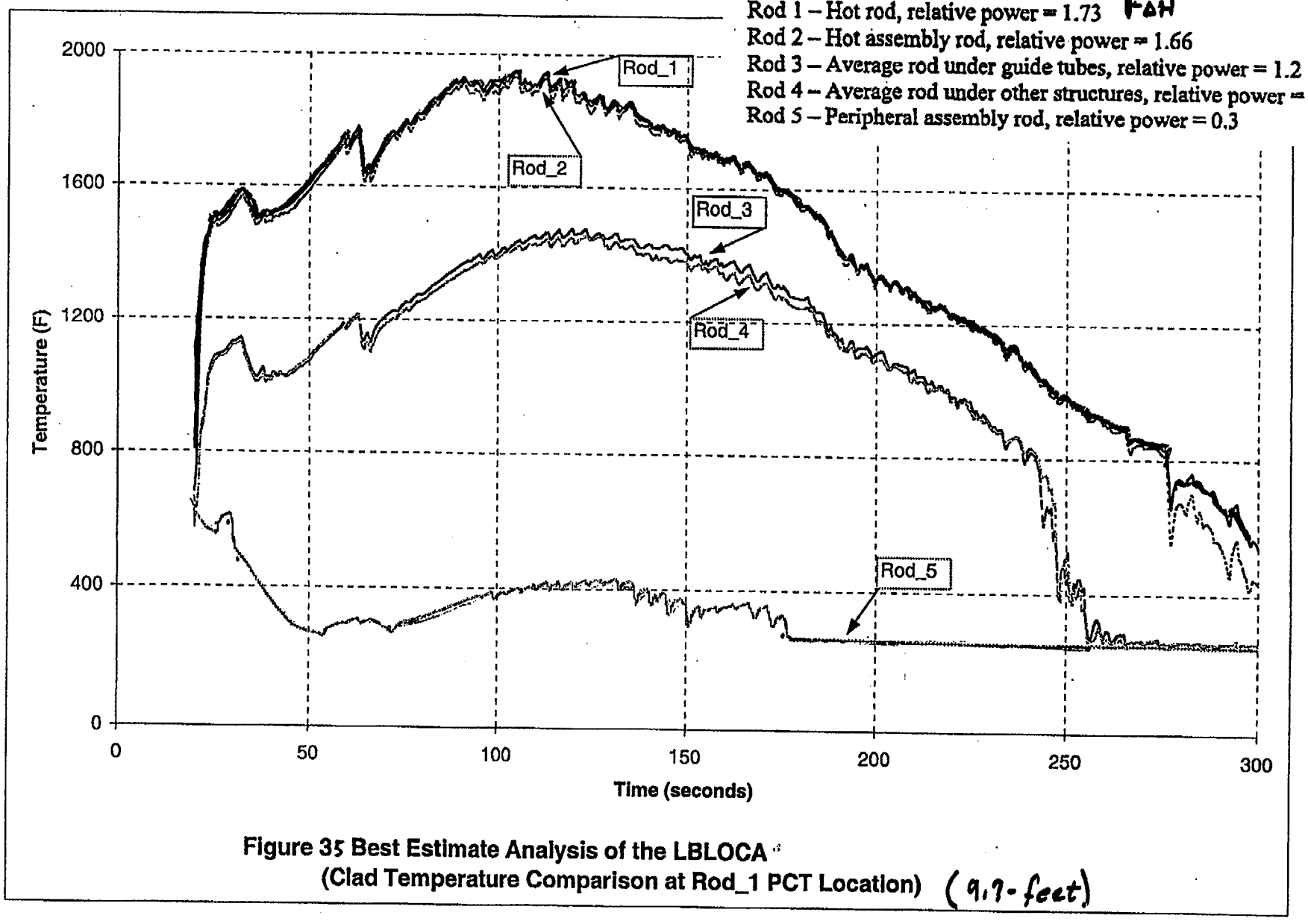

Figure 35 Best Estimate Analysis of the LBLOCA
(Clad Temperature Comparison at Rod_1 PCT Location)

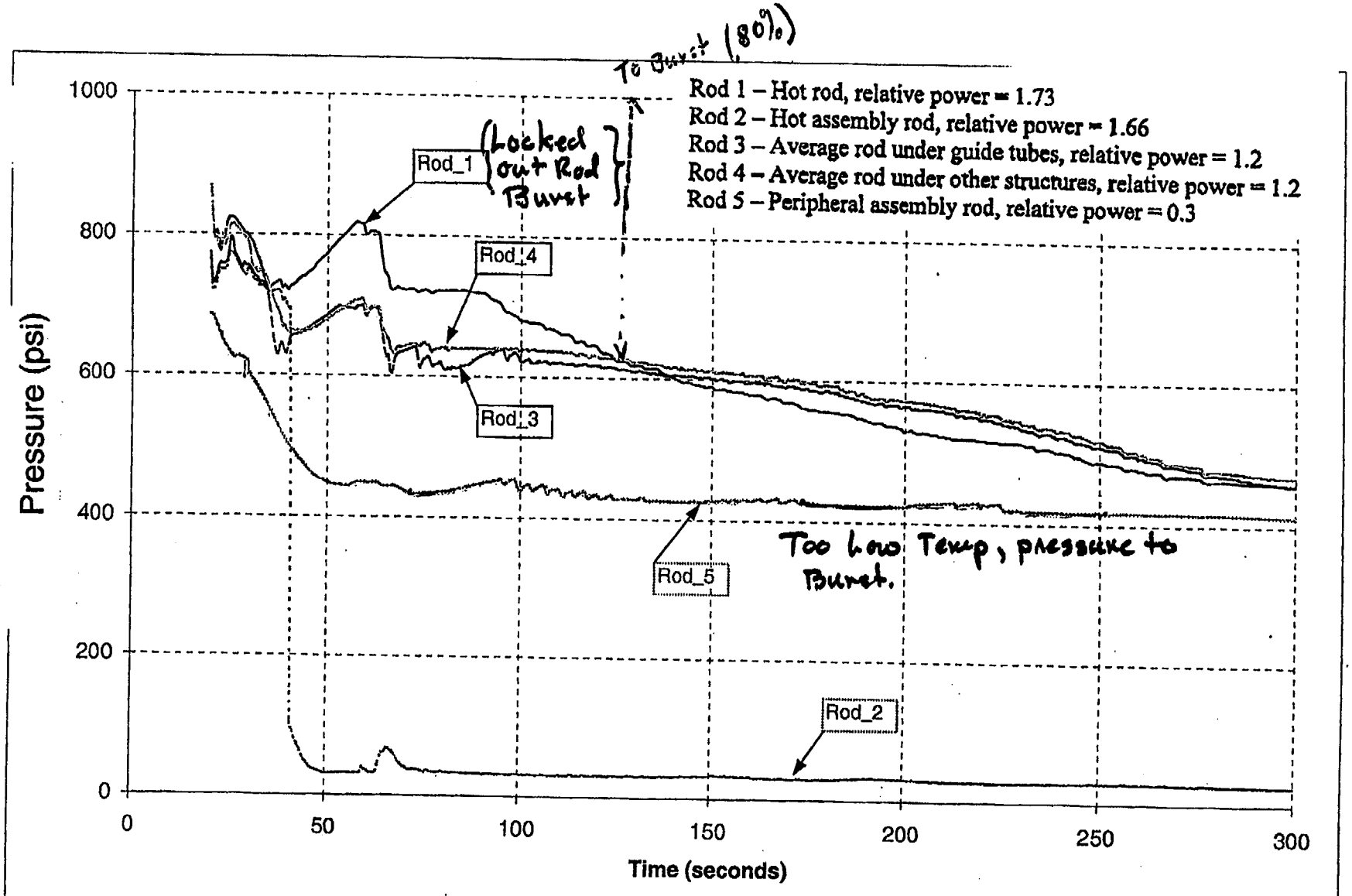

Figure Best Estimate Analysis of the LBLOCA
(Rod Internal Pressure Comparison)

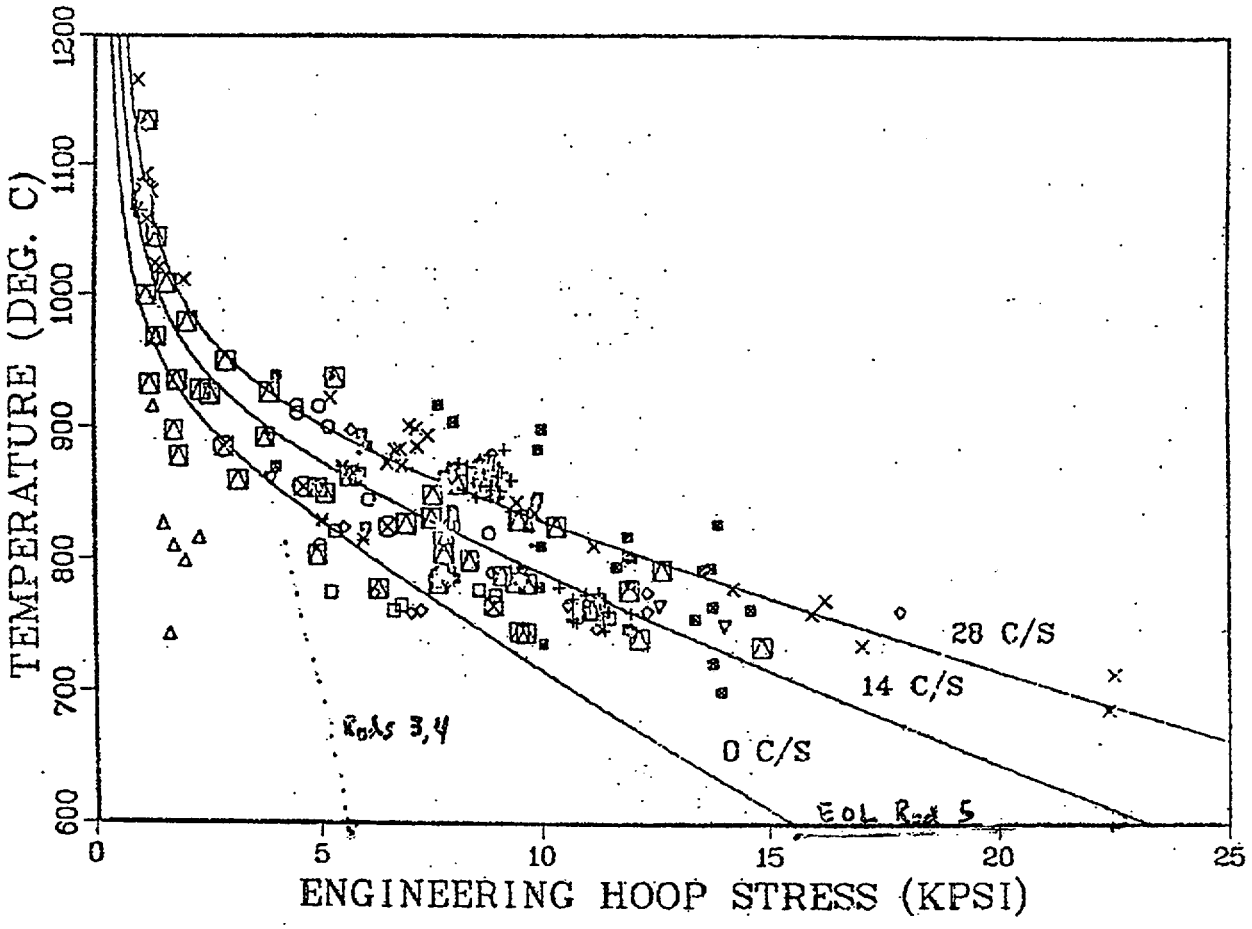

ORNL correlation of rupture temperature as a function of engineering hoop stress and temperature-ramp rate with data from internally heated Zircaloy cladding in aqueous atmospheres.

In a LOCA the fuel rod internal pressure decreases because the energy source has been removed as the reactor shuts down. Also, all system pressures come down and the fission gas plenum is at a much lower temperature so the internal pressure of the rod will decrease. This effect is shown in Fig. 38 for different fuel rods at the beginning of life (BOL), middle of life (MOL), and the end of life (EOL). This internal pressure calculation assumes perfect axial pressure transport such that there is no internal resistance to the gas pressure within the fuel rod. If the temperature for Rod 5 is examined, which is like about 400 degrees, this point is not even on this burst curve.

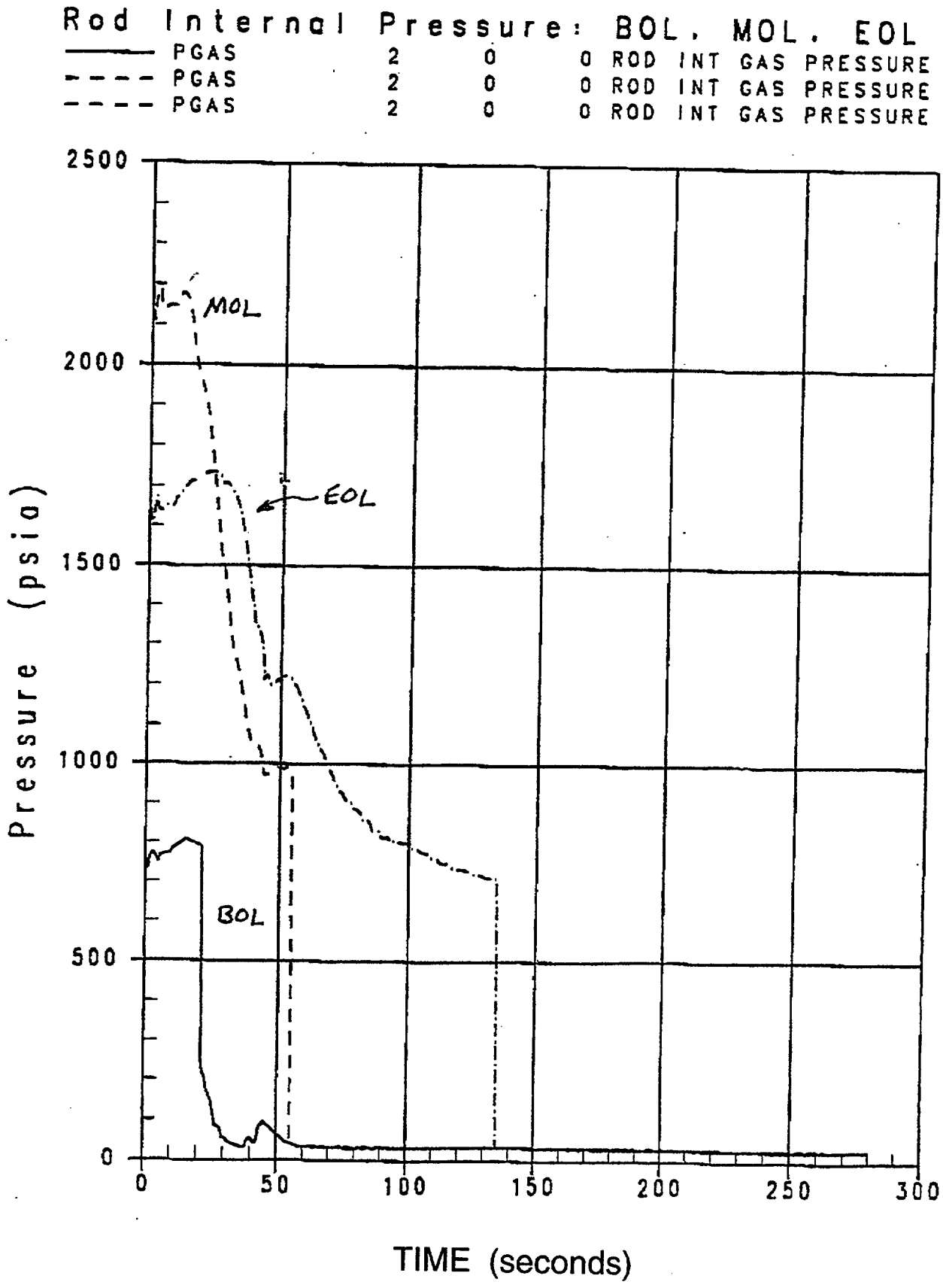
Rod Internal Pressure: BOL, MOL, EOL
PGAS 2 0 0 ROD INT GAS PRESSURE
PGAS 2 0 0 ROD INT GAS PRESSURE
PGAS 2 0 0 ROD INT GAS PRESSURE
MOL
EOL
BOL
2500
2000
1500
1000
500
0
0
50
100
150
200
250
300
Pressure (psia)
TIME (seconds)

This analysis indicates that at end of life, for the most burned fuel assemblies, which have the highest internal pressure, the rods are not likely to burst because their calculated temperatures are too low. If Rods 3 and 4, which constitute the majority of the rods in the core, don't burst, the majority of these fuel assemblies, which are going to have powers around 1.2 or lower, will not burst. Therefore it is only going to be the very high power fuel assemblies that burst, and these fuel assemblies are going to be the fuel assemblies with the least burnup.

WCOBRA TRAC was used for the transient calculations. The variations of the thermal conductivity of the fuel with burnup has not been considered since the majority of the fuel rods would seem to be at relatively modest burnup prior to where thermal conductivity degradation with burn up would become important.

I-1.7. Conclusions

The bottom line is that for the highest burnup fuel assemblies, particularly on the edge of the reactor core, the assembly power and the corresponding calculated temperatures, for a LOCA, are sufficiently low that fuel rod burst is not calculate even if these assemblies have the highest internal gas pressure. If the loading pattern places a twice-burned assembly at the center of the core, surrounded by high power assemblies; the effect of the higher power assemblies is to drive the burned assembly to higher powers than would otherwise be the case. In this situation, with the higher internal gas pressure within the fuel rods, the high burnup fuel assembly could experience burst. However, most of the burned assemblies, in which the relative power was 1.2 or less, were not calculated to fail. Therefore, in a realistic LOCA calculation, the majority of the higher burnup fuel assemblies are not calculated to fail. This result is dependent on the loading pattern, which is chosen. : For the purpose of satisfying the 10CFR50.46 criteria, the WCOBRA/TRAC plant model only analyzes the five fuel rods as discussed above. There is no fuel rod census throughout the core to see how many rods burst. That is not part of the acceptance criteria, although, perhaps, it should be.

I-2. PWR Small-Break LOCA: Impact of High Burnup Fuel

This review was prepared for the PIRT panel by A. F. Gagnon of Westinghouse Electric Company and panel member Lawrence E. Hochreiter of The Pennsylvania State University.

As part of the High Burnup Phenomena Identification and Ranking Table (PIRT) effort for the Loss of Coolant Accident, it was requested to put together a PWR small break LOCA tutorial for the PIRT panel. A loss of coolant accident is a failure of the reactor pressure boundary, either a crack, split, or a break in the main reactor piping or a failure of a connecting line, such that the break is large enough that the reactor system depressurizes. When the primary system depressurizes, safety injection and reactor scram signals will be activated. In Westinghouse plants, breaks larger than three-eighths of an inch, result in break flows which is lager than the normal make-up system capacity at full pressure, such that the reactor system depressurizes. Westinghouse plants have instrumentation lines that come out of the bottom of the reactor vessel and so one designs for failure of those instrumentation tubes, such that it becomes a leak, not a LOCA. The high head charging system is sized to have enough makeup flow capacity, that if one of the instrumentation tubes failed, which has happened, the safety injection signal does not occur.

Therefore, small-break LOCAs are breaks, which are typically larger than three-eighths of an inch, since smaller leaks don't depressurize the reactor coolant system, and are called leaks. Typically SBLOCA have break areas that are larger than three-eighths of an inch and less than one square foot. The limiting small break is determined by the interplay between the power level, and the axial power shape that is used, the capacity of the high head safety injection system, and the setpoint of the cold leg accumulators. The analysis and results that will be shown are typically what is calculated using a conservative Appendix K safety analysis model.

Typically, what's used in the Appendix K analysis is an artificial power shape, which is bounding for all expected operational power shapes. The bounding shape has the peak power location (peak kilowatts per foot) at the top of the core, because as the reactor vessel drains the core is uncovered from the top. As the two-phase mixture level drops below the peak power location, the fuel rod transitions from being cooled by nucleate boiling to being cooled by very low steam flow. As a result, the fuel rod temperature increases. The specific axial power shape is also chosen such that the integral of power is low at the bottom portion of the core. In this manner, only a small amount of steam is generated below the peak location, which then provides the steam flow for the cooling of the uncovered top portion of the core. With a high power at the top of the core and relatively low power at the bottom of the core, poor heat transfer and higher calculated peak cladding temperatures (PCTs) are calculated at the peak power location.

The break size is also important, because this is the leakage path from the primary system. The high-head safety injection performance is also very important, since this represents the make-up flow to the system. The accumulator set-point pressure is important since this determines if and when in the transient, the accumulators inject and refill the vessel.

Parameters such as the high head safety injection are plant dependent, and they can be different for different plants, and different vendors. The accumulator set-point pressure is also different for different vendor's plants. Therefore, the limiting break is that break size that is large enough such that the safety injection system can't make up the flow, such that the core uncovers. However, the limiting break must also be small enough such that the plant does not depressurize rapidly to the accumulator set -point, since at the set point the accumulators will inject and refill the reactor vessel. Therefore, the limiting breaks are those in the range where the break flow rate is significantly larger than the high head safety injection system; but, at the same time, not so large that the system is immediately depressurized to the point that the accumulators inject.

Figure 1 shows the types of safety systems for a typical PWR. The cold leg accumulators are passive tanks of cold borated water that are isolated from the primary system by check valves and when the primary system depressurizes below their set point pressure, water is injected into the reactor downcomer at a high flow rate. Figure 1 also shows the high pressure, intermediate pressure and low pressures safety injection pumped systems. Most plants have both high-pressure and low-pressure safety pumped systems. These systems can come on at a varying range of pressures. For some plants, the high head injection pressure can exceed the safety valve set-point, particularly for older plants. This is not necessarily a good idea, because if there is a spurious safety injection signal, the charging flow from the safety injection pump could result in a liquid solid system, which will result in opening the pressurizer safety valves. Most of the high-pressure safety injection systems inject starting at 1,800 PSI. The low-pressure safety injection systems start to inject at approximately 150 PSI. Reactor scram and safety injection typically occurs when the reactor coolant system depressurizes below 1,900 PSI.

Analysis of small break LOCAs is really verifying the performance or capacity of the high-pressure safety injection system to mitigate the small break transient. Single failure is assumed such that one of the high-pressure safety injection pumps is lost.

For most Westinghouse plants, the limiting break size is typically between two and four inch sizes. The smaller breaks are terminated by the high-pressure safety injection system, and the larger, small-breaks, are terminated due to the accumulator injection. So, it is this smaller range between two to four inches that's more limiting. For both Westinghouse and B&W plants have the accumulator set-point pressure at about 600 PSI. This pressure limits the maximum size of the small break, because the larger the break, the more quickly reactor system depressurizes and then the accumulator comes on and refills the vessel to terminate the accident.

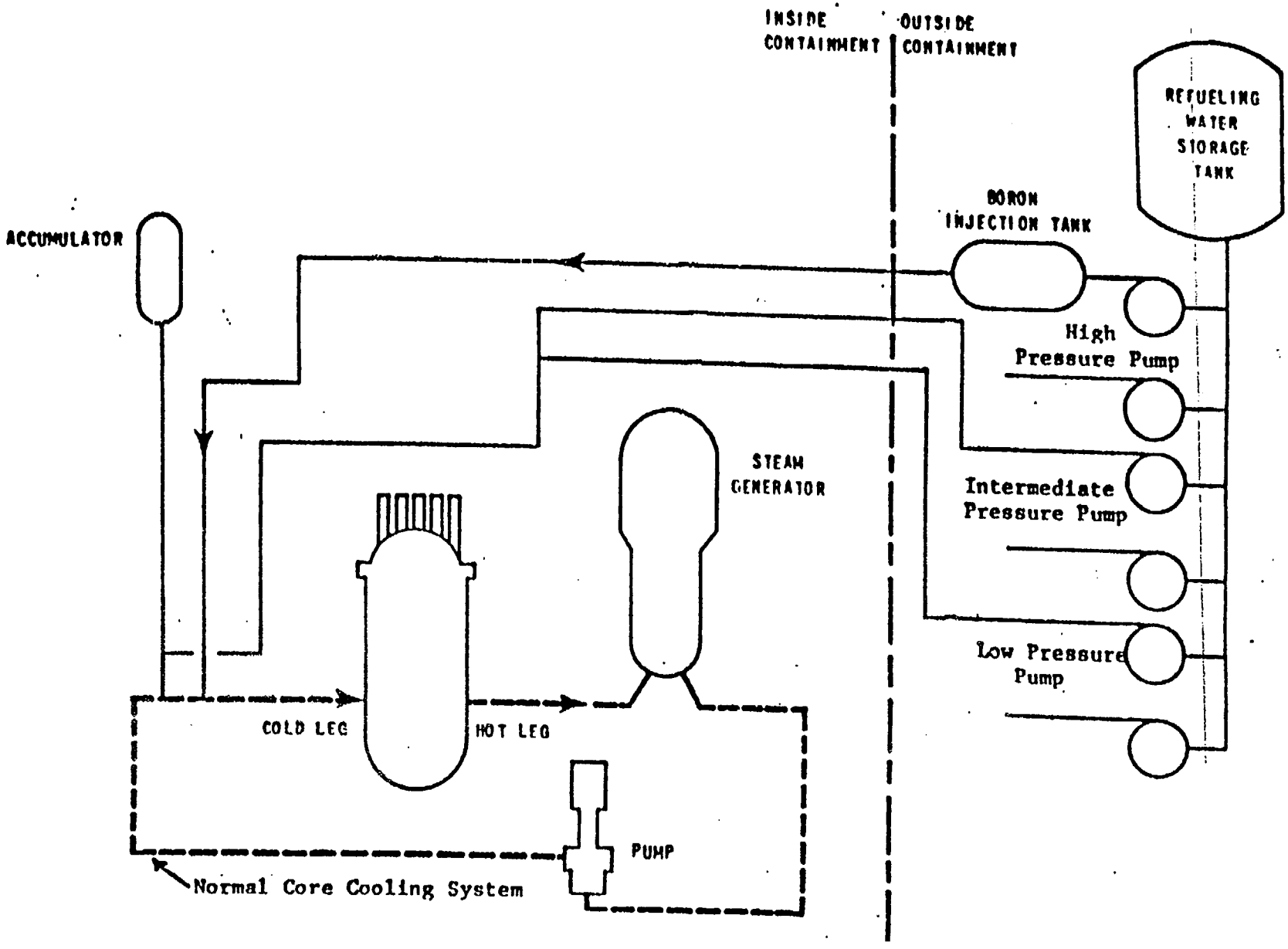

Figure 1. Emergency Core Cooling System (Schematic)

Combustion Engineering plants have lower accumulator set point pressures, typical 200 PSI. It is my understanding is that they dropped the pressure down to 200 PSI basically to improve the plant large break LOCA performance since less accumulator water would be bypassed. By decreasing the accumulator setpoint pressure, there is a larger range of small breaks, which can be more limiting. For the Combustion Engineering plants, the small break peak cladding temperature (PCTs) are typically higher than for Westinghouse and Babcock and Wilcox plants and are closer to the large-break LOCA PCTs.

A Westinghouse reactor system is shown in Fig. 2. For small break LOCA behavior, a reactor trip on low pressurizer pressure will occur at typically 1,900 PSI. Full credit is taken for control rod insertion, such that the high pressure safety injection system only has to remove the core decay heat and the stored energy that is in the primary system, mostly in the metal structures.

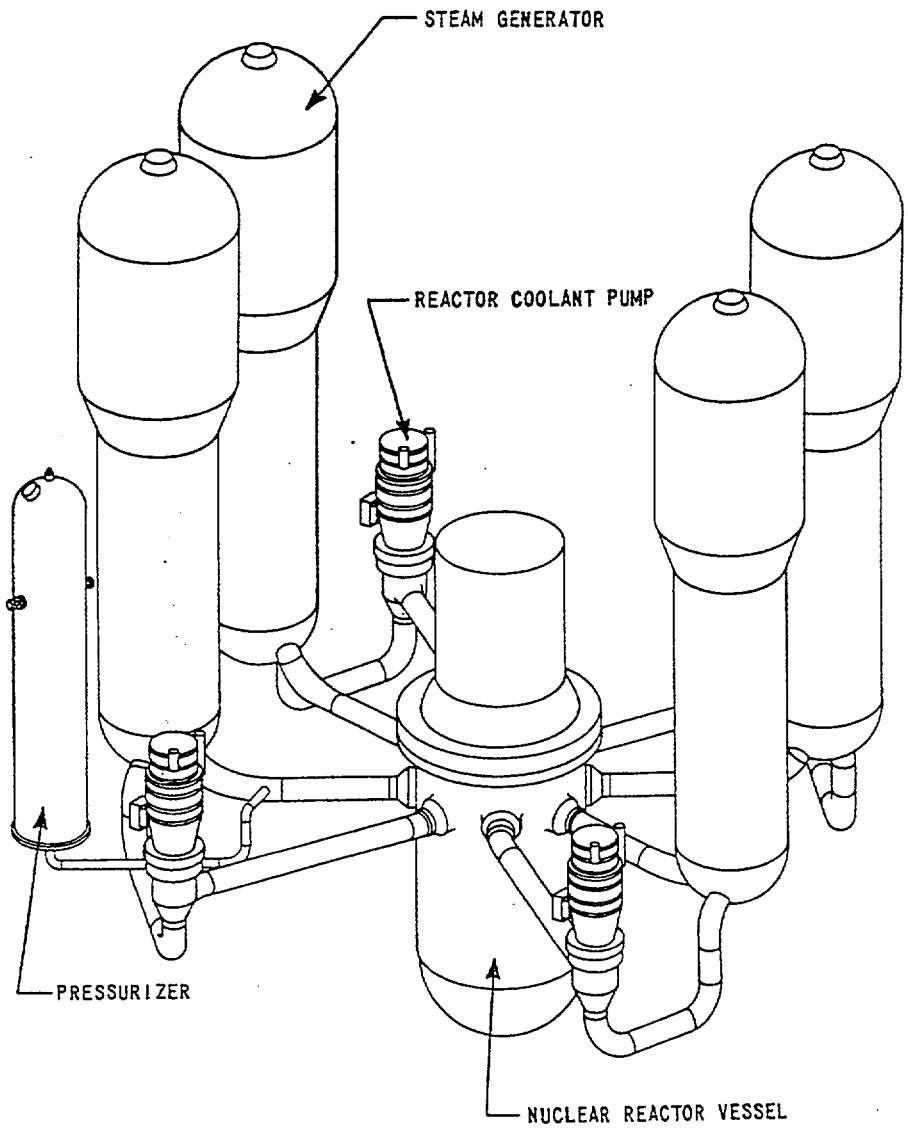

High-pressure safety injection system will occur about 1,800 PSI. The steam generators are isolated, and the emergency steam generator feed flow starts. Energy is removed from the primary system by both the break and the energy removal from the steam generators. The time period in which energy is removed by the steam generators depends on the break size, but usually for the limiting breaks it is for several hundred seconds. The primary system is in single and two-phase natural circulation with the energy being removed from the generators, in addition to energy going out the break. The plant decay heat is typically two or three percent and the generators are sized for 100 percent so it is easily remove the core decay energy from the generators, which will help cool the system down.

Single phase and then two-phase natural circulation will continue until the reactor system has drained sufficiently that there will be a break in natural circulation in the generators because the mixture level is low enough that liquid can no longer carry over the U-tubes in the generators. At this point the plant will transition into a reflux condensation mode in the generators. Vapor with, some liquid droplets, will be carried into the up-hill side of the generator where the steam will be condensed and the condensate will run back down into the upper plenum. Some of the steam will also be carried over the U-tube to the downhill side of the generator where it is condensed and the condensate flows into the cold leg. During all phases of natural circulation, the high-pressure safety injection system continues to inject subcooled borated water into either the cold legs or into the downcomer.

As the transient progresses, the primary system slowly looses mass and the mixture level in the vessel is decreasing until there is a level in the hot legs and in the cold legs, natural circulation has ended and basically, the reactor vessel is acting like a boiling pot in reflux condensation. The core is still covered, and is in nucleate boiling. There is really no temperature excursion at this point, and the stored energy in the fuel has been removed. The energy that is being removed is the core decay heat any stored energy that is in the structures.

As the mixture drains down further to the cold-leg elevation, the generators are empty, there can be a liquid level in the reactor cold-leg loop seals as seen in Fig. 2. The loop seals can be full of water and there will be a mixture level that may be in the upper plenum above the top of the core. For a cold leg break the loop seals will have to be vented such that core generated steam can vent out the break. To vent the loop seals, the upper plenum pressure will increase which will depress the mixture level in the vessel. Water will actually be forced out of the core, up into the down comer, to counterbalance the elevation head of the loop seals. This can lead to a core uncovery and a short temperature excursion. Once the loop seal vents, steam will then blow through the loop seal and out the break, and the mixture level will return to its original position in the vessel. Once steam vents out the break, the system depressurizes faster. Core uncovery can occur as the vessel mixture level is depressed to vent out the loop seal, however, it is only momentarily. It doesn't normally take very

long to vent the loop seal and then recover the mixture level, after which the system slowly continues to lose inventory.

The portion of the core that is covered with a two-phase mixture remains in nucleate boiling. When the mixture level drops down into the core, there is a very sharp interface that exists between the covered region in the core and that portion of the core, which is uncovered. The covered region is in nucleate boiling where the cladding temperature is approximately five degrees above the saturation temperature. The uncovered region of the core is in steam cooling, and is the region in which the peak cladding temperature is calculated to occur. The covered and uncovered regions of the core are shown in Fig. 3.

Depending upon how deep the core uncovers, the axial power shape that is assumed, and the core power level, the steam above the mixture level will quickly superheat. As a result there is very poor cooling, and the fuel rods heat up very quickly to high temperatures due to the decay power at the hot spot. From a fuel rod point of view, is the difference between the small and the large break, at this point is that in the small break, the stored heat in the fuel rod is not a factor and does not contribute to the fuel rod heat-up. In the large break, the fuel rod stored energy is a factor and does contribute to the fuel rod PCT.

The resulting small-break PCT does dependent on how long the heat-up occurs in the transient and the location of the mixture level in the core, or the location of where the front is between nucleate boiling and steam cooling.

The Westinghouse Appendix K small-break analysis method uses the NOTRUMP reactor systems code. It is a one-dimensional, network flow path, control volume type code that uses a five-equation drift flux formulation. NOTRUMP calculates the draining of the reactor system, counterflow and countercurrent flooding, and mixture levels in the core and different volumes in the reactor system. It treats thermodynamic non-equilibrium, since the steam can be superheated at temperatures much higher than the saturation temperature, in the presence of liquid droplets.

NOTRUMP has flow regime dependent drift flux models to predict the mixture levels, two-phase pressure drop and the void fraction distribution in the mixture within the reactor vessel. The code can also predict the two-phase stratification in the hot legs and the cold legs as the vessel drains. NOTRUMP models the core and the structural energy release into the fluid and the steam generators as well as the break from the primary system. It uses point kinetics for the neutronics modeling but this is a small effect because the reactor shuts down as the control rod scram and it is really the decay power that is being removed. NOTRUMP also models the safety injection system including the high-pressure safety injection as well as the accumulators.

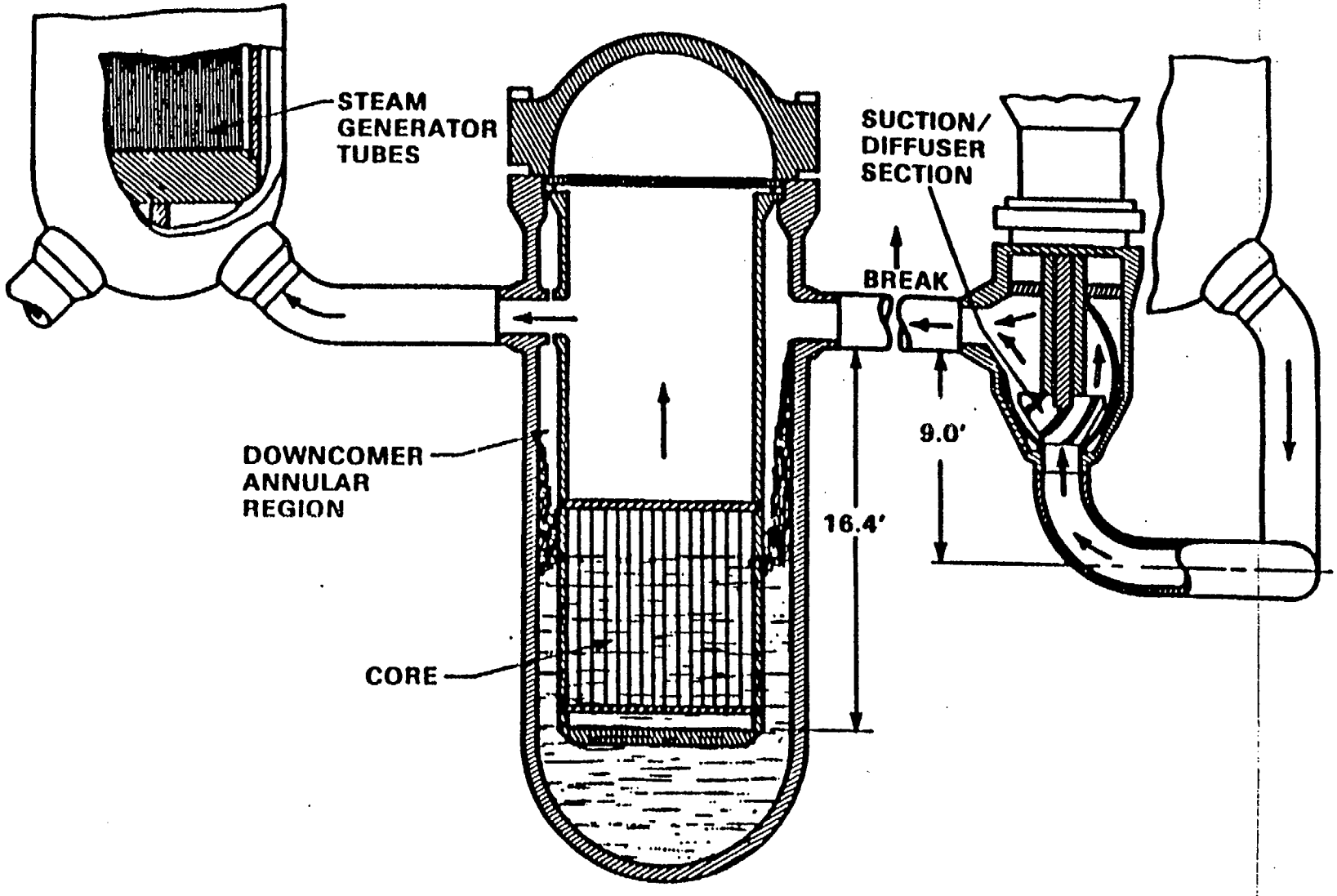

Figure 3. Cold Leg Break Steam Flow Path Schematic Drawing

Again, NOTRUMP is the hydraulic calculation, as seen in Fig. 4, and it passes the hydraulic information, such as the mixture level, the core flow, the pressure, and so forth, to a hot rod heat up calculation, which is the LOCTA code which is also seen in Fig. 4. LOCTA models the core average rod as well as the hot rod in the core. It has the thermal model for the rod as well as the mechanical model. The mechanical models is not the detailed mechanical design code model, but it's a suitable mechanical model that will predict the mechanical cladding behavior such as swelling, burst and rupture on the cladding as well as the peak cladding temperature. LOCTA also performs its own calculation of the local vapor temperature, which is the heat sink for the fuel rod model. The hot rod model in the LOCTA code has all the uncertainties added on such that the calculation represents the peak FQ, F delta H, and so forth. For the mechanical calculation, it includes the NUREG 0630, burst criteria and burst strain curve and includes the Appendix K required metal-water reaction and performs a double-sided reaction calculation if rod burst occurs.

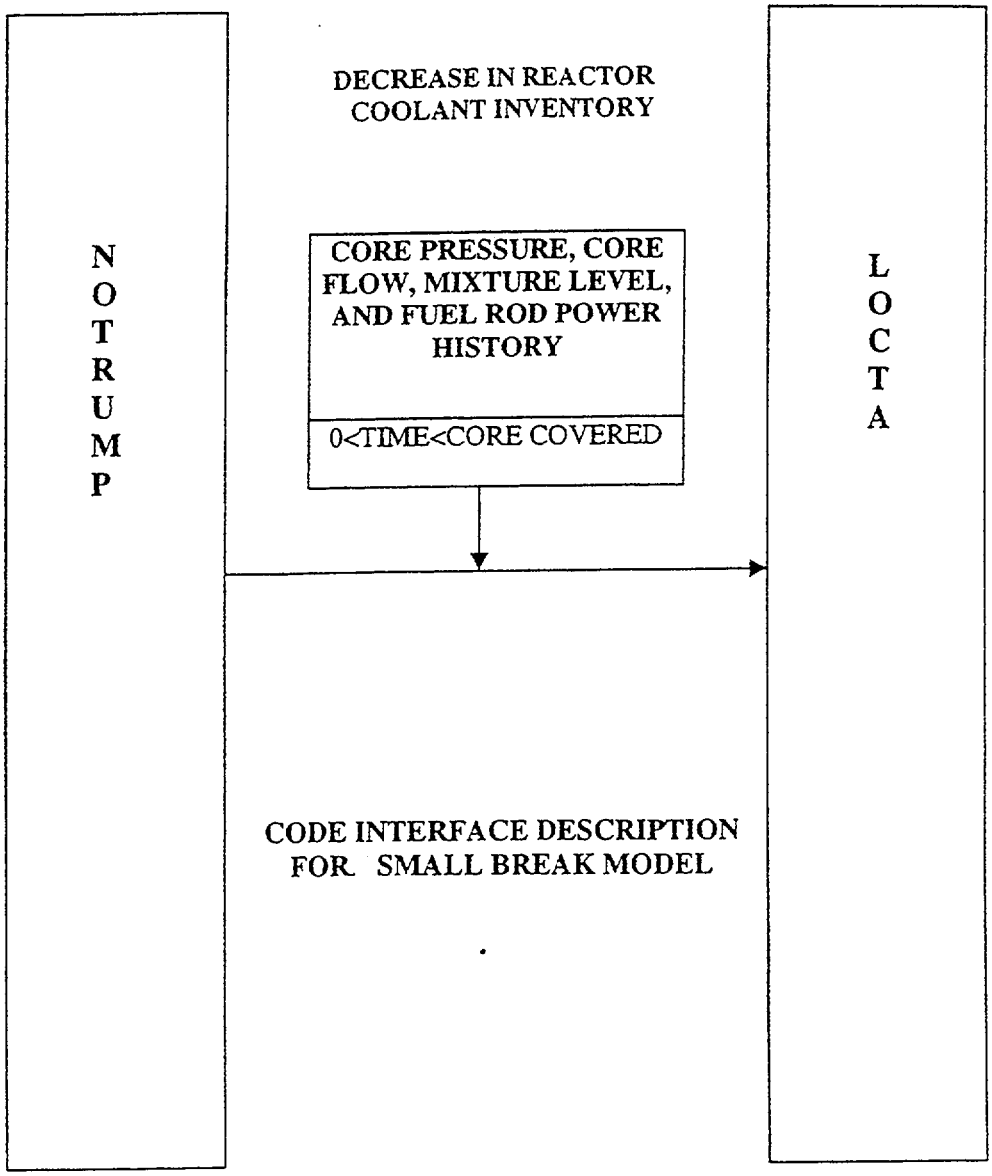

Two sets of Appendix K small-break calculations, one calculation for fresh fuel which has higher peaking factors and fuel which has higher burnup at 30 GWd/t and 54 Gwd/t will now be examined. These calculations are for typical Westinghouse three-loop plant. Different plants will respond differently to the small-break LOCA, because of the sizing of the high-head safety injection system. Typically, Westinghouse four-loop plants have higher high head safety injection capacity so the small break peak temperatures that are calculated for these plants are much lower than the temperatures calculated for three-loop plants.

The first set of calculations reflect typical FSAR small break LOCA calculations for fresh fuel. The initial conditions for the calculations are given in Table 1. Fresh fuel maximizes the peak linear heat rate in the calculation. However, at the same time, fresh fuel has very low burnup and the calculation tends not to predict fuel rod swelling, burst and ballooning, and failure of the cladding. The second set of calculations consider the effects of burnup on the fuel rod behavior and response. In these cases, the fuel rods do balloon and burst. The information in Table 1 is for a three-loop plant at the beginning of a cycle. The peak linear heat rate includes the effects of the calorimetric error or uncertainty. The plant power is 2775 megawatts. It has a rather high total peaking factor (FQ). This plant has fuel assemblies with a 17 by 17-rod array. The reactor system conditions are given in the table along with the plant initial conditions before the calculated transient. The accumulator set point pressure is 615 PSI, and it is assumed that the plant has10 percent steam generator tube plugging.

Table 1.

INPUT PARAMETERS USED IN THE ECCS SMALL BREAK ANALYSIS

Core Power	2775 MWt
Peak Linear Power (included 102% factor)	13.663 KWt/ft
Total Peaking Factor, F_Q	2.46
Axial Peaking Factor, F_{NZ}	1.4302
Power Shape	See Figure 15.6.5.2-3
Fuel Assembly Array	17x17
Accumulator Water Volume (nominal)	1,000 ft^3
Accumulator Tank Volume (nominal)	1,450 ft^3
Accumulator Gas Pressure	615 psia
Safety Injection Pumped flow	See Figures 15.6.5.2-1 and 15.6.5.2-2
Initial Loop Flow	9,612 lb/sec
Vessel Inlet Temperature	554.8 °F
Vessel Outlet Temperature	622.2 °F
Reactor Coolant Pressure	2300 psia
Steam Pressure	925.5 psia
Steam Generator Tube Plugging Level	10%

Table 2 gives the time sequence for a range of small breaks. In the analysis, a range of breaks need to be considered to examine the trade-off between performance of the high head safety injection system; the break size, the core power, and the accumulator set point. The interactions of all these parameters determine the most limiting break. Typically four breaks are examined; two, three, four, and six-inch breaks as shown in the table. The reactor trips on low pressurizer pressure. The S, or safety injection signal, quickly follows. Safety injection starts being delivered. In some plants, there is a delay time for safety injection. The time at which core uncover occurs is also given in the table. For the smallest break, it takes almost 1,500 seconds before core uncovery occurs. The larger the break the shorter the time scale for the accident transient. Also, the larger the break the quicker the reactor system will depressurize and the accumulator will terminate the transient because it will start to inject sooner.

The time when the peak cladding temperature occurs is also given in Table 2. For the two-inch break, there is no accumulator injection. In other words, as the decay heat falls off, and the high head safety injection is maintained, it will eventually overcome the loss of inventory in the system and recover the vessel.

The three-inch break has the highest PCT. This break requires the accumulator injection to terminate the transient and as the break size gets larger, the accumulator injection occurs earlier in time and the core is recovered earlier in time such that the resulting PCT is lower. The same criteria are used to evaluate the small-break LOCA as are used to evaluate the large-break LOCA. Usually the most limiting criteria is the calculated peak clad temperature which is limited to 2200 ^{0} F. The small-break LOCA transients are very long and for the smaller breaks it take several thousand seconds before the core is completely covered by a two-phase mixture and the fuel rods return to nucleate boiling.

While the cladding temperature is elevated, as long as it stays below the metal-water reaction temperature, the amount of oxidation of the cladding is small and the 17% criteria of Appendix K is not violated. If the cladding temperature does remain above 1800 ^{0} F for extended periods of time then the analysis would be limited by the cladding oxidation. The peak cladding temperature is still usually the most limiting criteria for the transient.

The results of the different break size calculations are given in Table 3 and indicate that the three-inch break is the most limiting and its peak clad temperature is slightly over 1800 ^{0}F. Again, this analysis has been performed for fresh fuel, so the fuel rods do not burst. The PCT elevation is at 11.75 feet which is due to the assumptions on the axial power distribution.. The maximum calculated oxidation is about 12 percent for the three-inch break. Therefore, the calculation has met the Appendix K criteria of a PCT is less than 2,200 degrees, oxidation is less than 17 percent, and less than one percent of core wide hydrogen generation. Since the peak cladding temperature and oxidation limits are within the Appendix K requirements the core remains in a coolable geometry. The plant has also been designed for long-term cooling.

Table 2.

NOTRUMP TRANSIENT RESULTS

Event Time (sec)	2 Inch	3 Inch	4 Inch	6 Inch
Break Initiation	0	0	0	0
Reactor Trip Signal	42.5	16.2	9.41	6.07
S-Signal	56.8	28.0	20.3	13.9
SI Delivered	83.8	55.0	47.3	40.6
Loop Seal Clearing*	960	416	210	42.5
Core Uncovery	1468	700	436	181.5
Accumulator Injection	N/A	1246	609	259.9
RWST Empty Time	3910	3878	N/A	N/A
PCT Time	2822.5	1482	764.2	317.7
Core Recovery**	> 6000	> 5000	2828	382.2

* Loop seal clearing is defined as break vapor flow > 1 lb/s

** For the 2 and 3 inch cases, where core recovery is > TMAX, basis for transient termination can be concluded based on the following arguments: (1) The RCS system pressure is decreasing which will increase SI flow, (2) Total RCS system mass is increasing, (3) Core mixture level has begun to increase and is expected to continue for the remainder of the accident

Table 3.

BEGINNING OF LIFE (BOL) ROD HEATUP RESULTS

	2 Inch	3 Inch	4 Inch	6 Inch
PCT (°F)	1276	1829	1531	1418
PCT Time (s)	2822.5	1482.0	764.2	317.7
PCT Elevation (ft)	11.5	11.75	11.5	10.75
Burst Time (s)	N/A	N/A	N/A	N/A
Burst Elevation (ft)	N/A	N/A	N/A	N/A
Max. Local ZrO_2 (%)	0.23	3.98	0.49	0.16
Max. Local ZrO_2 Elev (ft)	11.5	11.75	11.5	11.0
Core-Wide Avg. ZrO_2 (%)	0.03	0.53	0.08	0.03

Figure 5 shows the high head safety injection flow. The lower curve is the flow that's in the broken loop, and the higher curve is the flow that is in the two intact loops. As the figure indicates, as the system pressure drops, the flow rate increases as expected. In NOTRUMP, the intact loops are lumped, this is a three-loop plant, so the intact loop flow actually represents the flow that is in two loops. One of the things that is done for the ECCS system design relates to the orifices in the injection lines, which are designed it to minimize the amount of flow that is loss due to the break. Therefore, each line has roughly the same flow per loop, whether it discharges into a broken cold leg or into an intact loop. The flows are actually tested in the plant.

Figure 6 shows the axial power distribution that is used in the small break calculations. The peak power occurs near the very top of the core resulting in a very conservative shape. The peak power location is occurring roughly at the 10-foot elevation, and most of the power is in the upper portion of the core with lower power in the bottom part of the core. Since the core uncovers from the top, the two-phase mixture level is moving down and uncovering the top portion of the core. If there is lower power generation at the bottom of the core, the amount of steam that is generated is smaller, so that the steam flow flowing upward to cool the top portion of the core is smaller. Therefore a power shape of this type is specifically chosen to penalize the calculation.

Figure 7 shows the reactor system pressure. The pressure quickly drops from 2250 psia down to approximately the safety valve setpoint on the secondary side of the steam generators (approximately 1250 psia). The main reactor coolant pumps are tripped very early in the transient. Energy is then removed from the primary system in this time period, by natural circulation, using the steam generators. As the primary system loosing more and more inventory and the pressures starts to come down. It is the break that's doing the depressurization. At approximately 1,100 seconds or so, the accumulator setpoint pressure is reached and the accumulators can inject which is a large source of water to refill the vessel.

Figure 8 shows the mixture level in the vessel. The top of the core is at 22 feet in the figure. The mixture level decreases and then it starts to move into the core at approximately about 700 seconds or so, and reaches a level of approximately six feet in the core and then it slowly recovers. The accumulators start to come on at this point and then the core mixture level is recovered as shown in the figure. In this calculation, it does take a long time to completely refill the core.

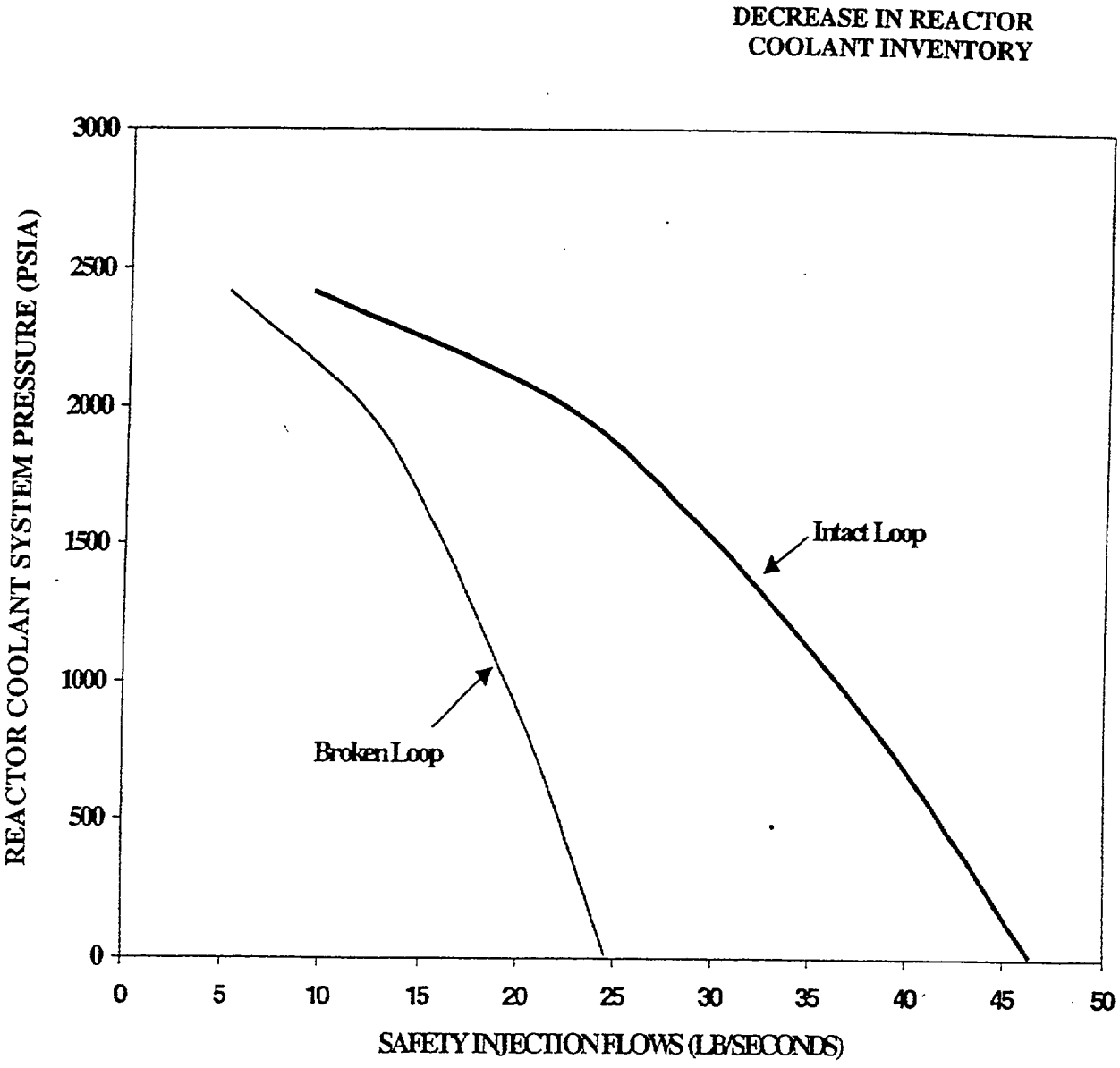

Figure 5.

SMALL BREAK SAFETY INJECION FLOW RATES
BREAKS LESS THAN 6 INCHES

DECREASE IN REACTOR
COOLANT INVENTORY

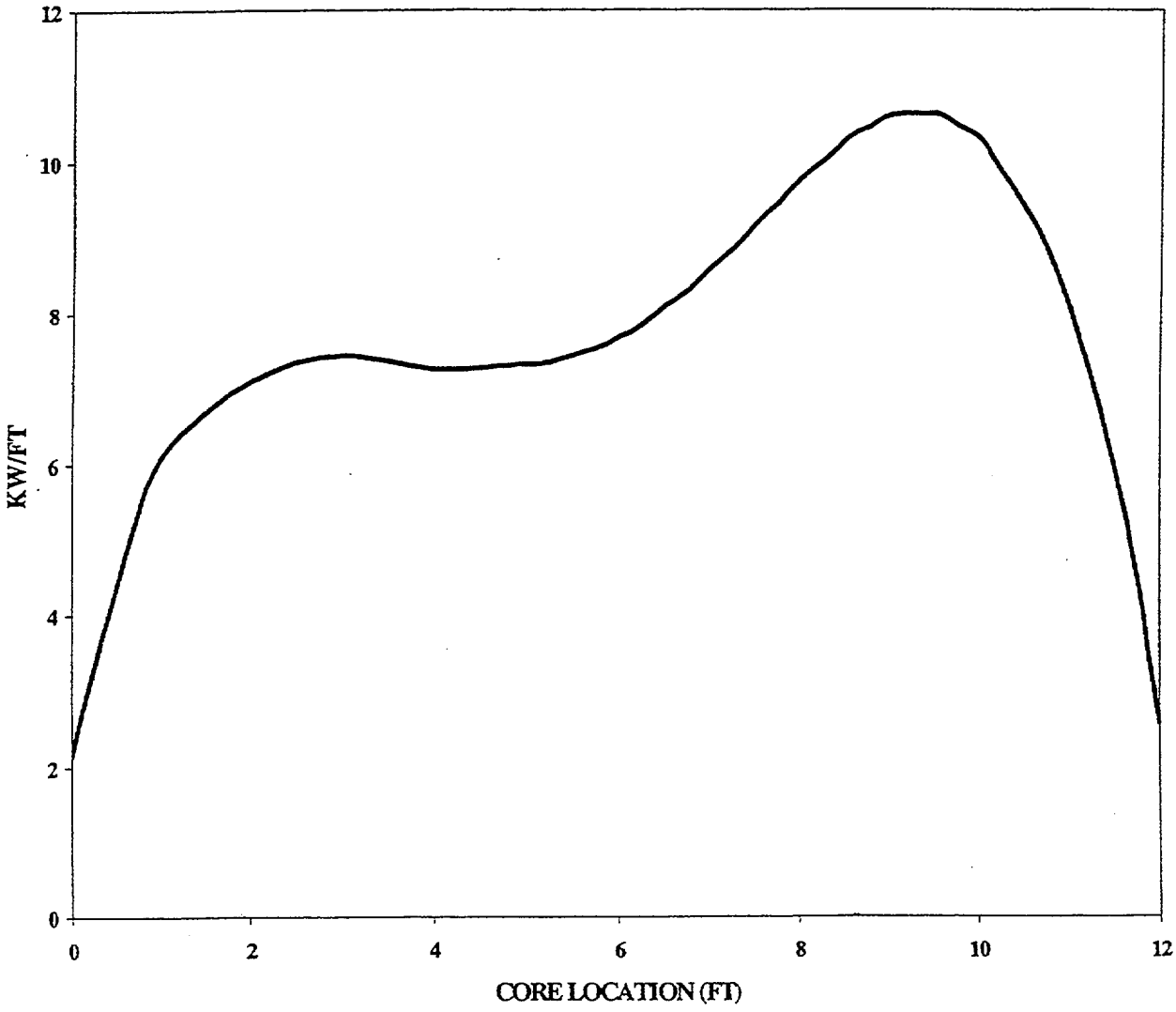

Figure 6.

SMALL BREAK HOT ROD POWER SHAPE

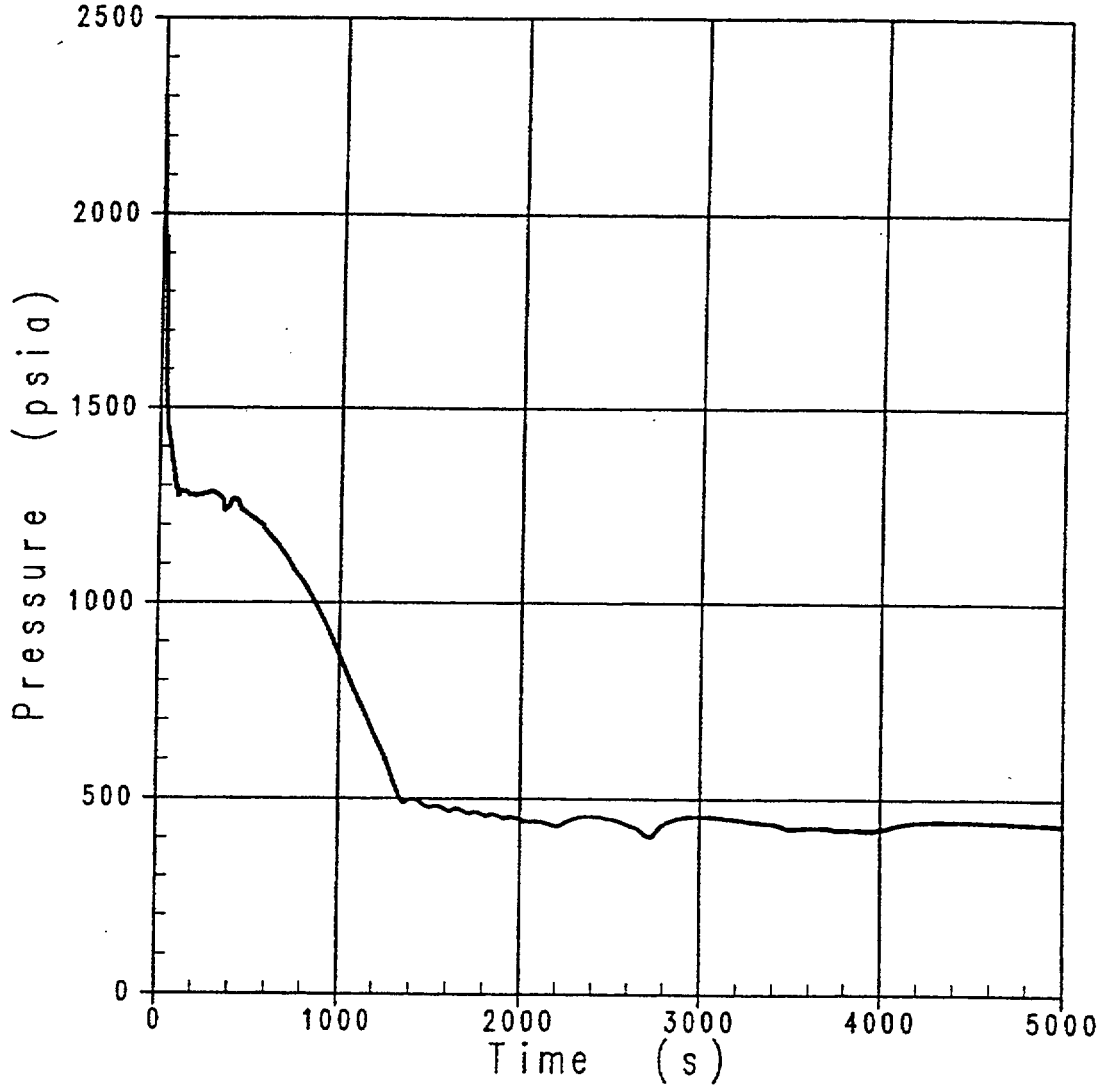

Figure 7.

3-INCH PRESSURIZER PRESSURE

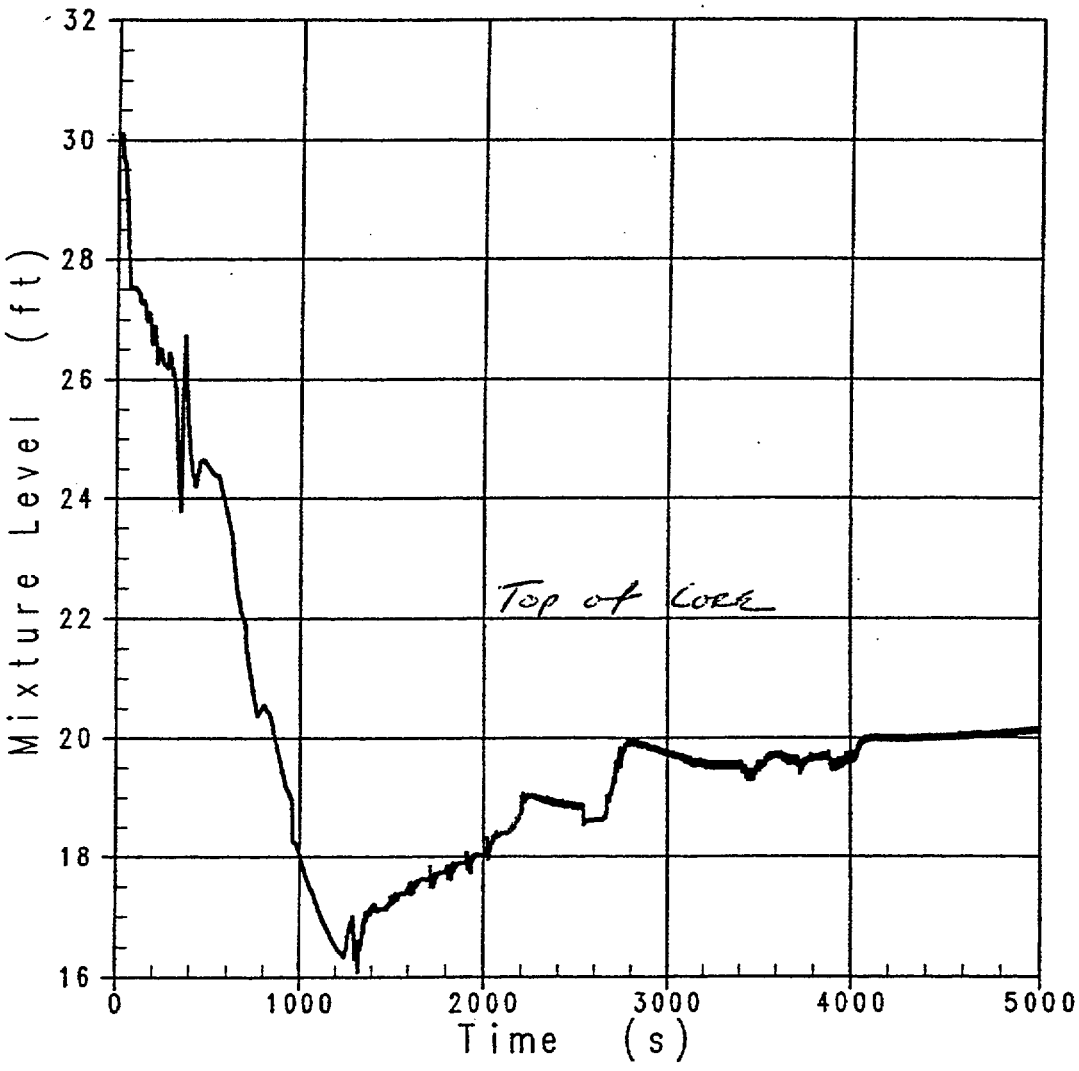

Figure 8.

3-INCH CORE MIXTURE LEVEL

Figure 9 shows the calculated peak cladding temperature, which indicates when the top of the core becomes uncovered. Once the core uncovers, the temperature immediately increases above the saturation temperature since the fuel is now being cooled by weak steam cooling. The calculated peak temperature reaches approximately 1,800 degrees before it turns-over and comes back down. In this calculation, the peak clad temperature is turning over as the vessel refills. As the core begins to refill two effects occur which help cool the peak temperature. Refilling the core reduces the vapor temperature, which is the heat sink for the heat transfer from the fuel rod. The second effect is that more of the core becomes covered with a two-phase mixture such that a higher steaming rate will occur which improves the single-phase steam convection heat transfer coefficient. Also, the figures indicate that the peak temperature is occurring over several hundred seconds during which the core is slowly refilling. During this time the decay heat is also decreasing slightly as time progresses. All of these small changes result in improved cooling at the peak location and the termination of the clad temperature rise.

Figure 10 shows the calculated heat transfer at the PCT location. The high heat transfer is when the core is covered with a two-phase mixture while the low heat transfer coefficient is when the PCT location is in steam cooling. There are two orders of magnitude difference.

Figure 11 shows the calculated vapor temperature at the PCT location. The steam does get quite superheated and it is not significantly different than the cladding temperature. The Steam temperature then decreases as the core refills, which decreases the cladding temperature. The heat flux at the hot spot sees the benefit of the increased steam flow, which results in a higher heat transfer coefficient, and the benefit of a larger delta T, both which increases the heat flux from the rod which turns the temperature over.

Westinghouse also ran some additional 3-inch small-break LOCA calculations to examine the effects of high burn up situations. The hydraulic transient for the high burn up calculations and the beginning of cycle calculations shown previously, is nearly identical as seen in Table 4. The higher burn up rods have reduced power to reflect the fuel burn down that has occurred. These rods also have higher internal pressures since there are additional fission gases within the rods due to the burn up effects.

Figure 12 shows the pressure behavior in the vessel, which is basically, the same, since the pressure is responding to the break and the safety injection systems. The accumulator set point is 615 PSI. The vessel mixture level shown in Fig. 13 is also the same. Twenty-two feet is the top of the core. As the figure indicates, the core becomes uncovered and then it slowly recovers due to the accumulator injection. Figure 14 shows the core average vapor temperature, which reaches 1,300 degrees Fahrenheit. The vapor temperature increases once the core location is uncovered. The same axial power shape is used for these calculations as was shown previously.

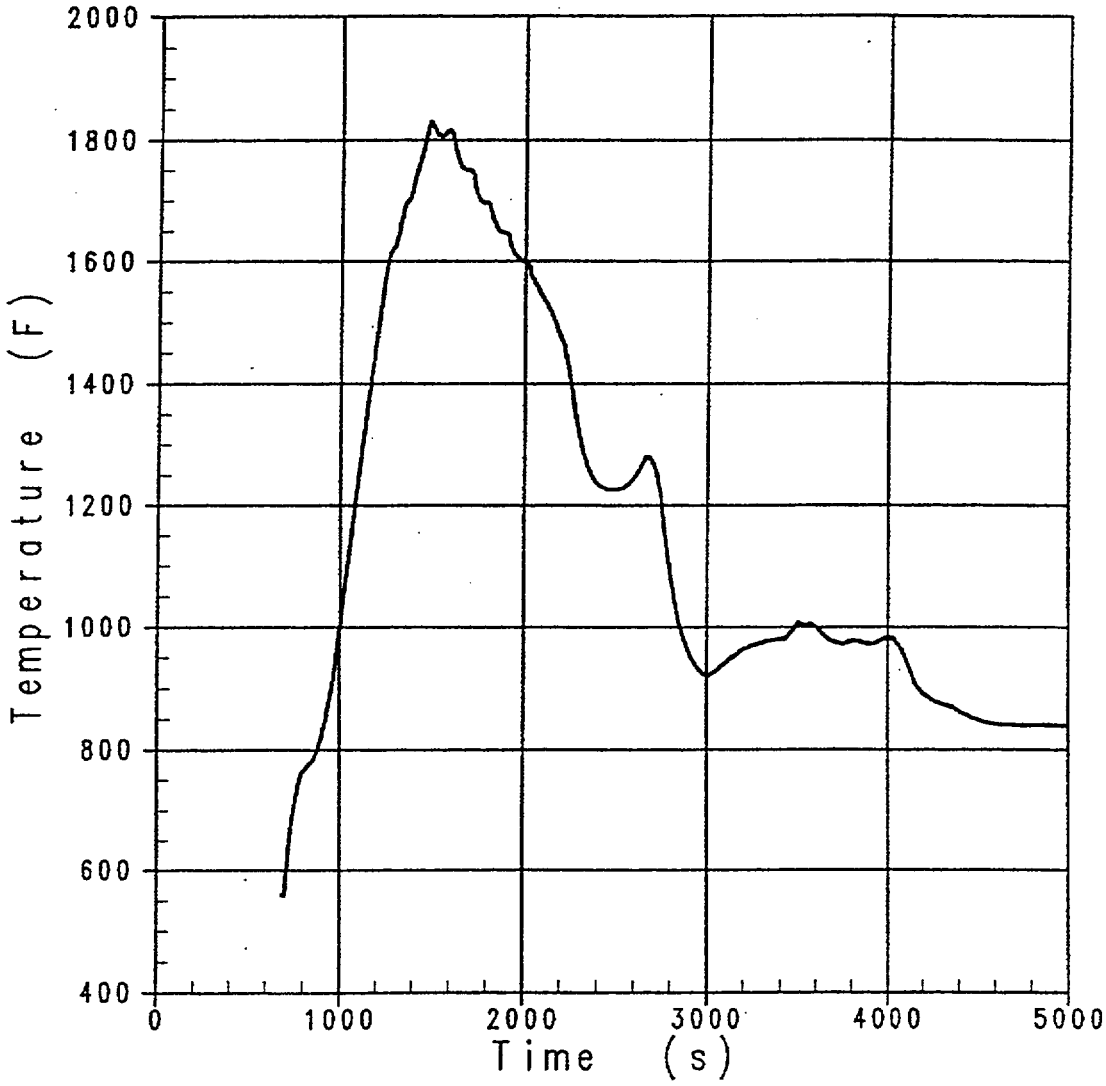

Figure 9.

3-INCH PEAK CLAD TEMPERATURE

DECREASE IN REACTOR
COOLANT INVENTORY

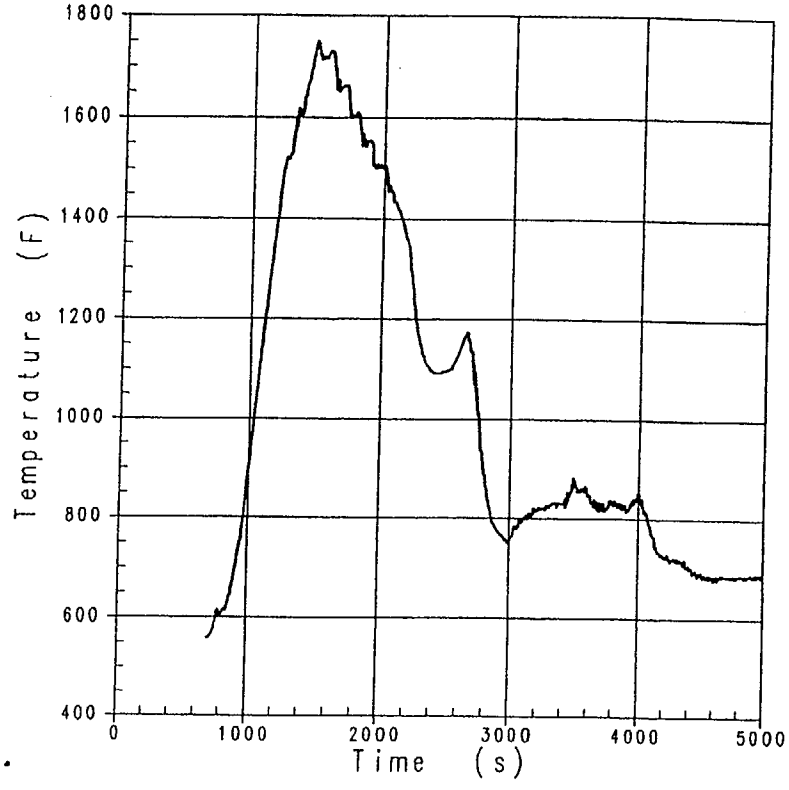

Figure 11.

3-INCH HOT SPOT FLUID TEMPERATURE

DECREASE IN REACTOR
COOLANT INVENTORY

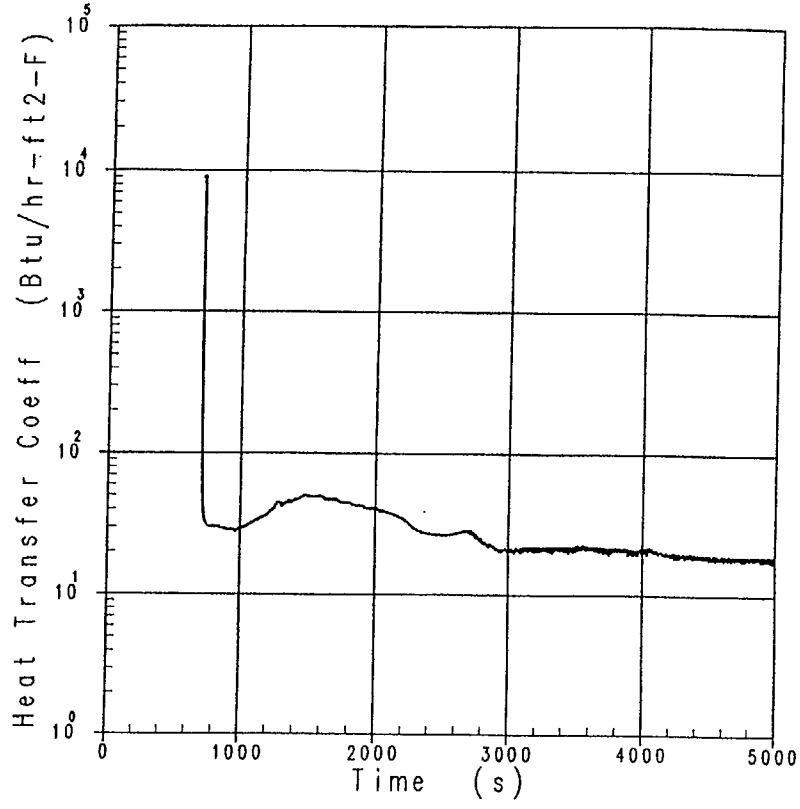

Figure 10.

3-INCH HOT SPOT HEAT TRANSFER COEFFICIENT

- **3 - Inch Cold Leg Break**

  - **RCP Trip** **16.8 sec**
  - **S - Signal** **30 sec**
  - **SI - Delivery** **64.5 sec**
  - **Loop seal clearing** **349.5 sec**
  - **Core Uncovery** **470.6 sec**
  - **Accumulator Injection** **1036.5 sec**
  - **Core Recovery** **3333.3 sec**

Figure 12. Transient Run 3 inch Break w/High Tavg

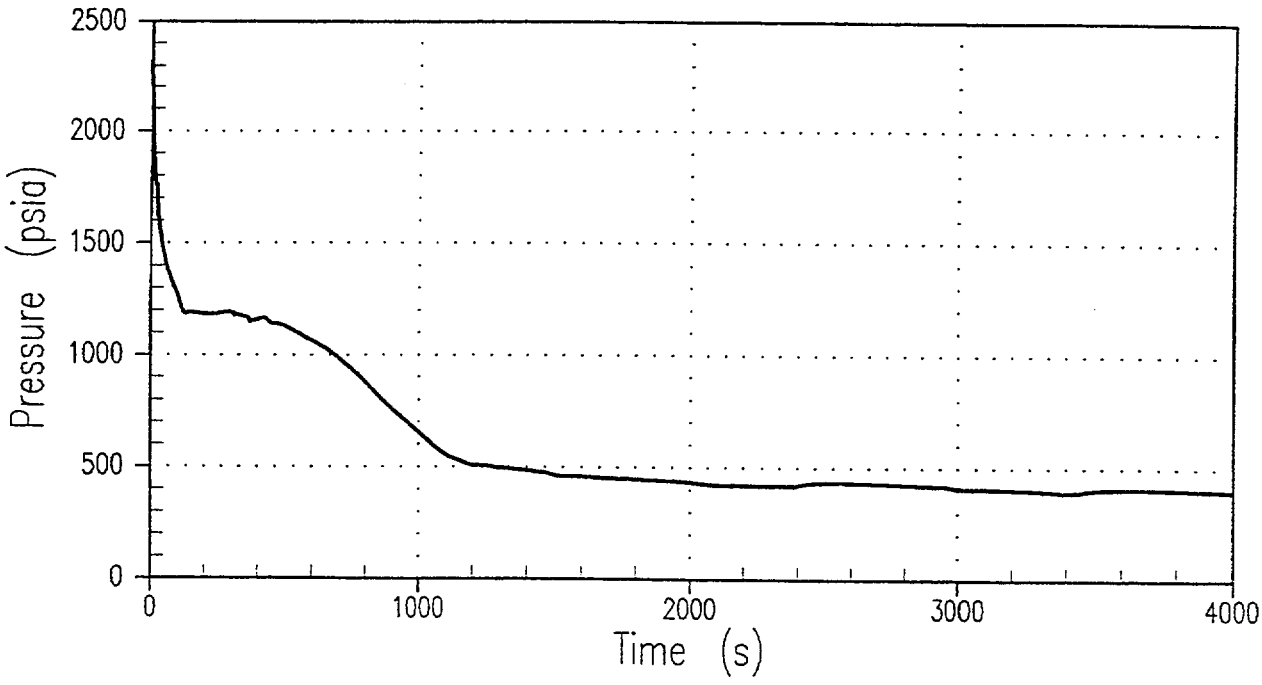

Figure 13. Transient Run 3 inch Break w/High Tavg

N 7 0 0 CORE

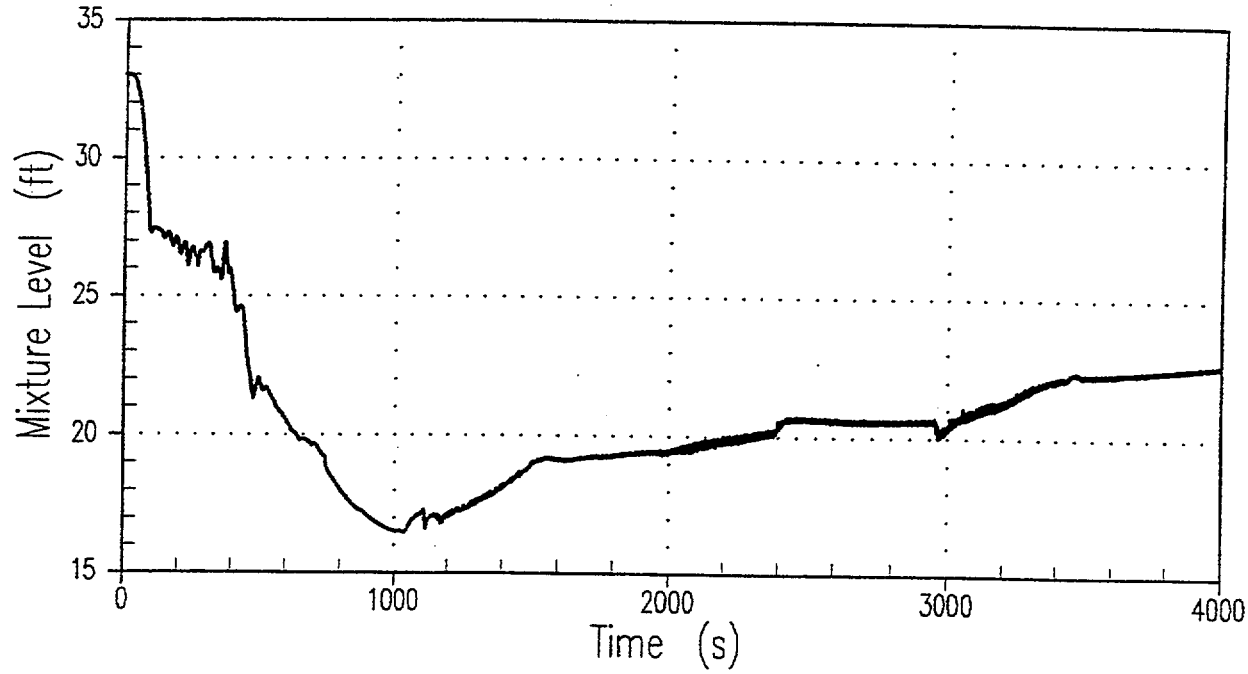

Figure 14. Transient Run 3 inch Break w/High Tavg

6 0 0 TOP CORE VAPOR

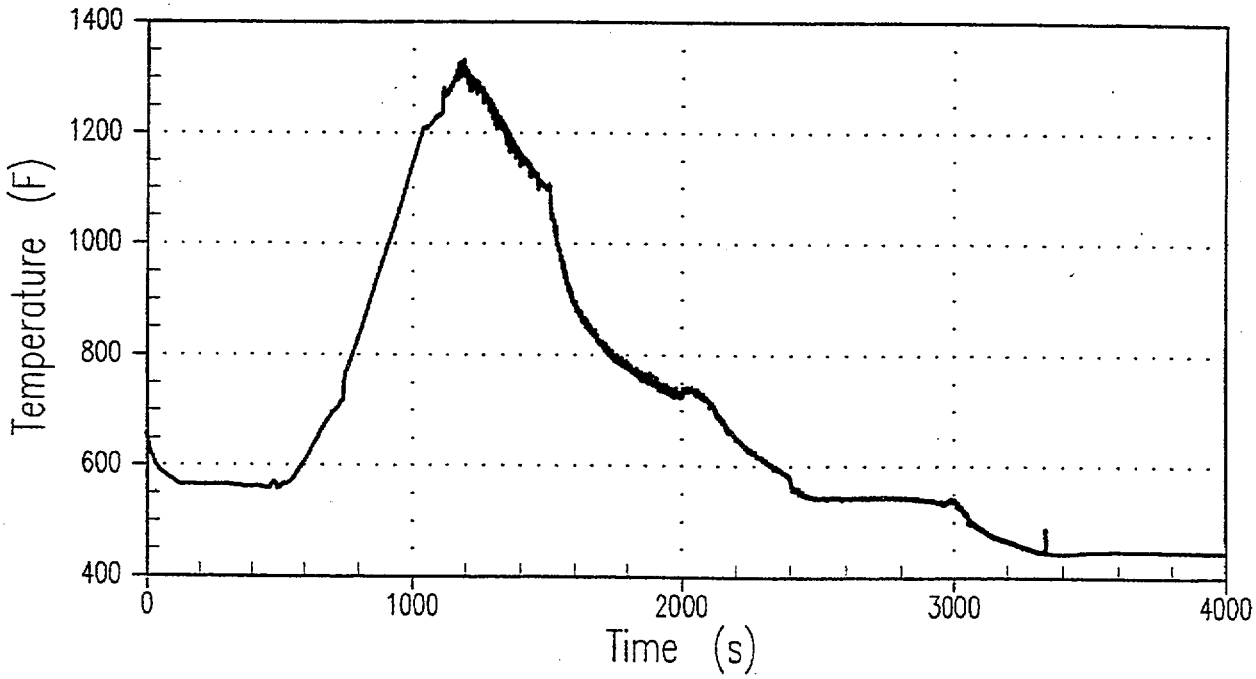

Figure 15 shows the rod temperatures and the local hot channel vapor temperatures. This particular rod has 30 thousand-megawatt days per tonne burn up. The hot channel vapor temperature is higher than the core average vapor temperature shown in Fig. 14 as expected since the hot channel enthalpy rise is larger than the core average enthalpy rise. Figure 16 shows the fuel rod internal pressure and the system pressure. There is an internal pressure increase, because the temperature of the rod is increasing, and then the pressure comes down, due to clad swelling and then burst occurs at approximately 1100 seconds and the rod internal pressure decreases to the system pressure. The differential pressure at burst or the delta P at burst is shown on the figure. Now, this point can be plotted on the NUREG-0630 burst curve, given in Fig. 17 , which is what's used in calculating the burst.

The calculated oxidation level can be calculated for the 30 thousand-megawatt day per tonne burn up fuel rod in the calculation. The oxidation level at the PCT location, without burst, in this calculation is around 4.1 percent as seen in Fig. 18. These were initially about 3.95% of initial oxidation before the transient so there was an increase in the oxidation that occurred due to the transient. However, since the calculated PCT is only around 1,600 degrees or a little bit less, so there is not a significant amount of oxidation generated during the transient. At the burst location, one has to calculate double sided oxidation as per the Appendix K requirements. As seen in Fig. 19, the fuel rod had initially roughly 3.9 percent oxidation, but total oxidation at the end of the transient is only about 5.3 percent. So because of the double-sided oxidation at the burst location, additional oxidation is calculated for the 30 thousand-megawatt days per tonne burn up rod. The total amount of oxidation is higher, but still within 17 percent requirement.

The results for a 54,000-megawatt day per tonne rod, for a 3-inch break are very similar. The small-break hydraulics are the same so only the hot rod behavior will be examined. Figure 20 shows the cladding temperature, which is increasing from the point of core uncovery and then turns-over as the core, is recovered. The hot channel vapor temperature is also plotted on Fig. 20. The core average vapor temperature peak was about 1,300 degrees Fahrenheit. The fuel rod temperature is lower than in the two previous cases since the rod power is lower due to the burn up. In this case the peak temperature was only 1500 ^{0}F so not much oxidation will occur. Since the burn up is now 54,000 megawatt days per tonne, the rod pressure is higher as seen in Fig. 21. The rod pressure increases as the rod temperature increases and there is some swelling which occurs, which brings it down, before it bursts. The rod then bursts with the differential pressure as seen on the figure. As Dr. Meyer indicated, the PIRT panel should think about the high burn up mechanical properties that could have an effect on this process, because the ballooning strains might be much smaller. The pressure would not drop as seen in the figure and burst could occur earlier. It might occur at a slightly different set of pressure and temperature conditions. This could have some effects in this area, since the NUREG-0630 curves that are used are all for fresh fuel.

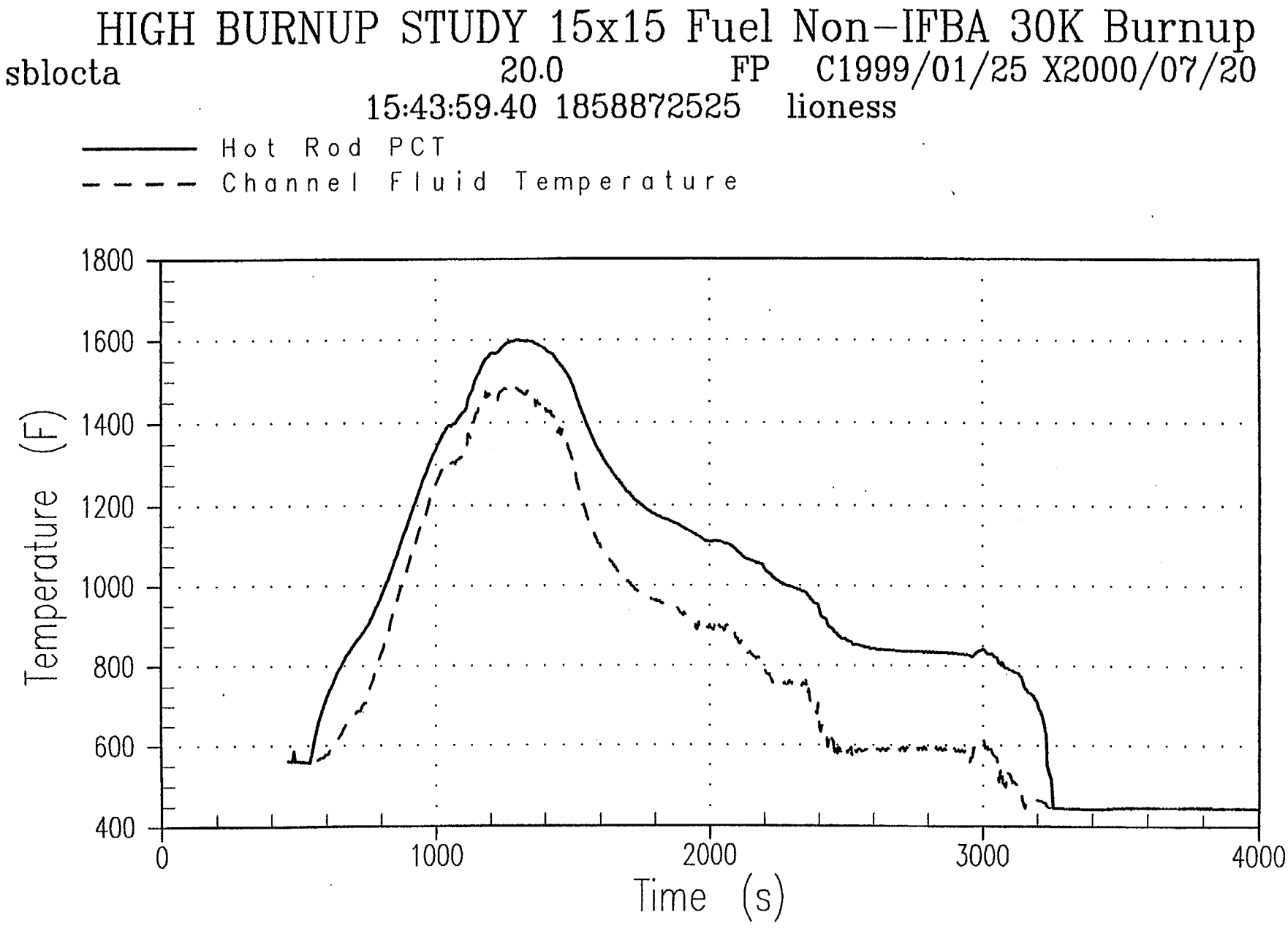
HIGH BURNUP STUDY 15x15 Fuel Non-IFBA 30K Burnup
sblocta 20.0 FP C1999/01/25 X2000/07/20
15:43:59.40 1858872525 lioness
Hot Rod PCT
Channel Fluid Temperature
Temperature (F)
1800
1600
1400
1200
1000
800
600
400
0
1000
2000
3000
4000
Time (s)

Figure 15

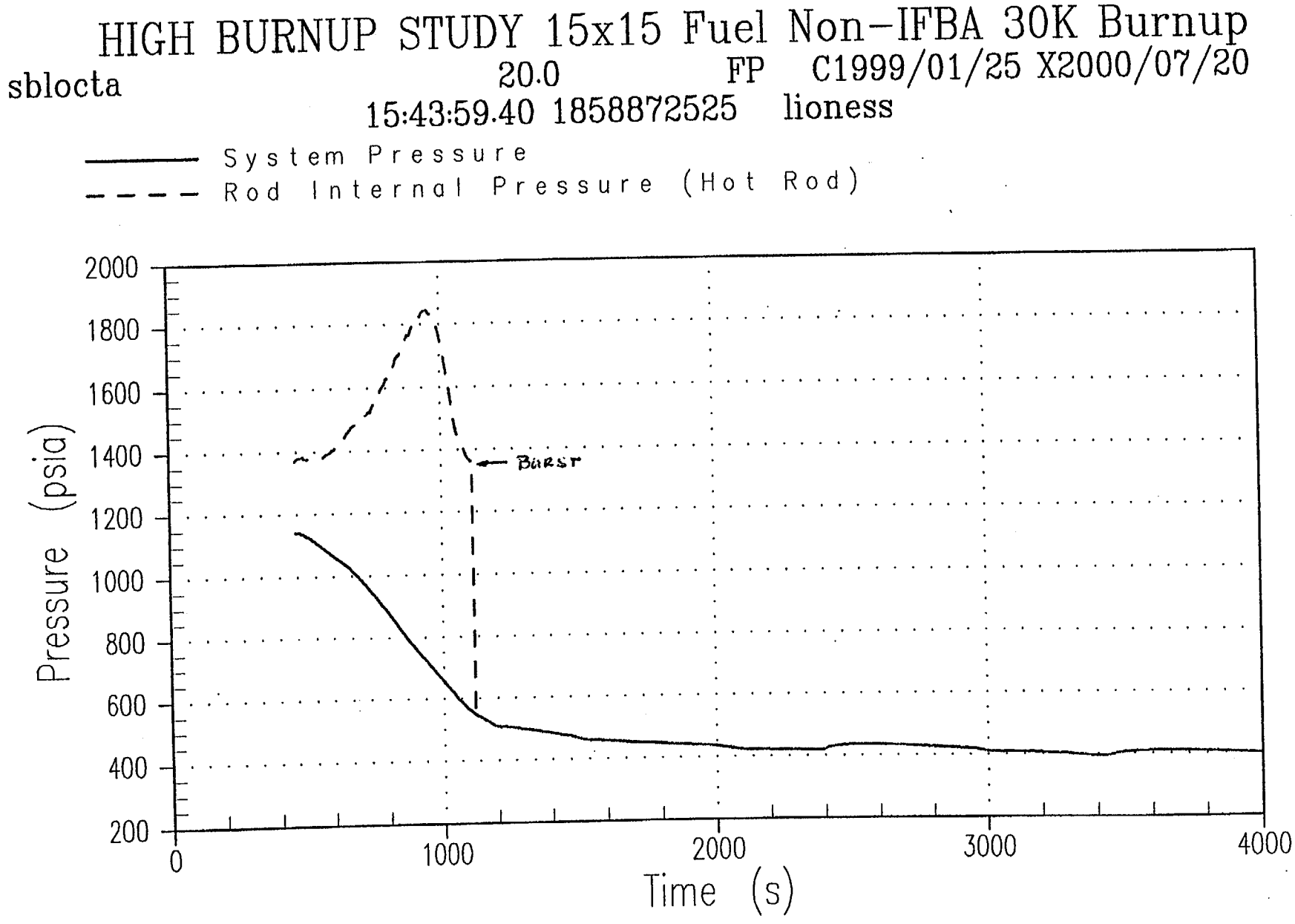
HIGH BURNUP STUDY 15x15 Fuel Non-IFBA 30K Burnup
sblocta 20.0 FP C1999/01/25 X2000/07/20
15:43:59.40 1858872525 lioness
System Pressure
Rod Internal Pressure (Hot Rod)
Burst
Pressure (psia)
2000
1800
1600
1400
1200
1000
800
600
400
200
0
1000
2000
3000
4000
Time (s)

Figure 16.

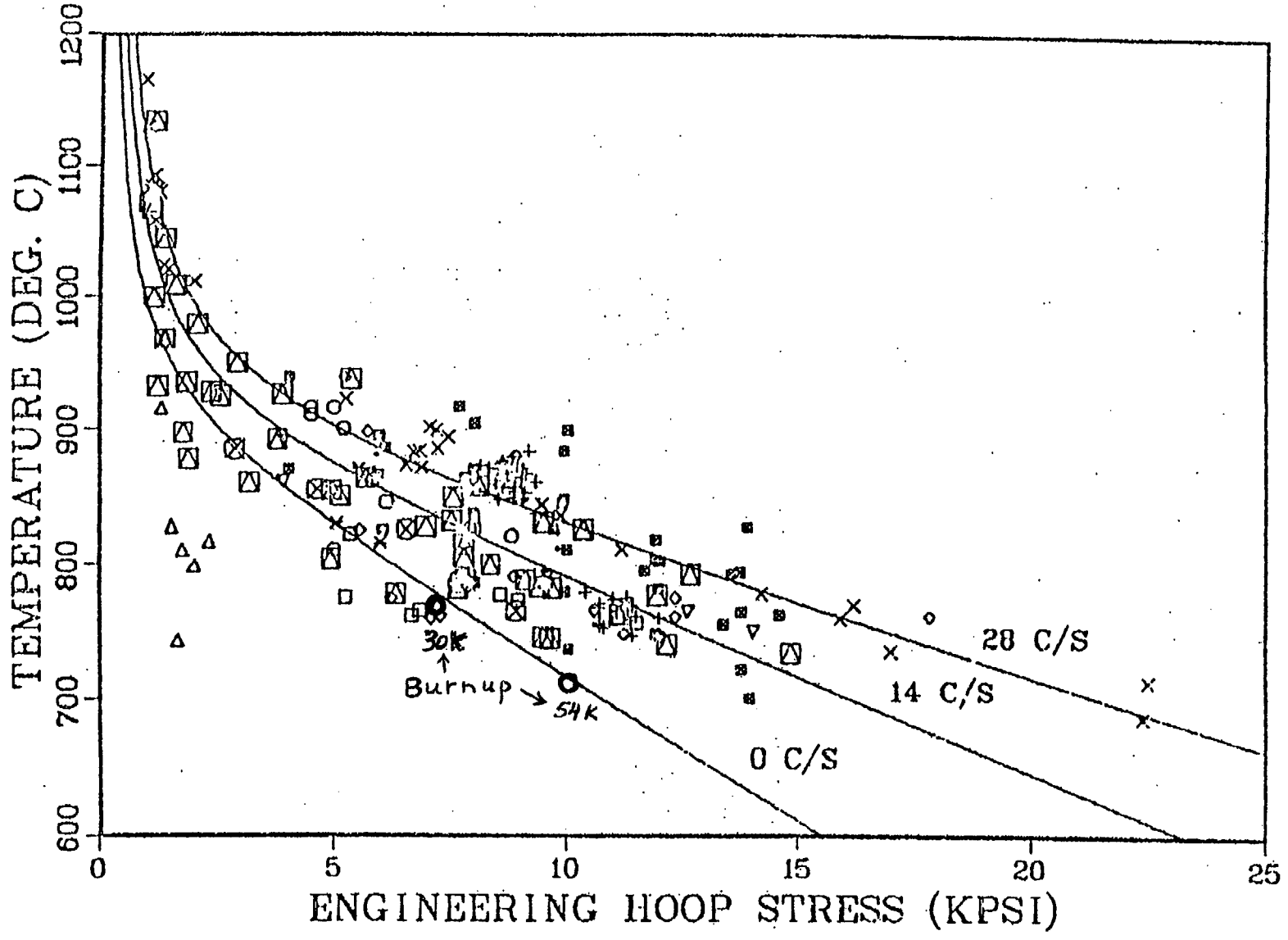

Figure 17. ORNL correlation of rupture temperature as a function of engineering hoop stress and temperature-ramp rate with data from internally heated Zircaloy cladding in aqueous atmospheres.

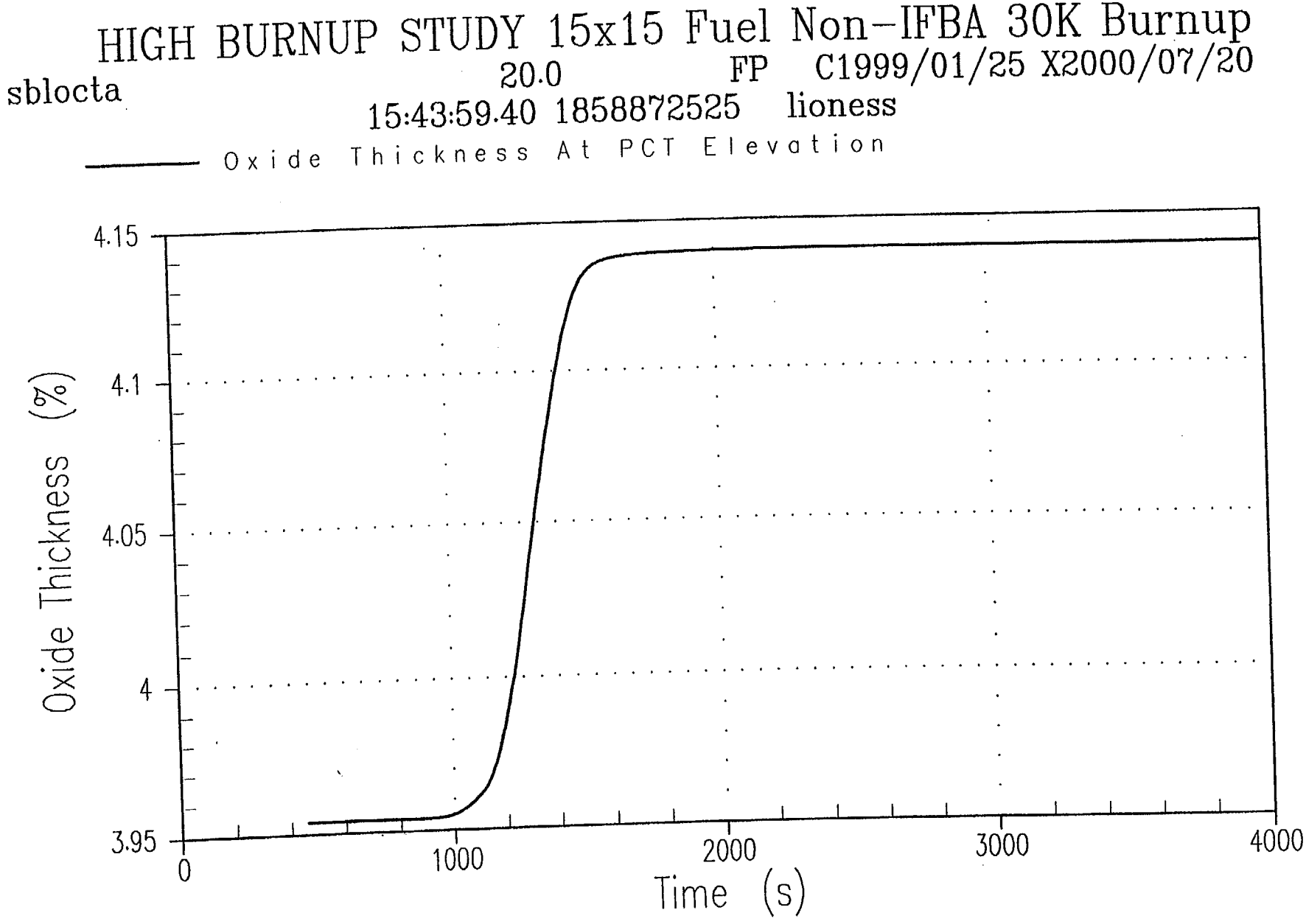
HIGH BURNUP STUDY 15x15 Fuel Non-IFBA 30K Burnup
sblocta
20.0
FP C1999/01/25 X2000/07/20
15:43:59.40 1858872525 lioness
Oxide Thickness At PCT Elevation
Oxide Thickness (%)
4.15
4.1
4.05
4
3.95
0
1000
2000
3000
4000
Time (s)

Figure 18

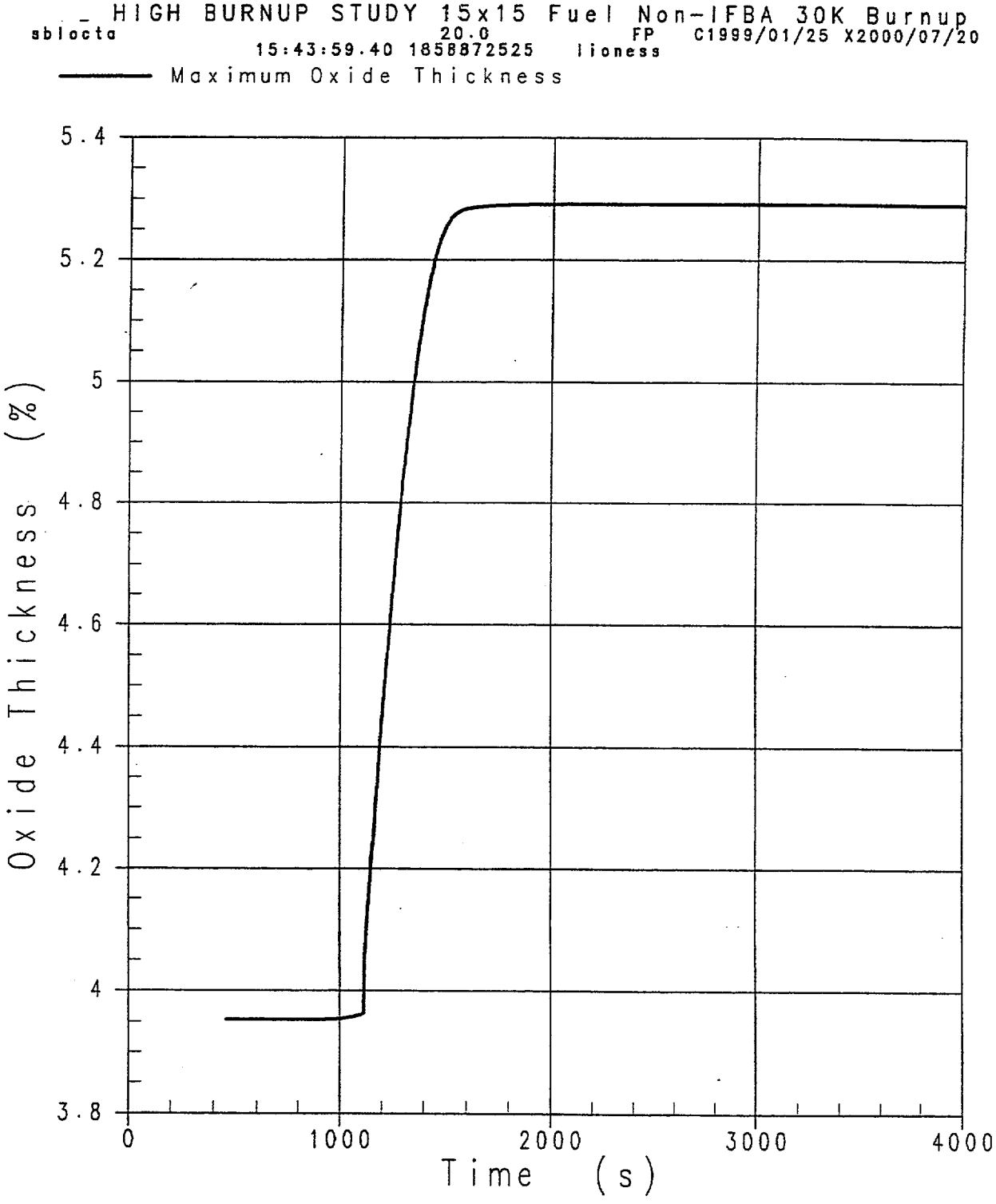
HIGH BURNUP STUDY 15x15 Fuel Non-IFBA 30K Burnup
sblocta 20.0 FP C1999/01/25 X2000/07/20
15:43:59.40 1858872525 lioness
Maximum Oxide Thickness
Oxide Thickness (%)
5.4
5.2
5
4.8
4.6
4.4
4.2
4
3.8
0
1000
2000
3000
4000
Time (s)

Figure 19.

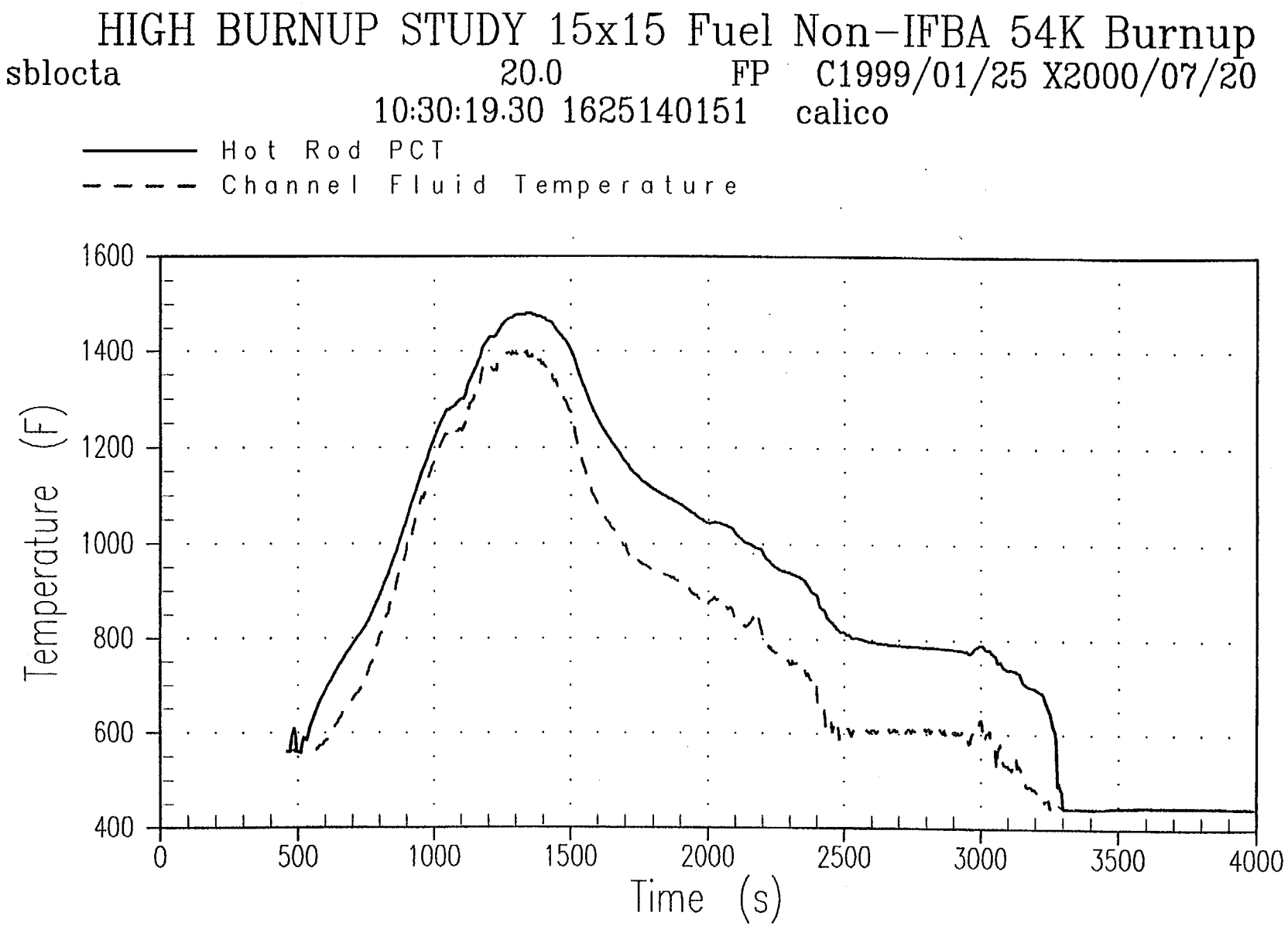
HIGH BURNUP STUDY 15x15 Fuel Non-IFBA 54K Burnup
sblocta 20.0 FP C1999/01/25 X2000/07/20
10:30:19.30 1625140151 calico
Hot Rod PCT
Channel Fluid Temperature
Temperature (F)
1600
1400
1200
1000
800
600
400
0
500
1000
1500
2000
2500
3000
3500
4000
Time (s)

Figure 20.

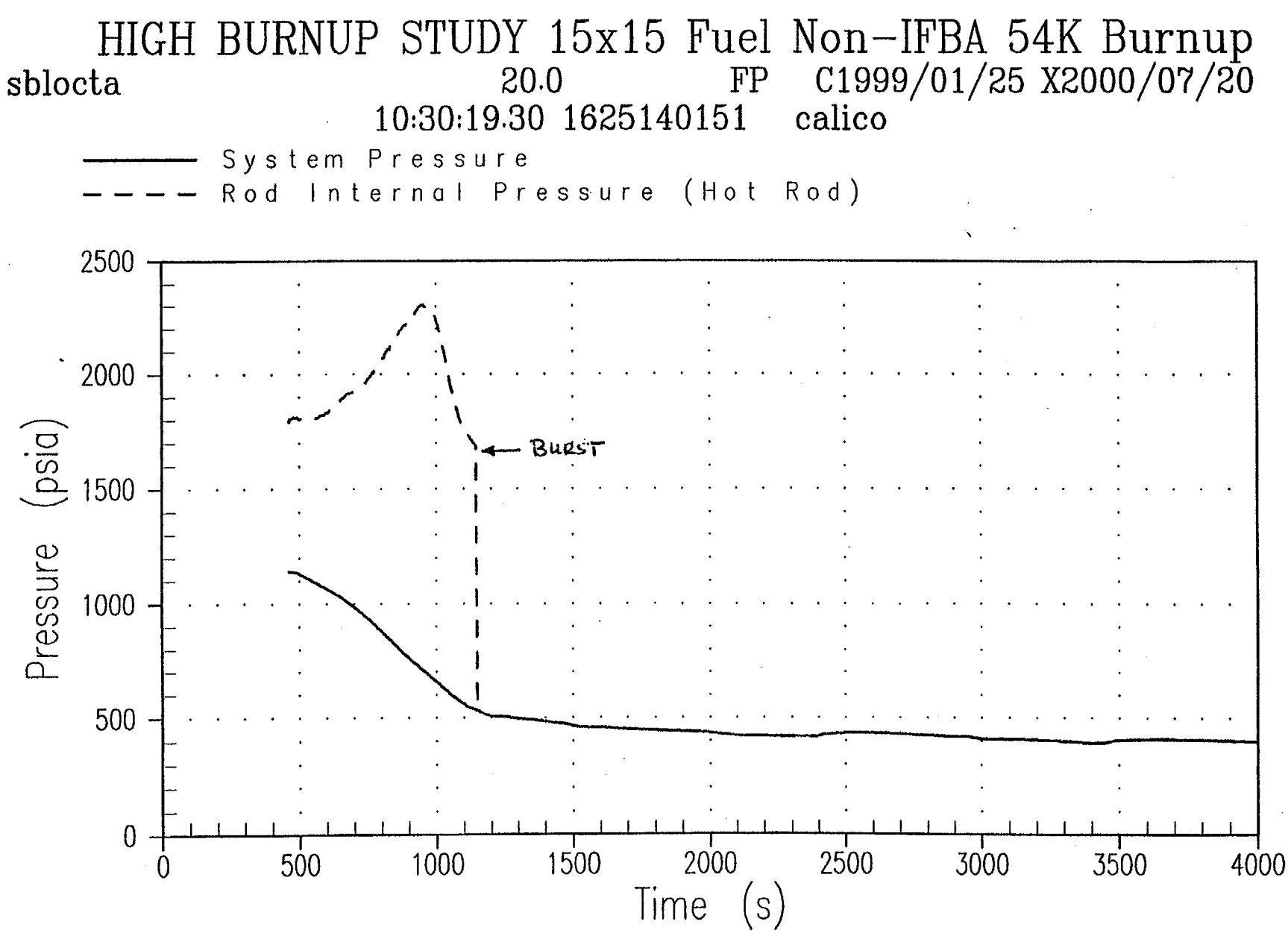
HIGH BURNUP STUDY 15x15 Fuel Non-IFBA 54K Burnup
sblocta 20.0 FP C1999/01/25 X2000/07/20
10:30:19.30 1625140151 calico
System Pressure
Rod Internal Pressure (Hot Rod)
Burst
Pressure (psia)
Time (s)
0
500
1000
1500
2000
2500
3000
3500
4000

Figure 21.

The calculated oxidation for the 54,000 megawatt days burn up case at the PCT location is shown in Fig. 22. The initial oxidation on the rod at the beginning of the calculation, due to the higher burn up is roughly 13 percent. The increase in the amount of oxidation at the PCT point is not very much due to the lower temperatures during the transient. The oxidation at the Burst node is shown in Fig. 23 and again there is a very small gain in the total oxidation even though the double-sided oxidation was considered. In these cases, the accident does not really add any significant oxidation, as compared to the initial oxidation level on the fuel rod at the beginning of the accident due to the increased burn up history. Therefore, as the fuel rod burn up increases, the initial oxidation value at the beginning of the transient increases, however, with the higher burn up, the rod power are sufficiently low that there is no significant heat up of the highly burn up rods and the additional oxidation due to the transient is very small.

Therefore, the Westinghouse small-break Appendix K calculations show that the calculated PCTs are well below the 2,200 degrees Fahrenheit limit for all burn ups considered. Fresh fuel, gives the highest PCTs since the linear heat rate is the highest but the hot rod is not calculated to burst in these calculations. As the burn up increases, the calculated PCT will decrease since the linear heat rate is lower but the fuel rod will burst due to the increased fission gas pressure within the rod. The fuel rod burn up does not have to be very large before a burst is calculated. Burst usually will be calculated at burn ups greater than about 10,000-megawatt days per ton.

If best-estimate small break calculations were performed, much lower PCTs would be calculated, primarily because of the lower decay heat. Lower decay heat helps in many different aspects. It will make the worst small break size larger, and since the accumulator setpoint is fixed, the window for which the core could uncover would become smaller. The transients are all going to be shorter, so the time at elevated temperatures will be less so the heat ups, for thousands of seconds, which was calculated in the Appendix K calculations, would not be calculated in the best-estimate calculations.

Also, best-estimate calculations would use more realistic power shapes, instead of bounding power shape and the peak power and the PCT will not be at 11-1/2 feet. In some of these Appendix K calculations, bursting is predicted to occur at 12 feet which is unrealistic because there is no fuel at 12 feet or perhaps just one pellet, and so the burst occurs where the fission gas plenum is, which is sort of crazy. So, a realistic power shape is going to reduce the power at the top of the core. Since the power will be reduced at the top of the core, there will be more power at the bottom of the core, which will increase the steam flow at the PCT elevation and improve heat transfer there.

Appendix K calculations use a conservative break flow model which maximizes the flow lost from the reactor system. If a best-estimate break flow model is used, the flow out of the system would be less, which will make the high head safety injection system perform more effective.

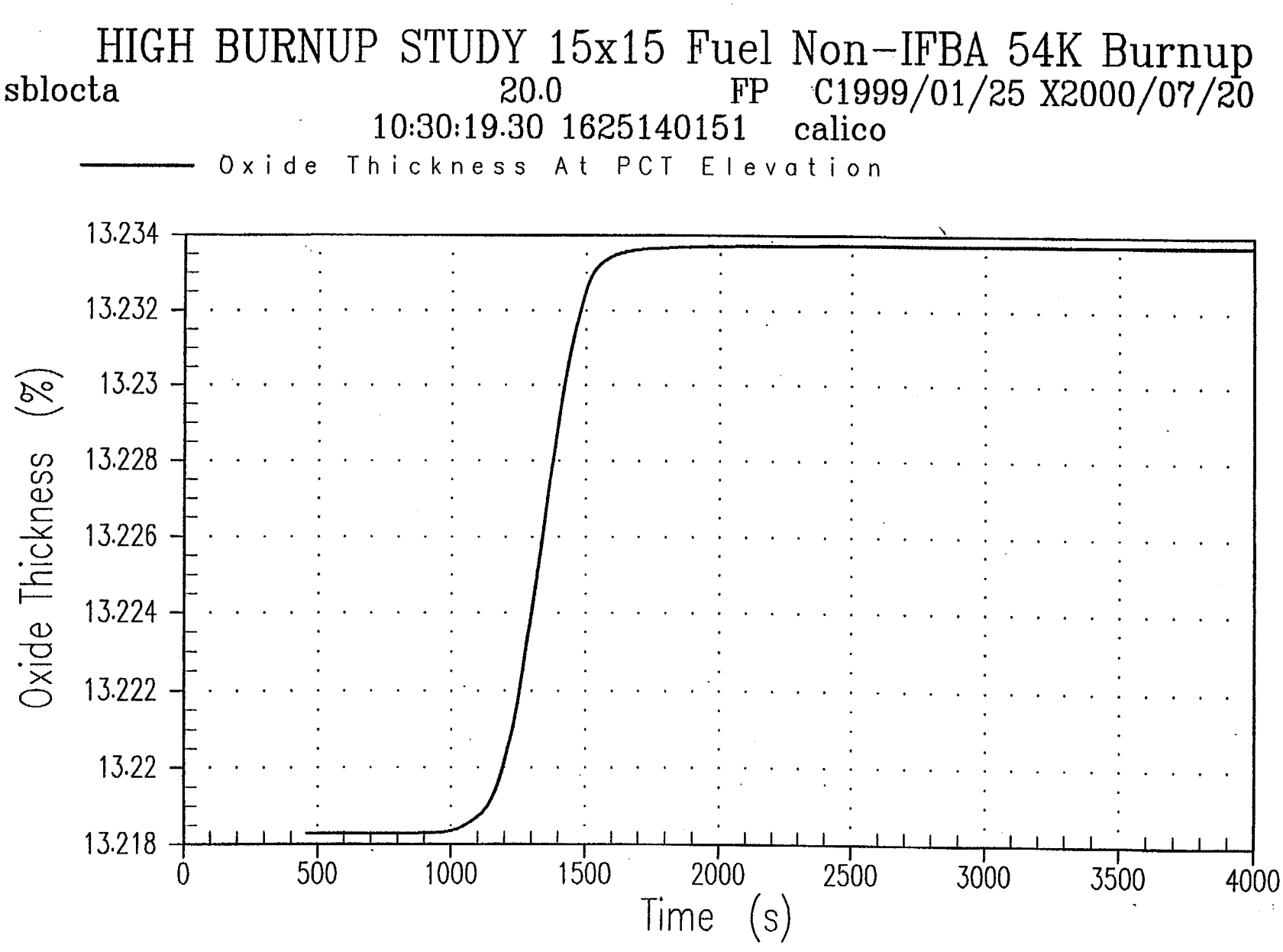
HIGH BURNUP STUDY 15x15 Fuel Non-IFBA 54K Burnup
sblocta 20.0 FP C1999/01/25 X2000/07/20
10:30:19.30 1625140151 calico
Oxide Thickness At PCT Elevation
Oxide Thickness (%)
13.234
13.232
13.23
13.228
13.226
13.224
13.222
13.22
13.218
0
500
1000
1500
2000
2500
3000
3500
4000
Time (s)

Figure 22.

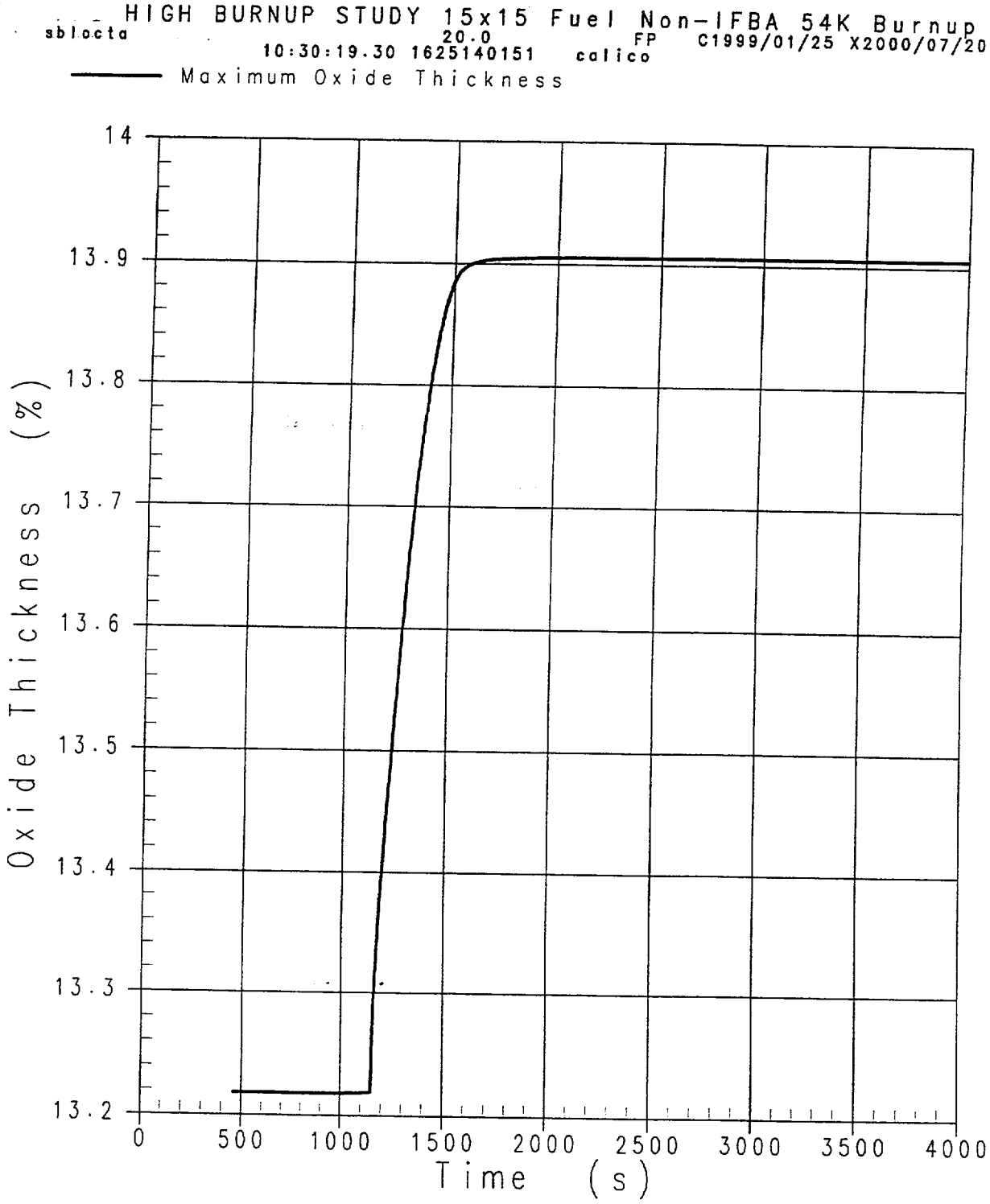
HIGH BURNUP STUDY 15x15 Fuel Non-IFBA 54K Burnup
sblocta 20.0 FP C1999/01/25 X2000/07/20
10:30:19.30 1625140151 calico
Maximum Oxide Thickness
Oxide Thickness (%)
14
13.9
13.8
13.7
13.6
13.5
13.4
13.3
13.2
0
500
1000
1500
2000
2500
3000
3500
4000
Time (s)

Figure 23.

There are also three-dimensional effects, which are not accounted for in the Appendix K calculations, which would result in a thermal siphon effect where the higher power regions will suck in steam from the lower power regions and a higher steam flow for the higher power fuel assemblies will be calculated. Also, for best-estimate calculations more realistic rod powers and fuel rod internal pressures would be used such that burst would probably not be calculated. So, if a true best estimate calculation were performed the expected PCTs would be nowhere near the licensing limit. In fact, it is likely that core would not uncover for some of the breaks that are now calculated to uncover with Appendix K calculations. The resulting PCTs would be much, much lower and none of the rods are likely to burst.

I-3 BWR LOCA

Panel member Jens G. M. Andersen prepared this review for the PIRT panel.

The following is a presentation of the BWR LOCA. The presentation is based on the GE BWRs. Slide 2 is a brief outline of the presentation. The presentation will be based on the design basis accident, which is the double-sided break in the suction side of the recirculation line. It will cover the phenomena that occur during the LOCA.

BWR LOCA GNF

- **Design Basis Accident**
  - Double Sided Break in Recirculation Line - Suction Line
- **Phenomena**
  - Blowdown
  - Refill Reflood
- **BWR/6** **BWR/4** **BWR/2**
- **Typical LOCA Transient**
- **Small Break LOCA**
- **Fuel Exposure**

JGMA May 2000 2

The discussion of the LOCA phenomena will be divided into two phases, the blowdown phase and the refill/reflood phase. The presentation will furthermore cover the differences between the different plant types, the BWR/6, which is the latest design in the U S., and the BWR/4 which is the design for which there are the most plants. Finally the BWR/2, which is the early BWR designed with the external recirculation loops without jet pumps, will be covered. There are two BWR/2 in the United States. In addition to the typical design basis LOCA transient, the presentation will address issues that exist for small break LOCAs, and it will discuss the effect of fuel exposure on the fuel performance during a LOCA transient.

The BWR/6 design basis accident (See Slide 3) will be covered first. During normal operation, the feedwater comes in at the top of the downcomer just below the dryer skirt. The feedwater will flow down the downcomer into the bottom of the downcomer where the suction for the recirculation line is located. Water is taken out through the recirculation line, enters the recirculation pump and is then reintroduced back into the jet pump in the downcomer through the drive line for the jet pump. There the drive flow mixes with the suction flow that comes directly from the downcomer. For simplicity, the driveline is shown at the drawing coming in at the top of the jet pump. In reality, the drive line enters the downcomer at the same elevation as the suction line and then continues vertically to the top of the jet pump inside the downcomer. There is a 180 degree bend at the top before the drive flow enters the jet pump. Both of the recirculation line connections are the bottom of the core, to avoid having any pipe connections on the vessel in the high flux region outside the core.

BWR/6 LOCA

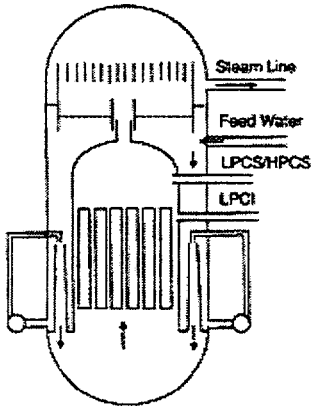

BWR/6 Design Basis Accident

Double Ended Break in Recirculation Line - Suction Line

JGMA May 2000 3

The flow then exits the bottom of the jet pump and continues up to the core.
The rectangular boxes in the core region on Slide 3 represent the fuel channels. The region in between the fuel channels is the bypass region. Typically, about 10-11% of the active recirculation flow flows in the bypass region. The dominant flow path for the bypass flow is up through the inlet orifice in the fuel channels, and then through the leakage paths which are small holes in the side of the nose pieces to the fuel channels.

The fluid flows from the inside of the channels through the leakage holes and couple of additional leakage paths into the bottom of the bypass region. The flow through the leakage holes is the dominant flow path into the bypass region. It is important, because it has a very significant impact on the performance during the refill/reflood phase of the LOCA.

Boiling and vapor generation will take place in the channels, and the two-phase mixture flows from the core region through the upper plenum and into the steam separators. The steam is separated from the liquid in the steam separators and flows through the steam dryers into the steam line. The main flow path for the liquid is from the separators into the mixing region and back into the downcomer where it mixes with the feedwater flow. The inlet subcooling at the bottom of the core is approximately 20 F.

The worst break, the design basis accident for the BWR/6, is a break in the suction side of the recirculation line. This is the lowest pipe connection for any large pipe relative to the position of the core.

The height of the jet pumps is two-thirds of the height of the core. With a break in the recirculation line, it is possible to reflood the core with a collapsed water level up to the height of two-thirds the height of the core before the water will spill out to the top of the jet pump and flow out to the break location.

There are other possible break locations - in the LPCI line or the spray lines, but those would be break locations above the top of the active fuel in the core, and the break sizes are smaller. There are also possibilities for break in the feedwater line and the steam lines. These other breaks are usually much less severe than the break in the recirculation line.

The design basis accident is a double-ended break in the suction line (See Slide 4). There are two suction lines going into two recirculation pumps in the BWR.

After the recirculation pumps, the flow continues to a header that feeds the drive lines for 10-12 jet pumps per recirculation loop. The suction pipe is a large pipe. Following a break, the reactor scrams, typically on high drywell pressure. However, because of the depressurization, and the associated fluid loss there is a very fast increase in the core average void fraction. The negative reactivity caused by the voiding shuts down the core immediately.

Immediately after the break, fluid will start flowing from the downcomer out through the suction line to the break. There will be flow reversal in the drive line and fluid will flow to the break from the other side. As a result of the flow reversal in the discharge side of the recirculation line, all the drive flow to half the jet pumps is lost.

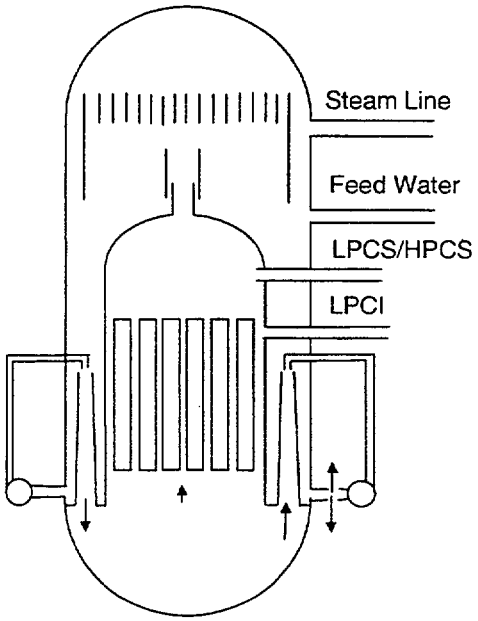

- **Break in Recirculation Line**
- **Scram**
- **Loss of Power**
- **Flow Reversal in Broken Loop Jet Pump**
- **Coast Down of Intact Pump**
- **Large Reduction in Core Flow and Early BT ≈ 1 sec.**
- **PCT Dominated by Stored Energy (kW/ft, h_{gap})**
- **Isolation**
- **Depressurization and Loss of Liquid Inventory**

JGMA May 2000

The flow reversal in the drive lines and the break flow out the suction line causes the exit flow from half of the jet pumps to reverse. It is conservatively assumed that all power is lost, which means that there is no power to the recirculation pumps and the flow in the intact recirculation loop will start to coast down. The coast-down time of the recirculation pumps is on the order of 10-15 seconds, so it's a relatively slow coast-down.

Consequently, there is a very large, almost instantaneous reduction in the core flow. This leads to an early boiling transition in the core, typically within one second after the break.

Following the early boiling transition, there is very fast increase in the cladding temperature. During steady state, there is a parabolic temperature profile in the fuel. Following the boiling transition, the film boiling heat transfer is much less than the nucleate boiling heat transfer in normal operation, and therefore the temperature distribution in the fuel will become equalized. Therefore the early peak cladding temperature (PCT) is dominated by how much stored energy there initially is in the fuel, and that is given primarily by the linear heat generation rates and the fuel heat transfer parameters. These are the two dominant parameters that control the amount of stored energy and the early PCT.

Subsequent to the break there is an isolation of the primary system. The closure of the isolation valves typically occurs four seconds into the transient.

As a result of the break, the system starts depressurizing and there is a loss of liquid inventory. The loss of liquid inventory leads to a drop in the water level in the downcomer, and when water level has reached the top of the jet pump, a flow path is established where steam can flow directly out to the break (See Slide 5). This leads to a significant increase in volume flow through the break and in the rate of depressurization.

BWR/6 LOCA

GNF

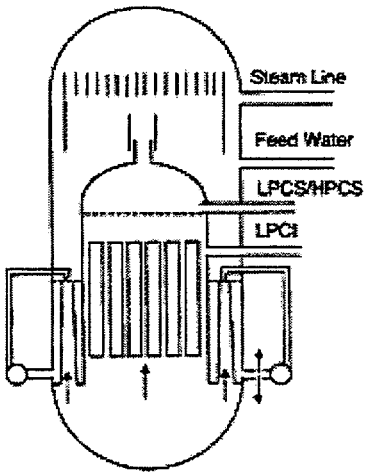

- **Increased Depressurization Following Jet Pump Uncovery**
- **Flashing when Tsat(P) < T_l**
- **Increased Core Flow from Lower Plenum Flashing Quenches Fuel**

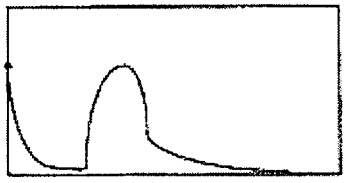

Core Flow

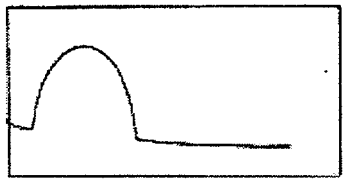

PCT

The initial subcooling in the downcomer and lower plenum is approximately 20 F, therefore when the pressure drops below the saturation pressure corresponding to the liquid temperature, flashing of the liquid will take place. The combination of the large increase in the depressurization following the jet pump uncovery and the flashing of super-heated liquid, causes a surge in core flow. The surge in core flow from the lower plenum quenches the fuel and the cladding temperature is returned to the saturation temperature. Lower plenum flashing typically occurs 10 seconds into the transient.

In summary there is a rapid reduction in the core due to the flow reversal in half the jet pumps and a subsequent early boiling transition. Once the pressure drops to the point of lower plenum flashing there is a surge in core flow, which quenches the core and brings the temperatures back to the saturation. This is referred to as the early boiling transition and the first peak in the cladding temperature for the BWR.

As the LOCA progresses, the liquid inventory and pressure continue to drop, and eventually the two-phase level drops inside the core region. A two-phase level will also form in the lower plenum region (See Slide 6).

The reason that levels may form in both in the lower plenum and the core region is counter current flow limitation (CCFL) at the inlet to the fuel bundles. This core uncovery leads to a second boiling transition, which typically happens 20 seconds into the transient.

BWR/6 LOCA

GNF

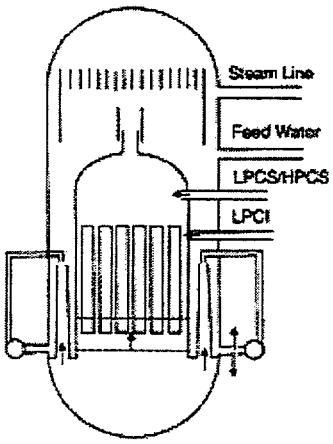

- **Continued Depressurization**
- **Loss of Liquid Inventory**
- **Core Uncovery Leads to Second BT**
- **HPCS comes on (D/G Startup)**
- **LPCS and LPCI Comes on when P < Shutoff Head**
- **Worst Single Failure**
  - **Failure: LPCI D/G**
  - **Available: HPCS/LPCS/LPCI/ADS**

The high pressure core spray into the upper plenum will come on early in the transient. It is controlled by the time it takes to start up the diesel generator that powers the high pressure core spray pump. This pump typically comes on 35-40 seconds into the transient.

Diesel generators also power the low-pressure core spray into the upper plenum and the low-pressure coolant injection into the top of the bypass region. These systems, however, will not come on until the system pressure has dropped below the shutoff head for the pumps, which is typically on the order of about 200 psi.

A conservative requirement for the LOCA analysis is to make the assumption of the worst single failure. The BWR/6 has one high pressure core spray system, one low pressure core spray system, and it has three LPCI systems injecting into the bypass region. In addition to this, there is the automatic depressurization system ADS). The ADS is of importance primarily for small breaks and it's purpose is to lower the pressure and allow the low pressure systems to come on. The worst single failure for the BWR/6 is to assume a failure of one of the diesel generators powering two of the LPCI systems.

Several different combinations of failures are analyzed, but the diesel generator failure is the worst and leaves only the high pressure core spray, the low pressure core spray and one LPCI system that injects into the bypass region.

When the pressures is low enough that it has dropped below the shutoff head for the LPCI pump, liquid is injected into the bypass region and quickly fills up the bypass region (See Slide 7). The only significant way this liquid can drain out of the bypass is to flow backwards through the leakage hole into the fuel channels and then drain through the side entry orifice into the lower plenum. However, because of the depressurization and release of stored energy from the vessel wall and guide tubes in the lower plenum, the liquid in the lower plenum will be flashing. The flashing leads to a significant flow of steam up into the core region and at the same time there is liquid trying to drain into the lower plenum. For the BWRs, in order to control core flow distribution and stability, there are relatively tight inlet orifices at the bottom of the channels. The flow area at the inlet orifice is typically a third or less of the active flow area in the channel. Counter current flow limitation will occur at this point and liquid will be held up in the core. Two-phase levels are therefore formed both in the core region and in the lower plenum.

In the upper plenum, there is injection of the high pressure and the low pressure core sprays. There is a flow restriction at the top of the fuel channel. In older fuel types, the most limiting flow area used to be the upper tie plate in the channel. For modern fuel designs, the flow area in the upper tie plate has been increase, and the limiting flow area is typically the top spacer in the fully rodded region of the bundle.

BWR/6 LOCA

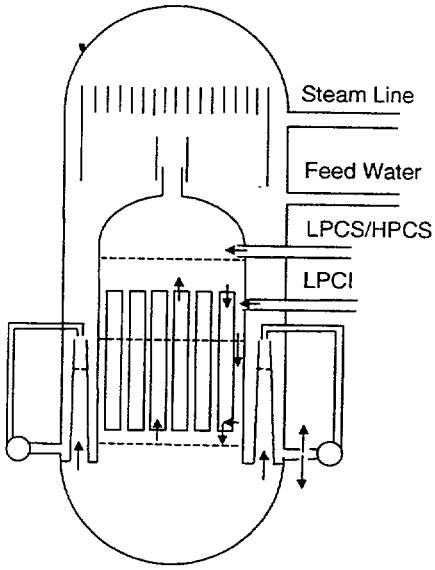

- **LPCI Fills Bypass Region**
  - Liquid Enters Core through Channel Leakage Path
  - Steam from Lower Plenum Flashing Holds up Liquid in Core due to CCFL in Inlet Orifice
- **HPCS/LPCS Enters Upper Plenum**
  - Liquid Level Forms in Upper Plenum. Holdup in Upper Plenum due to Steam from Lower Plenum (flashing) and Core (heat transfer). CCFL at Upper Tie Plate
  - Down Flow through Peripheral Low Power Bundles Helps Refill and Reflood Core

JGMA May 2000 7

Steam originating from the flashing of fluid in the lower plenum and core region plus steam generated in the core due to the heat transfer from the hot fuel will flow up through the top of the bundles. Counter current flow limitation can therefore occur at the spacers or the upper tie plate and will then hold up liquid in the upper plenum. CCFL typically exist for the average and high power bundles, while for the peripheral channels, which are at much lower power than the central channels there is typically not enough steam flow to cause CCFL and down-flow is likely.

The phenomena in the upper plenum and core regions are of particular interest for refill/reflood part of the transient. In the upper plenum, there is interaction between the core spray system and the water level, and in the core region there can be three different flow patterns (See Slide 8). There are two different scenarios dependent on whether the water level in the upper plenum is below or above the core spray spargers.

The cold ECC water is injected through the spargers, which are pipes that runs along the periphery of the upper plenum and contains spray nozzles along the length of the pipe.

BWR/6 LOCA

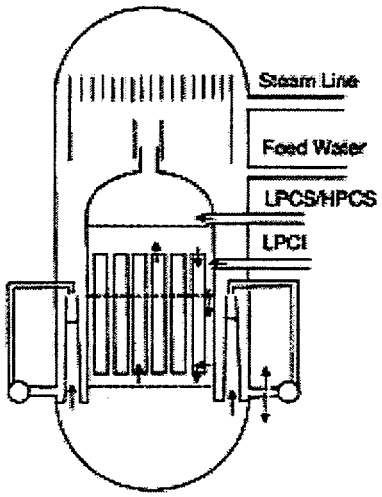

- **Upper Plenum Phenomena**
- **Level Below CS Sparger**
  - Condensation on ECC
  - Spray Distribution
  - CCFL at Upper Tie Plate Holds up Liquid in Upper Plenum
  - Upper Plenum Level Raises
- **Level Above CS Sparger**
  - Not Enough Steam for Condensation on ECC
  - Subcooling Reaches Peripheral Bundles Causing Subcooled CCFL Break Down
  - Upper Plenum Level Drops
- **Parallel Channel Effects in Core**
  - Co Current Up Flow
  - Counter Current Flow with Level
  - Co Current Down Flow
- **Reflooding of Core Prior to Refilling of Lower Plenum**

JGMA May 2000 8

When the water level is below the core spray sparger, the nozzles spray water as droplets into the vapor space m upper plenum. The condensation heat transfer is very large on these droplets and data have shown that there usually is enough condensation to remove all the subcooling once the droplets have traveled a distance on the order of 4 to 5 nozzle diameters into the upper plenum. There is complete condensation on the ECC water, which means that the water is saturated once it reaches the top of the two-phase level.

Therefore the water below the two-phase level in the upper plenum will be saturated.

CCFL will occur at the top of the bundles due to the up-flow of steam, and the water can not drain into the core as fast as it is supplied from the spray sparger. Consequently the water level in the upper plenum will start rising.

This quickly leads into the other situation where the two-phase level in the upper plenum is above the core spray sparger. In this scenario, the water essentially shields the cold water from the steam. Enough steam can not get to the cold ECC water to provide

sufficient condensation to heat the water up to saturation. Therefore, the liquid below the two-phase level becomes subcooled, and cold water starts penetrating to the top of the core and in particular along the shortest path down into the peripheral bundles.

These bundles are also the lowest power bundles, and subcooled CCFL breakdown will occur. Subcooled CCFL breakdown is a phenomenon that occurs when the amount of condensation required to remove the subcooling of the water flowing down exceeds the upward steam flow. When this condition occurs, the cold water penetrating into the channel condenses all the available steam flow and the flow pattern changes to co-current down-flow of cold water in these peripheral channels.

As a result of the subcooled CCFL breakdown in the peripheral channels, the upper plenum starts to drain and the two-phase level drops until the core spray is uncovered again. The upper plenum enters a mode where the water level slowly oscillates up and down around the location of the ECC sparger, the oscillation occurs with the time period of maybe 10 to 20 seconds. Consequently during the refill-reflood period a water level is maintained and oscillating around the core spray spargers.

In the channels three different flow patterns can occur. There can be down-flow in the peripheral channels because of the CCFL breakdown that occurs when the cold water gets down to the top of the channels. There can be a pattern of co-current up-flow where steam from the lower plenum and core is vented up through some of the channels at a rate close to or exceeding the shut-off point on the CCFL curve, i.e., the point where liquid down flow is not possible. This typically occurs in the highest power channels. For the remaining part of the channels, there will be a counter-current flow pattern. There is counter-current flow at the top of the channel where the upward flowing steam limits to the amount of liquid flowing down into the channels, and as a result a two-phase level is formed inside the channels. This flow pattern occurs for the majority of the channels.

The number of channels in co-current up-flow, co-current down-flow, counter-current flow is controlled by several phenomena. One of them is the requirement to have the same pressure drop between the inlet and the exit of the channels, which is a pressure drop between the lower plenum and the upper plenum. The number of co-current up-flow channels is given by the number of channels it takes the vent flow that is generated from lower plenum flashing plus the vapor generation in the channels. The number of co-current down-flow channel is given by the number of channels it takes to drain the core spray flow that is injected into the upper plenum. The remaining channels will be in the counter-current flow mode. The two-phase levels in these channels are such that the pressure drop between the upper and lower plena is the same for all channels.

This phenomenon was not seen in some of the earlier experiments in the seventies such as the Blow Down Heat Transfer (BDHT) loop, and then later on the Two Loop Test Apparatus (TLTA) and in the eighties the Full Integral Simulation Test (FIST) facilities under the Refill/Reflood and FIST programs. In those facilities, the simulation of the

boiling water reactor was scaled to one single fuel bundle. The three simultaneous flow patterns were not possible as only one channel existed, and the major flow pattern seen in the experiment was the counter-current flow pattern. As a result the liquid in the test facility with a single bundle would initially drain slower into the lower plenum and the two-phase level in the lower plenum would drop down to the bottom of the jet pumps. When the level drops below the bottom of the jet pumps, steam that is generated from the lower plenum flashing will vent up to the jet pumps. This reduced the amount of steam flowing up through the core and as a result of that counter-current flow limitation would diminish and allow more liquid to drain down from the upper plenum and core regions into the lower plenum. During the transient while the level existed at the bottom of the jet pump, liquid would be entrained out through the top of the jet pumps and flow out through the break.

During the refill-reflood program, however, tests were also conducted in the Steam Sector Test Facility (SSTF). In this test facility a full height 30 degree pie-shaped sector of the boiling water reactor was simulated. 58 parallel fuel channels were simulated in the SSTF and all three flow patterns were observed in this these tests. In these tests the level in the lower plenum did not drop down to the bottom of the jet pumps. Because of the parallel channel effects allowing all three flow patterns at the same time, there would be enough channels in down-flow to drain the flow out of the upper plenum while maintaining the level at the bottom of the core spray spargers.

Furthermore, as a result of holding up water due to CCFL at the side entry orifice at the bottom of the fuel channels, the core in the BWR typically refloods before the lower plenum is completely filled. Consequently, in the PIRT tables, we do not distinguish between the refill and the reflood phase, but we consider the two together, since they occur simultaneously. Eventually the refilling and reflooding will restore the liquid level in the core and it will completely quench the core. Inside the jet pumps the water level rises to the top of the jet pumps, which is two-thirds height of the core. With the vapor generation in the core region and the corresponding high void fraction, the two-phase level inside the core shroud needed to balance the static head is significantly above the top of the active fuel, and it completely quenches the core (See Slide 9).

To summarize the LOCA transient for the BWR/6, there is a second boiling transition that occurs, typically 20-35 second into the transient. A minor core heat up is experienced, and the core is reflooded and quenched 100-150 second into the transient. The PCT in a nominal best estimate calculation is below 1000 F. The upper bound PCT at the 95% probability / 95% confidence level is a couple hundred degrees higher and in the 1200-1300 F range. This is substantially lower than the 2200 F licensing limit set forth in 10CFR50 Appendix K.

For the BWR/4, the ECC configuration is slightly different (See Slide 10). There is a low-pressure core spray system that injects liquid into the upper plenum similar to the BWR/6. There is no high-pressure core spray system, instead, there is a high-pressure

coolant injection system that injects coolant into the downcomer region. The LPCI, instead of injecting into the bypass, connects to the drive line of the recirculation system. There are one low pressure core spray system, one high pressure coolant injection system, and four low pressure coolant injection systems, two into each recirculation system.

BWR/6 LOCA

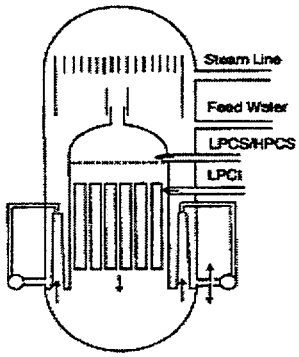

- **Refilling and Reflooding Restores Liquid Inventory and Quenches Core**
  - Downcomer Level at Top of Jet Pump
  - Two-Phase Level Above Core

BWR/6 PCT < 1000 °F

BWR/4 LOCA

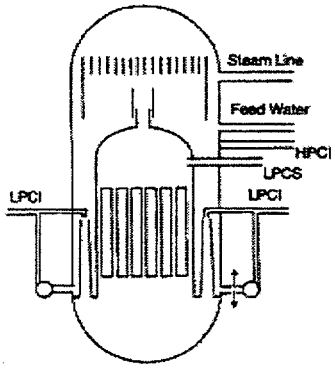

- **Early Part of Transient Similar to BWR/6**
  - Early Boiling Transition
  - Rewet due to Lower Plenum Flashing
- **LPCI Injection Into jet Pump Drive Line**
- **Core Uncovery Leads to Second BT**
- **HPCI Comes on (D/G Startup)**
- **LPCS and LPCI Comes on when P < Shutoff Head**
- **Worst Single Failure**
  - Failure: Battery
  - Available: 1 LPCS, 1 LPCI in each loop, ADS

The early part of the LOCA transient is very similar to the BWR/6 LOCA because it is dominated by the phenomena prior to the onset of the ECC systems (See Slide 11). Similar to the BWR/6, there is an early boiling transition, the fuel heats up and subsequently rewets due to lower plenum flashing, when the downcomer level has dropped below the top of the jet pump and the pressure has dropped below the saturation pressure corresponding to the liquid temperature in the lower plenum. The HPCI comes on based on the startup time for the diesel generators.

BWR/4 LOCA

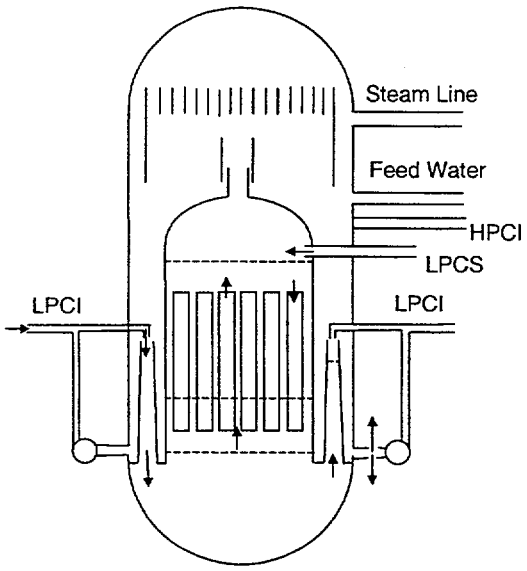

- **LPCS Injection**
  - **Phenomena Similar to BWR/6**
  - **Level Forms in Upper Plenum**
- **LPCI Injection**
  - **Condensation on LPCI**
  - **Lower Plenum Refills**
  - **Core Refloods**
- **Less Liquid Hold Up in Core During Refill Phase for BWR/4 Leads to Higher PCT for Second Peak**

The LPCI and the low pressure core spraying will come on when the pressure has dropped below the shutoff pressure for the pumps. Because of the time delay for the onset of these systems, the water level drops into the core region and there will be a second boiling transition as part of the core is uncovered.

Evaluating the various failure combinations and applying the single failure criterion, the worst failure for the BWR/4 is the battery failure. Battery failure will prevent the startup of one diesel generator, which will powers two of the LPCI pumps, and it will also prevent the opening of the injection valve for the high pressure coolant injection into the downcomer. This leaves one low pressure core spray system and two LPCI systems, one

for each recirculation loop. The LPCI is also affected by isolation valves in the discharge side of the recirculation loop preventing the LPCI from being lost out of the break location. The BWR/4 also have an ADS system, and similar to the BWR/6 the ADS system is not significant for the large break design basis accident.

For the BWR/4, when the two-phase level drops down into the lower part of the core, levels form in both the core and lower plenum (See Slide 11). This is very similar to the BWR/6. The phenomena associated with the low pressure core spray injection into the upper plenum are also very similar to the BWR/6.

For the low pressure coolant injection, cold water is injected into the jet pump drive line and enters the jet pump through the nozzles. There is a very large condensation rate on the LPCI flow right inside the mixing region of the jet pump and steam is drawn into the jet pump from the downcomer region to sustain this condensation. This was tested in the SSTF as part of the Refill-Reflood test program. These tests showed that, as long the water level in the jet pumps does not cover the injection flow there is close to complete condensation inside the jet pumps on the LPCI flow coming through the nozzles and therefore saturated liquid will penetrate into the lower plenum.

For the BWR/6, the LPCI liquid was injected into the bypass and it would flow through the leakage holes into the bottom of the channel and be held up inside the channel by the CCFL. This does not happen for the BWR/4. The liquid is injected into the jet pump and from there into the lower plenum. Therefore less liquid is held up inside the core region and the level drop in the core is larger compared to the equivalent level drop for the BWR/6 before the core starts to reflood, and it takes longer time to quench the core. Consequently, the second peak in the cladding temperature is higher for the BWR/4 than for the BWR/6. As the lower plenum fills and a corresponding filling of the jet pumps occur, the condensation on the LPCI in the jet pumps will be reduced and cold water will penetrate into the lower plenum. The subcooled water stratifies at the bottom of the lower plenum and has relatively little impact on the two-phase level and the refilling of the lower plenum. As a major part of the liquid in the lower plenum remain saturated, particularly at the two-phase level, the flashing from the lower plenum continues and holds up liquid in the core region providing some cooling of the fuel. The liquid from the LPCI injection quickly fills up the lower plenum and when the two-phase level gets up to the bottom of the core, the core starts reflooding and subsequently quenches to terminate the transient.

In summary the temperature transients for the BWR/4 is quite similar to the BWR/6 (See Slide 12). There is level inside the jet pump at the top of the jet pump, and a two-phase level inside the core shroud that is above the top of the active fuel.

BWR/4 LOCA

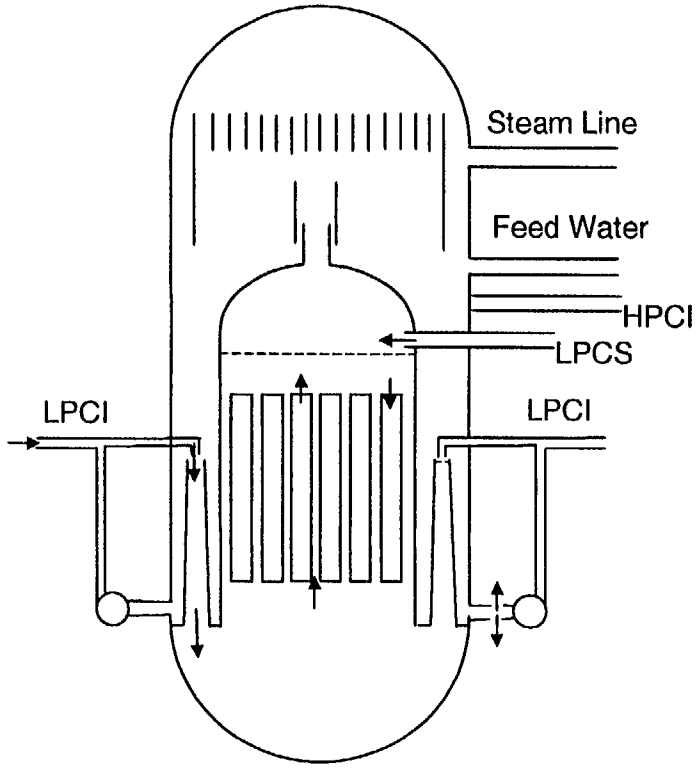

- **Refilling and Reflooding Restores Liquid Inventory and Quenches Core**
  - **Downcomer Level at Top of Jet Pump**
  - **Two-Phase Level Above Core**

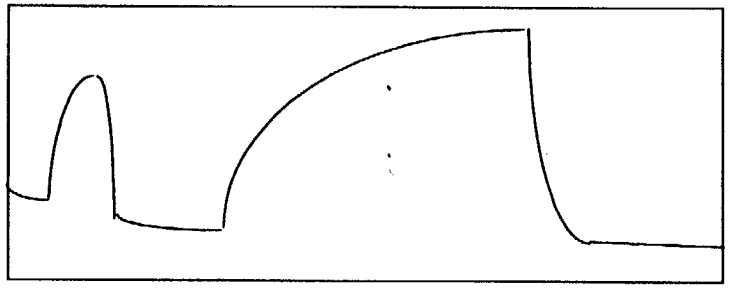

PCT

BWR/4 PCT ≈ 1000 °F

Because it takes a little longer to reflood the core for the BWR/4 the core heat-up is larger before it is quenched. Typically for BWR/4 the nominal best estimate PCT is in the order of 1000 F. The upper bound PCT at the 95/95 level is again a couple hundred degrees higher, and could be as high as 1400-1500 F.

Slide 13 summarizes the major phenomena for a LOCA in a the jet pump BWR. Critical flow in the break location affects the liquid loss from the primary system and the depressurization of the system. Interfacial shear, controls the void fractions in the system and the two-phase levels in the various regions. Counter-current flow limitation is extremely important for the BWR. It occurs at the side entry orifice and at the top restrictions in the fuel channel, which is either the upper tie plate or it is the top spacer in the fully rodded section of the fuel bundles (the last spacer before the end of the part length rods). Interfacial heat transfer together with the depressurization determines the flashing in the lower plenum and in the core region as well as other regions of the primary system. Interfacial heat transfer is also the controlling phenomenon for condensation on the ECC as it is injected into the system either through the core spray nozzles in the upper plenum, as LPCI into the bypass for the BWR/6 or into the jet pump drive lines for the BWR/4. Condensation is the controlling phenomenon for subcooled CCFL breakdown, which is a major controlling phenomenon for the parallel channel effects that exists in the core of the BWR during the refill/reflood phase. Wall friction is important, because, as discussed earlier in the presentation, there can be three parallel flow patterns in the core during the refill-reflood part, co-current up-flow, counter-current flow with the two-phase level and co-current down-flow. The pressure drop has to be matched between lower plenum and the upper plenum. For co-current up-flow the dominant part of the pressure drop is wall friction. For the down-flow it is friction and static head, and for the counter-current flow it is predominantly static head associated with the two-phase level in the channels. Finally heat transfer is important. Fuel heat transfer (pellet conductivity and gap conductance) controls the initial stored energy in the fuel. The early boiling transition in the core happens primarily because of the flow reduction while there is still plenty of liquid in the core region, and the stored energy has a major impact on the early PCT. Once boiling transition occurs, film boiling becomes the dominant mode of heat transfer and a major controlling phenomenon for the PCT.

Early in the transient, following the first boiling transition, the film boiling heat transfer is for the inverted annular type flow regime, and later on, for the co-current up-flow and counter-current flow regimes in the core region, prior to quenching, the film boiling heat transfer is for dispersed annular flow. Both modes of film boiling exist in the BWR.

Major Phenomena

- **Critical Flow**
- **Interfacial Shear**
  - Void Fraction
  - Two-Phase Levels
  - CCFL
- **Interfacial Heat Transfer**
  - Flashing
  - Condensation
  - Subcooled CCFL Break Down
- **Wall Friction**
- **Heat Transfer**
  - Boiling Transition
  - Film Boiling
  - Rewetting
  - Fuel Gap Conductance

JGMA May 2000 *13*

Finally rewetting is important, it is controlled by two phenomena: the minimum film boiling temperature and when sufficient liquid is present to maintain a wetted condition.

For the BWR/4 and /6, because the PCT is in the order 1000 degrees, metal-water reaction is not significant. There is no significant metal-water reactions at these low temperatures. Fuel rod failure mechanisms are also not significant because there is not enough stress on the cladding to cause failure at these low temperatures.

For the BWR/2, the situation is different. The BWR/2 is the older generation of the BWRs without jet pumps (See Slide 14). In the BWR/2, the recirculation flow is taken out at the bottom of the downcomer and recirculation pumps inject it back into the lower plenum. For the BWR/2, the design basis accident is the double-sided break in the discharge side of the loop. This produces a large break connected directly to the lower plenum, and due to the large size of the recirculation pipe, it becomes impossible to reflood the core for the BWR/2. The only means to maintain cooling is the core spray system There are two independent core spray systems that inject water into the upper plenum once a LOCA has occurred for the BWR/2, and because the design basis accident is a break connected to the lower plenum, all core flow is lost almost instantly and there is an early boiling transition. There is no early quenching from lower plenum flashing as most of the liquid from the lower plenum is lost out through the break.

BWR/2 LOCA

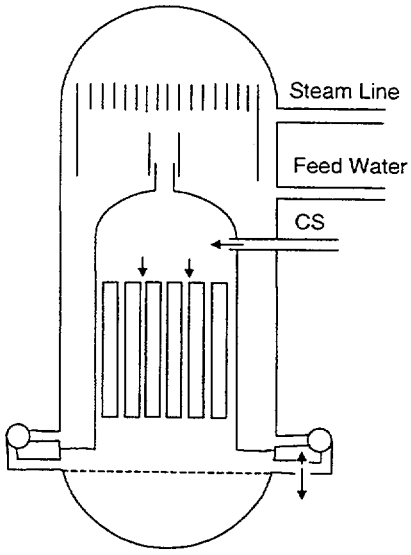

- **Early BT Like Jet Pump BWRs**
- **Core Can Not Be Reflooded**
- **Main Heat Transfer Phenomena: Core Spray Heat Transfer**
  - **Convective Heat transfer to Superheated Steam**
  - **Radiation Heat Transfer to Channel Box and to Two-Phase Mixture**
  - **Conduction Controlled Rewetting**
  - **Metal-Water Reaction**
- **PCT Controlled by Balance Between Decay Heat and CS Heat Transfer**

Quenching of the fuel for the BWR/2 does not occur until on the order of half an hour into the LOCA transient. During the heatup, the only cooling of the fuel is provided by the core spray system injecting water into the upper plenum and from there into the fuel channels. A two-phase level never forms in the upper plenum, because the up-flow of steam is not sufficient to hold up water in the upper plenum. The up-flow of steam into the upper plenum is low, because part of the steam generated trough vaporization in the core will leave the system through the bottom of the core and out through the break.

The spray distribution in the upper plenum and CCFL for the high power channels controls the drainage of liquid into the channels.

The core spray heat transfer is the dominant mode and the major controlling phenomenon for the PCT. Core spray heat transfer consists of convection heat transfer to superheated steam with entrained droplets and radiation heat transfer.

Film flow will occur on the channel box and the fuel rods after quenching. Thermal radiation heat transfer is a very dominant mode for the BWR/2. There is radiation heat transfer to the two-phase mixtures to the channel box. The radiation heat transfer to the channel box is the dominant mode as the channel box will quench relatively early in the transient because of the core spray water entering the channels and the bypass region.

The quenching of the channel box is dominated by conduction controlled rewetting, and the quench front moves down from the top to the bottom of the channel box.

The PCT becomes very high for the BWR/2 because of the relatively low value of the core spray heat transfer coefficient and because thermal radiation is only significant at high temperatures. Metal-water reaction will occur at high temperature, and at high temperatures close to the 2200F limit, it can become comparable in magnitude to the decay heat. The LOCA transient is significantly longer for the BWR/2 compared to the jet pump BWRs. The PCT typically occurred within 100-150 seconds for the jet pump BWRs. For the BWR/2, after the initial blowdown, the transient is an almost quasi-steady state transient, where the temperature of the fuel is determined by a balance between the energy that is being generated, which is the decay heat, plus some contribution from the metal-water reaction, and the heat transfer, which is the core spray heat transfer. Typically the PCT occurs 600-800 seconds into the transient. Quenching of the fuel rods could be very slow. It can be half an hour into the transient because the core never refloods and quenching of the fuel is mainly due to conduction controlled quenching from the top. For the fuel, the quench front propagates at a velocity that is in the order of millimeters per second.

In summary, for the BWR/2 there is an early boiling transition, and the system, once the blowdown is over, enters a quasi-steady state mode controlled by a balance between the decay heat and core spray heat transfer. The cladding temperature is controlled by the magnitude of the core spray heat transfer and the gradual reduction of the decay heat, and the PCT occurs at the point where the energy generation becomes less than the core spray heat transfer. In the order of half an hour into the transient, the quench front has moved low enough on the fuel rods to quench the temperatures.

Nominal best estimate PCT for BWR/2 is in the order of 1700 F (See Slide 15). Upper bound PCT at the 95/95 level is on the order of 2000 F. Licensing calculations for BWR/2 with the SAFER/CORCL codes can give PCTs close to the 2200 F limit.

BWR/2 LOCA

GNF

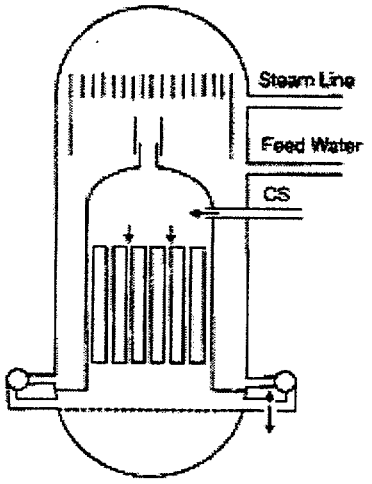

- **Core Spray Heat Transfer Controls PCT**

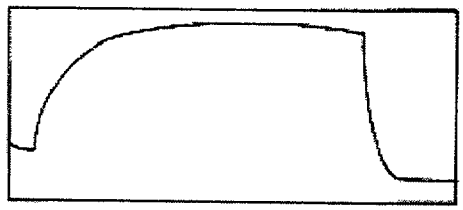

BWR/2 PCT = 1700 °F

Major phenomena for the BWR/2 are critical flow and interfacial shear (See Slide 16). Critical flow controls the blow down, while interfacial shear controls phenomena such as void fractions, two-phase levels, CCFL and the spray distribution in the upper plenum. The spray distribution in the upper plenum is very important for the BWR/2 as there will be no level in the upper plenum. It is not significant for the jet pump BWRs, because a level is maintained in the upper plenum during the refill and reflood phase. Similar as for the jet pump plants, interfacial heat transfer is significant for the BWR/2 as it controls flashing, condensation and subcooled CCFL breakdown.

Major Phenomena

GNF

- **Critical Flow**
- **Interfacial Shear**
  - **Void Fraction**
  - **Two-Phase Levels**
  - **CCFL**
  - **Spray Distribution**
- **Interfacial Heat Transfer**
  - **Flashing**
  - **Condensation**
  - **Subcooled CCFL Break Down**
- **Wall Friction**
- Heat Transfer
  - **Boiling Transition**
  - **Film Boiling**
  - **Rewetting**
  - **Radiation Heat Transfer**
  - **Conduction Controlled Rewetting**
- Metal-Water Reaction
- Fuel Rod Failure

JGMA May 2000 *16*

For heat transfer, thermal radiation heat transfer is a very dominant mode of heat transfer. For a fuel rod in a BWR/2, typically half or 50% of the heat transfer is thermal radiation. The dominant part of the radiation heat transfer is to the channel box once it is quenched by the core spray water flowing down on the inside and on the outside of the channel box. Quenching time for the channel is typically on the order of half a minute into the transient. Rewetting is a very important phenomenon for the BWR/2 because the quenching of the channel box and the associated change in emissivity has such a strong impact on the heat transfer. Finally because of the high temperatures obtained in a BWR/2 LOCA, metal-water reaction and fuel rod failure mechanisms are important phenomena.

The previous was a summary of the design basis LOCA for the various BWR types and the major controlling phenomena for these events. The following will contain a short discussion of the small break LOCA (SBLOCA).

When LOCAs are analyzed, the entire break spectrum is evaluated to demonstrate that the design basis accident is indeed the limiting LOCA. For a SBLOCA (See Slide 17), the system may not depressurize, because only small amount of liquid leaves the system through the break while the vapor generation can make up for the volume loss. In this case the system is not depressurizing, however, the level will drop slowly because of the loss of liquid inventory. This is where the ADS system becomes important for the BWR. The Automatic Depressurization System (ADS) is needed to lower the pressure, because as long as the pressure stays high liquid from any of the low pressure systems can not be injected into the BWR, and the single failure criterion can eliminate the high pressure system. Most of the ECC systems are low pressure systems. Once a low level in the downcomer occurs, the ADS is tripped. The ADS valves will open and depressurize the system, allowing the low pressure systems to come on. In a way, the ADS converts the small break LOCA to an event that resembles a large steam line break LOCA .

Small Break LOCA

GNF

- **No Depressurization**
- **Level Drop Due to Loss of Inventory**
- **ADS Trip on Low Level**
- **Low Pressure Activates LPCI and LPCS**

- **ADS Turns Small Break Into Large Break**

For the small break LOCA, there is no immediate reversal of the flow in half the jet pumps, therefore there is no drastic reduction in the core flow, but rater a slow reduction given by the coast down of the recirculation pumps. The early boiling transition is typically avoided for the small break LOCA and only the second boiling transition will occur.

The last slide (Slide 18) shows the impact of fuel exposure. Typically, the thermal mechanical design limit determines the maximum linear heat generation rate; in this case here, in this case, the maximum average planar linear heat generation rate (MAPLHGR) is shown. The thermal mechanical design limit is an envelope of power versus exposure and as long as the fuel operate within that envelope, all of the classic design and licensing limits are met. The top curve on Slide 18 shows the thermal mechanical design limit for the jet pump BWRs. It is the design and licensing limit for the fuel, and the PCT for the jet pump plants, as shown earlier, are calculated with the fuel operating at this limit. This is the reason for the conclusion that the jet pump BWRs are not limited by the LOCA events.

The BWR/2 is LOCA limited. Early in the transient, where the linear heat generation rate is high, the linear heat generation is limited by the peak cladding temperature. For the licensing calculation, the PCT gets close to the licensing limit of 2200F. The 2200F limit determines what the maximum linear heat generation can be in the fuel bundle. At some point, with increasing the exposure, as fission gas pressure or the pressure in the gap increases, the fuel rods may fail. When that happens, metal-water reaction is calculated on both sides of the cladding, both on the outside and on the inside.

Under these conditions the limit of 17% maximum local oxidation can be reached before the PCT reach the 2200F limit. Typically for intermediate exposures as shown in Slide 18, the linear heat generation rate is limited by oxidation limit. In the calculation of the LOCA transient, it is assumed that there is no initial oxidation of the cladding, which maximizes the energy generations from the calculated metal-water reaction. The assumption for the initial oxidation on the fuel is currently subject to some discussion in the technical community. In conclusion, while the jet pump BWRs are not limited by the LOCA, the BWR/2 is limited by the LOCA.

Fuel Exposure - MAPLHGR

GNF

- **MAPLHGR = Maximum Average Planar Linear Heat Generation Rate**

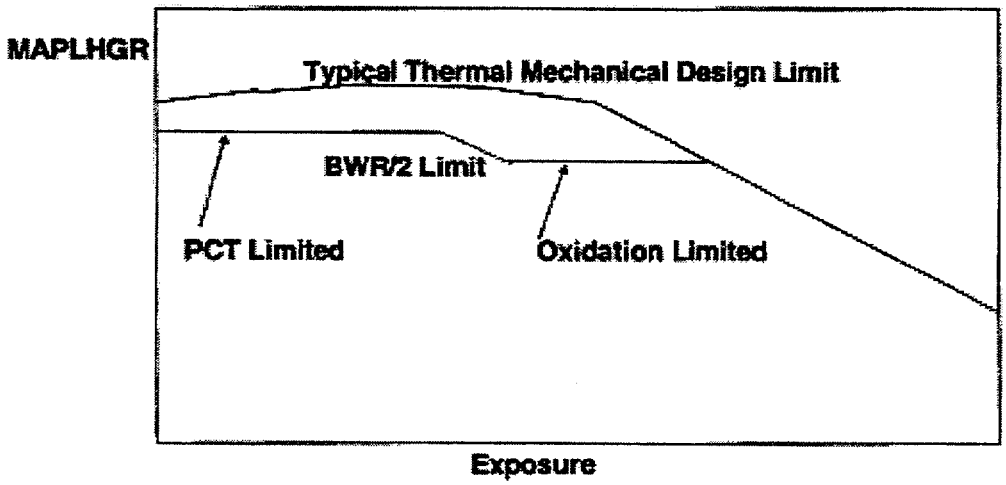

THE HISTORY OF LOCA EMBRITTLEMENT CRITERIA

G. Hache
Institut de Protection et de Sureté Nucléaire
Cadarache, France

H. M. Chung
Argonne National Laboratory
Argonne, Illinois, USA

Abstract

Performance of high-burnup fuel and fuel cladding fabricated from new types of alloys (such as Zirlo, M5, MDA, and duplex alloys) under loss-of-coolant-accident (LOCA) situations is not well understood at this time. To correctly interpret the results of investigations on the performance of the old and new types of fuel cladding, especially at high burnup, it is necessary to accurately understand the history and relevant databases of current LOCA embrittlement criteria. In this paper, documented records of the 1973 Emergency Core Cooling System (ECCS) Rule-Making Hearing were carefully examined to clarify the rationale and data bases used to establish the 1204°C peak cladding temperature and 17% maximum oxidation limits. A large amount of data, obtained for zero- or low-burnup Zircaloy cladding and reported in literature only after the 1973 Rule-Making Hearing, were also evaluated and compared with the current criteria to better quantify the margin of safety under LOCA conditions.

1. Introduction

Because of major advantages in fuel-cycle costs, reactor operation, and waste management, the current trend in the nuclear industry is to increase fuel discharge burnup. At high burnup, fuel rods fabricated from conventional Zircaloys often exhibit significant degradation in microstructure. This is especially pronounced in pressurized-water reactor (PWR) rods fabricated from standard Zircaloy-4 in which significant oxidation, hydriding, and oxide spallation can occur. Thus, many fuel vendors have developed and proposed the use of new cladding alloys, such as low-tin Zircaloy-4, Zirlo, M5, MDA, duplex cladding, and Zr-lined Zircaloy-2. Performance of these alloys under loss-of-coolant-accident (LOCA) situations, especially at high burnup, is not well understood at this time. Therefore, it is important to verify the safety margins for high-burnup fuel and fuels clad with new alloys. In recognition of this, LOCA-related behavior of various types of high-burnup fuel cladding is being actively investigated in several countries [1-6]. However, to correctly interpret the results of such investigations, and if necessary, to establish new embrittlement thresholds that maintain an adequate safety margin for high-burnup operation, it appears necessary to accurately understand the rationale,

history, and data bases used to establish the current LOCA criteria, i.e., maximum cladding temperature limit of 1204°C (2200°F) and maximum oxidation limit of 17%. For this purpose, documented records of the 1973 Atomic Energy Commission (AEC) Emergency Core Cooling System (ECCS) Rule-Making Hearing were carefully examined and the relevant databases were reevaluated in this paper. Since the establishment of the current criteria, large amounts of data were obtained in many countries for zero- or low-burnup fuel cladding. The results of these investigations were also critically evaluated to determine the validity of the current criteria and safety margins for a wider range of conditions.

2. Primary Objectives of Current Criteria

In 1967, an Advisory Task Force on Power Reactor Emergency Cooling [7], appointed to provide "additional assurance that substantial meltdown is prevented" by core cooling systems, concluded that:

> "The analysis of (a LOCA) requires that the core be maintained in place and essentially intact to preserve the heat-transfer area and coolant-flow geometry. Without preservation of heat-transfer area and coolant-flow geometry, fuel-element melting and core disassembly would be expected... Continuity of emergency core cooling **must be maintained after termination of the temperature transient for an indefinite period until the heat generation decays to an insignificant level**, or until disposition of the core is made."

This rationale makes it plainly clear that it is most important to preserve the heat transfer area and the coolant flow geometry not only during the short-term portion of the core temperature transient but also for long term.

Consistent with the conclusions of the Ergen Task Force, the U.S. Atomic Energy Commission (AEC) promulgated Criterion 35 of the General Design Criteria [8] which states that: "... fuel and clad damage that could interfere with **continued effective core cooling** is prevented." It also promulgated Criterion 3 of the Interim Acceptance Criteria for ECCS for LWR [9] which states that: "The clad temperature transient is terminated at a time when the core geometry is still amenable to cooling, and before the cladding is so embrittled as to fail **during or after quenching**."

These criteria were subjected to a Rule-Making Hearing in 1973, which was extensively documented in the Journal of Nuclear Safety in 1974 [10,11]. During the hearing process, the last part of the Criterion 3 was replaced by the modified Criterion 1 and the new Criterion 2 of the Code of Federal Regulations, Title 10, Part 50.46, Article (b), commonly referred to as 10 CFR 50.46 [12]. Thus, the AEC Commissioners wrote:

"In view of the fundamental and historical importance of maintaining core coolability, we retain this criterion as a basic objective, in a more general form than it appeared in the Interim Acceptance Criteria. It is not controversial as a criterion... Although most of the attention of the ECCS hearings has been focused on the events of the first few minutes after a postulated major cooling line break, up to the time that the cladding would be cooled to a temperature of 300°F or less, the **long-term maintenance of cooling** would be equally important [13]."

There are two key factors to consider to evaluate the change in coolable geometry of core, a brittle mode and a ductile mode of deformation in fuel cladding. The ductile mode is related to cladding ballooning, burst, and coolant channel blockage. This mode will not be treated in this paper. Our focus in this paper is on the change in coolable geometry due to cladding embrittlement and failure.

3. Metallurgy of Cladding Embrittlement

In 1960s, Wilson and Barnes performed laboratory tests simulating steam reactions with Zircaloy-clad fuel rods at high temperatures. They observed embrittlement of oxidized cladding well below the melting temperature of Zircaloy, either during the test itself or during removal of the specimen from the oxidizing furnace. The results were reported in Argonne National Laboratory (ANL) progress reports and synthesized later in Ref. 14. At the same period, investigators in Oak Ridge National Laboratory (ORNL) conducted TREAT Test No. 6 with Zircaloy cladding in steam and observed that the specimen was severely embrittled by oxidation [15]. Also at about the same period, many tests were conducted that simulated reactivity-initiated accident (RIA) in SPERT-CDC and TREAT reactors. Results of metallurgical examination in these tests showed that embrittlement was caused by severe microstructural modification of the cladding. Brittle cladding cross sections exhibited oxide layer, oxygen-stabilized alpha-phase layer and a region of acicular prior beta-phase. The results were later reported by Fujishiro et al. [16].

As a result of these observations, the scientific community was alerted to the fact that oxidation of Zircaloys above the alpha-to-beta transformation temperature results in the formation of inherently brittle phases, i.e., Zr oxide, oxygen stabilized alpha-Zr (fcc structure), and diffusion of oxygen into the underlying beta phase (bcc structure). This is shown schematically in Fig. 1. Ductility of cladding could be severely degraded if the degree of oxidation is high. It was also realized that, if the embrittled cladding fragments into small pieces, the coolability of the core could be seriously impaired.

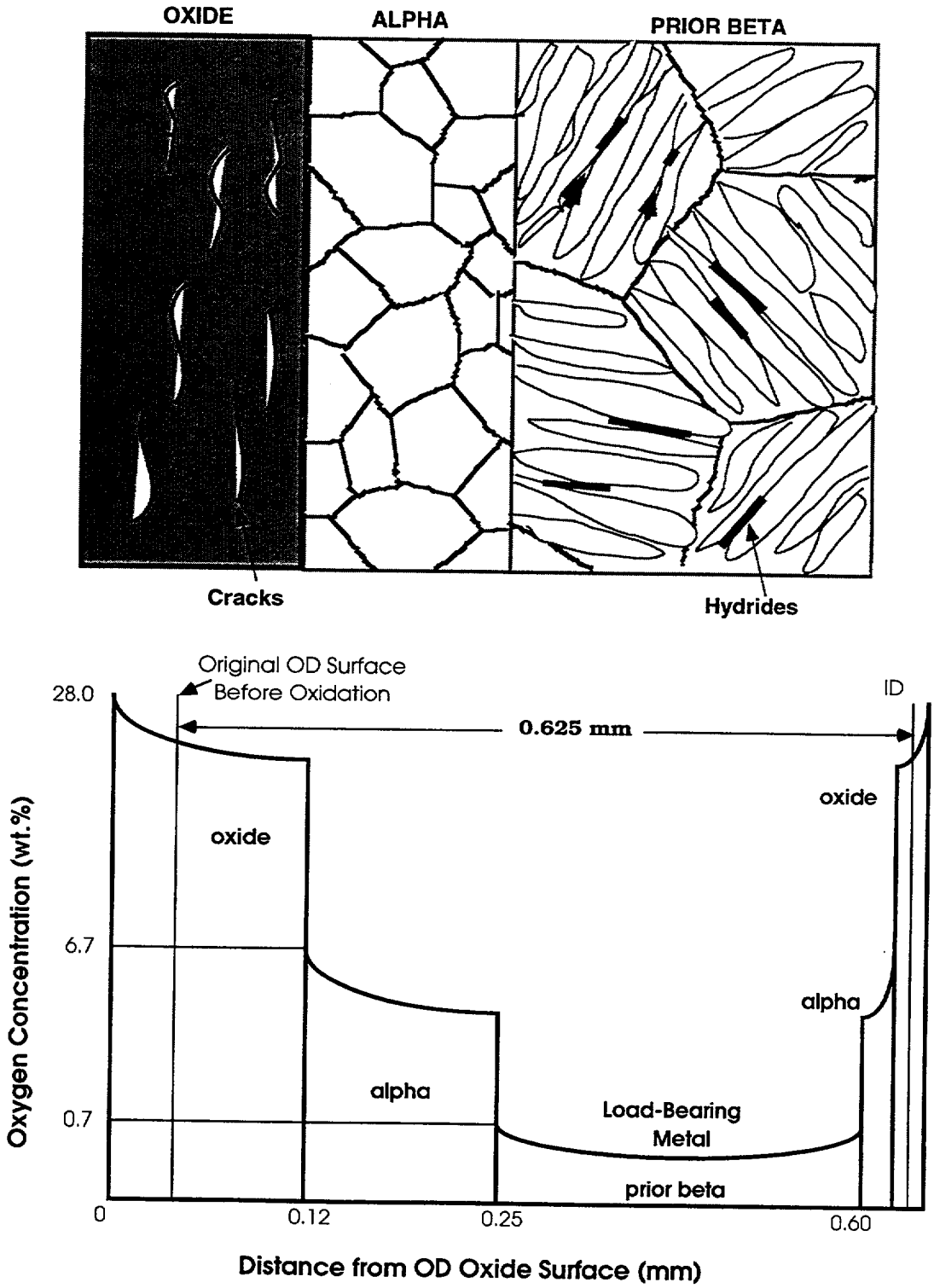

Fig. 1. Schematic illustration of microstructure (top) and oxygen distribution (bottom) in oxide, stabilized alpha, and prior-beta (transformed-beta) layers in Zircaloy cladding after oxidation near 1200°C.

Significantly embrittled cladding can fragment during the quenching phase of a LOCA. The action of rewetting by ECCS water involves the collapse of the vapor film that covers the cladding outer-diameter (OD) surface prior to subsequent transition to nucleate boiling. This event takes place at a more or less constant temperature, i.e., the Leidenfrost temperature. For oxidized Zircaloy-4 cladding rewetted by bottom-flooding water, ANL investigators reported that rewetting occurs in the range of 475-600°C [17]. The abrupt change in the heat transfer conditions induces large thermal-shock stress, which can fracture the cladding, if it is sufficiently embrittled by oxidation.

Below the Leidenfrost temperature, there is continued risk of fragmentation after quenching. In accordance with the opinions of the Ergen Task Force and the AEC staff and commissioners mentioned earlier, other experts also wrote a similar opinion for OECD Committee on Safety of Nuclear Installations (CSNI) [18]: "The ability of the cladding to withstand the thermal-shock stresses of quenching during rewetting **or post-LOCA forces** is related to the extent and detailed nature of oxidation during the transient. **The post-LOCA forces, which need to be taken into account, are the hydraulic, seismic, handling, and transport forces."**

There are two primary factors that exacerbate the susceptibility of oxidized cladding to post-quench embrittlement in comparison with susceptibility to fragmentation during quenching: i.e., (1) more pronounced effect of oxygen dissolved in beta phase at lower temperature of loading (i.e., more pronounced after quench than during quench) and (2) more pronounced effect of hydrogen uptake which may occur during irradiation (e.g., in high-burnup Zircaloy-4) or during transient oxidation in steam (e.g., from cladding inner surface in contact with stagnant steam near a ballooned and burst region). For cooling rates typical of bottom flooding of core (i.e., 1-5°C/s), most hydrogen atoms remain in solution in the beta phase at Leidenfrost temperature, and in such state, hydrogen has little effect on the fracture resistance of an oxidized Zircaloy. However, when load is imposed at temperatures below the Leidenfrost temperature, precipitated hydrides strongly influence the fracture resistance of cladding. Eutectoid decomposition of hydrogen-stabilized beta phase at temperatures below ≈550°C [19] is the major factor that causes this deleterious effect (see Fig. 2).

4. Opinion of Regulatory Staff and Commissioners during 1973 Rule-Making Hearing

4.1 Reluctance to Neglect Effects of Mechanical Constraints

Some factors during a LOCA, such as ballooning of the rod near the spacer grid, rod-grid spring chemical interaction, and the friction between the fuel rod and spacer grids, can restrict the axial movement of the cladding. Also, guide tubes in a PWR fuel assembly are mechanically fixed to the spacer grids.

Because of these factors, fuel rods during reflooding will be subject to tensile load that is produced due to the differential axial shrinkage between a cladding and the guide tube. Rods may interact each other due to ballooning or bowing. For high-burnup fuels in which tight pellet-cladding bonding is common, axial shrinkage can be restricted if the tight bonding remains unchanged after ballooning and burst. These constraints will remain after quench, when deleterious effects of oxygen and hydrogen are far more pronounced.

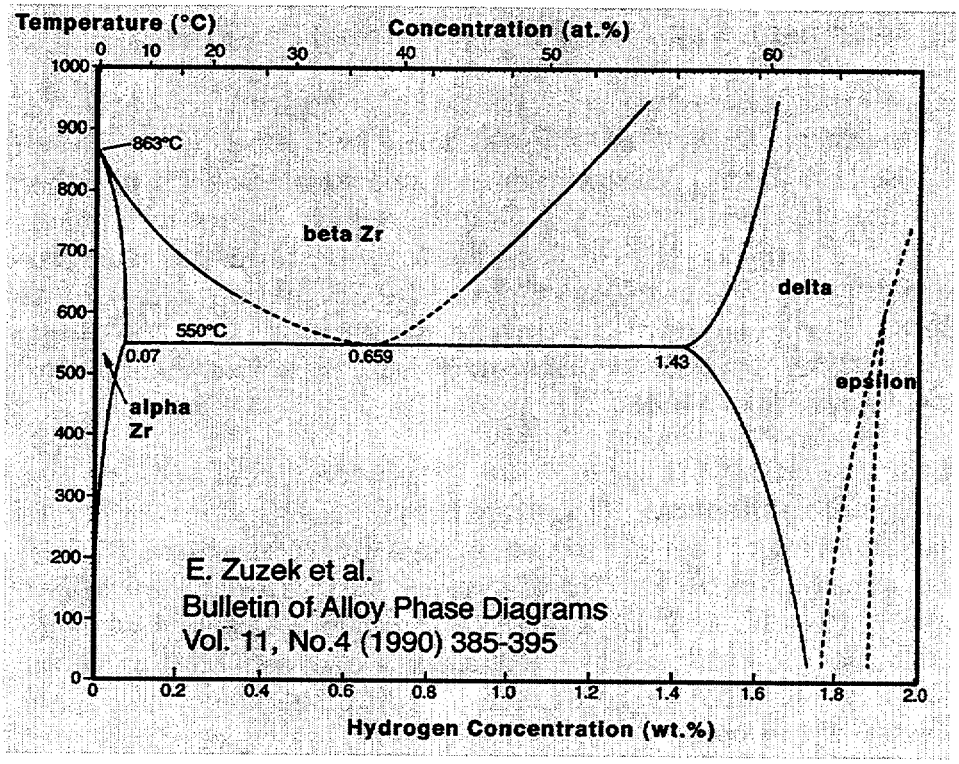

Figure 2.

Zr-H binary phase diagram (from E. Zuzek et al., Bulletin of Alloy Phase Diagrams, Vol. 11, No. 4, 1990, pp. 385-395).

In recognition of this, the AEC Staff wrote during the 1973 Rule-Making Hearing that "**the loads due to assembly restraint and rod-to-rod interaction may not be small compared to the thermal shock load and cannot be neglected** [20]." Subsequently, it was concluded that: "The staff believes that quench loads are likely the major loads, but **the staff does not believe that the evidence is as yet conclusive enough to ignore all other loads** [21]."

Then, the Commissioners added: "**There is some lack of certainty as to just what nature of stresses would be encountered during the LOCA**.... (We want) to draw attention to the fact that **it may not be possible to anticipate and calculate all of the stresses to which fuel rods would be subjected in a LOCA**. Although we believe the calculations of thermal shock stresses are worthwhile and informative, we agree with the regulatory staff that they are not sufficiently well defined to depend on for regulatory purposes [13]."

Before 1973, no thermal-shock quench test was performed on mechanically constrained cladding specimens. Then in early 1980s, Uetsuka et

al. performed quenching tests on cladding sections under severely constrained condition [22]. In their experiment, cladding tube was fixed at the bottom but was allowed to freely elongate in axial direction during oxidation at high temperature. As a result, cladding length increased freely because of thermal expansion and oxide-induced creep. At the end of the isothermal oxidation, the specimen top was fixed to the crosshead of an Instron tensile facility. Then, the load-time curve was continuously monitored during quenching. Thus, at Leidenfrost temperature, the cladding tube was subjected to combined axial-tensile and thermal-shock stresses. The results of the tests are summarized in the Fig. 3. Similar tests were also performed on unconstrained tubes (Fig. 4).

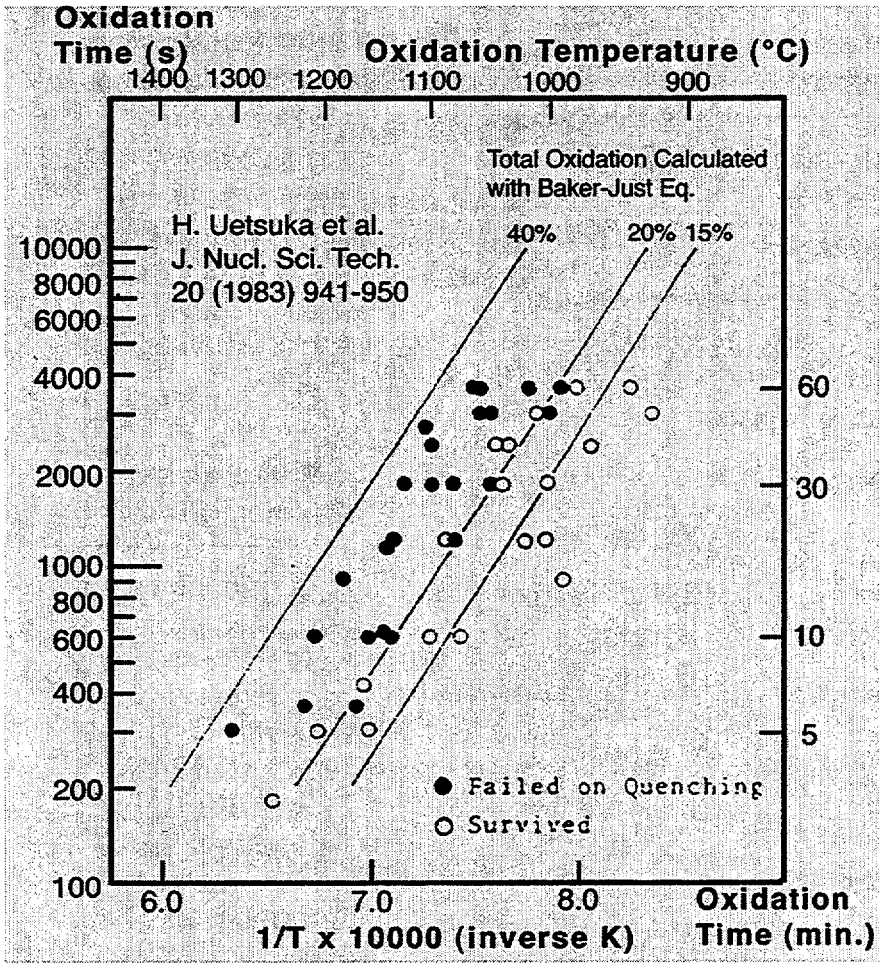

Figure 3.

Failure-nonfailure boundary for fully constrained Zircaloy-4 after oxidation in steam and quenching as function of oxidation time and temperature; total oxidation calculated with Baker-Just equation is also indicated (from Uetsuska et al., J. Nucl. Sci. Tech. 20, 1983, pp. 941-950).

A comparison of the results from the two contrasting types of test shows a large effect of the mechanical constraint. However, it is difficult to conclude whether the degree of constraint in the experiments of Uetsuka et al. is prototypic of a LOCA or unrealistically too severe. The 17% oxidation limit, calculated with Baker-Just correlation, appears to be adequate for protection of constrained rods against thermal-shock failure (Fig. 3), whereas a large margin is evident for unconstrained rods (Fig. 4).

Unlike other bundle tests such as NRU, REBEKA, JAERI and ORNL multirod tests that were entirely devoted to the study of ballooning, burst, and flow-channel blockage, some of the tests in Phebus LOCA program was devoted to the study of embrittlement [23]. The fragmented Rod 18 of the Test 219, exposed to ≈1330°C, is especially interesting (see Fig. 5). For this oxidation temperature, results of calculation with PRECIP-II Code [24] indicates that the O content in the beta phase was higher than 0.9 wt.%, a threshold O concentration found to be associated with thermal-shock failure or survival [17]. Rod 18 fragmented despite it was oxidized to an equivalent-cladding reacted (ECR) value of only ≈16%. This observation indicates a deleterious bundle effect, i.e., an additional mechanical constraint.

As a conclusion, results of the JAERI constraint quench test and the PHEBUS-LOCA Test appear to justify the reluctance of the AEC staff and commissioners to neglect the effect of mechanical constraints on the susceptibility to thermal-shock failure.

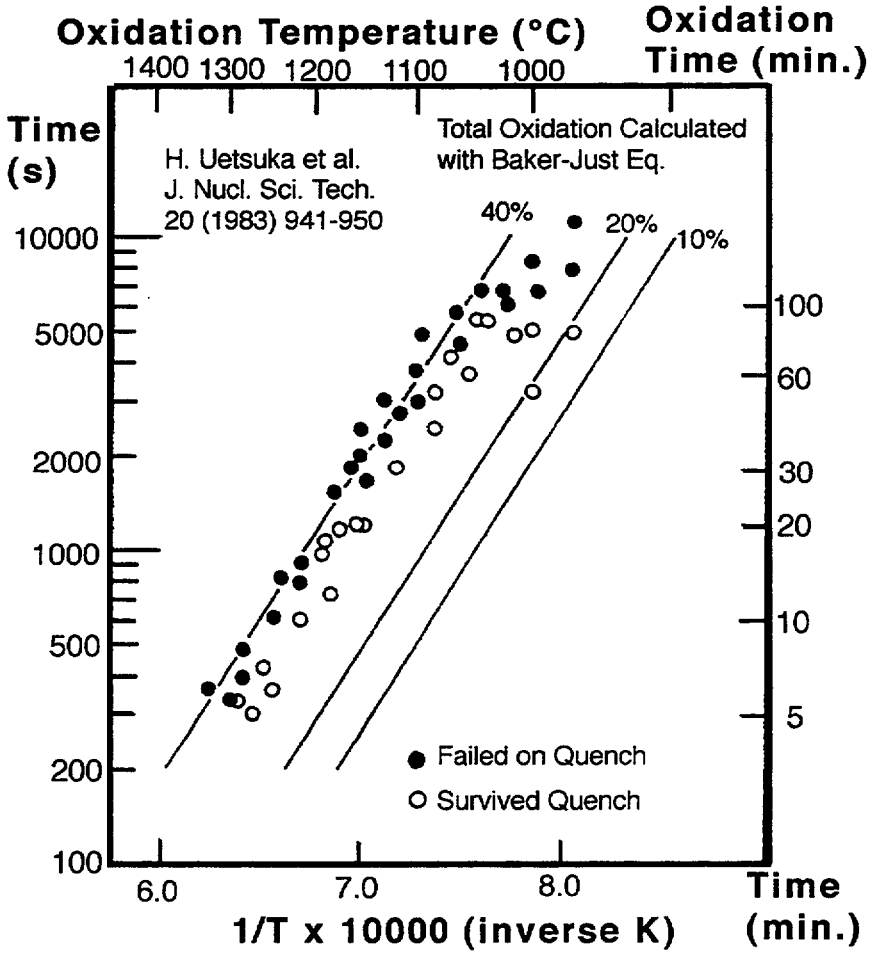

Figure 4.

Failure-nonfailure boundary for unconstrained Zircaloy-4 after oxidation in steam and quenching as function of oxidation time and temperature; total oxidation calculated with Baker-Just equation is also shown (from Uetsuska et al., J. Nucl. Sci. Tech. 20, 1983, pp. 941-950).

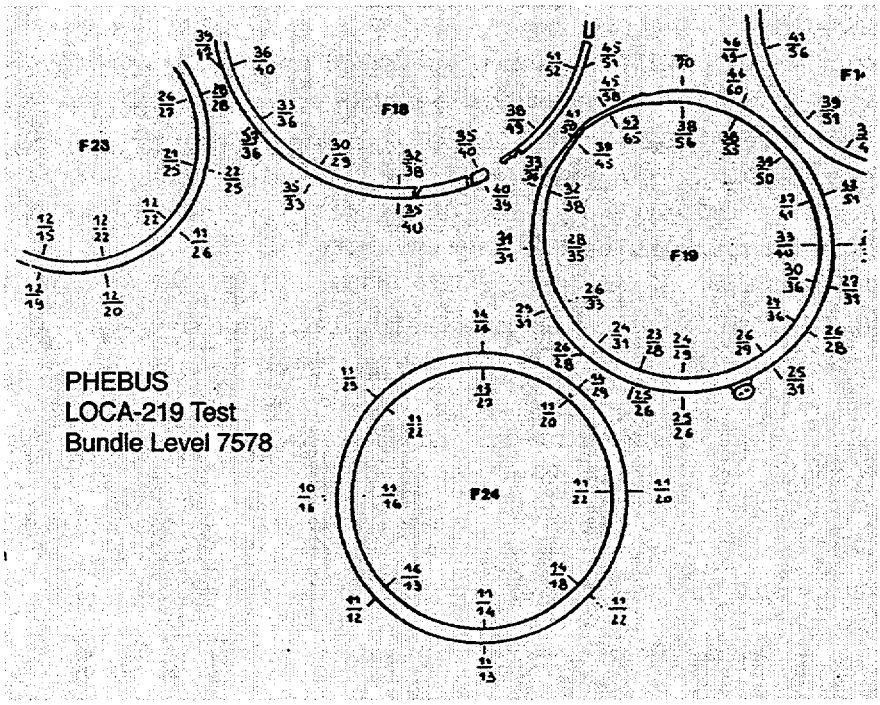

Figure 5.

Cross-section of portion of fuel assembly from PHEBUS LOCA-219 Test (Ref. 23), showing fragmentation of cladding.

4.2 Preservation of Ductility and Consideration of Results from Unconstrained Quench Test

At the end of the 1973 Hearing, the AEC Commissioners wrote: "...Nevertheless we find the quench results encouraging in that they provide assurance that the 2200°F limit is conservative. Our selection of the 2200°F limit results primarily from **our belief that retention of ductility in the Zircaloy is the best guarantee of its remaining intact during the hypothetical LOCA**... The thermal shock tests are reassuring, but **their use for licensing purposes** would involve an assumption of knowledge of the detailed process taking place in the core during a LOCA **that we do not believe is justified** [13]."

Without much ambiguity, this conclusion clearly expressed the belief that retention of ductility was considered the best guarantee against potential fragmentation under various types of loading (thermal-shock, bundle constraints, hydraulic, handling, and seismic forces). During the 1973 Hearing, results from unconstrained quench tests (simple thermal-shock test) were considered only corroborative and reassuring. However, their use for regulatory purposes was not accepted.

Results of later investigations on unconstrained or partially constrained cladding [17,18] showed a large margin of survival under thermal shock relative to 17%-ECR and 2200°F (1204°C) peak temperature limits. Such results are summarized in Fig. 6. No fragmentation occurred for ECR < 17% for all oxidation temperatures, whereas significant margin of survival was observed for

oxidation temperatures <1204°C. The results in Fig. 6 were limited for thermal-shock tests in which cladding tube or ring was directly quenched from the maximum oxidation temperature without slow cooling through the range of beta-to-alpha-prime transformation. For slow-cooling conditions, more pronounced margin of survival was observed [17].

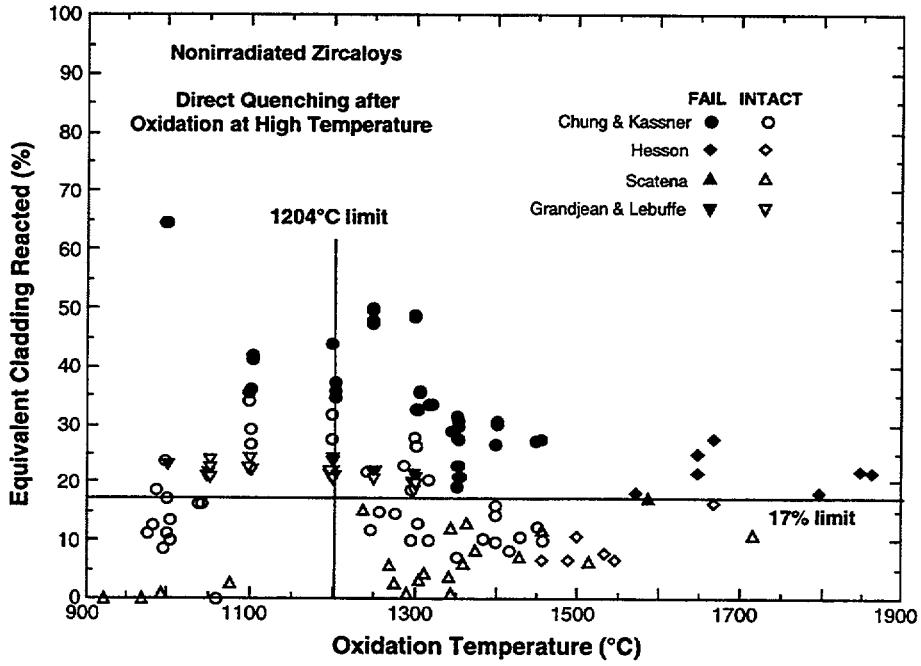

Figure 6. Failure boundary of partially constrained Zircaloy cladding tubes or unconstrained rings after oxidation at high temperature and direct quenching from peak oxidation temperature (from Refs. 17 and 29).

5. 17%-Oxidation Criterion

5.1 Establishment of 17% Criterion During 1973 Rule-Making Hearing

The rationale for establishment of the two criteria in 10 CFR 50.46(b) is described in this section. As indicated in a few reports [17,18] that reviewed the results of the LOCA-related tests performed before and after the 1973 Hearing, the 17%-ECR and 1204°C criteria were primarily based on the results of post-quench ductility tests conducted by Hobson [25,26].

Figure 7 summarizes the results of Hobson's ring compression tests performed at 23-150°C. Zircaloy-4 cladding tubes were oxidized in steam on two sides, followed by direct quenching into water. Then, short ring specimens cut from the oxidized tube were either compressed slowly to a total deflection of 3.8 mm or squashed by impact loading. After the test, the broken pieces of the ring was assembled back to determine the degree of brittleness. Zero ductility was defined on the basis of the macroscopic geometry of the broken pieces and the morphology of the fracture surface on microscopic scale. Each data point in Fig. 7 indicates failure type, test identification number, oxidation time in min., oxidation temperature in °F, and first maximum load in pound.

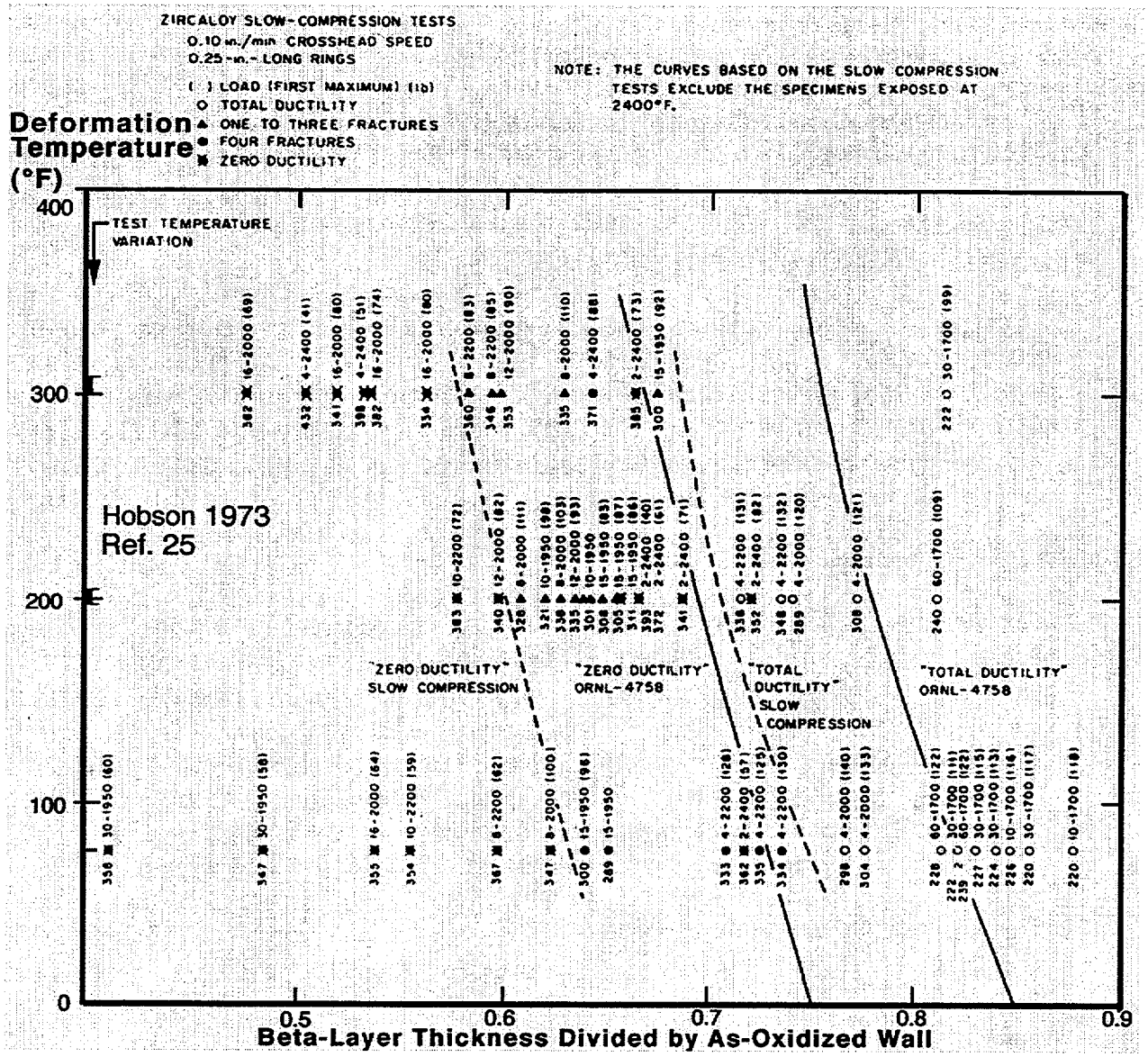

Figure 7.

Ductility of two-side-oxidized Zircaloy rings as function of slow- or fast-compression temperature and fraction of transformed-beta-layer (from Hobson, Ref. 25 and 26).

The dashed line on the left side of Fig. 7 denotes the zero ductility domain for slow-compression rate. This domain is valid only for oxidation temperatures of <2200°F or <1204°C. During the 1973 Hearing, ORNL investigators suggested to consider a zero-ductility temperature (ZDT) no higher than the saturation temperature during reflood, i.e., ≈135°C. Zero-ductility threshold at this temperature is equivalent to a beta-layer fraction of ≈0.58, or a fraction of combined oxide layer plus alpha layer thickness (defined as X_T) of ≈0.42 (based

on as-oxidized cladding wall). The latter fraction corresponds to ≈0.44 if it is calculated based on fresh nonoxidized cladding wall (defined as Wo).

The threshold fractional thickness of the combined oxide and alpha layer (X_T/Wo, defined as Xoa in Fig. 8) of 0.44, which corresponds to zero ductility threshold for slow compression at 135°C, was the key number in the establishment of 17% oxidation criterion in the 1973 Hearing. During the hearing, the AEC Regulatory Staff wrote:

> "Giving due credit to the numerous quench experiments and the ORNL zero ductility experimental data points for both impact and slow compression, the staff suggests that an embrittlement criterion be based on a **calculated X_T/Wo that shall not exceed 0.44. This is equivalent to a zero ductility temperature of about ... 275°F based on the slow compression tests** [20]."

Then, it was concluded:

> "To preclude clad fragmentation and to account for effects noted in the tests described above, **a limit of X_T/Wo ≤ 0.44** was earlier suggested by the Regulatory staff as an embrittlement criterion (Exhibit 1113, page 18-18). This limit was inferred from quench tests and mechanical tests. Criterion (b)(2) is now proposed as a better method of specifying a similar limit on the extent of cladding oxidation. The bases for proposing this method are described below: (The) use (of the **17 percent reaction limit) with the Baker-Just equation** is conservative when compared to the previously suggested limits of **X_T/Wo ≤ 0.44**. This is shown in Figure 8 (of this paper) for isothermal conditions. Four lines of **constant calculated X_T/Wo** (two for 0.44 and two for 0.35) are constructed on the plot of percent reaction versus a parameter proportional to the square root of exposure time. The solid X_T/Wo lines are based on Pawel's equation (Exhibit 1133) (Ref. 27 of this paper), and the dashed lines are based on Exhibit 09, page 9, Figure 5 (Ref. 25 of this paper). As can be seen, **the X_T/Wo = 0.44 lines are both above the 17 percent reaction line..."**

Results of a total of five key tests and calculations are summarized in Fig. 8, a complex but the most important step used to reach the 17% oxidation limit. They are: (1) equivalent cladding reacted (ECR) calculated as function of oxidation temperature and square root of time based on Baker-Just correlation, (2) two broken curves which define the time and temperature to reach the threshold fractional thickness of the combined oxide and alpha layer (denoted as Xoa) of 0.44 and 0.35, as determined based on the data given in Ref. 25, Page 9, Fig.5, (3) two solid curves that define the time and temperature to reach the threshold fractional thickness of the combined oxide and alpha layer of 0.44

and 0.35, as determined based on the method of Ref. 27, (4) six ECR-(time)$^{0.5}$ curves from the thermal-shock tests of Hesson et al., Ref. 14, and (5) results from Combustion Engineering (CE) ring compression tests after one-sided oxidation.

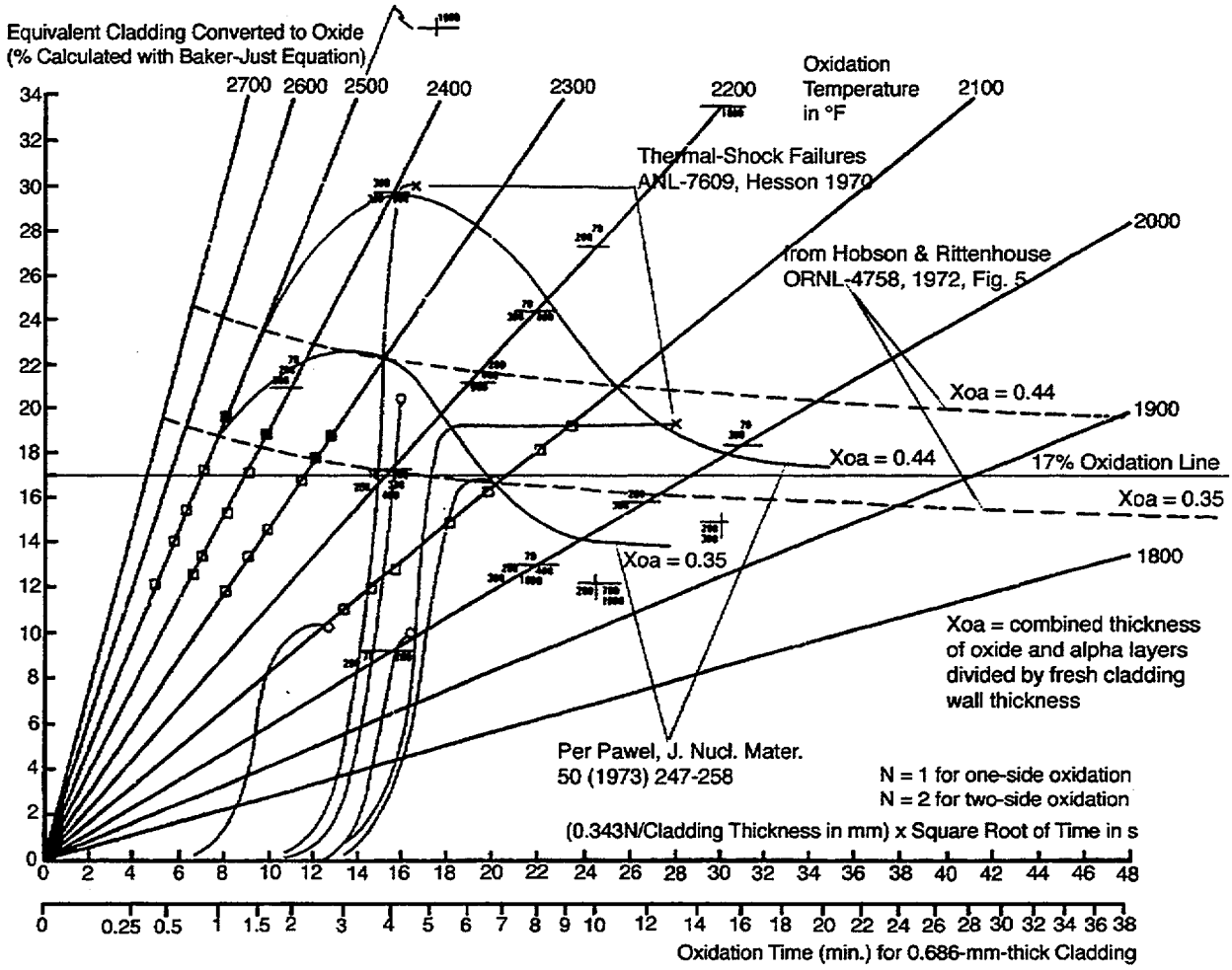

Figure 8.

Summary of multistep procedure used to establish 17% oxidation criterion during 1973 Rule-Making Hearing (from Docket RM-50-1, April 16, 1973). Note equivalent cladding oxidized was calculated per Baker-Just correlation. For comparison, time to reach threshold fraction of combined oxide and alpha layers of 0.44 is shown as determined per Hobson and Rittenhouse (ORNL-4758, January 1972) and Pawel (J. Nucl. Mater. 50, 1973, pp. 247-258).

By definition, **ECR parameter varies depending on cladding wall thickness,** either due to differences in fuel design or due to ballooning and

burst during the heatup phase in a LOCA. Figure 8 shows how to take account of the effects of variations in wall thickness and one- vs. two-sided oxidation.

Two of Hesson's thermal-shock experiments resulted in cladding fragmentation at calculated ECR values of ≈19 and ≈30%, as indicated in the figure. The other four did not fail at ECR values of ≈21, ≈16.5, ≈10, and ≈9.5%. The time-temperature transients in Hesson's tests were integrated also by **using the Baker-Just equation.**

The CE data, discussed in the Hearing, are represented by squares on the oxidation isotherms of 2500, 2400, 2300, and 2100°F. If the sample fractured on compression by CE's load standard, it was considered to have failed and is denoted with a filled square. Open squares denote CE's non-failed specimens. By the CE's load standard, only those samples with calculated ECR values >17% failed.

Based on the results given in Fig. 7 and the five sets of information shown in Fig. 8, one can conclude that **no samples tested by slow compression at >135°C failed with zero ductility if equivalent cladding reacted (ECR), calculated on the basis of Baker-Just correlation, was less than 17%.** Furthermore, all samples oxidized to <17% ECR (again calculated with Baker-Just correlation) survived direct quenching.

In summary, the AEC Commissioners concluded that the very good consistency between the **17% limit, if calculated with the Baker-Just equation,** and a wide variety of experiments supports adoption of this procedure [21], and it was further stated:

> "There is relatively good agreement among the industrial participants as to what the limit on total oxidation should be.... The regulatory staff in their concluding statement compared various measures of oxidation and concluded that a 17 % total oxidation limit is satisfactory, **if calculated by the Baker-Just equation**... As argued by the regulatory staff, it appears that the 17% oxidation limit is within the Rittenhouse criteria. Thus a remarkable uniformity of opinion seems to exist with regard to the 17% oxidation limit [13]."

It is clear that the primary **rationale of the 17% criterion is retention of cladding ductility** at temperatures higher than 275°F (135°C, i.e., the saturation temperature during reflood). Of major importance in this proceeding is that the **threshold ECR value of 17% is tied with the use of Baker-Just correlation.** That is, the 17% ECR criterion is specific to Baker-Just correlation that must be used to determine the degree of total oxidation. If an oxidation correlation other than the Baker-Just equation (e.g., Cathcart-Pawel correlation) were used, the threshold ECR would have been less than 17%.

This means that use of a best-estimate correlation may not necessarily be conservative in evaluating post-quench cladding ductility.

5.2 Other Embrittlement Criteria Proposed after the 1973 Hearing

Few months after the 1973 Hearing, Pawel proposed a new criterion based on <95 % saturation of the average oxygen concentration in the beta phase [27]. However, such a criterion fails to recognize that in addition to a sufficiently low O concentration, a minimum thickness of beta layer is required to ensure adequate resistance to failure. Such criterion is less facilitated to handle, especially during non-isothermal LOCA transients, and it requires a computer code that can accurately calculate O diffusion under moving-phase-boundary conditions, a task more difficult than the calculation of a simple parabolic oxidation correlation. Nevertheless, many of such computer codes have been developed after the 1973 Hearing, e.g., those reported in Refs. 17 and 24.

Sawatzky performed room-temperature tensile tests on specimens exposed to high-temperature spikes in steam [28]. Based on results of microhardness measurement, the distribution of O in the transformed beta (or prior beta) layer was found to be nonuniform, an observation confirmed subsequently by ANL investigators by Auger electron spectroscopy (Fig. 32-43, Ref. 17). In spite of total oxidation of only 16 %, a specimen with average O concentration >0.8 wt% in the prior beta exhibited very low strength and negligible elongation, whereas a specimen with O content <0.6 wt% in the prior beta retained some ductility. Based on this observation, Sawatzky proposed to replace the 1204°C PCT and the 17% ECR criteria by a unified criterion, that is, oxygen concentration in beta layer shall be <0.7 wt% over at least half of the cladding thickness. At temperatures >1280°C, Sawatzky's criterion is virtually identical to Pawel's criterion (see Fig. 9).

Validity of the three criteria illustrated in Fig. 9 is, however, subject to variations in cladding wall thickness, because the time to reach the specified threshold state of material is strongly influenced by the clad wall thickness which may vary with fuel design and the degree of ballooning and burst. Thus, it was deemed desirable to develop a unified embrittlement criterion that would be valid independent of variations in wall thickness and oxidation temperature [17].

5.3 One- vs. Two-Side Oxidation and Thermal-Shock Failure

Grandjean et al. have reported results of extensive thermal-shock tests which were performed in TAGCIS facility [29,30]. Hydrogen uptake in their short ring specimens was not excessive. In their investigation, ECR was calculated with PECLOX oxidation code [31], and failure-survival behavior was determined based on the result of gas-leakage check. The results of the tests were included in Fig. 6. The effect of one- vs, two-side oxidation on thermal-

shock failure was the focus of investigation. As indicated in Fig. 8, such effect was considered negligible in establishing the 17% ECR limit in the 1973 Rule-Making Hearing. Interestingly, Grandjean et al.'s failure threshold for two-side oxidation appears to be slightly higher than the threshold for one-sided oxidation, i.e., ≈21 vs. ≈20% ECR. Nonetheless, this study provides an independent confirmation of the validity of the 17% ECR criterion relative to susceptibility to thermal-shock failure.

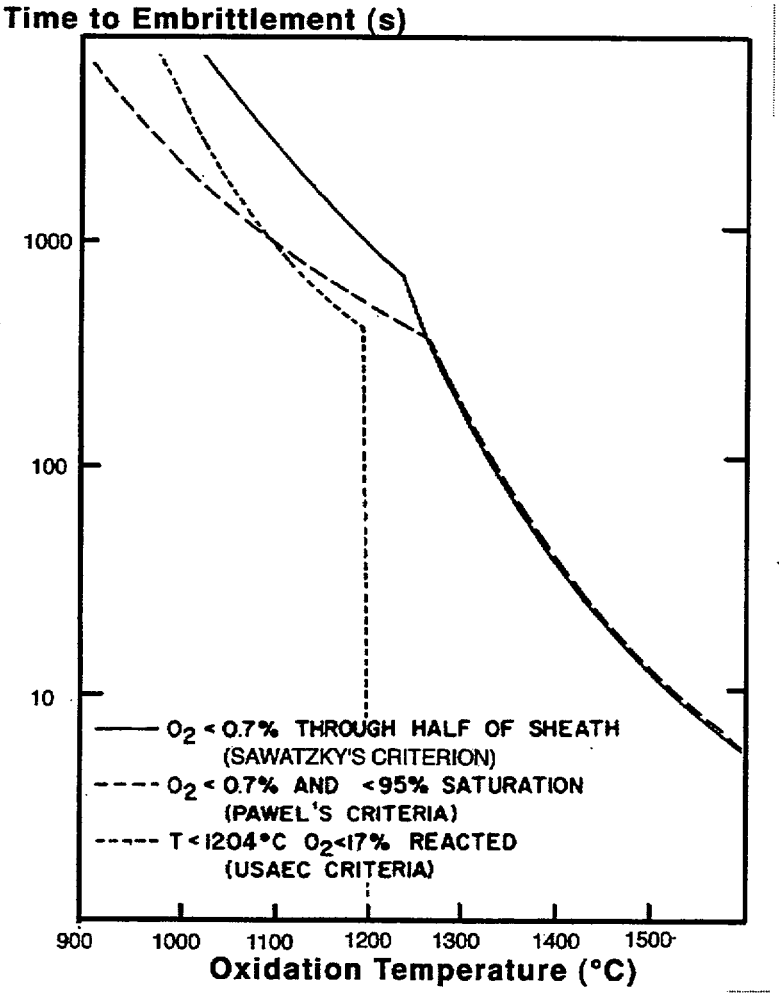

Figure 9.

Comparison of current embrittlement criteria with those proposed by Pawel (Ref. 27) and Sawatzky (Ref. 28).

5.4 17% Oxidation Limit and Impact Failure at Small Hydrogen Uptake

After the 1973 Hearing, ANL investigators conducted impact tests to provide an independent verification of the validity of 17% ECR threshold with respect to cladding resistance to impact failure [17]. Impact tests were performed at room temperature on non-pressurized open-ended Zircaloy-4 tubes that were oxidized on two sides in steam at 1100-1400°C and cooled through the beta-to-alpha-prime transformation range at 5 or ≈100°C/s. Because the sample was oxidized on both OD and ID sides, hydrogen uptake was limited to <130 wppm. Therefore, microstructure and oxygen and hydrogen distributions in the specimens were similar to those of the ring-

compression specimens of Hobson [25,26] that were cooled fast through the beta-to-alpha-prime transformation range.

It was found that slow-cooled specimens were more resistant to impact failure than fast-cooled specimens (Fig. 65, Ref. 17]. Results obtained for slow-cooled specimens are summarized in Fig. 10. The ECR values in Fig. 10 were directly determined based on measured phase layer thickness, therefore, are considered more accurate than values calculated based on Baker-Just correlation. The results in Fig. 10 show that for cladding oxidized at <1315°C to <17% ECR, a sufficient level of resistance to impact failure is retained at 23°C, i.e., failure impact energy of >0.8 J.

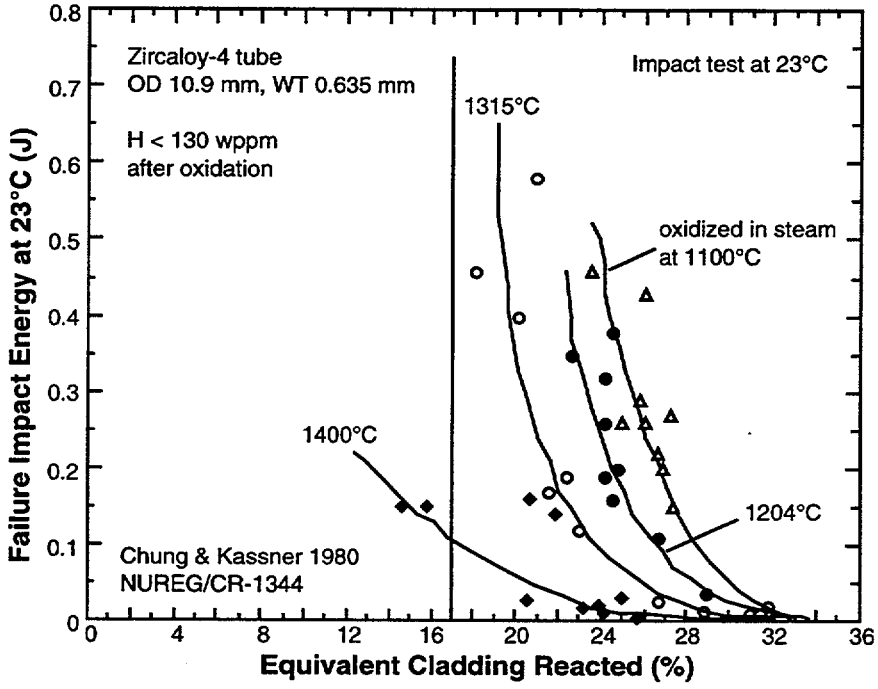

Figure 10.

Failure impact energy vs. equivalent cladding reacted, from tests at 23°C on undeformed Zircaloy-4 tube oxidized on two-sides and cooled at 5°C/s (Ref. 17).

5.5 17% Limit and Ring-Compression Ductility at Small Hydrogen Uptake

As shown in Fig. 8, the 17% threshold ECR was derived by indirect multistep procedure. Of particular importance in this procedure is the accuracy of two key factors, i.e., (1) temperature measurement in the experiments of Baker-Just and Hobson-Rittenhouse [25,26] and (2) definition of nil-ductility as given in Fig. 7. In consideration of this, ANL investigators performed independent compression tests at room temperature on short Zircaloy-4 ring specimens. Rings were sectioned from long tubes that were oxidized in steam at 1100-1400°C and cooled through the beta-to-alpha-prime transformation range at 5 or ≈100°C/s. Hydrogen uptake in the ring specimens was <130 wppm. This procedure reproduced the conditions of the ring-compression tests of Hobson. In the ANL compression tests, however, load-

deflection curves were obtained to better quantify the degree of remaining ductility and the magnitude of load that a ring can sustain.

It was found that slow-cooled specimens retained more ductility than fast-cooled specimens under otherwise identical conditions (Fig. 67, Ref. 17]. Figure 11 summarizes results obtained for a slow-cooling rate of ≈5°C/s, a rate probably more prototypic of a LOCA than fast cooling. The ECR values in the figure were determined based on measured phase layer thickness and time-temperature history. This result shows that for cladding oxidized at <1315°C to <17% ECR, ductility is retained at 23°C (i.e., relative diametral deflection >16%); no brittle failure was observed. This experiment provides an independent confirmation of the validity of the 17% oxidation limit for undeformed Zircaloy specimens that contain hydrogen <130 wppm.

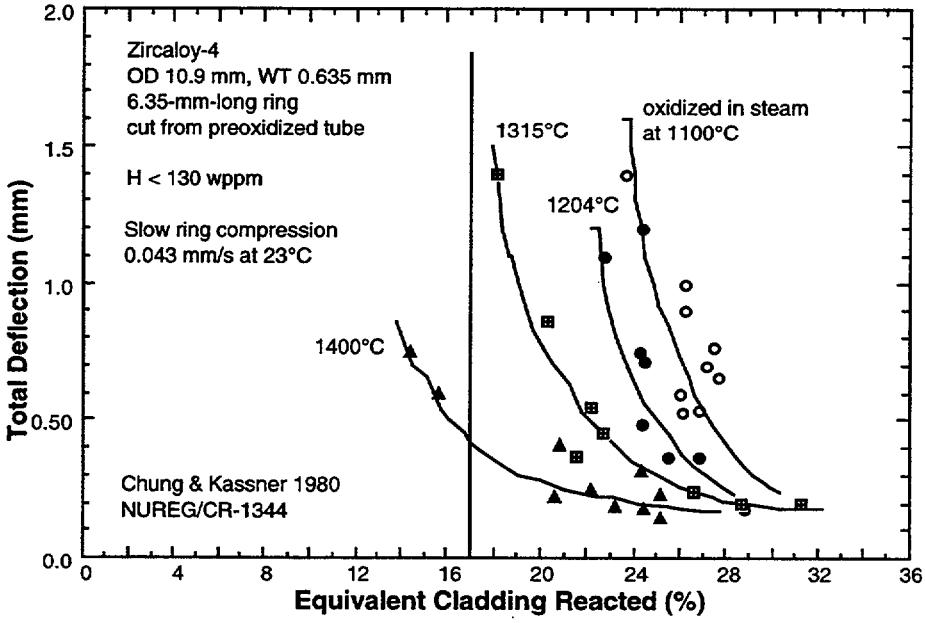

Figure 11.

Total deflection at 23°C vs. equivalent cladding reacted, from ring-compression tests on Zircaloy-4 oxidized on two-sides and cooled at 5°C/s (Ref. 17).

5.6 Resistance to Impact Failure at Large Hydrogen Uptake

In addition to the impact tests on non-ruptured empty tubes, ANL investigators performed 0.15- and 0.3-J pendulum impact tests at 23°C on pressurized Zircaloy-4 tubes that were burst, oxidized, cooled at ≈5°C/s, and survived quenching thermal shock [17]. The CSNI experts [18] considered that: "Ambient impact of 0.3 J were thought to be a reasonable approximation to post LOCA quench ambient impact loads." The results of the 0.3-J impact tests, summarized in Fig. 12, indicate that the 17%-ECR limit is adequate to prevent a burst-and-oxidized cladding from failure under 0.3-J impact at 23°C, as long as peak cladding temperature remained ≤1204°C. The ECR values in the figure were determined based on measured thickness of oxide, alpha, and beta phase

layers, rather than calculated based on Baker-Just correlation, and hence, are considered more accurate.

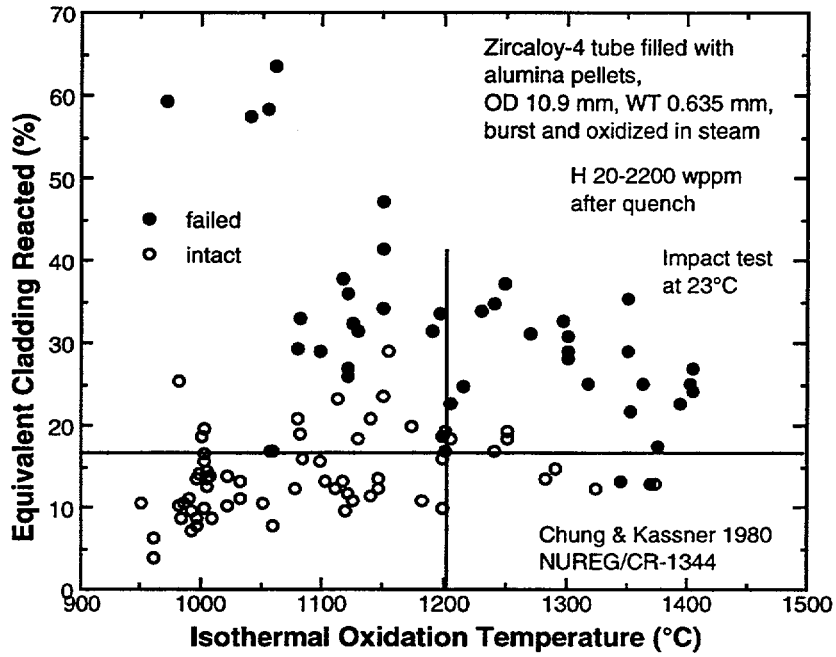

Figure 12.

Impact failure threshold as function of equivalent cladding reacted and oxidation temperature of burst, oxidized, slow-cooled, and quenched Zircaloy-4 tube containing 20-2200 wppm hydrogen (from Ref. 17).

In contrast to two-side-oxidized non-pressurized non-ruptured tubes in which hydrogen uptake was small (<130 wppm), burst Zircaloy-4 tubes exhibited peculiar oxidation behavior near the burst opening. The inner-diameter (ID) surfaces of the top and bottom "necks," ≈30-mm away from the burst center, were exposed to hydrogen-rich stagnant steam-hydrogen mixture which is produced because of poor mixing of steam and hydrogen at the narrow gap between the alumina pellets and the ID surface of the necks. As a consequence, thick breakaway oxides formed at 900-1120°C [17], and hydrogen uptake as high as ≈2200 wppm was observed at the "necked" regions. Subsequently, JAERI investigators confirmed occurrence of the same phenomenon [32,33].

The results from the same tests shown in Fig. 12 were converted to failure-survival map based on average hydrogen content of the impact-loaded local region and the thickness of transformed-beta layer containing <0.7 wt.% oxygen. This failure-survival map is shown in Fig. 13. . On the basis of the figure, ANL investigators proposed to replace the 1204°C PCT and 17% ECR criteria by a unified criterion which specifies that the thickness of transformed-beta layer containing <0.7 wt.% oxygen shall be >0.3 mm [17]. The criterion implicitly incorporates a limit in peak cladding temperature. This limiting temperature corresponds to the temperature at which oxygen solubility is 0.7 wt.% in Zircaloy that contains 700-1200 wppm hydrogen. This temperature is believed to be between 1200 and 1250°C, although the exact data from

applicable Zircaloy-O-H ternary diagrams are not. This criterion is not subject to variations in cladding wall thickness and oxidation temperature.

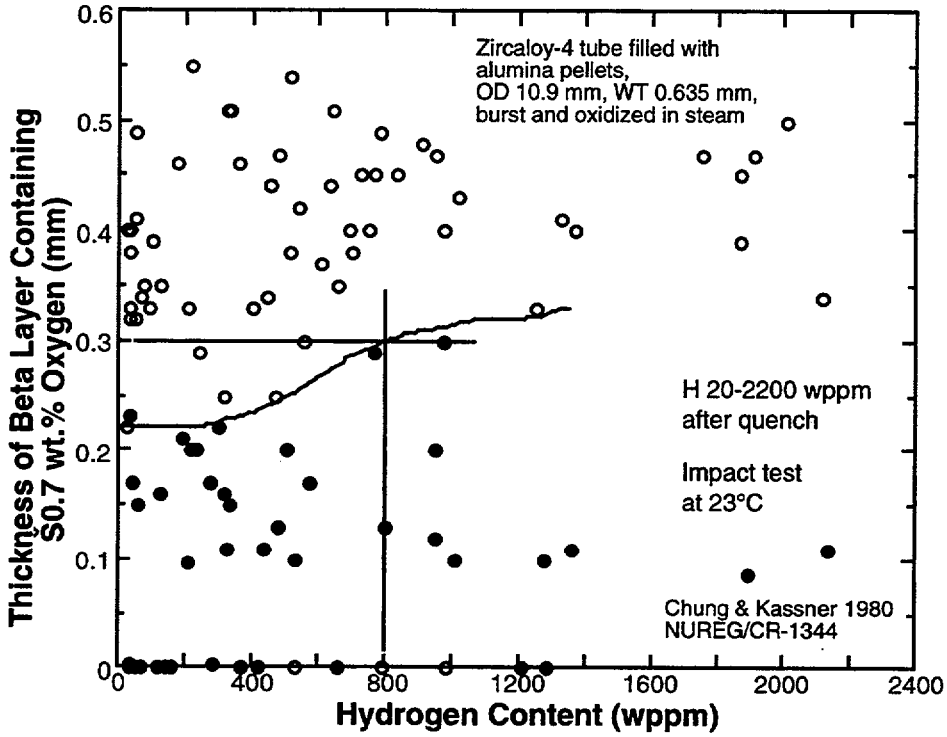

Figure 13.

Impact failure map as function of hydrogen content and thickness of beta layer containing ≤0.7 wt.% oxygen; Zircaloy-4 tube burst, oxidized, slow-cooled, and quenched (from Ref. 17).

The results in Fig. 13 show that for a given thickness and a given oxygen content in transformed-beta layer, resistance of cladding to impact failure is significantly reduced if hydrogen uptake exceeds ≈700 wppm. Such situation does not occur in non-pressurized, non-ruptured, two-side-oxidized Zircaloy cladding, such as those tested by Hobson [26] or discussed in Figs. 10 or 11.

5.7 Ring-Compression Ductility at Large Hydrogen Uptake

Investigators in ANL [17] and JAERI [32,33] conducted extensive tests on tube or ring specimens of Zircaloy-4 that contained high concentrations of hydrogen. In the former investigation, Zircaloy-4 tubes filled with alumina "pellets" were pressurized, heated, burst, oxidized, slow-cooled, and quenched with bottom-flooding water. Then, the tubes that survived the quenching thermal shock were compressed diametrically at 23°C [17]. Such specimens contained H up to ≈2200 wppm. In the latter investigation, short rings, sectioned from tubes that were exposed to similar conditions, were compressed at 100°C. The ring specimens contained H up to ≈1800 wppm. Typical distributions of oxide layer thickness, hydrogen concentration, and ring deflection to failure are shown in Fig. 14. The top and bottom "necks" that contained the highest concentration of hydrogen and the thinnest transformed-beta layer exhibited the lowest ductility.

However, ANL investigators observed that the rate of hydrogen generation, amount of hydrogen uptake, and hence, the degree of embrittlement of the necked regions are strongly influenced by the method of heating cladding tubes during LOCA-like transients, i.e., more uniform (indirect heating in JAERI) vs. less uniform (direct heating in ANL) heating [17]. This is schematically illustrated in Fig. 15.

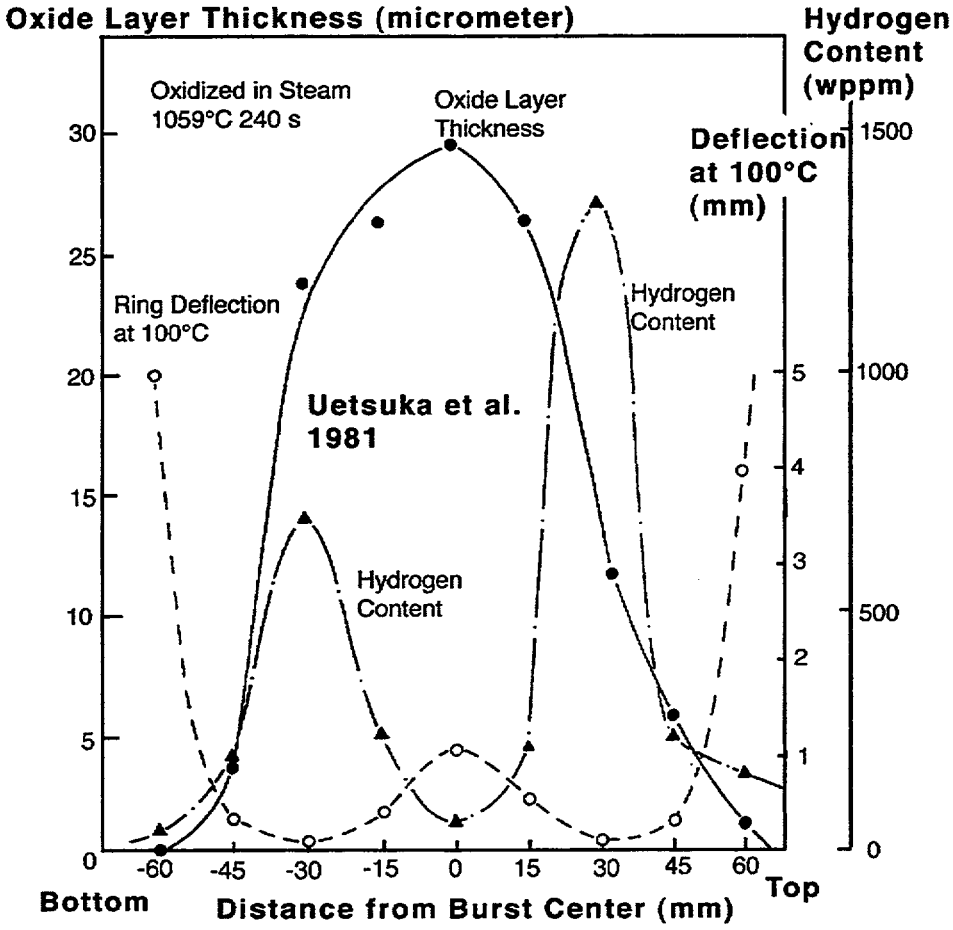

Figure 14.

Distributions of hydrogen content, inner-diameter oxide layer thickness, and total deflection at 100°C of ring specimens sectioned from burst region (from Uetsuka et al., Refs. 32 and 33).

The effect of hydrogen uptake on post-quench ductility, determined either from diametral-compression test of burst-and-oxidized tubes at 23°C [17] or compression at 100°C of ring specimens sectioned from burst-and-oxidized tubes [32,33], is summarized in Fig. 16. At hydrogen uptake >700 wppm, significant embrittlement of cladding is evident, even if total oxidation is <17% (see Fig. 14). Similar dependencies of plastic deflection on beta-layer oxygen content and total hydrogen content have been also reported in Fig. 88, Ref. 17 and Fig. 89, Ref. 17, respectively. These results show that post-quench ductility of Zircaloy is strongly influenced by not only oxidation but also

hydrogen uptake. This is shown in Fig. 17. Apparently, the important effect of hydrogen uptake on post-quench ductility was not well realized at the time of 1973 Hearing.

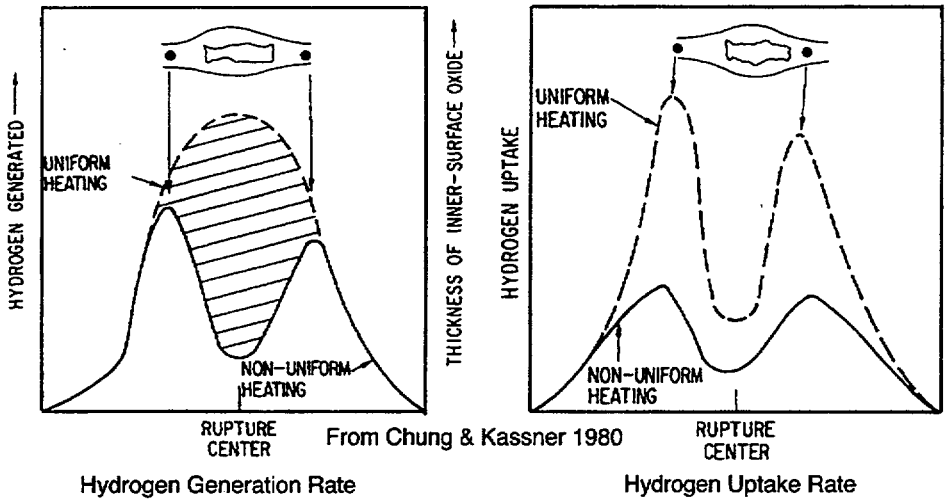

Figure 15.

Effect of heating method (uniform vs. nonuniform heating) on hydrogen generation and uptake near burst opening (from Ref. 17)

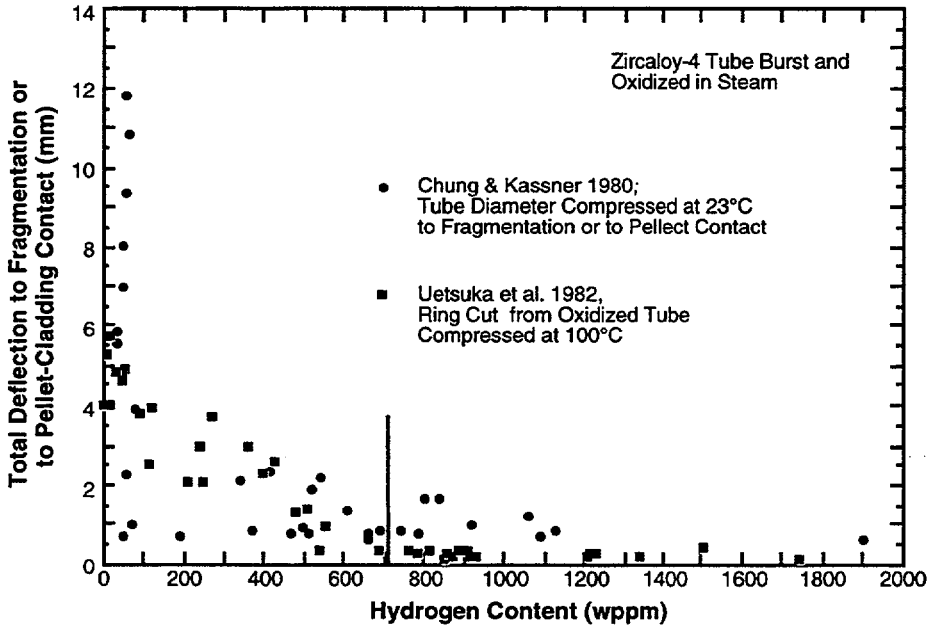

Figure 16.

Effect of hydrogen uptake on diametral deflection of burst, oxidized, and quenched Zircaloy-4 tube or sectioned ring.

Essentially similar observation has also been reported by Komatsu et al. [34,35]. They reported that the load to initial ring cracking is strongly influenced by total oxidation and hydrogen uptake. For oxidation temperatures >1260°C in which the oxygen content in the beta layer exceeds ≈0.7 wt.% in short period of time, the embrittling effect of oxygen appears to be predominant (see Fig. 18). The "zero-ductility" region denoted in Fig. 18 appears to have

been determined based on a threshold load to initial cracking rather than based on ductility consideration. As such, this "zero-ductility" threshold differs significantly from that defined by Hobson [25,26].

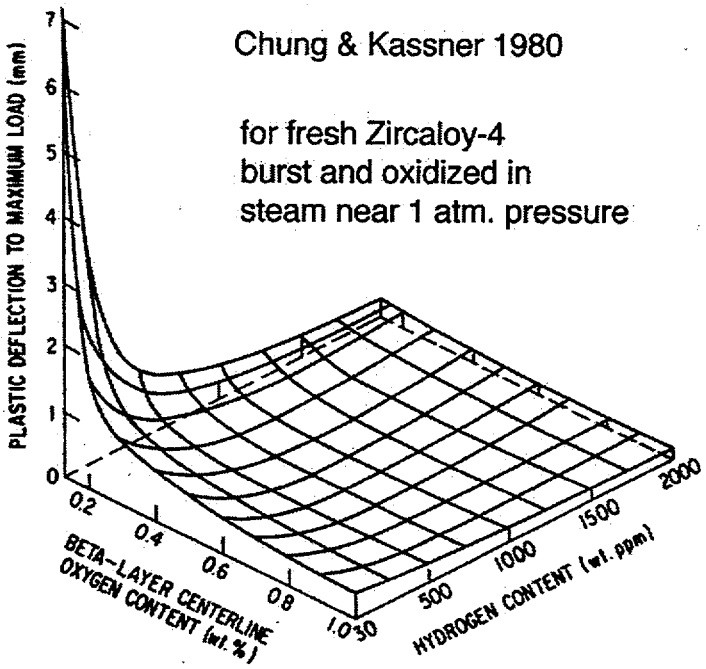

Figure 17.

Post-quench ductility shown as function of oxidation (beta-layer centerline oxygen content) and total hydrogen content, from diametral compression test at 23°C on burst, oxidized, slow-cooled, and quenched Zircaloy-4 tubes (for database see Ref. 17).

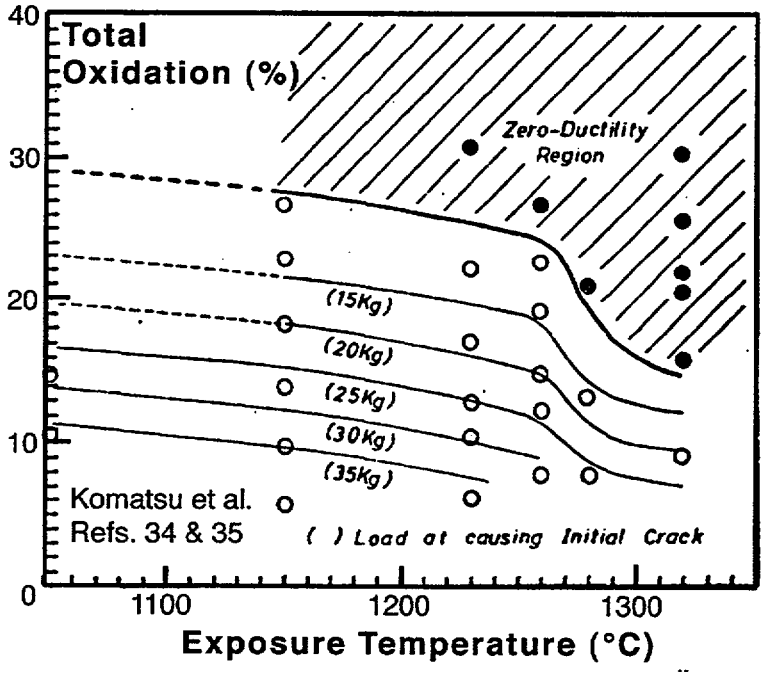

Figure 18.

Applied load at initial cracking of ring as function of total oxidation and exposure temperature, from Komatsu et al., Refs. 34 and 35.

5.8 17% Oxidation Criterion - Summary

It is clear that the primary rationale of the 17% ECR criterion is retention of cladding ductility at temperatures higher than 275°F (135°C), i.e., the

saturation temperature during reflood. The threshold ECR value of 17% is tied with the use of Baker-Just correlation. If a best-estimate correlation other than Baker-Just equation (e.g., Cathcart-Pawel correlation) were used, the threshold ECR would have been <17%.

Investigations conducted after the 1973 Rule-Making Hearing showed that for oxidation temperatures ≤1204°C, the 17% oxidation limit (as calculated with Baker-Just correlation) is adequate to ensure survival of fully constrained or unconstrained cladding under quenching thermal shock. It was also shown that the 17% limit (ECR determined on the basis of measured phase layer thickness) is adequate to ensure retention of ductility and resistance to 0.3-J impact failure in non-irradiated, non-ruptured, two-side-oxidized Zircaloy cladding in which hydrogen uptake during a LOCA-like transient is small.

However, the 17% limit appears to be inadequate to ensure post-quench ductility for hydrogen uptake >700 wppm. Such level of large hydrogen uptake could occur in some types of fuel rods during normal operation, especially at high burnup, or during a LOCA-like transient in localized regions in a ballooned and ruptured node.

6. 1204°C (2200°F) Peak Cladding Temperature Criterion

6.1 Selection of 1204°C Criterion in 1973 Hearing

From the results of posttest metallographic analysis of the slow-ring-compression specimens, Hobson [26] observed a good correlation between zero ductility temperature (ZDT) and fractional thickness of transformed-beta layer (or the sum of oxide plus alpha layer thickness) as long as the specimen was oxidized at ≤2200°F (1204°C) (see Fig. 7). However, in spite of comparable thickness of transformed beta layer, specimens oxidized at 2400°F (1315°C) were far more brittle. This observation was explained on the basis of excessive solid-solution hardening of transformed-beta phase at high oxygen concentrations. For mechanical properties near room temperature the critical concentration of oxygen in the transformed-beta was estimated to be ≈0.7 wt%. Above this concentration, transformed beta phase becomes brittle near room temperature. Because of the solubility limit of oxygen in the beta phase, this high O concentration cannot be reached at 2200°F (1204°C) but can be reached at 2400°F (1315°C). Hobson concluded that: "embrittlement is not simply a function of the extent of oxidation alone, but is related in yet another way to the exposure temperature."

During the 1973 Rule-Making Hearing, AEC Staff endorsed Hobson's conclusion and wrote: "The staff recognizes the importance of oxygen concentration in the beta phase in determining the load bearing ability of Zircaloy cladding, and the implication from the recent compression tests that this may not be satisfactorily characterized above 2200°F by a ZDT as a

function of remaining beta fraction only. We therefore believe that **peak cladding temperatures should be limited to 2200°F** [20]."

Subsequently, it was also concluded that:

"Additional metallurgical and slow compression mechanical tests on other quenched samples from the ORNL experiments indicated that an important consideration was the amount and distribution of oxygen in the nominally ductile prior-beta phase. However, these factors could not be correlated as functions of time and temperature in the same manner as the (combined oxide and alpha layer) penetration. In particular, the slow compression tests indicated a greater degradation in cladding ductility at higher temperatures than would be expected from considerations of (combined oxide and alpha layer) penetration alone. It was on this basis that **the staff previously suggested a 2200°F maximum cladding temperature**... What was observed in the slow compression tests was that 6 samples exposed at 2400°F for only two minutes and with relatively high values of Fw (Fw being fractional thickness of prior beta, all greater than 0.65) all fractured with nil ductility... Only when brittle failure was detected at high Fw in the slow compression tests did the suspicion arise that ductility was a function of both Fw and the exposure temperature... As the temperature rises above 2200-2300°F, solid solution hardening in the beta phase appears to contribute significantly to formation of a brittle structure. That is, brittle failure occurs even though alpha incursions are not observed, and the fraction of remaining beta is greater than that observed in lower temperature tests. This is confirmed by examination of the six samples from the ORNL exposed at 2400°F for two minutes (Exhibit 1126)... From the foregoing, there is ample evidence that load bearing ability and ductility decrease with increasing exposure temperatures, even for transients with comparable Fw. Increased solubility of oxygen in the prior-beta phase has been discussed as a contributing factor... The staff believes that because of high temperature degradation ... phenomena (... strongly suggested by the experimental evidence cited), **the suggested 2200°F limit should be imposed** [21]."

Then it was added:

"The situation is complicated by the fact that not all of the prior beta phase is equally strong or ductile, since these properties depend on the amount of dissolved oxygen. This fact has been suspected for some time... From the phase diagram, given by both Scatena and Westinghouse, it is obvious that it is possible for the beta phase zirconium to take on a higher oxygen content at 2600°F than at 2000°F. Furthermore, since the diffusion rate depends exponentially upon temperature, one might expect a greater incursion of oxygen into the beta phase for a given thickness of oxide and stabilized alpha phase at higher temperatures... Others (than Hobson) have also observed that the resistance to rupture depends upon the temperature at which oxidation occurs

as well as the extent of oxidation... To recapitulate, measures of Zircaloy oxidation, whether by percent, X_T, or F_W, are largely or wholly determined from the brittle layers of zirconium oxide or stabilized alpha phase, while the ductility and strength of oxidized zirconium depend upon the condition and the thickness of the prior beta phase... Thus a criterion based **solely on the extent of total oxidation is not enough, and some additional criterion is needed** to assure that the prior beta phase is not too brittle. The specification of a maximum temperature of 2200°F will accomplish this **adequately. The data cited in exhibit 1113 would not support a choice of a less conservative limit** [13]."

Few months after the Hearing, Pawel [27] explained Hobson's observation based on data that indicate oxygen solubility in the beta Zr at 2200-2400°F (1204-1316°C) is ≈0.7 wt.%. The O solubility in beta Zircaloy is significantly influenced by not only temperature but also the concentration of hydrogen, a strong beta stabilizer. Nevertheless, Pawel endorsed that: "...the above reasoning easily explains why the mechanical or load bearing properties of the oxidized specimens should not be a unique function of the extent of (total) oxidation." Consequently, Pawel proposed to replace the peak cladding temperature (PCT) criterion by a new criterion that specifies the average oxygen concentration in the beta phase shall be less than 0.7 wt% [see Fig. 9].

6.2 1204°C Limit vs. In-Pile Test Results

In 1970s, high-temperature oxidation and embrittlement behaviors were investigated extensively in TREAT and PBF test reactors. During the TREAT-FRF2 test, a seven-rod cluster was oxidized at 2400°F (≈1315°C) [36]. According to hardness measurements, all rods contained portions that possessed no ductility at room temperature. Three rods were broken accidentally during handling in ORNL hot cell, which indicates the degree of brittleness of a badly embrittled rod and the magnitude of a typical load during handling in hot cell (see Fig. 19).

Some fuel rods tested in the Power Burst Facility (PBF) were also known to have failed during handling or posttest examination in hot cell. This information is summarized in Fig. 20 [37]. Total oxidation of several failed rods were <17 %. Of particular interest is Rod IE-019 of Test IE 5, because ballooning and burst occurred in the rod before exposure to temperatures >1100°C. In spite of the fact that ECR was only ≈12%, the rod broke into pieces after exposure to an "equivalent" oxidation temperature of ≈1262°C. Most likely, actual peak temperature was higher than this equivalent temperature. Rod A-0021 also ruptured before entering high temperature transient; this caused ingress of steam to the rod interior. The rod failed after exposure to ≈1307°C, although ECR was only ≈6%. Hydrogen uptake in the two rods was excessive because of exposure to stagnant steam near the rupture opening.

Figure 19.

Fuel pellet released through fragmented cladding section of Rod 11, TREAT-FRF 2 Test (from Ref. 37).

It is not clear if the failure behavior of Rods IE-019 and A-0021 is predicted based on Pawel's criterion (Fig. 9). However, because the exposure temperatures of the rods exceeded ≈1262°C, the thickness of beta layer that contained ≤0.7 wt.% oxygen should have been zero or close to zero. However, because oxygen solubility in beta is influenced by hydrogen and because accurate peak temperatures reached in the rods are not well known, it is difficult to calculate accurately the thickness of beta layer that contains O ≤0.7 wt.%. Therefore, it is not clear if the failure behavior of the two rods is consistent with the criterion shown in Fig. 13.

As long as clad oxidation temperature was limited to ≤1204°C, a handling failure at measured ECR <17% was not observed from the TREAT and PBF tests or the ANL 0.3-J impact tests (see Fig. 20). This observation clearly demonstrates the importance of the 1204°C PCT limit. That is, the 1204°C PCT and the 17% ECR limits are inseparable, and as such, constitute an integral criterion.

6.3 Summary of 1204°C Criterion

The 2200°F (1204°C) peak cladding temperature (PCT) criterion was selected on the basis of Hobson's slow-ring-compression tests that were performed at 25-150°C. Samples oxidized at 2400°F (1315°C) were far more brittle than samples oxidized at <2200°F (<1204°C) in spite of comparable level of total oxidation. This is because oxygen solid-solution hardening of the prior-beta phase is excessive at oxygen concentrations >0.7 wt%.

The selection of the 1204°C criterion was subsequently justified by the observations from the ANL 0.3-J impact tests and the handling failure of rods

tested in the Power Burst Facility. These results also take into account of the effect of large hydrogen uptake that occurred near the burst opening. Consideration of potential for runaway oxidation alone would have lead to a PCT limit somewhat higher than 2200°F (1204°C). In conjunction with the 17% oxidation criterion, the primary objective of the PCT criterion is to ensure adequate margin of protection against post-quench failure that may occur under hydraulic, impact, handling, and seismic loading.

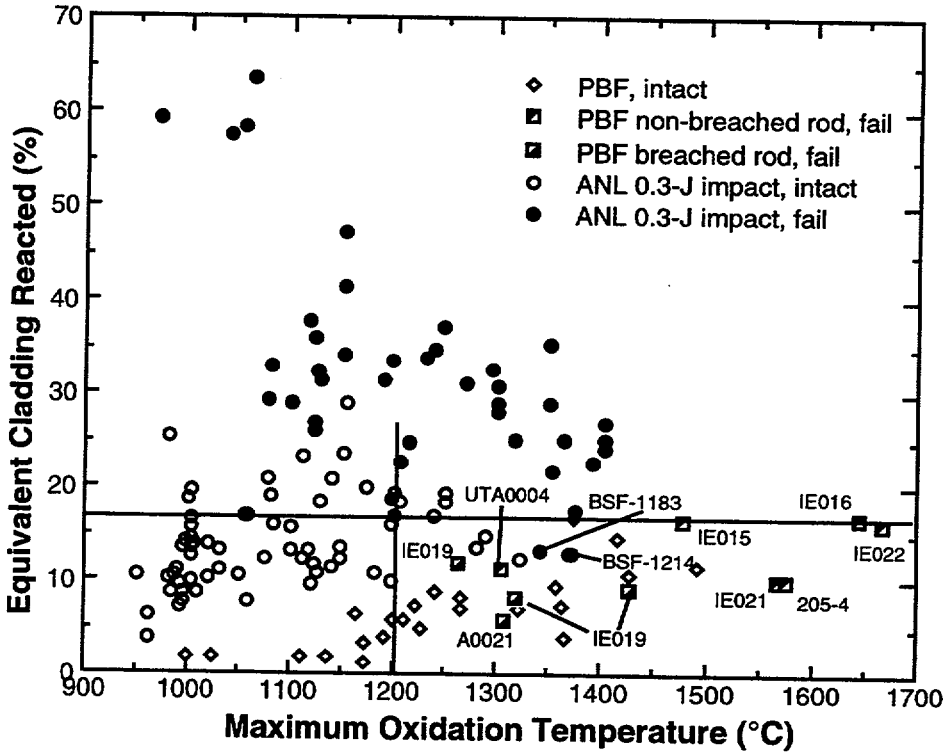

Figure 20.

Comparison of data from hot-cell handling failure of Zircaloy rods exposed to high temperature in Power Burst Facility (Ref. 37) and 0.3-J impact tests in ANL (Ref. 17).

7. Conclusions

1. In the 1973 Rule-Making Hearing, the U. S. Atomic Energy Commission (AEC) staff and commissioners were clearly reluctant to neglect the effect of mechanical constraints on the susceptibility of oxidized fuel cladding to thermal-shock fragmentation. Subsequent test results appear to justify this rationale. Results from unconstrained or partially constrained quench tests were considered only corroborative; their use for regulatory purposes was not accepted.

2. The AEC staff and commissioners and OECD-CSNI specialists were of the opinion that retention of ductility was the best guarantee against potential fragmentation of fuel cladding under various types of not-so-well-quantified loading, such as thermal shock, hydraulic, and seismic forces, and the forces related with handling and transportation.

3. Primary rationale of the 17% oxidation criterion was retention of cladding ductility at temperatures higher than 275°F (135°C), i.e., the saturation temperature during reflood. The threshold equivalent cladding reacted (ECR) of 17% is tied with the use of Baker-Just correlation. If a best-estimate correlation other than Baker-Just equation (e.g., Cathcart-Pawel correlation) had been used, the threshold ECR would have been <17%.

4. Investigations conducted after the 1973 Rule-Making Hearing show that for oxidation temperatures ≤1204°C, the 17% oxidation limit (calculated with Baker-Just correlation) is adequate to ensure survival of unconstrained or fully constrained cladding under quenching thermal shock. It was also shown that the 17% limit (ECR determined on the basis of measured phase layer thickness) is adequate to ensure retention of ductility and resistance to 0.3-J impact failure in non-irradiated non-ruptured two-side-oxidized Zircaloy cladding in which hydrogen uptake during a LOCA-like transient is small.

5. However, the 17% ECR limit appears to be inadequate to ensure post-quench ductility at hydrogen concentrations >700 wppm. A major finding from tests performed after the 1973 Rule-Making Hearing shows that post-quench ductility is strongly influenced by not only oxidation but also hydrogen uptake. It seems that this effect of large hydrogen uptake was not known at the time of 1973 Hearing.

6. By definition, an embrittlement criterion expressed in terms of ECR is subject to uncertainties because calculated ECR varies with variations in cladding wall thickness and the degree of ballooning.

7. The 1204°C peak cladding temperature (PCT) limit was selected on the basis of slow-ring-compression tests that were performed at 25-150°C. Samples oxidized at 1315°C were far more brittle than samples oxidized at 1204°C in spite of comparable level of total oxidation. This is because oxygen solid-solution hardening of the prior-beta phase is excessive at oxygen concentrations >0.7wt%. Consideration of potential for runaway oxidation was a secondary factor in selecting the 1204°C limit. The 1204°C limit was subsequently justified by the observations from impact tests and handling failure of fuel rods exposed to high temperatures in the Power Burst Facility. The 1204°C PCT and the 17% ECR limits are inseparable, and as such, constitute an integral criterion.

8. The degree of oxygen saturation and the thickness of beta layer that contains oxygen concentrations ≤0.7 wt.% were important parameters used by investigators to develop new embrittlement criteria based on beta phase thickness rather than total oxidation. Such a criterion is not subject to inherent uncertainties associated with variations in cladding wall thickness and pre-LOCA oxidation.

9. Post-quench ductility and toughness are determined primarily by the thickness and the mechanical properties of transformed-beta layer. The mechanical properties are strongly influenced by several factors such as: oxygen solubility in beta, concentrations of alpha- (tin and oxygen) and beta-stabilizing elements (niobium and hydrogen), the nature of beta-to-alpha-prime transformation, redistribution of oxygen, niobium, and hydrogen during the transformation, and precipitation of hydrides. Significantly large hydrogen uptake can occur in some types of fuel cladding, during normal operation to high burnup, during breakaway oxidation at <1120°C, and, for localized regions near a rupture opening, during LOCA transients. Hydrogen uptake and its effect on the properties of transformed beta could differ significantly in Zircaloys and in niobium-containing alloys. Considering these factors, it is recommended to obtain a better understanding of the effects of more realistic hydrogen uptake and niobium addition on the properties of transformed-beta layer and post-quench ductility.

Acknowledgments

The authors would like to express thanks to C. Grandjean, R. O. Meyer, and S. Basu for helpful discussions.

References

1. Grandjean, C. et al., "Oxidation and quenching experiments with high burnup cladding under LOCA conditions," Proc. 26th Water Reactor Safety Information Meeting, Bethesda, USA, 26-28 October, 1998.
2. Mardon, J.P. et al., "The M5 fuel rod cladding," Proc. ENS TOP'FUEL 99, Avignon, France, 13-15 September, 1999.
3. Nagase, F. et al., "Experiments on high burnup fuel behavior under LOCA conditions at JAERI," Proc. ANS Topical Meeting on LWR fuel Performance, Park City, USA, 10-13 April, 2000.
4. Ozawa, M. et al., "Behavior of irradiated zircaloy4 fuel cladding under simulated LOCA conditions," Proc. 12th Symp. on Zirconium in the Nuclear Industry, Toronto, Canada, 15-18 June, 1998.
5. Aomi, M. et al., "Behavior of irradiated BWR fuel cladding tubes under simulated LOCA conditions," Proc. ANS Topical Meeting on LWR fuel Performance, Park City, USA, 10-13 April, 2000.
6. Chung, H.M. et al., "Test plan for high-burnup fuel cladding behavior under loss-of-coolant accident conditions," Proc. 24th Water Reactor Safety Information Meeting, Bethesda, USA, 21-23 October, 1996.
7. Report of Advisory Task Force on Power Reactor Emergency Cooling, TID-24226, 1967.

8. General Design Criteria for Nuclear Power Plants, U.S. Code of Federal Regulations, Title 10, Part 50, Appendix A, 20 February, 1971, amended.

9. Interim Acceptance Criteria for Emergency Core-Cooling Systems for Light-Water Power Reactors, U.S. Federal Register 36 (125), pp. 12247-12250, 29 June, 1971.

10. Cottrell, W.B., "ECCS rule-making hearing," Nucl. Safety 15 (1974) 30-55.

11. New acceptance criteria for emergency core-cooling systems of light-water-cooled nuclear power reactors, Nucl. Safety 15 (1974) 173-184.

12. Acceptance Criteria for Emergency Core Cooling Systems for Light-Water Nuclear Power Reactors, U.S. Code of Federal Regulations, Title 10, Part 50, Section 46, 4 January, 1974, Amended.

13 Atomic Energy Commission Rule-Making Hearing, Opinion of the Commission, Docket RM-50-1, 28 December, 1973.

14. Hesson, J.C. et al., Laboratory Simulations of Cladding-Steam Reactions Following Loss-of-Coolant Accidents in Water-Cooled Power Reactors, ANL-7609, January 1970.

15. Parker, G.W. et al., "Release of fission products from reactor fuels during transient accidents simulated in TREAT," Proc. Intl. Symp. Fission Product Release and Transport under Accident Conditions, Oak Ridge, USA, 5-7 April, 1965.

16. Fujishiro, T. et al., "Light water reactor fuel response during reactivity initiated accident experiments," NUREG/CR-0269, August 1978.

17. Chung, H.M. and Kassner, T.F., Embrittlement Criteria for Zircaloy Fuel Cladding Applicable to Accident Situations in Light-Water Reactors, NUREG/CR-1344, January 1980.

18. Parsons, P.D. et al., The Deformation, Oxidation and Embrittlement of PWR Fuel Cladding in a Loss-of-Coolant Accident: A State-of-the-Art Report, CSNI Report 129, December 1986.

19. Zuzek, E. et al., "The H-Zr (hydrogen-zirconium) system," Bulletin of Alloy Phase Diagrams, 11 (1990) 385-395.

20. Atomic Energy Commission Rule-Making Hearing, Supplemental Testimony of the Regulatory Staff Docket RM-50-1, 26 October, 1972.

21. Atomic Energy Commission Rule-Making Hearing, Concluding Statement of the Regulatory Staff, Docket RM-50-1, 16 April, 1973.

22. Uetsuka, H. et al., "Failure-bearing capability of oxidized Zircaloy-4 cladding under simulated loss-of-coolant condition," J. Nucl. Sci. Tech. 20 (1983) 941-950.

23. Reocreux, M. and Scott de Martinville, E., "A study of fuel behavior in PWR design basis accident: An analysis of results from the PHEBUS and EDGAR experiments," Nucl. Eng. Design 124 (1990) 363-378.

24. Suzuki, M. and Kawasaki, S., "Development of computer code PRECIP-II for calculation of Zr-steam reaction," J. Nucl. Sci. Tech. 17 (1980) 291.

25. Hobson, D.O., and Rittenhouse, P. L., "Embrittlement of Zircaloy Clad Fuel Rods by Steam During LOCA Transients," ORNL-4758, Oak Ridge National Laboratory, January 1972.

26. Hobson, D.O., "Ductile-brittle behavior of Zircaloy fuel cladding," Proc. ANS Topical Mtg. on Water Reactor Safety, Salt Lake City, 26 March, 1973.

27. Pawel, R.E., "Oxygen diffusion in beta Zircaloy during steam oxidation," J. Nucl. Mater. 50 (1974) 247-258.

28. Sawatzky, A., "Proposed criterion for the oxygen embrittlement of Zircaloy-4 fuel cladding," Proc. 4th Symp. on Zirconium in the Nuclear Industry, Stratford-on-Avon, UK, 27-29 June, 1978.

29. Grandjean, C., "Oxidation and quenching experiments under simulated LOCA conditions with high burnup clad material," Proc. 24th Water Reactor Safety Information Meeting, Bethesda, USA, 21-23 October, 1996.

30. Grandjean, C. et al., "High burnup UO2 fuel LOCA calculations to evaluate the possible impact of fuel relocation after burst," ANL Program Review Meeting, Rockville (USA), 22 October, 1999.

31. Hofmann, P. et al., PECLOX: A Computer Model for the Calculation of the Internal and the External Zircaloy Cladding Oxidation, KFK-4422 Part 2, October 1988.

32. Uetsuka, H. et al., "Zircaloy-4 cladding embrittlement due to inner surface oxidation under simulated loss-of-coolant condition," J. Nucl. Sci. Tech. 18 (1981) 705-717.

33. Uetsuka, H. et al., "Embrittlement of Zircaloy-4 due to oxidation in environment of stagnant steam," J. Nucl. Sci. Tech. 19 (1982), 158-165.

34. Komatsu, K., "The effects of oxidation temperature and slow cooldown on ductile-brittle behavior of Zircaloy fuel cladding," Proc. CSNI Specialists' meeting on the behavior of water reactor fuel elements under accident conditions, Spaatind, Norway, 13-16 September, 1976.

35. Komatsu, K. et al., "Load-bearing capability in deformed and oxidized Zircaloy cladding," Proc. CSNI Specialist Mtg. on Safety Aspects of Fuel Behavior in Off-Normal and Accident Conditions, Espoo, Finland, 1-4 September, 1980.

36. Lorenz, R.A., "Fuel rod failure under loss-of-coolant conditions in TREAT," Nucl. Tech. 11 (1971) 502-520.

37. Haggag, F. M., Zircaloy-Cladding-Embrittlement Criteria: Comparison of In-Pile and Out-of-Pile Results, NUREG/CR-2757, July 1982.

NRC FORM 335 (2-89) NRCM 1102, 3201, 3202

U.S. NUCLEAR REGULATORY COMMISSION

BIBLIOGRAPHIC DATA SHEET

(See instructions on the reverse)

1. REPORT NUMBER (Assigned by NRC, Add Vol., Supp., Rev., and Addendum Numbers, if any.)

NUREG/CR-6744
LA-UR-00-5079

2. TITLE AND SUBTITLE

Phenomenon Identification and Ranking Tables (PIRTs) for Loss-of-Coolant Accidents in Pressurized and Boiling Water Reactors Containing High Burnup Fuel

3. DATE REPORT PUBLISHED

MONTH	YEAR
December	2001

4. FIN OR GRANT NUMBER

W6245

5. AUTHOR(S)

B.E. Boyack, A.T. Motta, K.L. Peddicord, C.A. Alexander, J.G.M. Andersen, J.A. Blaisdell, B.M. Dunn, D. Ebeling-Koning, T. Fuketa, G. Hache, L.E. Hochreiter, S.E. Jensen, S. Langenbuch, F.J. Moody, M.E. Nissley, K. Ohkawa, G. Potts, J. Rashid, R.J. Rohrer, J.S. Tulenko, K. Valtonen, N. Waeckel, W. Wiesenack

6. TYPE OF REPORT

Technical

7. PERIOD COVERED *(Inclusive Dates)*

04/00 to 11/00

8. PERFORMING ORGANIZATION - NAME AND ADDRESS *(If NRC, provide Division, Office or Region, U.S. Nuclear Regulatory Commission, and mailing address; if contractor, provide name and mailing address.)*

Los Alamos National Laboratory
Los Alamos, NM 87545

9. SPONSORING ORGANIZATION - NAME AND ADDRESS *(If NRC, type "Same as above"; if contractor, provide NRC Division, Office or Region, U.S. Nuclear Regulatory Commission, and mailing address.)*

Division of Systems Analysis and Regulatory Effectiveness
Office of Nuclear Regulatory Research
U.S. Nuclear Regulatory Commission
Washington, DC 20555-0001

10. SUPPLEMENTARY NOTES

H. Scott, NRC Project Manager

11. ABSTRACT *(200 words or less)*

In the United States, cladding embrittlement criteria and related evaluation models are used to address loss-of-coolant accidents. The embrittlement criteria are a peak cladding temperature of 1204 C (2200 F) and an equivalent oxidation of 17% of the cladding wall thickness calculated with the Baker-Just correlation. Evaluation models address ballooning, rupture, flow blockage, and oxidation kinetics. The NRC is performing research with respect to high burnup fuel to acquire and develop the requisite understanding of the performance of high burnup fuel under accident conditions. It is also conducting research to determine if current embrittlement criteria and evaluation models are adequate for high-burnup fuel or if modifications are needed. To support these efforts, the NRC has commissioned the formation of a Phenomena Identification and Ranking Table (PIRT) panel to identify and rank the phenomena occurring during selected transient and accident scenarios in both pressurized water reactors and boiling water reactors containing high burnup fuel. Because the PIRT identifies and ranks phenomena for importance, currently existing experimental data, planned experiments, computational tools (codes), and code-calculated results can be screened to determine applicability and adequacy using the PIRT results. This PIRT identifies and ranks phenomena for loss-of-coolant accidents in both pressurized and boiling water reactors.

12. KEY WORDS/DESCRIPTORS *(List words or phrases that will assist researchers in locating the report.)*

cladding, oxidation, embrittlement, rankings and rationales, LOCA, PWR, BWR, break-size, primary evaluation criterion, expert elicitation, plant transient analysis

13. AVAILABILITY STATEMENT

unlimited

14. SECURITY CLASSIFICATION

(This Page) unclassified

(This Report) unclassified

15. NUMBER OF PAGES

16. PRICE

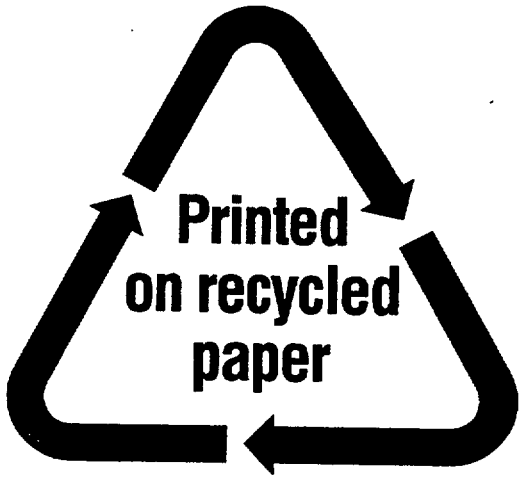

Federal Recycling Program

UNITED STATES
NUCLEAR REGULATORY COMMISSION
WASHINGTON, DC 20555-0001